

GEOCHEMICAL AND GEOCHRONOLOGICAL CONSTRAINTS ON MINERALIZATION
WITHIN THE HILLTOP, LEWIS, AND BULLION MINING DISTRICTS, BATTLE
MOUNTAIN-EUREKA TREND, NEVADA

by

CHRISTOPHER RONALD KELSON

(Under the Direction of Douglas E. Crowe)

ABSTRACT

The Hilltop, Lewis, and Bullion mining districts (northern Shoshone Range, Nevada) are part of the Battle Mountain-Eureka trend and contain both vein- and porphyry-type deposits.

New geochronology data from igneous rocks, porphyry-style Cu-Mo mineralization, and vein-hosted minerals elucidate the relationship between magmatic activity, hydrothermal fluid flow, and mineralization. Mostly felsic intrusive rocks were emplaced throughout the area between 39.3 ± 0.4 and 38.1 ± 0.4 Ma and weak Cu + Mo porphyry-style mineralization is associated with some of the intrusions. Ages of igneous rocks are nearly coincident with molybdenite ages, supporting a relation between pluton emplacement and porphyry Cu-Mo mineralization. Ages of quartz vein-hosted gold (35.9 ± 0.1 Ma, Hilltop deposit) and base-metal minerals (38.3 ± 0.07 Ma, Gray Eagle mine), established via ages of associated gangue clay minerals, are younger than nearby intrusive igneous rocks and may suggest the vein mineralization formed during prolonged hydrothermal activity related to igneous rock emplacement.

Quartz vein-hosted sulfide minerals from the northern Shoshone Range are isotopically similar ($\delta^{34}\text{S}_{\text{CDT}}$ range from -6 to +9 per mil) to sulfide minerals from other Cu-Mo porphyry deposits and Cordilleran vein-type deposits, supporting a mostly magmatic sulfur source. Carbon isotope data from vein gangue carbonate minerals also support a magmatic origin for ore-forming fluids with variable contributions from host rock organic matter or carbonate rocks ($\delta^{13}\text{C}_{\text{PDB}}$ range from -0.2 to -11.6 per mil); carbonate oxygen was derived mainly from magmatic fluids ($\delta^{18}\text{O}_{\text{VSMOW}}$ range from -1.3 to +14.4 per mil). Primary fluid inclusion data (salinity range from 0 to 6.4 equiv. wt. % NaCl; T_h range from 109-425°C) and measured $\delta^{18}\text{O}_{\text{VSMOW}}$ data (-0.97 to +17.3‰) suggest the ore-bearing vein quartz formed from variable amounts of meteoric and magmatic components (calculated $\delta^{18}\text{O}_{\text{VSMOW}}$ -16.2 to +13.3‰).

Depositional temperatures of base metal minerals, calculated using sulfide sulfur isotope geothermometry, range from 249-502°C and agree with vein quartz primary fluid inclusion T_h values.

Geochronology, stable isotope, and geothermometry data show that vein- and porphyry-type mineralization is genetically related to Eocene magmatism and that some vein mineralization temperatures exceeded relatively low-temperature epithermal conditions and were more closely related to higher temperature porphyry-style processes.

INDEX WORDS: Base Metals, Battle Mountain-Eureka Trend, Bullion District, Carbon, Carbonate, Copper, Cu, Eocene Magmatism, Epithermal, Fluid Inclusions, Geochronology, Geothermometry, Gold, Hilltop District, Hydrothermal, Lewis District, Mineralization, Mo, Molybdenite, Nevada, Oxygen, Porphyry, Quartz, Shoshone Range, Silver, Stable Isotopes, Sulfide, Sulfur, Vein

GEOCHEMICAL AND GEOCHRONOLOGICAL CONSTRAINTS ON MINERALIZATION
WITHIN THE HILLTOP, LEWIS, AND BULLION MINING DISTRICTS, BATTLE
MOUNTAIN-EUREKA TREND, NEVADA

by

CHRISTOPHER RONALD KELSON

B.S., University of Utah, 1994

M.S., Brigham Young University, 1999

A Dissertation Submitted to the Graduate Faculty of The University of Georgia in Partial
Fulfillment of the Requirements for the Degree

DOCTOR OF PHILOSOPHY

ATHENS, GEORGIA

2006

© 2006

Christopher Ronald Kelson

All Rights Reserved

GEOCHEMICAL AND GEOCHRONOLOGICAL CONSTRAINTS ON MINERALIZATION
WITHIN THE HILLTOP, LEWIS, AND BULLION MINING DISTRICTS, BATTLE
MOUNTAIN-EUREKA TREND, NEVADA

by

CHRISTOPHER RONALD KELSON

Major Professor: Douglas E. Crowe
Committee: Robert B. Hawman
Michael F. Roden
Paul A. Schroeder
Sandra J. Wyld

Electronic Version Approved:

Maureen Grasso
Dean of the Graduate School
The University of Georgia
May 2006

DEDICATION

This dissertation, representing five years' worth of being away from home and family while either working in the field or spending long days, weekends, and odd hours in the laboratory and office, is dedicated to my wife Christa. Without her love, support, and patience, I would not have made it through this.

ACKNOWLEDGEMENTS

This research would not have been possible without the generous support of the Cortez Joint Venture, and very special thanks to Mr. Robert C. Hays, Jr., Technical Services Superintendent, Cortez Joint Venture. This research was also funded by the Society of Economic Geologists (Hugh E. McKinstry Grant), the Geological Society of America (Grant No. 7180-02), and the Department of Geology, University of Georgia. Permission of the Cortez Joint Venture to publish this investigation is gratefully acknowledged. Thanks to: Dr. Kenneth A. Foland (OSU), Dr. Matthew T. Heizler (NMT), and Mr. Thomas D. Ullrich (UBC) for their assistance and insight with the $^{40}\text{Ar}/^{39}\text{Ar}$ data. Dr. Chris Romanek (SREL) and Mr. Tom Maddux (UGA) assisted with the organic carbon isotope data. Dr. Zachary D. Sharp (UNM) provided the silicate oxygen isotope analyses. Richard Markey (AIRIE, Colorado State University) provided the Re-Os analyses. Ms. Julia Cox and Mr. Chris Fleisher (UGA) assisted with stable isotope and electron microprobe analyses, respectively.

I would especially like to thank the members of my dissertation committee for many informative discussions regarding every facet of this study, and for their review of this dissertation.

TABLE OF CONTENTS

	Page
ACKNOWLEDGEMENTS	v
LIST OF TABLES	viii
LIST OF FIGURES	x
CHAPTER	
1 INTRODUCTION	1
REFERENCES	9
2 GEOCHRONOLOGY AND GEOCHEMISTRY OF THE HILLTOP, LEWIS, AND BULLION MINING DISTRICTS AND SURROUNDING AREA, BATTLE MOUNTAIN-EUREKA TREND, NEVADA	11
Abstract	12
Purpose of Study	13
General Geology of the northern Shoshone Range	14
Description of Mines in this Study	14
Analytical Methods	20
Results	24
Discussion	37
Conclusion	48
Acknowledgements	49
References	51

3	GEOCHEMICAL AND GEOCHRONOLOGICAL CONSTRAINTS ON MINERALIZATION WITHIN THE HILLTOP, LEWIS, AND BULLION MINING DISTRICTS, BATTLE MOUNTAIN-EUREKA TREND, NEVADA ..54	
	Abstract	55
	Introduction	57
	Regional Geologic Setting.....	62
	Northern Shoshone Range and District Geology	65
	Battle Mountain – Eureka trend	67
	Northern Shoshone Range Mineral Deposits	68
	Methods	81
	Intrusive Igneous Rocks	87
	Geochronology	98
	Relationship between Magmatism and Mineralization	105
	Discussion: Northern Shoshone Range Vein-Hosted Mineralization	116
	Summary and Conclusion	124
	Acknowledgements	125
	References	126
4	CONCLUSION.....	137
	APPENDICES	139
A	Geochemical data and location information for northern Shoshone Range samples.	139
B	⁴⁰ Ar/ ³⁹ Ar data	188
C	Quartz vein-hosted mineral species delineated by sample and deposit.	208

LIST OF TABLES

	Page
Table 2.1: Molybdenite Re-Os data from Tenabo, Hilltop, and Park Saddle areas.....	21
Table 2.2: Selenium-sulfide mineral associated with Hilltop molybdenite.....	27
Table 2.3: $^{40}\text{Ar}/^{39}\text{Ar}$ data from the northern Shoshone Range, Nevada.....	28
Table 2.4: Microprobe analyses of ore minerals from the northern Shoshone Range, Lander County, Nevada.....	33
Table 2.5: Carbon and oxygen stable isotope data from carbonate minerals associated with base- and precious-metal mineralization, northern Shoshone Range, Lander County, Nevada.....	35
Table 2.6: Sulfur stable isotope data from sulfide and sulfate minerals associated with base- and precious-metal mineralization, northern Shoshone Range, Lander County, Nevada....	36
Table 2.7: Sulfur isotope geothermometry data from four mines and prospects, northern Shoshone Range, Lander County, Nevada.....	47
Table 3.1: Types and orientations of ore-bearing structures and Ag:Au ratios for northern Shoshone Range vein deposits.....	69
Table 3.2: Electron microprobe analyses of sulfide minerals from northern Shoshone Range vein deposits.....	77
Table 3.3: Major and trace element chemical data for northern Shoshone Range igneous rocks.....	82
Table 3.4: $\delta^{13}\text{C}$ data for organic carbon-bearing rocks, breccias, and fault gouge, northern Shoshone Range.....	85

Table 3.5: Summary of all K-Ar, Ar/Ar, and Re-Os geochronology data for northern Shoshone Range igneous rocks, molybdenite (porphyry) mineralization, and vein-hosted mineralization.	100
Table 3.6: Salinity and homogenization temperatures for primary fluid inclusion as well as oxygen isotope compositions of host vein quartz, northern Shoshone Range vein deposits.	107
Table 3.7: $\delta^{13}\text{C}$ and $\delta^{18}\text{O}$ data for carbonate gangue minerals and upper plate (?) limestone, northern Shoshone Range vein deposits.	112
Table 3.8: $\delta^{34}\text{S}$ data for sulfide and sulfate minerals from northern Shoshone Range vein deposits.	115
Table 3.9: Calculated depositional temperatures based on sulfur isotope fractionation between two coexisting mineral phases using fractionation equations of Kajiwara and Krause (1971)	118

LIST OF FIGURES

	Page
Figure 1.1: Location of the Great Basin, Nevada, and mineral trends within north-central Nevada.....	2
Figure 1.2: Location of study area with respect to the Golconda thrust and Roberts Mountains thrust and major mining trends.....	3
Figure 1.3: Generalized stratigraphic column of the northern Shoshone Range in the vicinity of Mt. Lewis.....	6
Figure 2.1: Back scattered electron images (BEI) of Betty O’Neal mine samples.....	16
Figure 2.2: Generalized geologic map of the northern Shoshone Range	26
Figure 2.3a: $^{40}\text{Ar}/^{39}\text{Ar}$ age spectra and correlation diagrams for GM-3 biotite, DSC BXA clay, and HT02-1 clay (analyzed by RIL).....	29
Figure 2.3b: $^{40}\text{Ar}/^{39}\text{Ar}$ age spectra and correlation diagrams for GM-6 biotite and hornblende, GM-15 biotite and hornblende, and T99413-570 biotite (analyzed by NMGRL)	30
Figure 2.4: Carbonate and oxygen isotope data from four mineralized areas within the northern Shoshone Range, Lander County, Nevada.....	41
Figure 2.5: Carbonate carbon isotope data from four mineralized areas within the northern Shoshone Range, Lander County, Nevada.....	43
Figure 2.6: Sulfide and sulfate sulfur stable isotope data from six mineralized areas within the northern Shoshone Range, Lander County, Nevada	45
Figure 3.1: Location of the Lewis, Hilltop, and Bullion mining districts and mineralized areas studied here, northern Shoshone Range, Lander County, Nevada.....	58

Figure 3.2: Simplified geologic map of the northern Shoshone Range study area, Lander County, Nevada.....	59
Figure 3.3: Examples of northern Shoshone Range vein mineralization.....	71
Figure 3.4: Aeromagnetic map of the northern Shoshone Range study area and adjacent areas, band pass filtered to emphasize magnetic structures and bodies between the surface and 500 m.....	89
Figure 3.5: Whole rock chemical data plot for least altered northern Shoshone Range igneous rocks compared to igneous rocks related to porphyry systems (modified from Le Maitre, 2002; Seedorff et al., 2005).....	90
Figure 3.6: Chondrite-normalized REE diagrams for least altered igneous rocks, northern Shoshone Range, compared to other Eocene igneous rocks associated with mineralization in the Carlin trend (data from Ressel et al., in review).	94
Figure 3.7: MORB-normalized spider diagrams for least altered igneous rocks, northern Shoshone Range.....	96
Figure 3.8: Summary of all geochronology (K-Ar, Ar/Ar, Re-Os) data for igneous rocks and molybdenite mineralization and vein-associated minerals, northern Shoshone Range.	102
Figure 3.9: Salinity vs. homogenization temperature plot of primary fluid inclusion data from northern Shoshone Range ore-bearing quartz veins.....	109
Figure 3.10: Plot of salinity vs. calculated $\delta^{18}\text{O}$ for fluids associated with ore-bearing vein quartz.	110

Figure 3.11: Plot of primary fluid inclusion homogenization temperatures vs. calculated $\delta^{18}\text{O}$ for fluids associated with vein quartz carrying epithermal – porphyry-type base- and precious metal mineralization.111

Figure 3.12: Plot of carbon and oxygen isotope data from carbonate gangue minerals compared to Cortez (lower plate) carbonate rocks, Lovie (upper plate?) limestone and organic carbon (this study), and calcite in equilibrium with meteoric water and primary granodioritic magmatic water at 250°C.....113

Figure 3.13: Sulfide and sulfate (barite) sulfur isotope data from northern Shoshone Range vein deposits.....117

CHAPTER 1

INTRODUCTION

The state of Nevada, located within the Great Basin physiographic province of the western United States, has been an important producer of base- and precious-metals, especially silver, since the 1850s. Economically, gold has surpassed silver as the dominant commodity produced in Nevada since the discovery of sediment (carbonate)-hosted, low-grade, bulk-tonnage gold deposits (Carlin-type deposits) in the 1960s, although base- and precious-metals are mined from a wide variety of deposit types. In 2001, Nevada accounted for nearly 75% of United States gold production and 10% of world gold production, behind only South Africa and Australia (Price and Meeuwig, 2002).

Roberts (1966) first identified 12 mineral “belts” or “trends” – alignments of mines and deposits – throughout Nevada. Each mineral trend consists of several mining districts composed of hundreds of mines, deposits, and prospects. The origin of these mineral trends is not completely understood, although the existence of deep-penetrating crustal structures that acted as conduits for intrusive igneous rocks and/or mineralizing fluids have been postulated by several workers (Roberts, 1966; Shawe, 1991; Zamudio and Atkinson, 1991; Grauch et al., 2003; Howard, 2003; among others). In north-central Nevada, five mineral trends are identified: Getchell, Crescent Valley-Independence, Carlin, Alligator Ridge, and Battle Mountain-Eureka (John et al., 2003). This study focuses on mineralization within part of the Battle Mountain-Eureka trend (Figs. 1.1 and 1.2).

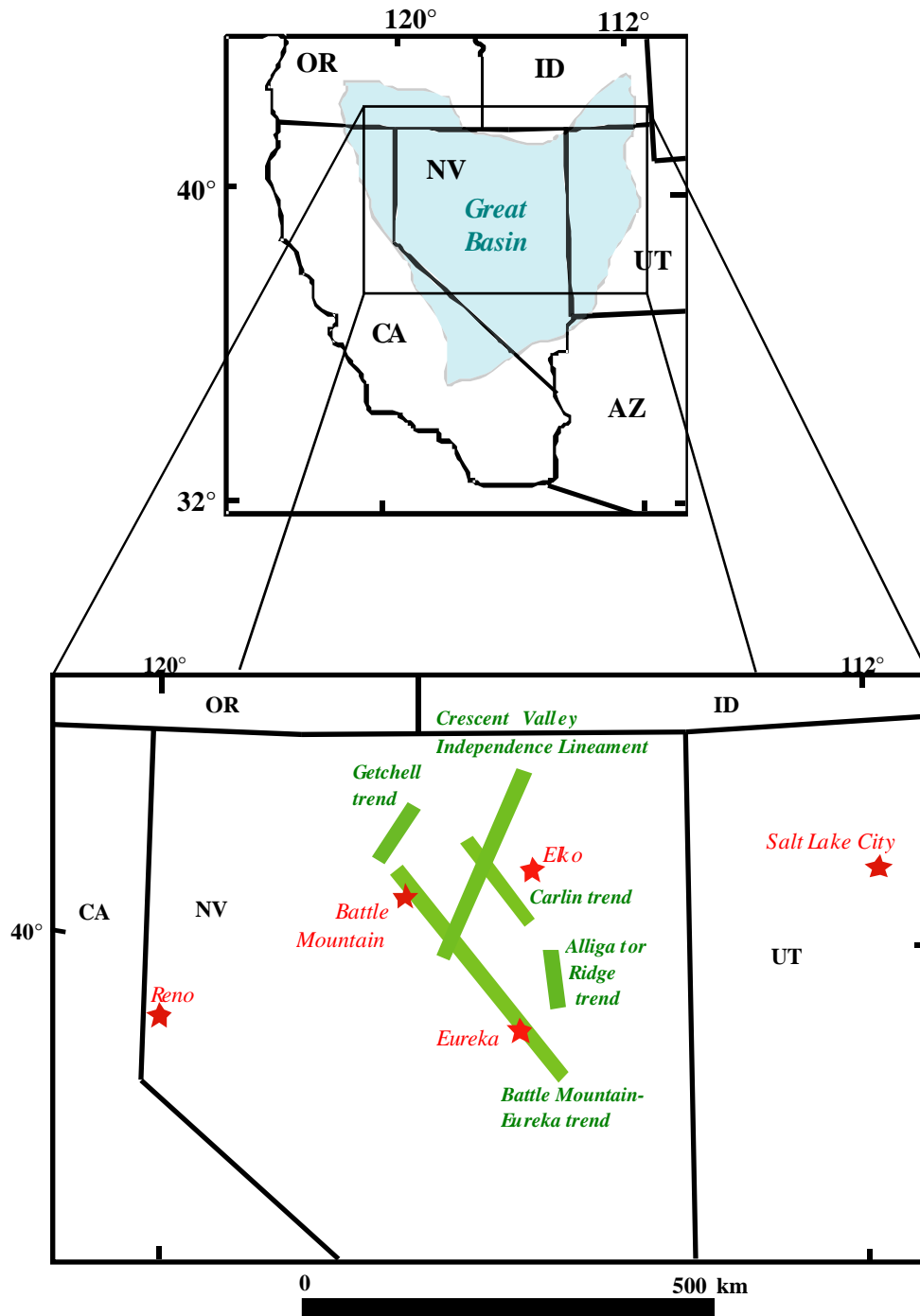
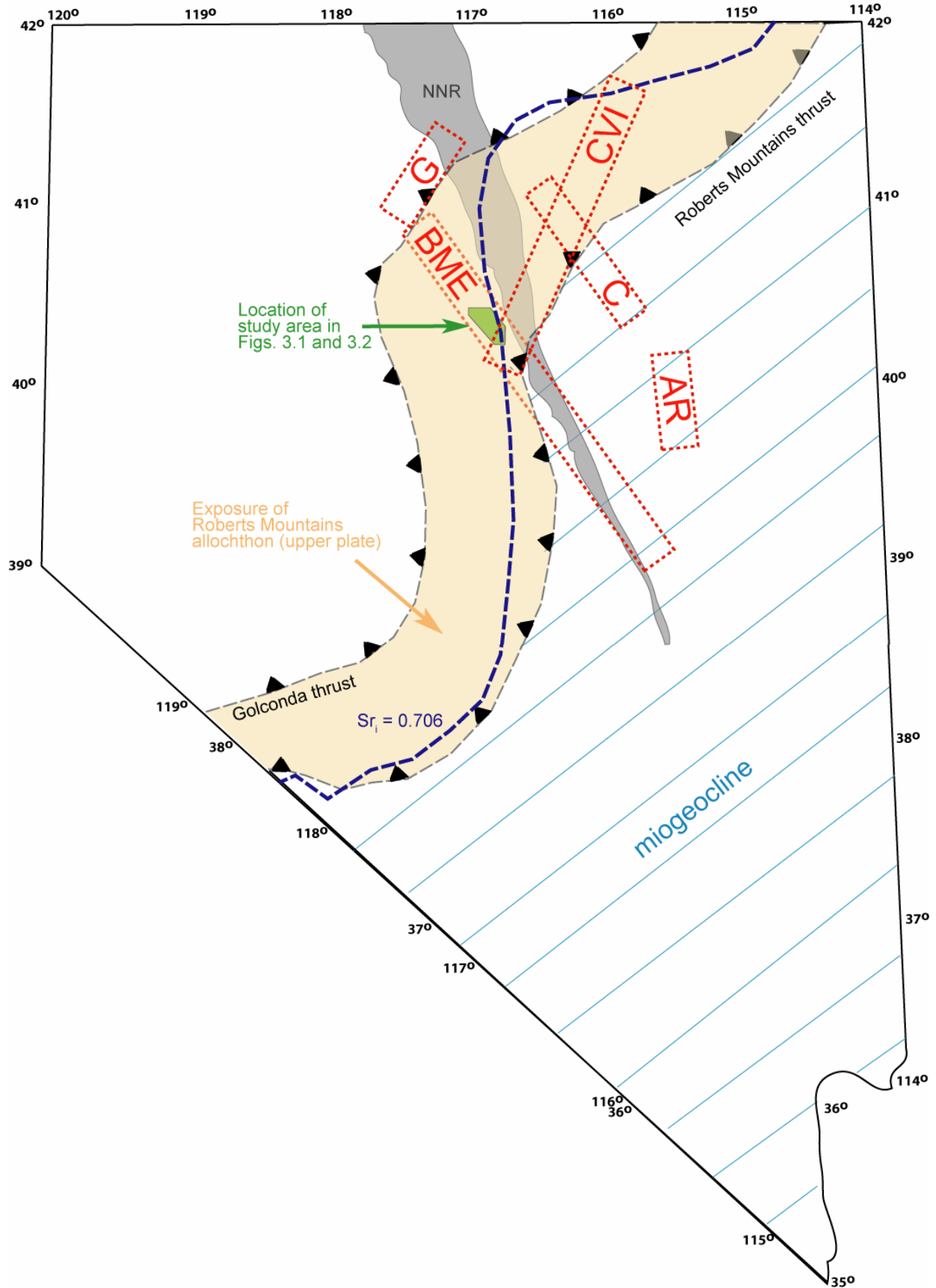


Figure 1.1: Location of the Great Basin, Nevada, and mineral trends within north-central Nevada (modified from John et al., 2003).

Figure 1.2 (next page): Location of study area with respect to the Golconda thrust and Roberts Mountains thrust and major mining trends. Also shown: Inferred western edge of the Precambrian crust ($Sr_i=0.706$), Northern Nevada Rift (NNR), Battle Mountain-Eureka trend (BME), Alligator Ridge trend (AR), Carlin trend (C), Crescent Valley-Independence lineament (CVI), and Getchell trend (G). Miogeoclinal ("lower plate") rocks of the Cordillera also shown. Modified from Saleeby and Busby-Spera (1992), and Grauch et al. (2003).



The Battle Mountain-Eureka trend consists of 10 mining districts, three of which (Hilltop, Lewis, and Bullion, collectively containing over 140 mines and prospects) were organized shortly after the 1859 Comstock Lode discovery and are located within the northern Shoshone Range in Lander County. Between 1860 and 1936, more than 33 Koz gold (placer and lode), 5 Moz silver, 53 Moz lead, and 20 Moz copper have collectively been produced from the Hilltop, Lewis, and Bullion mining districts (Vanderburg, 1939). Other commodities include mercury, antimony, manganese, turquoise, fluorspar, and barite.

This study focuses on mineralization from eight different locales within the northern Shoshone Range: the Hilltop deposit and Blue Dick and Kattenhorn mines (Hilltop district); the Betty O'Neal mine (Lewis district); the Gray Eagle and Lovie mines, Tenabo deposit, and an unnamed prospect (Bullion district). Although most mines within the silver-rich northern Shoshone Range have been inactive since the 1930s, the area is periodically evaluated and explored for further (gold) mineralization potential.

Most mineralization within the northern Shoshone Range occurs as vein and fracture-fill within early Paleozoic siliceous and siliciclastic rocks (Ordovician Valmy Formation, upper plate, Roberts Mountains allochthon; Fig. 1.3) and/or Tertiary intrusive rocks. Weak Cu + Mo ± Au porphyry-type mineralization is also locally associated with some granitic intrusive rocks.

The most abundant vein-hosted ore minerals include pyrite, galena, sphalerite, arsenopyrite, chalcopyrite, fahlore and other sulfosalts. Major silver-bearing minerals include sulfosalts (e.g. fahlore [(Cu,Ag)₁₂(Zn,Fe)₂(As,Sb)₄S₁₃]), Ag-halogens (e.g. chlorargyrite), and lesser argentiferous galena and electrum. Native gold and electrum are rare. Vein-hosted gangue minerals include quartz, calcite with Fe, Mn, and/or Mg, Ba- and/or Ca- sulfates, chlorite, illite (“sericite”), muscovite, smectite and other clays, and remobilized organic carbon.

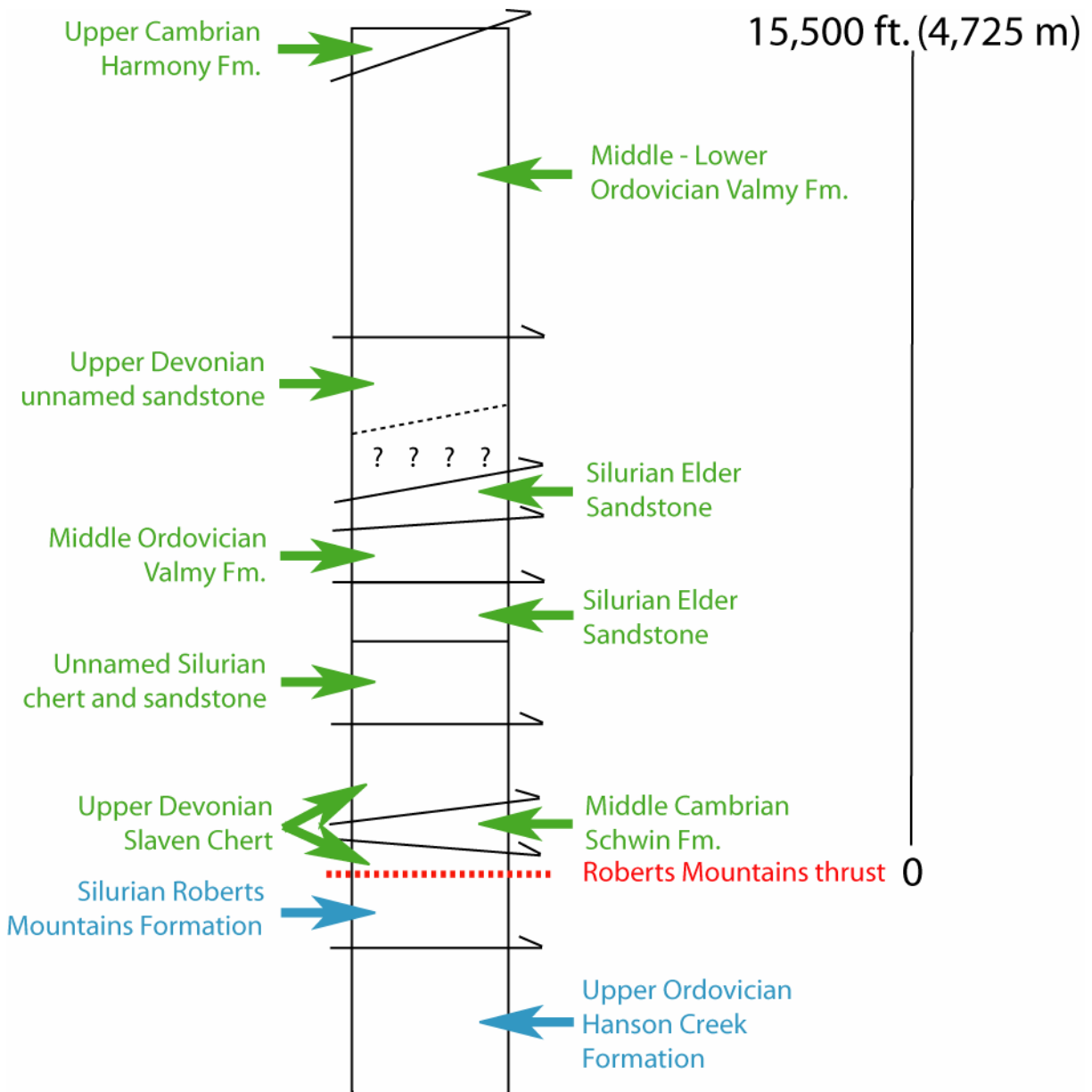


Figure 1.3: Generalized stratigraphic column of the northern Shoshone Range in the vicinity of Mt. Lewis. Green indicates upper plate units of the Roberts Mountains allochthon; blue indicates autochthonous (lower plate) units. Arrows indicate thrust fault contacts; contact dashed where inferred. Modified from Poole et al. (1992).

Sulfide (ore) minerals are always associated with quartz, commonly with clays, and rarely with chlorite, remobilized organic carbon, or carbonate and sulfate minerals.

Due to the poor primary permeability and porosity of the siliceous and siliciclastic host rocks, mineralization is mostly localized in areas of strong structural preparation, i.e. fault, fracture, and shear zones. Alteration normally associated with vein- or porphyry-type mineralization is largely absent within the host rocks, attesting to the inability of the mineralizing fluids to circulate through the host rocks outside of areas exhibiting pronounced secondary permeability.

Except for the Hilltop gold deposit (Hilltop district), no detailed investigation exists concerning any particular mine within the Hilltop, Lewis, or Bullion mining districts, and only a few investigations (mostly reconnaissance in nature) exist regarding the geology or mining history of the entire area (King, 1876; Spurr, 1903; Emmons, 1910; Lee et al., 1916; Vanderburg, 1939; Gilluly and Gates, 1965; Stewart and McKee, 1977).

This study is the first in-depth, multi-faceted examination of northern Shoshone Range mineralization. The second and third chapters investigate geochronological and geochemical aspects of mineralization including:

1. $^{40}\text{Ar}/^{39}\text{Ar}$ ages of intrusive igneous rocks located proximal and distal to mineralized areas;
2. $^{40}\text{Ar}/^{39}\text{Ar}$ ages of gangue minerals associated with vein-hosted base- and precious-metal mineralization;
3. Re-Os ages of molybdenite (porphyry) mineralization;
4. The temporal relationship between igneous activity and mineralization;

5. Major- and trace-element analysis and geochemical characterization of intrusive igneous rocks;
6. Identification and paragenesis of ore and gangue minerals within each mineralized area;
7. Stable isotope analysis of sulfide, sulfate minerals (sulfur), carbonate minerals (carbon, oxygen), and vein quartz from each mineralized area;
8. Depositional parameters (temperature, salinity) of ore-bearing solutions from each mineralized area;
9. Ore-bearing fluid source characterization of each mineralized area.

The results of this study provide new insight into the timing and genesis of ore deposition and the relationship between intrusive igneous rocks and ore, and may elucidate new avenues of base- and precious-metal exploration within this portion of the Battle Mountain-Eureka trend.

REFERENCES

- Emmons, W.H., 1910, A reconnaissance of some mining camps in Elko, Lander, and Eureka Counties, Nevada: U. S. Geological Survey Bulletin 408, 130 p.
- Gilluly, J., and Gates, O., 1965, Tectonic and igneous geology of the northern Shoshone Range, Nevada: U.S. Geological Survey Professional Paper 465, 153 p.
- Grauch, V.J.S., Rodriguez, B.D., and Wooden, J.L., 2003, Geophysical and isotopic constraints on crustal structure related to mineral trends in north-central Nevada and implications for tectonic history: *Economic Geology*, v. 98, p. 269-286.
- Howard, K.A., 2003, Crustal structure in the Elko-Carlin region, Nevada during Eocene gold mineralization: Ruby-East Humboldt metamorphic core complex as a guide to the deep crust: *Economic Geology*, v. 98, p. 249-268.
- John, D.A., Hofstra, A.H., and Theodore, T.G., 2003, Preface, *in A Special Issue Devoted to Gold Deposits in Northern Nevada: Part 1. Regional Studies and Epithermal Deposits: Economic Geology*, v. 98, p. 225-234.
- Kelson, C.R., Keith, J.D., Christiansen, E.H., and Meyer, P.E., 2000, Mineral paragenesis and depositional model of the Hilltop gold deposit, Lander County, NV, *in Cluer, J.K., Price, J.G., Struhsacker, E.M., Hardyman, R.F., and Morris, C.L., eds., Geology and ore Deposits 2000: The Great Basin and Beyond: Geological Society of Nevada Symposium Proceedings, Reno/Sparks, May 2000*, p. 1107-1132.
- King, C., 1876, Geological and topographical atlas accompanying the report of the Geological Exploration of the Fortieth Parallel.
- Lee, W.T., Stone, R.W., Gale, H.S., and others, 1916, The Overland Route, with a side trip to Yellowstone Park, Pt. B *of Guidebook of the western United States: U.S. Geological Survey Bulletin* 612.

- Poole, F.G., Stewart, J.H., Palmer, A.R., Sandberg, C.A., Madrid, R.J., Ross, R.J., Jr., Hintze, L.F., Miller, M.M., and Wrucke, C.T., 1992, Latest Precambrian to latest Devonian time; Development of a continental margin, *in* Burchfiel, B.C., Lipman, P.W., and Zoback, M.L. eds., *The Cordilleran Orogen: Conterminous U.S.*: Boulder, Colorado, Geological Society of America, *The Geology of North America*, v. G-3, p. 9.56.
- Price, J.G., and Meeuwig, R.O., 2002, Overview, *in* *The Nevada Mineral Industry 2001*: Nevada Bureau of Mines and Geology Special Publication MI-2001, p. 3-12.
- Roberts, R.J., 1966, Metallogenic provinces and mineral belts in Nevada: Nevada Bureau of Mines and Geology Report 13, part A, p. 47-72.
- Saleeby, J.B., and Busby-Spera, C., 1992, Early Mesozoic tectonic evolution of the western U.S. Cordillera, *in* Burchfiel, B.C., Lipman, P.W., and Zoback, M.L. eds., *The Cordilleran Orogen: Conterminous U.S.*: Boulder, Colorado, Geological Society of America, *The Geology of North America*, v. G-3, p. 107-168.
- Shawe, D.R., 1991, Structurally controlled gold trends imply large gold resources in Nevada: In Raines, G.L., Lisle, R.E., Schafer, R. W., and Wilkenson, W.H.. (eds.), *Geology and ore deposits of the Great Basin*: Geological Society of Nevada, p. 199-212.
- Spurr, J.E., 1903, Descriptive geology of Nevada south of the 40th Parallel and adjacent portions of California: U.S. Geological Survey Bulletin 208.
- Stewart, J.H., and McKee, E.H., 1977, *Geology and Mineral Deposits of Lander County, Nevada*: Nevada Bureau of Mines and Geology Bulletin 88, 106 p.
- Vanderburg, W.O., 1939, Reconnaissance of some mining districts in Lander County, Nevada: U.S. Bureau of Mines Information Circular 7043, p. 47-50.
- Zamudio, J.A., and Atkinson, Jr., W.W., 1991, Igneous rocks of the northeastern Great Basin and their relation to tectonic activity and ore deposits, *in* Buffa, R.H., and Coyner, A.R., eds., *Geology and ore deposits of the Great Basin, Field Trip Guidebook Compendium*, v. 1: Geological Society of Nevada, p. 229-242.

CHAPTER 2

GEOCHRONOLOGY AND GEOCHEMISTRY OF THE HILLTOP, LEWIS, AND BULLION MINING DISTRICTS AND SURROUNDING AREA, BATTLE MOUNTAIN-EUREKA TREND, NEVADA ¹

¹ Kelson, Chris R., Crowe, Douglas E., and Stein, Holly J., 2005, Geochronology and geochemistry of the Hilltop, Lewis, and Bullion mining districts and surrounding area, Battle Mountain-Eureka trend, Nevada, *in* Rhoden, H.N., Steininger, R.C., and Vikre, P.G., eds., Geological Society of Nevada Symposium 2005: Window to the World, Reno, Nevada, May 2005, p. 25-42.

Reprinted here with permission from the publisher.

Abstract

Recent work in the northern Shoshone Range, Lander County, Nevada, provides new insight into the relationship between precious- and base-metal deposits within the Hilltop, Lewis, and Bullion mining districts and to nearby igneous intrusions. Radiogenic and stable isotope data, combined with geochemical analyses, allow us to elucidate the timing and origin of hydrothermal events within the districts.

Five molybdenites from four samples associated with Cu + Mo ± Au porphyry-style mineralization from the Hilltop district yield ages from 40.1 ± 0.2 to 40.6 ± 1.2 Ma with a weighted mean of 40.23 ± 1.7 Ma (MSWD = 2.4, 95% CL). A single molybdenite sample from Cu + Mo ± Au porphyry-style mineralization at the Tenabo deposit (Bullion district) provides a 39.0 ± 1.4 Ma age. $^{40}\text{Ar}/^{39}\text{Ar}$ ages for biotite and amphibole from unaltered igneous units within and/or proximal to mineralized areas (i.e. Tenabo granodiorite biotite: 38.85 ± 0.07 Ma) are nearly coincident with molybdenite ages, supporting a relation between pluton emplacement and porphyry mineralization.

Sulfur isotope data suggest a magmatic origin ($\delta^{34}\text{S}_{\text{CDT}}$ range from -4 to +4 per mil) for most sulfide minerals. Carbon isotope data ($\delta^{13}\text{C}_{\text{CDT}}$ range from -0.2 to -11.6 per mil) from carbonate minerals associated with ore also support a magmatic origin for the ore-forming fluids; carbonate oxygen isotope data ($\delta^{18}\text{O}_{\text{VSMOW}}$ range from -1.3 to +14.4 per mil) indicate predominantly magmatic to mixed magmatic/meteoric source fluids.

Temperatures of base metal-rich ore-forming fluids calculated using sulfur isotope fractionation between co-existing sulfides are 304-502°C (Gray Eagle mine), 339°C (unnamed prospect), 249°C (Lovie mine), and 434°C (Hilltop deposit).

Geochronology and stable isotope data suggest base- and precious-metal mineralization within the Hilltop, Lewis, and Bullion mining districts is genetically related to Eocene magmatism. Geothermometry indicates that some mineralization temperatures exceeded relatively low-temperature epithermal conditions and were more closely related to higher temperature porphyry-style processes.

Purpose of Study

The numerous precious ± base metal occurrences within the northern Shoshone Range contain dissimilar ore minerals and represent epithermal- and/or porphyry-style mineralization. Several granodioritic plutons are emplaced along a west-northwest trend through the area; some are barren and others are associated with Cu ± Mo ± Au porphyry-style mineralization. Prior to this study, the temporal relationship between mineralization and intrusive igneous rocks within the northern Shoshone Range was poorly understood, and mineralization fluid source(s) and depositional conditions unknown.

The purpose of this study is to: 1) determine the ages of intrusive igneous rocks and mineralization, 2) constrain fluid sources and depositional temperatures of mineralization, 3) elucidate the relationship between intrusive igneous rocks and mineralization, and 4) characterize geochemical differences between mineralized areas within the northern Shoshone Range.

General Geology of the northern Shoshone Range

The Shoshone Range is a northeast-trending mountain range that extends across north central Nevada. The northern half of the range contains the Lewis and Hilltop mining districts (which include the Betty O’Neal, Hilltop, Blue Dick, and Kattenhorn mines) and a portion of the Bullion mining district (including the Gray Eagle, Lovie, and Tenabo mines); all part of the Battle Mountain-Eureka mineral belt. The northern Shoshone Range is underlain mostly by highly-fractured and faulted Late Cambrian-Middle Devonian siliceous, siliciclastic, and volcanic rocks (allochthonous “upper plate” sequence, Roberts Mountains thrust). Cambrian-Early Mississippian carbonate rocks (lower plate) are rare (Gilluly and Gates, 1965). Eocene-Oligocene and mid-Miocene igneous rocks intrude or overlie the upper plate rocks (Stager, 1977). All of the mines, prospects, and deposits in this study are hosted within fractured and faulted upper plate rocks. Granodioritic intrusions occur within, proximal, and/or distal to each mineralized area.

Description of Mines in this Study

Lewis district: Betty O’Neal mine

The Betty O’Neal mine is one of 22 mines that comprise the Lewis mining district. It is the largest producer, having produced more than \$3 million in silver, gold, lead, and copper intermittently from 1880 to 1929 (Stager, 1977).

Precious- and base-metal mineralization at the Betty O'Neal mine is associated with two of at least seven temporally-distinct episodes of mineralization:

1. Quartz (early)
2. Carbonate + gypsum/anhydrite + epidote ± sericite ± chlorite ± pyrite ± fahlore
3. Euhedral quartz + fahlore ± carbonate + sphalerite + galena + chalcopyrite + bournonite
4. Quartz + barite
5. Fine grained quartz ± pyrite ± sericite
6. Sericite ± quartz ± pyrite ± clay
7. Quartz (late)

Mineralization is controlled and localized in quartz veins along four major shear zones that strike NW to NE and dip between 10-70° NE to NW (Stager, 1977). Ordovician Valmy Formation siliciclastic and siliceous rocks, not the igneous rocks, are hosts for mineralization. Barite does not appear to be associated with precious-metal mineralization, and no gold-bearing mineral was observed. The most abundant ore minerals are Ag-fahlore and other sulfosalts (i.e. chlorargyrite, bromargyrite). "Individual" fahlore grains are typically mixtures of As, Zn, Fe, ± Ag-bearing tetrahedrite-tennantite and occasional base-metal minerals (Figure 2-1a).

Betty O'Neal mine ore commonly exhibits minerals and textures indicative of significant amounts of supergene oxidation. Evidence includes: a) Cu and Ag oxidation products along fractures in fahlore; b) malachite, azurite, and Cu-oxides derived from fahlore oxidation; c) fragments of chlorargyrite and bromargyrite in banded lead manganate similar to coronadite (Hewett, 1971) (Figure 2-1b); d) vein pyrite frequently oxidized to hematite.

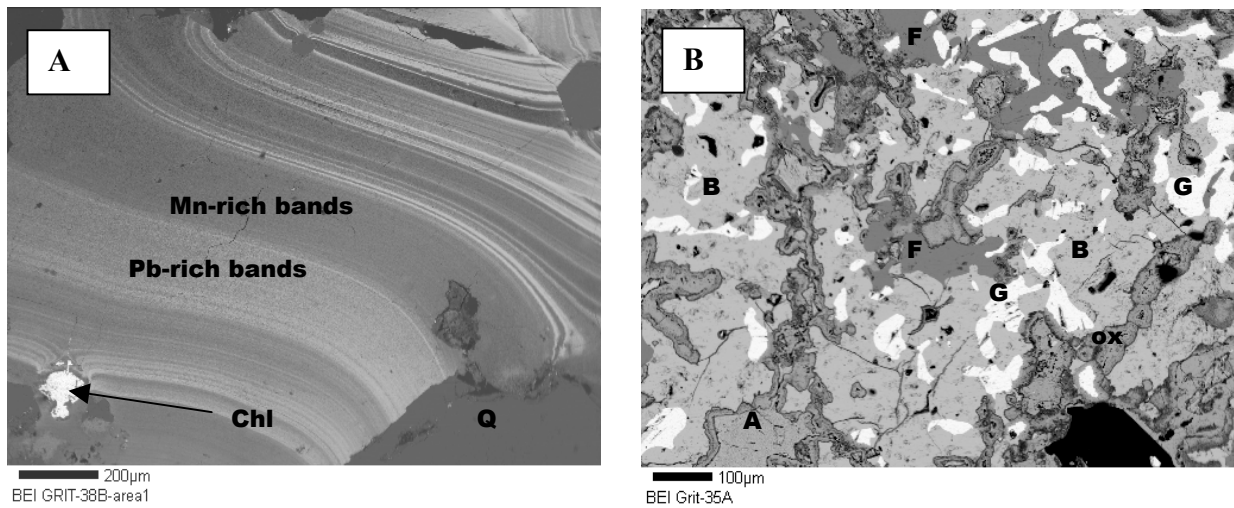


Figure 2.1: Back scattered electron images (BEI) of Betty O’Neal mine samples. A) Chlorargyrite (chl) grain in banded lead-manganate (e.g. coronadite) surrounded by quartz (q). B) Ag-rich fahlore (F) intergrown with bournonite (B), galena (G), acanthite (A), and oxidized bournonite (ox).

Hilltop district

The Hilltop district includes the Hilltop, Red Top, Independence, Blue Dick, and Kattenhorn mines, plus over 20 other mines and prospects, and has produced more than \$1 million in gold, silver, copper, lead, barite, antimony, and manganese intermittently from 1880 to 1969 (Stager, 1977).

The Hilltop, Red Top, and Independence mines are collectively referred to as the Hilltop deposit (Lisle and Desrochers, 1988; Kelson et al., 2000). Faulted and brecciated chert, argillite, siltstone, and quartzite of the Ordovician Valmy Formation host the Hilltop deposit. Initial Cu + Mo ± Au porphyry-style mineralization is associated with granodioritic intrusives that altered (bleached and recrystallized) the Valmy host rocks. Subsequent epithermal-style precious- and base-metal mineralization is localized in a breccia (the “Main Zone”) between two sub-parallel, north-striking and west-dipping faults (the Independence and Hilltop Mine faults). Main Zone mineralization consists of at least six temporally-distinct events:

1. Galena + sphalerite + pyrite + fahlore + chalcopyrite + sulfosalts (oldest)
2. Quartz + arsenopyrite + pyrite + gold
3. Quartz ± arsenopyrite ± kaolinite-group mineral ± pyrite ± carbonate ± barite ± marcasite ± stibnite + gold
4. Quartz + arsenopyrite + pyrite + gold
5. Melnikovite pyrite + marcasite + pyrite ± kaolinite
6. Sphalerite/wurtzite (youngest)

Gold also occurs within a discordant quartz breccia pipe located on the east flank of Hilltop. The pipe contains altered Valmy Formation siliciclastic fragments in a matrix of

ehedral, cockade quartz and is offset by the hanging wall Independence fault and floored by the Hilltop Mine fault. The precise relationship between breccia pipe and Main Zone mineralization is not clearly understood (Kelson et al., 2000).

The Kattenhorn and Blue Dick mines sporadically produced more than \$300,000 in silver ore from 1880 to 1923 (Stager, 1977). Silver in both deposits occurs mostly within fahlore, and mineralization is localized in northwest-striking quartz veins (up to five feet wide) that dip 45-50° SW (Vanderberg, 1939). Kattenhorn ore contains galena, chlorargyrite, and Sn- and Se-bearing fahlore while Blue Dick ore contains acanthite, arsenopyrite, sphalerite, and miargyrite. Barite is associated with quartz and sulfides in both deposits and at least one generation of barren quartz precedes sulfide mineralization.

Bullion district

The Bullion district consists of more than 90 mines and prospects. The Gray Eagle and Lovie mines, and an unnamed prospect, are considered in this study. Silver, gold, copper, lead, barite, and turquoise were produced from 1869 to 1961. The total value of production from the district is about \$16 million, mostly in gold from the Gold Acres mine (Stager, 1977). The Gold Acres mine is not part of this study. The silver-bearing deposits are quartz veins hosted by both siliciclastic and granitic rocks.

The Gray Eagle mine is located on the west flank of the Granite Mountain stock, and produced more than several hundred thousand dollars in gold, silver, and lead intermittently between 1870 and 1907. The deposit is a fissure vein of banded quartz + sulfide ± sericite that strikes N70E and dips 70°N within the Granite Mountain stock (Emmons, 1910; Vanderburg,

1939). Sulfides (arsenopyrite, pyrite, galena, sphalerite, chalcopyrite, fahlore, and rare hessite) and electrum are hosted within quartz veins that exhibit a range of color (clear or milky-white) and crystal size (sucrosic or euhedral, $\leq 1''$ crystals). Sulfides occur in vugs within the quartz vein or between individual vein quartz crystals; the host rock is weakly to strongly argillized and locally silicified.

The Lovie mine is hosted within Ordovician Valmy Formation siltstone, quartzite, and argillite and Devonian Slaven Formation chert. Sulfide minerals (galena, sphalerite, pyrite, Ag-rich fahlore, arsenopyrite, and chalcopyrite) \pm carbonate \pm quartz occur in $\leq 3''$ -wide veins. Most sulfide mineralization occurs within the northern and central portion of the deposit. Manganese-rich gossan commonly surrounds fresh, massive, galena and sphalerite veins and Mn-oxide typically replaces sphalerite along crystallographic boundaries and fractures. The Mn-oxide is not pervasive throughout the deposit and may only be associated with the galena and sphalerite. It clearly post-dates base metal deposition and probably reflects localized mobilization of Mn-rich fluids under supergene (oxidation zone) conditions. The source of the Mn is unknown. Massive barren carbonate veins occur in the southern portion of the deposit, and are cut by barren veins of chlorite + epidote. The paragenetic relationship of the carbonate veins to base-metal mineralization is unclear.

An unnamed prospect, located on the eastern flank of the Granite Mountain stock less than one mile east of the Gray Eagle mine, consists of several caved adits and trenches, and consists of 1-2''-wide quartz + carbonate \pm sericite veins with sulfides within Granite Mountain granite. Sulfides include galena, sphalerite, pyrite, arsenopyrite, Ag-fahlore, and geffroyite. Gold was not directly observed, but assay data reveal it to be present in anomalous concentrations.

Analytical Methods

Rhenium-Osmium (Re-Os)

For this study, a Carius-tube digestion was used. Molybdenite was dissolved and equilibrated with a mixed double Os spike (^{185}Re - ^{188}Os - ^{190}Os) in HNO_3 - HCl (inverse aqua regia) and sealed in a thick-walled glass ampoule and heated for 12 hours at 230°C (Markey et al. 2003). The double Os spike permits a check for common Os and mass fractionation correction, leading to high precision results. The Os was recovered by distilling directly from the Carius tube aqua regia into HBr , and was subsequently purified by micro-distillation. The Re was recovered by anion exchange. The Re and Os were loaded onto Pt filaments and isotopic compositions were determined using NTIMS on NBS 12-inch radius, 68° and 90° sector mass spectrometer at Colorado State University. Two in-house molybdenite standards, calibrated at AIRIE (Applied Isotope Research for Industry and the Environment), were run as an internal check. The Re-Os data acquired in this study are reported in Table 2-1, accompanied by pertinent information on the samples analyzed and data reduction.

$^{40}\text{Ar}/^{39}\text{Ar}$ – (NMGRRL)

Mineral separates (GM-6 hornblende and biotite; GM-15 hornblende and biotite; T99413-570 biotite) were loaded into machined Al discs together with a neutron flux monitor (27.84 Ma Fish Canyon Tuff sanidine FC-1) and irradiated for seven hours in D-3 position at the Nuclear Science Center, College Station, Texas.

Table 2.1: Molybdenite Re-Os data from Tenabo, Hilltop, and Park Saddle areas.

Location	Sample	AIRIE Run #	Description	Re, ppm	¹⁸⁷ Os, ppb	Age, Ma
Tenabo	99413 560	MDID-49	Molybdenite aggrerates (0.5 mm) and occassional pyrite in unaltered biotite + quartz + feldspar granodiorite	58 (2)	23.82 (7)	39.0 + 1.4*
Hilltop	97-6 80	MDID-63	Molybdenite flakes in 0.5 cm wide quartz vein in Valmy argillite	142.34 (3)	59.7 (2)	40.1 + 0.2
Hilltop	97-10 106.1	MDID-51	Abundant molybdenite laths with pyrite and sericite in 0.5 cm wide quartz vein in phyllically-altered intrusive-matrix breccia	51 (2)	21.88 (3)	40.6 + 1.2*
Hilltop	97-10 106.1	MDID-64	Replicate analysis	49.59 (3)	21.06 (4)	40.5 + 0.2
Hilltop	PH-136 270-380	MDID-290	Composite molybdenite sample. Trace molybdenite + chalcopyrite in ~1 mm wide quartz veins in brecciated Valmy quartzite, siltstone, and argillite with minor feldspar porphyry matrix	18.5 (2)	7.79 (5)	40.2 + 0.4
Park Saddle	XCR-6 340-380	MDID-291	Composite molybdenite sample. Trace molybdenite + common pyrite disseminated in strongly phyllically-altered and silicified feldspar porphyry	0.5769 (2)	0.2432 (2)	40.2 + 0.1

Notes:

Samples (6-302 mg) run using Carius tube dissolution with mixed double Os spike to decrease uncertainties
 Data are blank corrected, account for common Os, and are corrected for Os mass fractionation
 Blank corrections include Re and Os concentrations, ¹⁸⁷Os/¹⁸⁸Os isotopic compositions, and their uncertainties
 For Re and ¹⁸⁷Os concentration data, absolute uncertainties shown, all at 2-sigma level, for last digit indicated
 Decay constant is ¹⁸⁷Re is 1.666 x 10⁻¹¹yr⁻¹ (Smoliar et al. 1996) and ages assume initial ¹⁸⁷Os/¹⁸⁸Os of 0.2 ± 0.1
 Ages calculated using ¹⁸⁷Os = ¹⁸⁷Re (e^{λt} - 1) include all analytical uncertainties and ¹⁸⁷Re decay constant uncertainty
 Replicate analyses of molybdenite were made from new or added mineral separate
 XCR-6 had very limited molybdenite and low Re concentration results from silica dilution, and is not the true concentration of Re in molybdenite
 Blanks are Re = 1.3 ± 0.2 pg, Os = 2.0 ± 0.6 pg, and ¹⁸⁷Os/¹⁸⁸Os composition = 0.3 ± 0.9 for MDID-49, 51, 63, 64.
 Blanks are Re = 8.5 ± 0.6 pg, Os = 1.9 ± 0.1 pg, and ¹⁸⁷Os/¹⁸⁸Os composition = 0.3 ± 0.05 for MDID-263, 264, 266, 276, 290, 291.

Samples and monitors were step-heated in a Mo resistance furnace and analyzed with a Mass Analyzer Products 215-50 mass spectrometer on line with an automated all-metal extraction system at the New Mexico Geochronological Research Laboratory (NMGRL). Heating times were ten minutes for hornblende and nine minutes for biotite. Reactive gases were removed during heating with a SAES GP-50 getter operated at ~450°C. Additional cleanup (biotite 6 minutes, hornblende 7 minutes) following heating was accomplished with 2 SAES GP-50 getters, one operated at ~150°C and one at 20°C. Gas also exposed to a W filament operated at ~2000°C.

⁴⁰Ar / ³⁹Ar – (RIL)

Three samples (GM-3, biotite; HT02-1, clay; DSC BXA, clay) were irradiated for 31 hours at McMaster University, Ontario, and analyzed at the Radiogenic Isotopes Laboratory (RIL), Department of Geological Sciences, The Ohio State University.

The clay samples were irradiated in Al foil capsules in vacuum (runs #72B10 and #72B11) or in evacuated SiO₂ glass ampoules (run #72B4). For sample run #72C4, aliquots 1 and 2 were for step-heating analyses using sample removed from the ampoule after measuring the recoiled Ar. The amount of sample DSC BXA was severely limited so that only a single aliquot was feasible for the step-heating analysis using sample removed from the #72C7 ampoule after measuring the recoiled Ar. Both the biotite and clay samples were packed into a quartz ampoule (1mm ID, 3mm OD, ~25mm long), and a small piece of Al foil was put on top of the sample to keep it in place. The ampoule was attached to an ultra-high vacuum line and baked at 150°C and pumped to achieve a vacuum with a pressure of ~3 x 10⁻⁸ mbar. The ampoule was

sealed while under vacuum taking special care not to displace the sample. After irradiation the ampoule was loaded into a small chamber with a quartz glass window on an ultra-high vacuum line. The chamber was heated to 150°C during pumping to achieve a pressure of $\sim 3 \times 10^{-9}$ mbar. The ampoule was pierced using a focused UV laser beam to release the gas contained in it. The Ar was purified and analyzed on a MAP 215-50 mass spectrometer. The percentage of ^{39}Ar and ^{37}Ar lost by the sample in the ampoule was calculated by comparing amounts of each isotope in the ampoule gas to the concentrations measured for the same sample in normal step- heating analyses. All fractions were corrected uniformly using the recoil % for ^{39}Ar and for ^{37}Ar measured independently for each sample. The monitors used were the 27.84 Ma Fish Canyon Tuff sanidine FC-1 and an intralaboratory muscovite with a $^{40}\text{Ar}/^{39}\text{Ar}$ age of 165.3 Ma that is assigned an uncertainty of $\pm 1\%$.

Electron Microprobe

Mineral composition data were collected from polished thin sections with a JEOL 8600 Electron Microprobe (Department of Geology, University of Georgia) utilizing Geller dQant automation with Heinrich matrix correction and dPict imaging software. Operating conditions included a 1- μm beam diameter, 15 nA current, and 15 keV accelerating voltage. Standards included pyrite (Fe, S), galena (Pb), cinnabar (Hg), InAs (As), diopside (Si), halite (Cl), and pure metal each for Cd, Zn, Ge, Au, Ag, Cu, Se, Sb, Mn, Sn, and Te.

Carbon, Oxygen, and Sulfur Stable Isotopes

Carbonate minerals were reacted overnight with H₃PO₄ at 50°C using a modification of the McCrea (1950) technique. Sulfide and sulfate minerals were ground together with V₂O₅, silica, and Cu-metal and combusted at 1050°C. The resultant CO₂ or SO₂ gas was cryogenically isolated on a vacuum extraction line and analyzed via dual inlet mass spectrometry on a Finnigan MAT 252 in the Stable Isotope Laboratory, Department of Geology, University of Georgia. Laboratory standards NBS-18 carbonatite, NBS-19 limestone (for C, O isotopes) and IAEA-S1 silver sulfide, NBS-123 sphalerite, NBS-127 barium sulfate (for S isotopes) were prepared and analyzed daily with CO₂ or SO₂ samples, respectively. Internal precision was determined to be ± 0.1 per mil (1σ). Compositions are reported in per mil notation relative to PDB (Pee Dee belemnite) for carbon, VSMOW (Vienna Standard Mean Ocean Water) for oxygen, and CDT (Canyon Diablo troilite) for sulfur (Hoefs, 1997).

Results

Re-Os Ages of Molybdenite

The Re-Os chronometer in molybdenite (MoS₂) provides the tool to date mineralization directly. Molybdenite is a common accessory or major mineral in a wide variety of geologic environments and ore-deposit types. The substitution of Re for Mo in molybdenite is common but can be complete, as the discovery of rheniite (ReS₂) supports the existence of a Re-Mo solid

solution series (Korzhinsky et al., 1994). Essentially no Os is incorporated into molybdenite, so all measured Os is generally assumed to be ^{187}Os produced by the decay of parent ^{187}Re . Unlike other isotopic chronometers (Rb-Sr, K-Ar, $^{40}\text{Ar}/^{39}\text{Ar}$) that are more susceptible to subsequent thermal disturbances, the Re-Os chronometer in molybdenite appears to be remarkably robust under most geologic conditions (Stein et al., 1998; 2001, 2003) and remains isotopically closed following molybdenite crystallization.

Six molybdenite samples were collected from molybdenite occurrences (Hilltop, Park Saddle, Tenabo) within the northern Shoshone Range (Figure 2-2 and Table 2-1). The molybdenite occurs within quartz veins or is disseminated within the host rock. Molybdenite in quartz veins is commonly intergrown or associated with small ($\leq 10\mu\text{m}$) laths of an unidentified selenium-sulfide mineral similar to poubaite and other selenium- sulfides (Fleischer, 1978) (Table 2-2). However, Hilltop's selenium-sulfide mineral contains Sb and at least eight wt. % more Te than similar species, and may represent a previously undescribed mineral.

The five molybdenite samples associated with Cu + Mo \pm Au porphyry-style mineralization within the Hilltop district yield ages from 40.1 ± 0.2 to 40.6 ± 1.2 Ma with a weighted mean of 40.23 ± 1.7 Ma (MSWD = 2.4, 95% CL). A single molybdenite sample from Cu + Mo \pm Au porphyry-style mineralization at the Tenabo deposit (Bullion district) yielded a 39.0 ± 1.4 Ma age. The larger errors in Re concentration and age for runs MDID-49 and MDID-51 are due to imperfect spiking. There was enough molybdenite remaining in the Hilltop sample to run a second time (MDID-64).

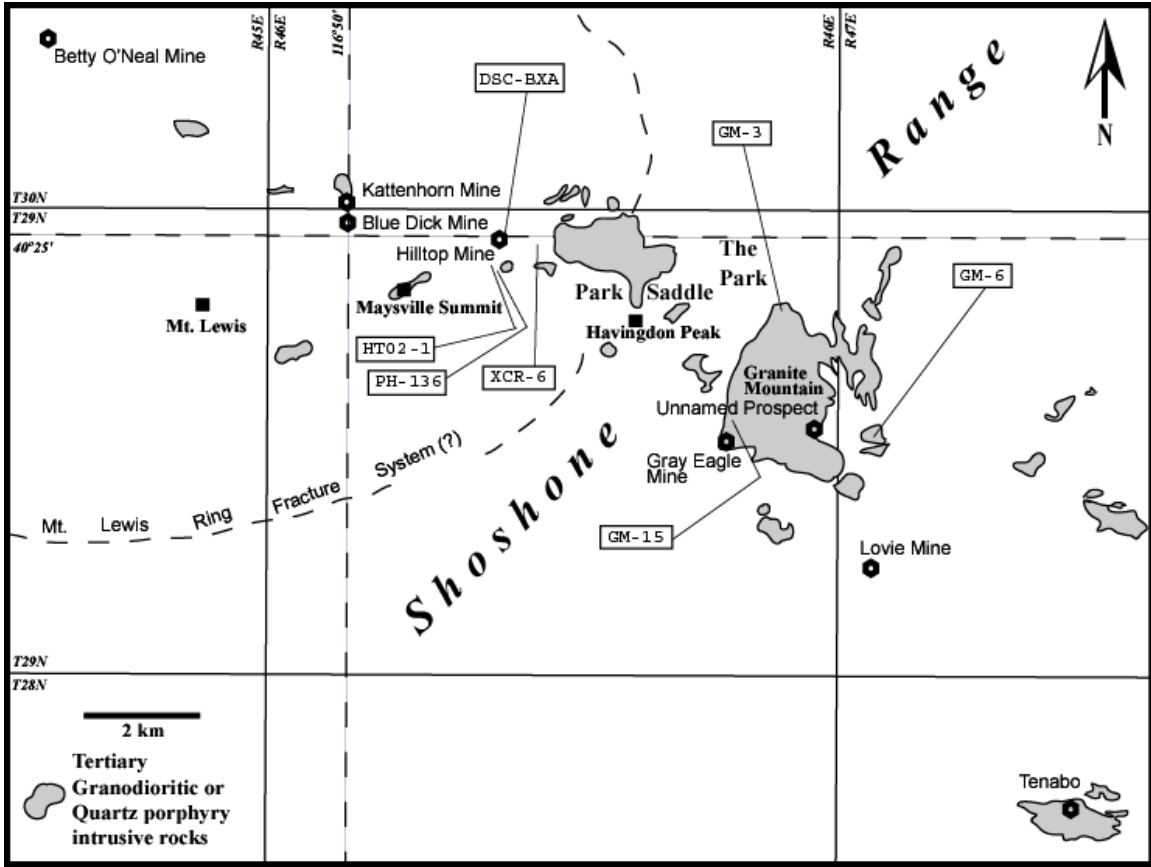


Figure 2.2: Generalized geologic map of the northern Shoshone Range. Select sample locations and mines, prospects, and deposits considered in this study. Only Tertiary granodioritic and quartz porphyry intrusive rocks shown; all else is undivided upper plate rocks of the Roberts Mountains allochthon (after Gilluly and Gates, 1965).

Table 2.2: Selenium-sulfide mineral associated with Hilltop molybdenite (n=44).

	S	Sb	Pb	Se	Bi	Te	O	U	total
Avg. wt. %	4.6	0.2	5.4	2.4	56.5	28.2	1.9	1.1	100.3

⁴⁰Ar/³⁹Ar Data

Eight individual mineral separates from six different samples collected throughout the northern Shoshone Range (Figure 2-2) were analyzed via ⁴⁰Ar/³⁹Ar. These samples include unaltered Tertiary intrusive rocks (both proximal and distal to base- and precious-metal mineralization) and gangue minerals directly associated with mineralization. Samples were collected from outcrop, surface and underground workings, and drill core/chips. The results and analytical precision of each argon analysis are in Table 2-3 and Figures 2-3a and 2-3b.

⁴⁰Ar/³⁹Ar ages for biotite and hornblende from unaltered igneous units (Table 2-3) within and/or proximal to mineralized areas are nearly coincident with molybdenite ages, supporting a relationship between pluton emplacement and porphyry mineralization. The ⁴⁰Ar/³⁹Ar age for Tenabo granodiorite biotite is 38.85 ± 0.07 Ma, similar to the 38.88 ± 0.13 Ma (hornblende average, n = 2) and 38.64 ± 0.19 Ma (biotite average, n = 3) ages for the Granite Mountain stock located midway between the Hilltop and Bullion districts and approximately five miles northwest of Tenabo.

Each age plateau for GM-6 and GM-15 biotite and hornblende, and T99413-570 and GM-3 biotite analyses includes five or more contiguous gas fractions that together represent at least 60% of the total ³⁹Ar released from each sample. Concordance of the biotite and

Table 2.3: $^{40}\text{Ar}/^{39}\text{Ar}$ data from the northern Shoshone Range, Nevada.

Location	Sample	Description	Mineral separate	Mineral Chemistry	Age (Ma)
Granite Mountain	GM-3	Granodiorite (outcrop)	Biotite	$\text{K}_2\text{O} = 7.90\%$	$38.1 \pm 0.40^{\text{R}}$
Hilltop	HT02-1	Clay-filled vug inside matrix of unmineralized breccia pipe mantling quartz monzonite (Hobo Gulch) intrusion (outcrop)	clay*	$\text{K}_2\text{O} = 0.57\%$ avg.	$31.45 \pm 0.45^{\text{R} **}$
Hilltop	DSC BXA	Clay (+ visible gold) partially filling vug inside quartz vein from discordant quartz breccia pipe (outcrop)	clay*	$\text{K}_2\text{O} = 3.30\%$	$42.1 \pm 0.40^{\text{R}}$ (IP) $35.7 \pm 0.40^{\text{R}}$ (ISO)
Granite Mountain	GM-6	Granodiorite (outcrop)	Biotite Hornblende	$\text{K}_2\text{O} = 7.97\%$ $\text{K}_2\text{O} = 1.29\%$	$38.77 \pm 0.10^{\text{N}}$ $38.98 \pm 0.17^{\text{N}}$
Granite Mountain	GM-15	Granodiorite (outcrop)	Biotite Hornblende	$\text{K}_2\text{O} = 8.31\%$ $\text{K}_2\text{O} = 1.09\%$	$39.04 \pm 0.07^{\text{N}}$ $38.78 \pm 0.09^{\text{N}}$
Tenabo	99413-570	Granodiorite (drill chips from DDH99413-570)	Biotite	$\text{K}_2\text{O} = 8.04\%$	$38.85 \pm 0.07^{\text{N}}$

* = See text for detailed sample description

** = Average of two age plateaus

R = Analysis performed at the Radiogenic Isotopes Laboratory (RIL), Department of Geological Sciences, The Ohio State University.

N = Analysis performed at the New Mexico Geochronological Research Laboratory (NMGRL).

IP = Corrected integrated plateau age

ISO = Corrected isochron age

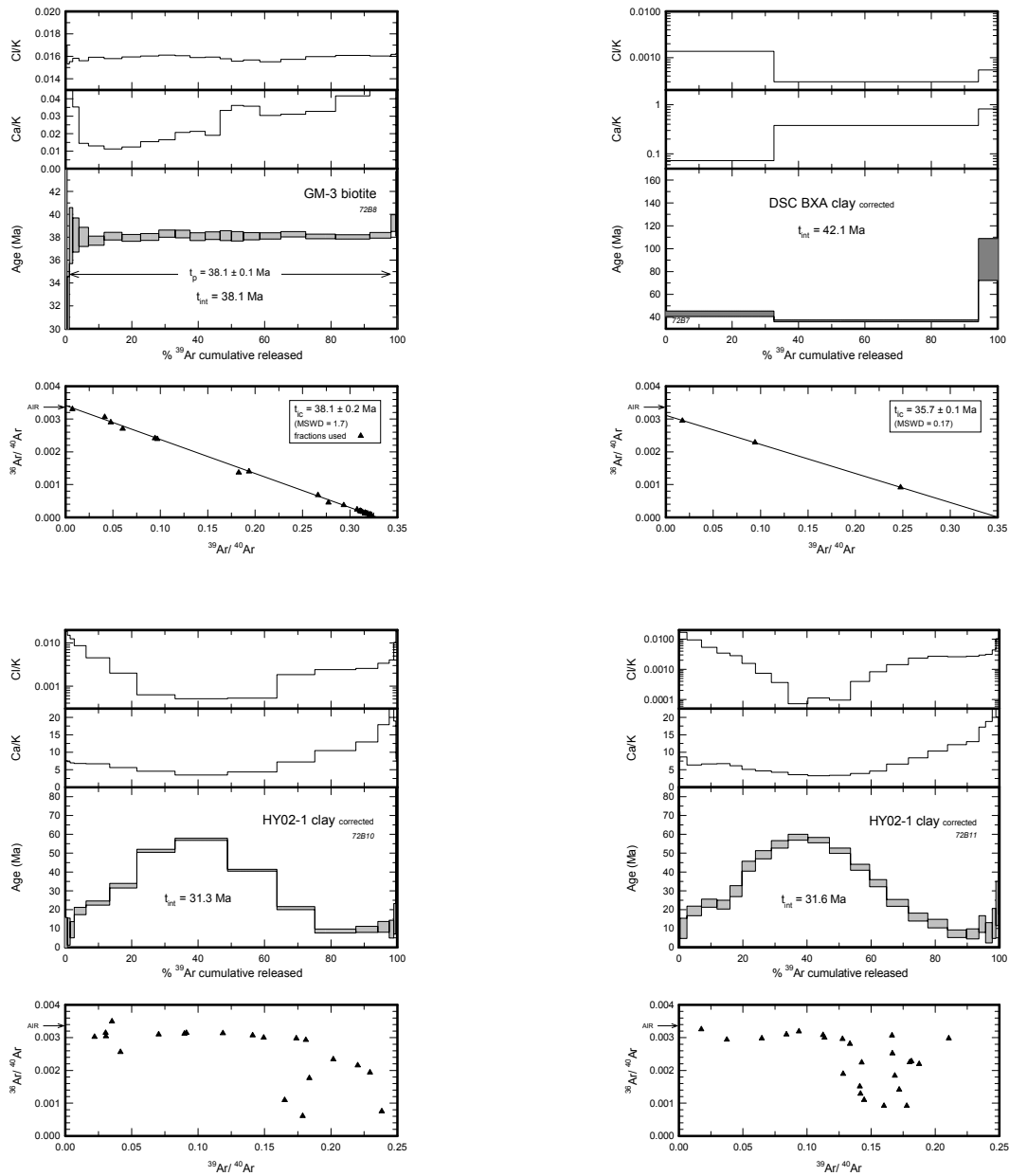


Figure 2.3a: $^{40}\text{Ar}/^{39}\text{Ar}$ age spectra and correlation diagrams for GM-3 biotite, DSC BXA clay, and HT02-1 clay (analyzed by RIL). The arrow indicates steps included in the weighted average plateau ages. All steps included in weighted average plateau age if no arrow is shown. Clay plateaus corrected for argon recoil.

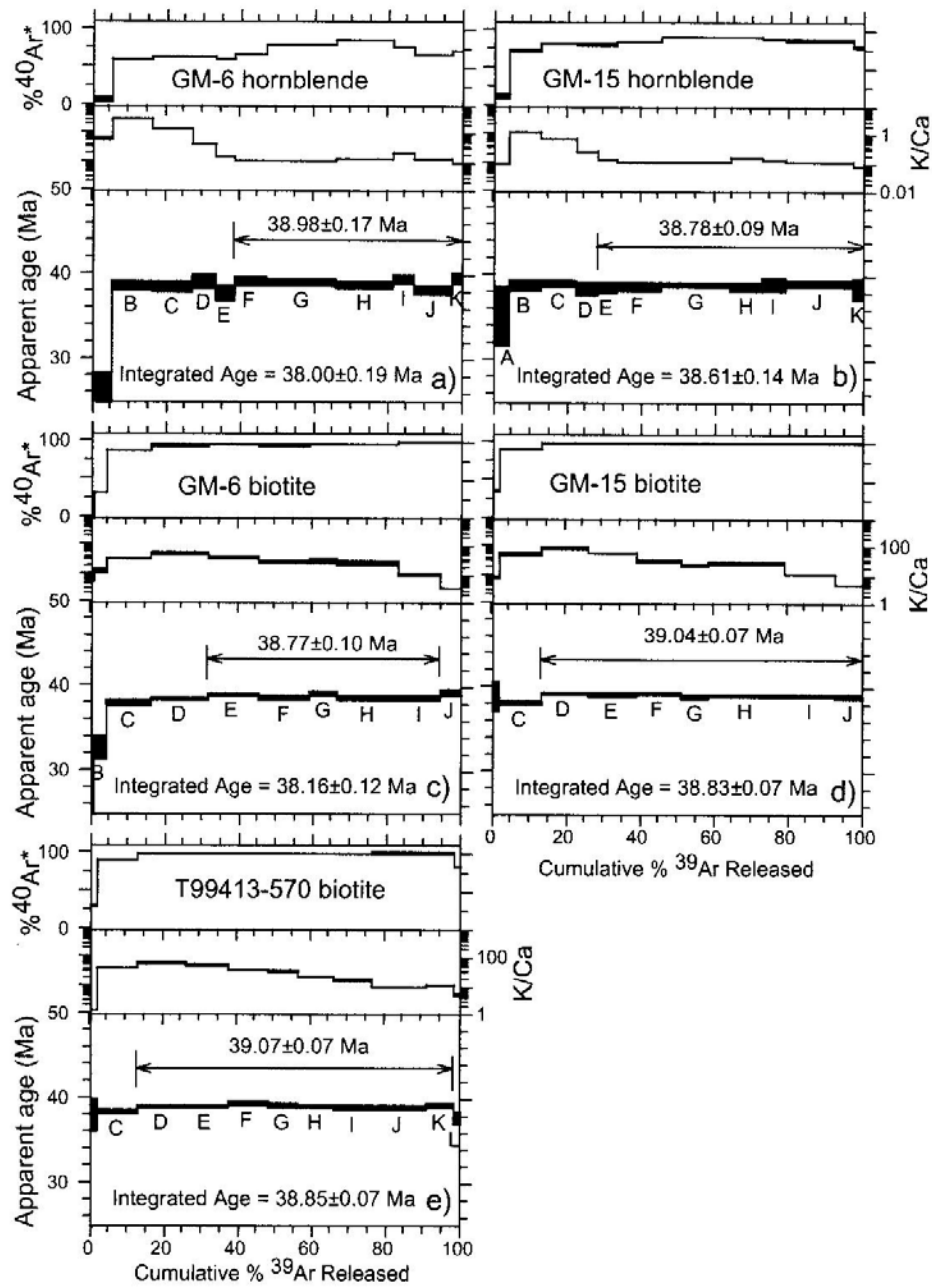


Figure 2.3b: $^{40}\text{Ar}/^{39}\text{Ar}$ age spectra and correlation diagrams for GM-6 biotite and hornblende, GM-15 biotite and hornblende, and T99413-570 biotite (analyzed by NMGR). The arrow indicates steps included in the weighted average plateau ages.

hornblende mineral pairs from Granite Mountain (GM-6, -15) help constrain the cooling rate of the Granite Mountain pluton, as each minerals' closure to argon loss is different (~500°C and ~300°C for hornblende and biotite, respectively; McDougall and Harrison, 1999). Assuming cooling via simple conduction, the Granite Mountain pluton cooled 200°C during a ~100,000 to 480,000-year span.

Two K-bearing clay samples were collected for Ar-Ar analysis. Sample HT02-1 is from the matrix of an unmineralized breccia pipe that mantles the quartz monzonite-granodiorite Hobo Gulch intrusive immediately southeast of Hilltop. Sample DSC BXA is from the discordant quartz breccia pipe located on the east flank of Hilltop.

Neither clay sample (HT02-1 or DSC BXA) yields a clear age plateau (Figure 2-3a). The age for HT02-1 (31.45 ± 0.45 Ma) is the average of two integrated plateau ages from two separate runs, as each run yielded a different plateau age (31.3 ± 0.4 Ma and 31.6 ± 0.5 Ma, respectively). The very limited amount of sample DSC BXA allowed only one analysis, yielding different ages between the corrected integrated plateau age (42.1 ± 0.9 Ma) and the corrected isochron age (35.7 ± 0.4 Ma). The true age of DSC BXA clay lies between these two values.

Electron Microprobe Data

Major- and trace-element compositions of base- and precious-metal-bearing minerals were determined via electron microprobe from seven deposits/mineralized areas (Betty O'Neal, Hilltop, Kattenhorn, Blue Dick, Grey Eagle and Lovie mines and an unnamed prospect) within the northern Shoshone Range. The 18-element routine (Fe, S, Pb, Hg, As, Si, Cl, Cd, Zn, Ge, Au, Ag, Cu, Se, Sb, Mn, Sn, and Te) was also utilized to verify ore mineral identification.

Low (96-99%) totals are probably the result of sulfur volatilization from sample during exposure to the electron beam and/or rough or uneven sample topography. Widening the beam diameter to 5µm and analyzing sulfur first minimized sulfur volatilization. Most analyses were collected from polished thin sections, polished slabs and fluid inclusion thick-sections. Mineral compositions were verified via EDS prior to each analysis to account for all constituent elements. A summary of ore mineral compositions from each deposit is reported in Table 2-4.

Stable Isotope Data – Carbonate, Sulfide, and Sulfate Minerals

Carbon and oxygen stable isotope data were collected from 18 carbonate minerals from the Hilltop, Betty O’Neal, and Lovie mines, and an unnamed prospect. The carbonate minerals occur with base- or precious-metal minerals or alone in veins or breccia matrix.

Ten carbonate samples were collected from the Hilltop deposit. Isotope values range from -11.7 to -2.5 per mil ($\delta^{13}\text{C}_{\text{PDB}}$) and from +2.4 to +14.4 ($\delta^{18}\text{O}_{\text{VSMOW}}$). Six samples from the Betty O’Neal mine yield -4.5 to -2.9 per mil ($\delta^{13}\text{C}_{\text{PDB}}$) and -1.3 to +8.7 per mil ($\delta^{18}\text{O}_{\text{VSMOW}}$). See Table 2-5 for complete data summary.

Ninety-two sulfide and sulfate minerals were collected from Granite Mountain and the Betty O’Neal, Lovie, Kattenhorn, Gray Eagle, and Hilltop mines and are summarized in Table 2-6.

Table 2.4: Microprobe analyses of ore minerals from the Blue Dick, Betty O’Neal, Gray Eagle mines and the unnamed prospect, northern Shoshone Range, Lander County, Nevada.

Blue Dick mine (Hilltop district)						Betty O’Neal mine (Lewis district)								
	py	fah	ac	mia	asp		py	fah	ac	sph	gal	cpy	chl	bn
Fe	46.03	1.77	0.26	0.01	31.72	Fe	44.83	2.36	0.06	2.21	0.20	27.81	0.04	0.08
S	51.87	23.21	13.60	18.59	18.87	S	52.15	22.73	15.40	32.34	13.42	33.87	0.01	19.83
Sb	0.02	25.85	0.56	37.12	0.77	Sb	0.01	25.54	0.00	0.02	0.09	0.05	0.02	25.31
As	0.00	0.89	0.02	0.40	43.10	As	0.16	1.05	0.00	0.00	0.00	0.00	0.01	0.53
Zn	0.04	5.13	0.07	0.02	0.00	Zn	0.06	4.68	0.22	61.85	0.76	0.08	0.05	0.02
Pb	0.01	0.01	0.02	0.17	0.11	Pb	0.00	0.01	0.00	0.01	88.29	0.00	0.04	41.69
Si	0.09	0.04	0.24	0.07	3.84	Si	0.03	0.03	0.03	0.10	0.04	0.05	0.19	0.01
Ag	0.01	17.23	84.45	39.97	0.04	Ag	0.04	21.91	86.40	0.57	0.07	0.08	88.23	0.03
Cu	0.04	25.94	0.06	0.00	0.09	Cu	0.06	22.52	2.21	0.09	0.31	32.78	0.05	13.12
Mn	0.03	0.05	0.04	0.00	0.00	Mn	0.05	0.05	0.00	0.43	0.00	0.03	0.41	0.00
Au	0.00	0.00	0.00	0.00	0.00	Au	0.06	0.02	0.08	0.00	0.02	0.02	0.02	0.00
Sn	0.00	0.06	0.00	0.00	0.00	Sn	0.00	0.03	0.00	0.00	0.01	0.00	0.00	0.02
Se	0.01	0.05	0.10	1.36	0.00	Se	0.01	0.00	1.03	0.00	0.17	0.00	0.00	0.18
Cd	0.03	0.10	0.43	0.00	0.00	Cd	0.02	0.20	0.46	0.62	0.05	0.01	0.41	0.00
Ge	0.00	0.00	0.01	0.00	0.00	Ge	0.00	0.00	0.00	0.01	0.02	0.00	0.04	0.00
Cl	0.00	0.03	0.08	0.03	0.01	Cl	0.01	0.02	0.08	0.00	0.05	0.00	3.41	0.01
Te	0.00	0.00	0.13	0.00	0.00	Te	0.02	0.00	0.15	0.02	0.05	0.04	0.09	0.00
Hg	0.02	0.12	0.04	0.32	0.00	Hg	0.00	0.02	0.00	0.00	0.01	0.01	0.01	0.03
Total	98.17	100.43	100.10	98.06	98.56	Total	96.75	101.19	106.11	98.25	103.57	94.81	91.55	100.87
n	11	3	3	1	1	n	6	10	1	5	10	2	11	1

Grey Eagle mine (Bullion district)									Unnamed prospect (Bullion district)						
	py	fah	asp	sph	gal	cpy	hes	elec		py	fah	asp	sph	gal	geo
Fe	45.58	3.43	35.04	9.63	0.19	28.70	--	0.00	Fe	45.25	3.10	34.76	6.24	0.04	24.62
S	52.35	24.06	21.92	32.76	13.58	34.05	--	0.17	S	53.84	25.84	21.80	34.18	14.42	32.77
Sb	0.02	28.10	0.17	0.02	0.02	0.04	--	0.00	Sb	0.01	27.33	0.04	0.03	0.19	0.00
As	0.19	0.88	43.54	0.00	0.00	0.00	--	0.00	As	0.00	1.06	43.63	0.00	0.00	0.00
Zn	0.14	4.09	0.01	54.99	0.10	0.04	--	0.00	Zn	0.01	4.20	0.00	58.01	0.06	0.12
Pb	0.00	0.01	0.00	0.00	85.44	0.00	--	0.00	Pb	0.00	0.00	0.01	0.02	87.71	0.00
Si	0.07	0.04	0.01	0.04	0.03	0.08	--	0.04	Si	0.01	0.01	0.01	0.01	0.05	0.00
Ag	0.02	5.22	0.02	0.01	0.96	0.02	60.39	22.83	Ag	0.03	8.02	0.01	0.01	0.08	12.79
Cu	0.05	34.72	0.04	0.04	0.07	34.66	--	0.12	Cu	0.04	33.50	0.06	0.09	0.07	27.26
Mn	0.01	0.04	0.02	0.22	0.02	0.01	--	0.04	Mn	0.02	0.00	0.01	0.21	0.02	0.00
Au	0.04	0.03	0.05	0.03	0.00	0.02	--	77.29	Au	0.02	0.00	0.05	0.00	0.03	0.07
Sn	0.00	0.08	0.00	0.00	0.00	0.00	--	0.00	Sn	0.00	0.03	0.00	0.00	0.01	0.00
Se	0.01	0.01	0.00	0.01	0.00	0.01	--	0.02	Se	0.00	0.00	0.00	0.01	0.00	0.00
Cd	0.00	0.06	0.00	1.34	0.06	0.02	--	0.10	Cd	0.00	0.00	0.00	1.05	0.08	0.05
Ge	0.00	0.00	0.00	0.00	0.05	0.00	--	0.00	Ge	0.00	0.00	0.00	0.00	0.00	0.00
Cl	0.01	0.01	0.00	0.01	0.05	0.01	--	0.03	Cl	0.00	0.01	0.01	0.01	0.05	0.04
Te	0.03	0.00	0.02	0.02	0.12	0.00	37.99	0.03	Te	--	--	--	--	--	--
Hg	0.04	0.00	0.02	0.05	0.03	0.00	--	0.00	Hg	--	--	--	--	--	--
Total	98.54	100.78	100.88	99.16	100.74	97.66	98.38	100.67	Total	99.23	103.10	100.38	99.85	102.80	97.72
n	5	5	4	4	5	3	2	1	n	3	2	3	5	3	1

Table 2.4 (continued): Microprobe analyses of ore minerals from the Hilltop, Lovie, and Kattenhorn mines, northern Shoshone Range, Lander County, Nevada.

Hilltop mine and immediate area (Hilltop district)											
	py	fah	mia	asp	sph	gal	cpy	stib	bn	cst	elec
Fe	44.84	3.88	0.00	34.10	7.94	0.21	29.22	0.04	0.04	3.09	--
S	51.03	27.16	20.77	20.49	32.93	11.88	33.49	27.51	19.43	26.08	--
Sb	0.04	17.58	40.38	0.46	0.02	0.21	0.03	70.83	24.29	25.85	--
As	0.34	1.36	0.35	43.51	0.00	0.00	0.00	0.56	1.16	2.79	--
Zn	0.08	13.30	0.06	0.05	55.56	0.31	0.21	0.02	0.26	5.26	--
Pb	0.84	0.00	0.00	0.06	0.00	83.44	0.00	0.00	43.41	0.01	--
Si	0.25	0.03	0.04	0.03	0.07	0.04	0.02	0.04	0.02	0.00	--
Ag	0.01	1.14	39.26	0.01	0.03	0.42	0.02	0.05	0.03	1.58	13.40
Cu	0.10	30.20	0.11	0.10	0.76	0.23	33.23	0.06	13.39	35.59	--
Mn	0.02	0.07	0.03	0.04	0.78	0.03	0.01	0.02	0.02	0.04	--
Au	0.02	0.03	0.00	0.03	0.03	0.01	0.01	0.02	0.00	0.00	85.07
Sn	0.00	4.91	0.00	0.00	0.06	0.00	0.05	0.26	0.04	0.15	--
Se	0.01	0.02	0.72	0.00	0.02	2.15	0.01	0.24	0.09	0.00	--
Cd	0.01	0.12	0.01	0.02	1.21	0.04	0.01	0.00	0.00	0.00	--
Ge	0.00	0.00	0.00	0.00	0.01	0.01	0.02	0.00	0.05	0.00	--
Cl	0.00	0.00	0.03	0.01	0.01	0.07	0.00	0.01	0.03	0.01	--
Te	0.01	0.00	0.00	0.02	0.02	0.08	0.01	0.00	0.00	0.00	--
Hg	0.01	0.11	--	0.00	0.01	0.01	0.04	0.01	0.00	--	--
Total	97.61	99.85	101.51	98.89	99.44	99.13	96.37	99.61	102.25	100.45	98.46
n	22	9	3	13	11	14	7	5	3	1	10

Lovie mine (Bullion district)						Kattenhorn mine (Hilltop district)				
	py	fah	asp	sph	gal		py	fah	gal	chl
Fe	45.61	4.48	36.23	7.80	0.23	Fe	44.12	1.21	0.00	0.14
S	52.59	23.36	21.11	33.27	13.46	S	49.48	15.33	12.62	0.08
Sb	0.01	21.45	0.03	0.01	0.24	Sb	0.06	7.69	0.16	0.00
As	0.09	0.48	44.95	0.00	0.00	As	0.00	0.16	0.00	0.00
Zn	0.06	11.60	0.11	56.69	0.09	Zn	0.07	19.28	0.06	0.00
Pb	0.00	0.00	0.14	0.00	85.96	Pb	0.00	0.17	84.27	0.00
Si	0.05	0.03	0.00	0.01	0.01	Si	0.55	1.17	0.96	6.62
Ag	0.01	19.33	0.02	0.02	0.22	Ag	0.04	16.82	0.16	65.75
Cu	0.02	17.78	0.03	0.14	0.15	Cu	0.06	30.01	0.03	0.00
Mn	0.02	0.10	0.02	1.59	0.02	Mn	0.02	0.36	0.01	0.00
Au	0.02	0.02	0.00	0.05	0.03	Au	0.01	0.06	0.02	0.18
Sn	0.00	0.93	0.00	0.00	0.01	Sn	0.00	4.58	0.01	0.00
Se	0.00	0.01	0.00	0.00	0.01	Se	0.01	0.84	1.41	0.06
Cd	0.04	0.11	0.02	1.01	0.03	Cd	0.00	0.14	0.04	0.32
Ge	0.00	0.01	0.00	0.00	0.01	Ge	0.00	0.01	0.00	0.00
Cl	0.00	0.03	0.00	0.01	0.06	Cl	0.01	0.05	0.08	4.50
Te	0.04	0.00	0.02	0.07	0.05	Te	0.03	0.25	0.01	0.18
Hg	0.01	0.00	0.10	--	0.01	Hg	0.01	0.13	0.00	0.02
Total	98.56	99.69	102.73	99.84	100.55	Total	94.47	98.26	99.86	77.84
n	5	6	2	4	8	n	2	5	2	1

Notes: Py, pyrite; fah, fahlore; mia, miargyrite; asp, arsenopyrite; sph, sphalerite; gal, galena; cpy, chalcopyrite; chl, chlorargyrite-bromargyrite; stib, stibnite; bn, bournonite; cst, chalcostibnite; ac, acanthite; ele, electrum; geo, geffroyite.

n = number of analyses

All data in average wt. %

-- = not analyzed

Minerals not listed in tables = not present in samples analyzed.

Table 2.5: Carbon and oxygen stable isotope data from carbonate minerals associated with base- and precious metal mineralization, northern Shoshone Range, Lander County, Nevada.

Deposit	Sample	Description	Host Rock	$\delta^{13}\text{C}_{\text{PDB}}$	$\delta^{18}\text{O}_{\text{VSMOW}}$
HT	97-8-106.8-1	1/2"-wide qtz vein with carb + py +cpy in center	Phyl. altered Tgd	-6.1	2.9
HT	97-8-136-1	F.g. carb in center of 3/4"-wide euhedral qtz vein.	Prop. altered Tgd	-8.8	3.3
HT	97-8-136-2	1/4"-wide envelope of euhedral carb bordering 97-8-136-1 vein.	Prop. altered Tgd	-11.7	6.0
HT	97-10-305.8	1/8"-wide envelope of carb+bar+kaol bordering qtz vein.	Prop. altered Tfp	-2.5	3.3
HT	97-11-168	1/2"-wide cal veinlet	Valmy siliciclastics	-8.7	9.3
HT	97-11-700-2	1/8"-wide envelope of carb+bar bordering 97-11-700-3 vein.	Valmy siliciclastics	-6.0	12.8
HT	97-11-700-3	1/2" -wide carb+qtz+bar+rock frag vein.	Valmy siliciclastics	-5.2	7.9
HT	97-13-221-1	Euhedral cal xtals in f.g. groundmass (97-13-221-3)	Phyl-prop alt Tgd	-5.4	2.4
HT	97-13-221-3	F.g. carb+ser groundmass	Phyl-prop alt Tgd	-4.9	2.7
HT	97-13-92.5	$\leq 1/2"$ -wide carb vein.	Phyl. altered Tfp	-5.9	14.4
BON	1-8S-B-2	$\leq 3/4"$ -wide carb vein between massive qtz and wall rock	n/a	-3.4	8.7
BON	05A-1	Carb+qtz matrix between rock clasts	Breccia	-4.5	7.3
BON	06A-1	Carb matrix between rock clasts w/ gal+fah+sph	Breccia	-3.4	0.1
BON	29A-1	1/2"-wide cal vein (with rock clasts)	Massive qtz vein	-3.7	-0.6
BON	32-1	Massive carb	Massive carb vein	-2.9	-1.3
BON	55-1	Massive carb	Massive carb vein	-3.4	2.9
Lovie	42-2	Massive cal cut by chl+ep veins	Massive cal vein	-0.2	17.0
UN	CK02-11-1	Qtz+cal vein with ser+py+gal+sph+fah+asp	Phyl-arg. altered Tgd	-2.3	2.6

Notes:

HT = Hilltop mine; BON = Betty O'Neal mine; Lovie = Lovie mine; UN = unnamed prospect.

Alteration: Phyl = phyllic; Prop = propylitic; Arg = argillic.

Tgd = Tertiary granodiorite; Tfp = Tertiary feldspar porphyry.

Carb = carbonate; py = pyrite; cpy = chalcopyrite; qtz = quartz; kaol = kaolinite; bar = barite; gal = galena; fah = fahlore; sph = sphalerite; asp = arsenopyrite; ser = sericite; chl = chlorite; cal = calcite; ep = epidote.

All data corrected using the fractionation factor of calcite at 50°C = 1.00922525

Unless specified, "carb" refers to CaCO₃ with small impurities of Fe, Mg, or Mn.

For all carbon and oxygen isotope values $\sigma = 0.1$ per mil

Table 2.6: Sulfur stable isotope data from sulfide and sulfate minerals associated with base- and precious metal mineralization, northern Shoshone Range, Lander County, Nevada.

Deposit	Sample	Mineral	$\delta^{34}\text{S}_{\text{CDT}}$	Deposit	Sample	Mineral	$\delta^{34}\text{S}_{\text{CDT}}$
BON	49-1	bar	19.3	HT	97-8-380.6-B7	mel py	-0.4
BON	04B-1	py	4.9	HT	97-8-380.6-B6	mel py	-12.1
BON	52	bar	18.2	HT	97-8-380.6-B4	mel py	-7.2
Lovie	03B-2	sph	6.2	HT	97-8-380.6-B5	mel py	-7.6
Lovie	05-1	sph	5	HT	97-8-466	bar	15.2
Lovie	35A-1	gal	5.6	HT	97-8-380.6-B8	mel py	5.6
Lovie	09-1	bar	20.9	HT	97-8-416	stib	5.5
Lovie	27-1	py	7.1	HT	97-8-106.8-2	py	5.5
Lovie	03A-1	py	5.1	HT	97-8-380.6-C	mel py	2
KATT	27A-1	bar	13.6	HT	97-8-380.6-B3	mel py	-5.4
KATT	31-1	bar	11	HT	97-8-380.6-B1	mel py	4.6
KATT	12-1	bar	16.3	HT	97-8-380.6-B2	mel py	1.1
KATT	09-1	bar	21.5	HT	97-9-358-1	py/asp	5.8
GE	05-1	sph	6.7	HT	97-10-1084.5-2	py	5.1
GE	04-2	py	6.6	HT	97-10-1084.5-1	sph	4.9
GE	X1-1	py	6.3	HT	97-10-106.1-1	moly	4.3
GE	10-1	py	6.2	HT	97-10-1181.5-2	py	6
GE	05-2	py	5.8	HT	97-10-1161.7	py	6.4
GE	09-2	py	6.8	HT	97-10-1160.6-2	py	5.4
GE	07-2	py	6.5	HT	97-10-1160.6-1	gal	3.2
GE	04-4	sph	7.1	HT	97-11-665.3-1	bar	10.4
GE	04-1	gal	5.8	HT	97-11-700-1	bar	5.9
GM	18	bar	17.7	HT	97-11-665.3-4	py	5.8
HT	HT02-12-SITE	stib	3.8	HT	97-11-1232.5-1	py	22
HT	HT02-14-1	py	4.3	HT	97-11-1235.4-1	bar	16.3
HT	HT02-8-1	stib	3.9	HT	97-11-1106-1	bar	10.9
HT	CK02-4/5-1	py	-2.1	HT	97-11-665.3-3	sph	5.2
HT	CK02-4/5-2	py	4.5	HT	97-11-1027.5-1	py	4.4
HT	CK02-4/5-3	py/asp	3.5	HT	97-11-991	py	6.2
HT	CK02-22	bar	18	HT	97-11-1235.4-2	py	14.4
HT	CK02-31	gal	3.1	HT	97-13-221-2	py	5.8
HT	CK02-28	py	4.1	HT	97-13-373-1	py	4.8
HT	CK02-29-1	py	4.4	HT	97-14-212	stib	2.9
HT	CK02-21	bar	17.7	HT	97-15-488.5-3	py	5.3
UN	CK02-11-3	py	7	HT	97-15-488.5-1	py	-2.7
UN	CK02-11-2	sph	6.2	HT	97-15-488.5-2	py	6.9
UN	CK02-11	py	6.9	HT	97-15-488.5-5	py	7.1
HT	Sb-P-1	bar	14.8	HT	97-16-484-1	py	-15.6
HT	Sb-P-2-2	bar	21.3	HT	97-16-484-2	py	5.3
HT	Sb-P-2-1	stib	3.3	HT	97-16-503.3-3	py	-1.9
HT	97-1-497B-1	bar	12.7	HT	97-16-503.3-1	py	-15.9
HT	97-5-473.5-1	bar	14.3	HT	97-16-339	py	4.1
HT	97-6-434	stib	3.3	HT	97-16-430.9-2	py	-1.0
HT	97-6-80-1	moly	5.6	HT	97-16-503.3-2	py	-10.6
HT	97-7-365-PY3	py	2	HT	97-16-430.9-1	py	-2.1
HT	97-7-365-PY4	py	2.3	HT	97-16-430.9-3	py	4.2
HT	97-7-365-PY2	py	-2.6	HT	BURNS-05	bar	16
HT	97-8-436-1	py	-2.7	HT	IND. N. ADIT-1	py	4.9

BON = Betty O'Neal mine; Lovie = Lovie mine; KATT = Kattenhorn mine; GE = Grey Eagle mine; GM = Granite Mountain; HT = Hilltop deposit / area; UN = Unnamed prospect.

bar = barite; py = pyrite; sph = sphalerite; gal = galena; stib = stibnite; asp = arsenopyrite; moly = molybdenite; mel py = melnikovite pyrite (b=band)

For all sulfur isotope data $\sigma = 0.1$.

Discussion

Age of Igneous rocks and Mineralization

Igneous rocks within the Battle Mountain-Eureka trend comprise three distinct age groups: 100-85 Ma (Middle to Late Cretaceous), 43-37 Ma (Eocene to early Oligocene), and ~15 Ma (middle Miocene) (Christiansen and Yeats, 1992; Maher and Browne, 1993). Data from this study (Table 2-3) and others (McKee and Silberman, 1970; Lisle and Desrochers, 1988) support an Eocene age for intrusive igneous rocks within the northern Shoshone range. These Eocene igneous rocks are part of the Tuscarora magmatic belt; a belt of 43 to 37 Ma calc-alkalic plutonic and volcanic rocks extending east-southeast across northern Nevada and west-central Utah. Several mineral deposits are associated with the Tuscarora magmatic belt, most notably the Bingham porphyry-copper deposit (Christiansen and Yeats, 1992).

Igneous rocks representing all three age groups occur with at least 20 base- and precious-metal mineral deposits within the Battle Mountain-Eureka trend, although establishing a definitive link between each deposit and its nearby igneous body is often impossible (Maher and Browne, 1993). However, the age of the Cu+Mo±Au porphyry-style mineralization within the northern Shoshone range has been established via molybdenite and the Re-Os method (Table 2-1).

Rhenium-osmium data from Tenabo, Park Saddle, and Hilltop molybdenite and $^{40}\text{Ar}/^{39}\text{Ar}$ data from nearby intrusive rocks support contemporaneous emplacement of both barren and molybdenite-bearing plutons throughout the northern Shoshone range. However, the paragenetic position of molybdenite at the Hilltop deposit has been difficult to establish as the relative ages

of molybdenite-bearing veins and base- and precious-metal-bearing veins have not been directly observed. The temporal relationship between molybdenite, the granodioritic intrusions within and proximal to the Hilltop deposit, and Hilltop's Au-bearing epithermal mineralization is not completely clear; however, soil geochemistry verifies a spatial relationship between the intrusions and molybdenite (Kelson et al., 2000). The alteration (recrystallization, bleaching \pm sericitization) of Hilltop's Ordovician Valmy Formation host rocks has been attributed to the nearby granodioritic intrusions. Assuming the granodioritic intrusions are responsible for molybdenite mineralization, then the presence of altered Valmy clasts within base- and precious-metal-bearing veins (Lisle and Desrochers, 1988; Kelson et al., 2000) may infer the earliest position of molybdenite within the Hilltop deposits' paragenetic sequence of mineralization.

Radiometrically determining the age of gold is not possible unless a datable phase (e.g. molybdenite, illite) is deposited with the gold. Gold at the Hilltop deposit occurs within the Main Zone and the discordant quartz breccia pipe, possibly representing two separate gold-bearing events (Kelson et al., 2000). Main Zone gold is sub-microscopic and intimately associated with arsenopyrite, pyrite, and silica; discordant quartz breccia pipe gold is frequently macroscopic and occurs as native Au or electrum.

A small (< 1mg) sample of K-bearing clay was recovered from a vug containing visible gold within the quartz matrix of the discordant quartz breccia pipe. The discordant quartz breccia pipe contains clasts of altered (bleached + recrystallized) Ordovician Valmy Formation rock types supported in a matrix of euhedral quartz \pm gold. XRD analysis and NEWMOD modeling of the XRD pattern suggest a mixture of 70% di-octahedral mica and 30% di-octahedral smectite. The single K-bearing phase was probably either muscovite or illite – both common accessory minerals in hydrothermal deposits – as K is not a principal interlayer cation in di- (or

tri-) octahedral smectites (Deer et al., 1999; Guilbert and Park, 1999). $^{40}\text{Ar}/^{39}\text{Ar}$ analysis of DSC BXA yields corrected ages of 42.1 ± 0.9 Ma (integrated plateau age) and 35.7 ± 0.4 Ma (isochron age) respectively. The age of DSC BXA clay (and associated gold within the discordant quartz breccia pipe) is between 42.1 ± 0.9 and 35.7 ± 0.4 Ma, assuming the clay + gold assemblage is hypogene and was not deposited/remobilized under supergene conditions.

Sample HT02-1 is a kaolinite-group clay with an illitic (10 \AA d-spacing 2θ) component from the unmineralized breccia pipe that mantles Hilltop's Hobo Gulch intrusion (41.2 ± 0.5 Ma (K-Ar); Kelson et al., 2000). The pipe contains angular, variably-sized, altered, angular clasts of Ordovician Valmy Formation quartzite, siltstone, chert, and argillite, and Hobo Gulch (?) intrusion in a matrix of rock flour and clay (sample HT02-1). Two separate HT02-1 $^{40}\text{Ar}/^{39}\text{Ar}$ analyses yield corrected integrated plateau ages of 31.6 ± 0.4 Ma and 31.3 ± 0.5 Ma, respectively (average 31.45 ± 0.45 Ma).

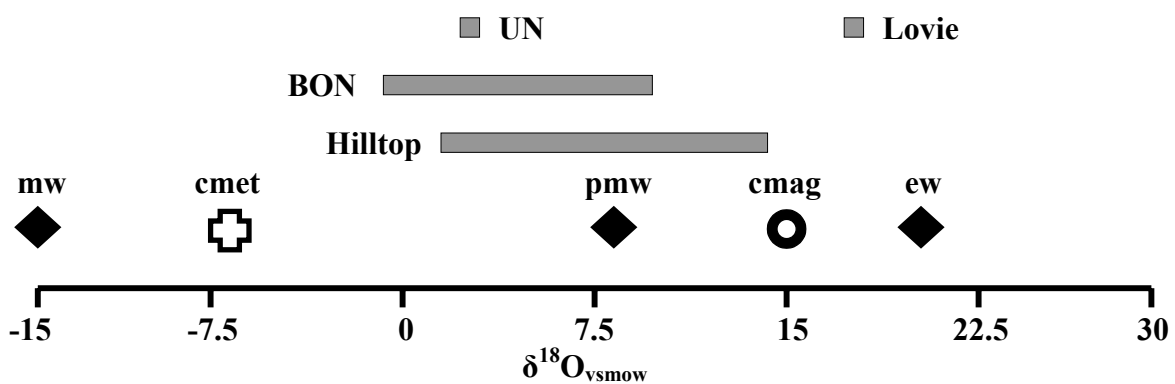
It is unlikely that the breccia pipe mantling the Hobo Gulch intrusion formed ~ 10 Ma after emplacement of the Hobo Gulch intrusion. Alternatively, the age of sample HT02-1 may reflect: 1) Initial mineral formation under supergene conditions, 2) remobilization and deposition of original breccia pipe matrix material under supergene conditions, 3) remobilization (or Ar-Ar resetting) of original mineral ~ 31.45 Ma by another hydrothermal "event" that did not reset nearby primary igneous minerals, or 4) the Ar-Ar age reported for sample HT02-1 is completely erroneous.

Fluid Sources: Stable Isotope Data

Stable isotope (carbon, oxygen, sulfur) data from carbonate, sulfide, and sulfate ore and gangue minerals were collected from several mineralized areas within the northern Shoshone Range (Tables 2-5 and 2-6) to elucidate fluid sources and calculate formation temperatures.

Hydrothermal calcite deposition was probably initiated by degassing of CO₂ and/or a change in fluid pH, not cooling, as a decrease in fluid temperature will actually raise calcite solubility. Loss of CO₂ will increase the fluid's pH resulting in calcite super-saturation and deposition. Fluid boiling is also an important process influencing calcite precipitation (Zheng, 1990).

$\delta^{18}\text{O}$ data from carbonate minerals are plotted in Figure 2-4 relative to meteoric water, primary magmatic (granodiorite) water, and water in equilibrium with limestone. $\delta^{18}\text{O}$ values from the Betty O'Neal mine and Hilltop deposit range from -1.3 to +8.7 per mil and +2.4 to +14.4 per mil, respectively. Comparatively, calcite in equilibrium with pure magmatic water at 250°C (cmag) and calcite in equilibrium with pure meteoric water at 250°C (cmet) are also plotted. The carbonate $\delta^{18}\text{O}$ data suggest varying degrees of fluid mixing between primary magmatic water and meteoric water without interaction with any carbonate (i.e. limestone) rock types. Generally, the data support a stronger meteoric signature for Betty O'Neal mine carbonate minerals than for Hilltop carbonate minerals. Likewise, unnamed prospect carbonate mineral $\delta^{18}\text{O}$ data support a strong meteoric water influence. One Lovie mine carbonate mineral ($\delta^{18}\text{O} = +17$ per mil) clearly reflects a non-meteoric water fluid source, and may be explained by either oxygen isotope fractionation between the carbonate mineral and primary magmatic water at ~



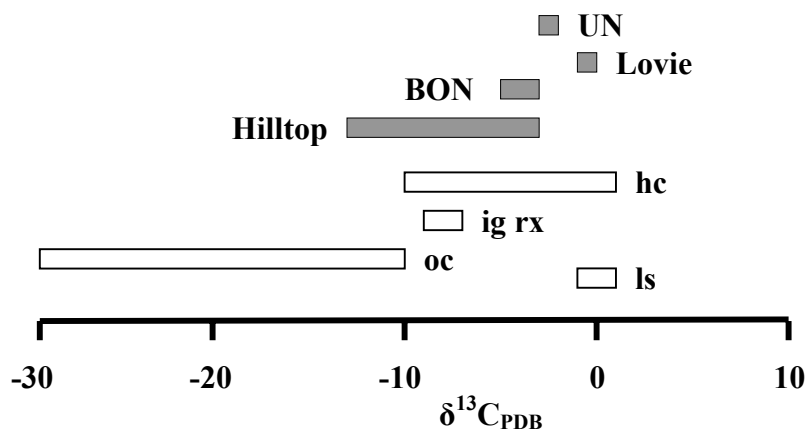
Notes: mw = Central-north central Nevada meteoric water; pmw = Primary magmatic (granodiorite) water; ew = Water in equilibrium with limestone (all reference values from Field and Ficarek, 1985); cmag = calcite in equilibrium with pmw @ 250°C; cmet = calcite in equilibrium with mw @ 250°C (Friedman and O'Neil, 1977); UN = unnamed prospect (n=1); Lovie = Lovie mine (n=1); BON = Betty O'Neal mine (n=6); Hilltop = Hilltop deposit (n=10).

Figure 2.4: Carbonate oxygen isotope data from four mineralized areas within the northern Shoshone Range, Lander County, Nevada.

200°C instead of 250°C or minimal interaction between mostly primary magmatic water and a calcareous (i.e. limestone) lithology.

Three key observations may be derived from these oxygen isotope data. First, the autochthonous “lower plate” carbonate rocks below the Roberts Mountains thrust did not isotopically influence the formation of the carbonate minerals, attesting to a shallow, near-surface source of the original hydrothermal systems and/or great depth of the underlying lower plate assemblage. Second, hydrothermal fluids did not ascend through (or interact with) lower plate carbonate rocks from some deep-seated source. Third, the $\delta^{18}\text{O}$ value of carbonate from a carbonate + sulfide-bearing vein at the unnamed prospect (UN) reflects mixing of meteoric and magmatic fluids. Since the vein is hosted by Granite Mountain granodiorite, the lack of a dominant magmatic signature suggests the Granite Mountain stock was almost or completely devoid of any magmatic water at the time the carbonate + sulfide-bearing vein formed, or the magmatic water emanated from another source.

$\delta^{13}\text{C}$ data of carbonate minerals are plotted in Figure 2-5 relative to limestone, organic carbon, igneous rocks, and hydrothermal carbonate minerals. $\delta^{13}\text{C}$ values from the Betty O’Neal mine and Hilltop deposit range from -4.5 to -2.9 per mil and -11.7 to -2.5 per mil, respectively. $\delta^{13}\text{C}$ of the Lovie mine (-0.2 per mil) and the unnamed prospect (-2.3 per mil) samples are also plotted. The data are typical of carbonate mineral values from other porphyry- or vein-type deposits (Field and Fifarek, 1985). The Hilltop, Lovie, and Betty O’Neal mines are all hosted by upper plate rocks, some of which contain an appreciable amount of organic carbon, i.e. Ordovician Valmy Formation chert (Gilluly and Gates, 1965; Kelson et al., 2000). However, only one of 17 samples (Hilltop sample 97-8-136-2, $\delta^{13}\text{C} = -11.7$ per mil) suggest organic carbon contribution. Although organic carbon is common in most upper plate rocks, its absence here



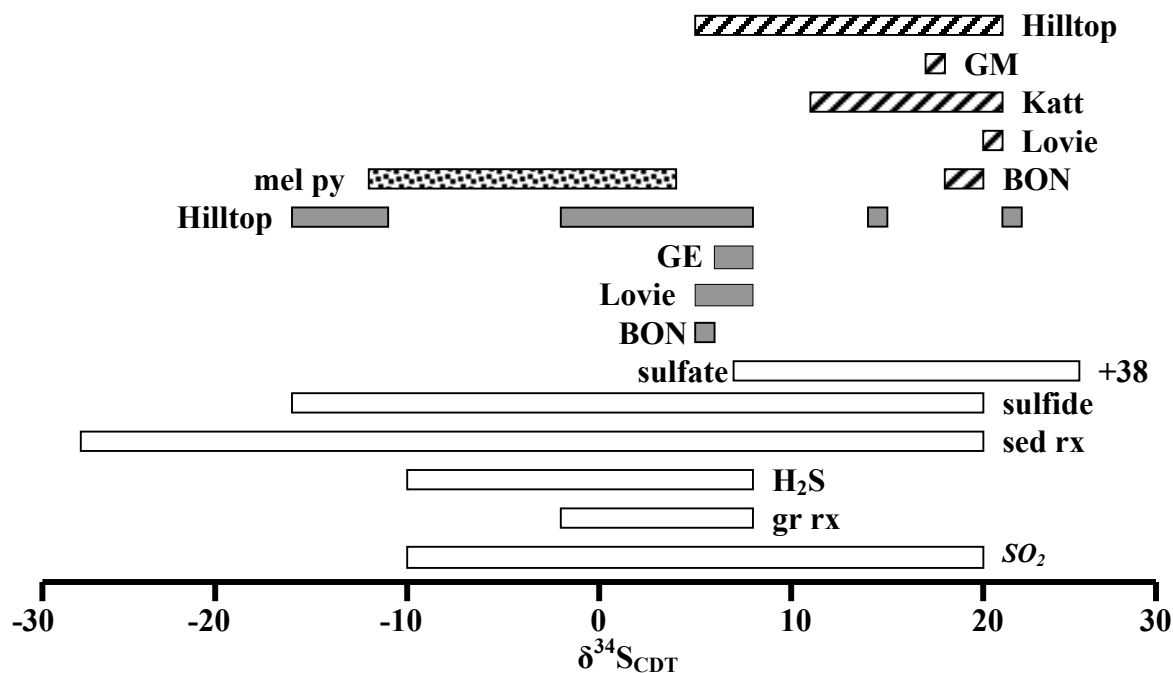
Notes: ls = limestone; oc = organic carbon; ig rx = igneous rocks (total C); hc = hydrothermal carbonates (all reference values from Field and Ficarek, 1985); UN = unnamed prospect (n=1); Lovie = Lovie mine (n=1); BON = Betty O'Neal mine (n=6); Hilltop = Hilltop deposit (n=10).

Figure 2.5: Carbonate carbon isotope data from four mineralized areas within the northern Shoshone Range, Lander County, Nevada.

attests to the overall low primary permeability of the upper plate rock types. A high water:rock ratio and channeled fluid flow may be inferred, as circulating hydrothermal fluids mostly followed faulted, fractured, brecciated, and sheared zones and interacted minimally with the surrounding rocks.

The lack of an organic carbon signature in Hilltop's vein carbonate minerals may indicate separate alteration (removal of organic carbon) and mineralization (deposition of carbonate minerals) events. Drill hole data document the lack of organic carbon from the entire hanging wall of the Hilltop deposit, i.e. most/all organic carbon in the Valmy Formation host rocks was probably removed during initial Cu+Mo±Au porphyry mineralization. Kelson et al. (2000) showed that later epithermal fluids at Hilltop lacked the ability to remove (bleach) organic carbon from surrounding host rock, and suggested vein carbonates + sulfides were associated with the initial porphyry event. However, the paucity of organic carbon in the $\delta^{13}\text{C}$ data may indicate two separate events, one that bleached Hilltop's hanging wall rocks and one that formed the carbonate + sulfide veins (studied here) emplaced in the hanging wall.

Sulfide and sulfate $\delta^{34}\text{S}$ data (Table 2-6) from six mineralized areas are illustrated in Figure 2-6. All sulfide data from the Gray Eagle, Lovie, and Betty O'Neal mines and most of Hilltop's sulfide data cluster together near $\delta^{34}\text{S}$ values of granitic rocks and hydrothermal sulfides (Field and Fifarek, 1985). Hilltop's most depleted sulfide values ($\delta^{34}\text{S}$ range from -15.9 to -10.6 per mil) probably reflect a biologic influence on sulfide formation (Hoefs, 1997). Sulfate data from the Hilltop, Kattenhorn, Lovie, and Betty O'Neal mines and a Granite Mountain-hosted barite vein cluster together and fall within documented hydrothermal sulfate ranges (Field and Fifarek, 1985).



Notes: SO_2 = Volcanic gas; gr rx = granitic rocks; H_2S = volcanic gas; sed rx = sedimentary rocks; sulfide = hydrothermal sulfides; sulfate = hydrothermal sulfates (Field and Ficarek, 1985; Hoefs, 1997). Gray boxes indicate sulfide data: GE = Gray Eagle mine (n=9); Lovie = Lovie mine (n=5); BON = Betty O'Neal mine (n=1); Hilltop = Hilltop deposit / area (n=54, including UN). Striped boxes = sulfate data: BON (n=2); Lovie (n=1); Katt = Kattenhorn mine (n=3); GM = Granite Mountain (n=1); Hilltop (n=12). Stippled box = melnikovite pyrite (Hilltop, n=9).

Figure 2.6: Sulfide and sulfate sulfur isotope data from six mineralized areas within the northern Shoshone Range, Lander County, Nevada.

$\delta^{34}\text{S}$ data from Hilltop Cu + Mo \pm Au porphyry- and four of six subsequent epithermal-style mineralizing events illustrate variable sulfur sources that contributed to the development of the Hilltop deposit. A magmatic fluid source is reflected in sulfide $\delta^{34}\text{S}$ values for: Initial porphyry event (molybdenite, +4.3 to +5.6 per mil); Event 1 (galena, sphalerite, +3.2 to +5.4 per mil); Event 2 (pyrite, arsenopyrite - main Au-bearing event, +3.5 to +4.5 per mil), and Event 3 (stibnite, +2.9-+5.5 per mil). $\delta^{34}\text{S}$ values of pyrite, marcasite, and melnikovite pyrite (-12.1 to +5.4 per mil) support both biologic and magmatic sulfur sources for the Event 5 assemblage.

Geothermometry

Temperatures of ore mineral formation are calculated using sulfur-isotope fractionation between coexisting sphalerite, galena, and/or pyrite.

The isotopic composition of sulfur in coexisting sulfide minerals is a function of their formation temperature; therefore, cogenetic sulfide minerals exhibit slight isotope ratio differences as a function of temperature. The extent of isotope fractionation depends on temperature, and the amount varies between different minerals. The extent of isotope fractionation between phases is minimal at higher (>600°C) temperatures and becomes more pronounced at lower (<300°C) temperatures (Bethke and Barton, 1971; Krauskopf and Bird, 1995).

Geothermometry calculations using $\delta^{34}\text{S}$ values (Kajiwara and Krouse, 1971) of co-existing sulfide mineral pairs (sphalerite-pyrite, sphalerite-galena, galena-pyrite) from the Lovie mine, Gray Eagle mine, the unnamed prospect, and the Hilltop deposit are reported in Table 2-7. Extraordinarily high calculated temperatures (>900°C) certainly represent mineral formation

Deposit	Sample Pair	Mineral pair	Δ per mil	Temp °C
Lovie	03A, B	sph-py	1.1	249
GE	05-1,2	sph-py	0.9	304
GE	04-1,2	gal-py	0.8	900
GE	04-1,4	gal-sph	1.3	511
GE	04-2,4	py-sph	0.5	502
UN	CK02-11-2,3	sph-py	0.8	339
Hilltop	97-10-1084.5-1,2	sph-py	0.2	952
Hilltop	97-10-1160.6-1,2	gal-py	2.2	434
Hilltop	97-11-665.3-3,4	sph-py	0.6	434

Table 2.7: Sulfur isotope geothermometry data from four mines and prospects, northern Shoshone Range, Lander County, Nevada.

under isotopic disequilibrium conditions; temperatures $<500^{\circ}\text{C}$ may represent isotopic equilibrium. Lower temperatures from the Lovie and Gray Eagle mines and the unnamed prospect ($249\text{-}339^{\circ}\text{C}$) fall within typical epithermal temperature ranges (Henley and Brown, 1985). Temperatures $>400^{\circ}\text{C}$ have been measured within active geothermal systems (Henley, 1985), supporting the calculated temperatures of Hilltop's Event 1 assemblage (434°C) that may represent the porphyry-epithermal mineralization transition (Kelson et al., 2000).

Conclusions

This study of upper plate mineralization within part of the Battle Mountain-Eureka mineral belt (northern Shoshone Range, Lander County, Nevada) has established:

1. The temporal relationship between molybdenum porphyry mineralization (~ 40 Ma) and granodioritic igneous rocks (~ 39 Ma);
2. The age of gold mineralization (between 42.1 ± 0.9 and 35.7 ± 0.4 Ma) of hypogene(?) smectite-illite clay associated with visible gold within the discordant quartz breccia pipe at the Hilltop deposit;
3. Identification of and geochemical differences between base- and precious metal-bearing minerals from seven mines, prospects, and deposits. Some minerals (e.g. pyrite, fahlore) are ubiquitous in all deposits, while others (e.g. electrum, sphalerite, arsenopyrite, bournonite) are not. Variable fahlore composition between deposits may reflect differences in the physical (i.e. temperature) and/or chemical (fahlore equilibration with other minerals) nature of each respective ore-forming fluid.

4. Identification of source fluid(s) for ore and gangue minerals via C, O, and S stable isotopes. Carbonate $\delta^{13}\text{C}$ data suggest a magmatic, not organic, source for carbon; carbonate $\delta^{18}\text{O}$ data support variable mixing between magmatic and meteoric water. Sulfide $\delta^{34}\text{S}$ data mostly support a magmatic source for sulfur, except for depleted $\delta^{34}\text{S}$ values (-12.1 per mil; biogenic influence) of Event 5 melnikovite pyrite and pyrite from Hilltop.
5. Geothermometry of ore minerals using sulfur isotope fractionation between coexisting sulfide minerals. Calculated formation temperatures (249-339°C) of sulfides at the Lovie and Gray Eagle mines and the unnamed prospect fall within typical epithermal temperature ranges. Temperatures of 434°C from Hilltop's Event 1 assemblage may indicate the transition between porphyry-epithermal mineralization.

Future work includes fluid inclusion analysis, oxygen and hydrogen (silicate minerals) and additional sulfur (sulfide minerals) isotope analysis to help constrain fluid sources and depositional temperatures. Additional $^{40}\text{Ar}/^{39}\text{Ar}$ ages of other intrusive rocks within the northern Shoshone Range are forthcoming.

Acknowledgements

This research would not have been possible without the generous support of Placer Dome U.S., Inc. and the Cortez Joint Venture, and special thanks to Mr. Robert C. Hays, Jr., Technical Services Superintendent, Cortez Gold Mines. This research was also funded by the Society of Economic Geologists (Hugh E. McKinstry Grant), Geological Society of America (Grant No.

7180-02), and the Department of Geology, University of Georgia. Permission of Placer Dome U.S., Inc. and the Cortez Joint Venture to publish this investigation is gratefully acknowledged. Thanks to Dr. Kenneth Foland (RIL) and Dr. Matthew Heizler (NMGRL) for their assistance and insight with the $^{40}\text{Ar}/^{39}\text{Ar}$ data. Richard Markey (AIRIE, Colorado State University) provided the Re-Os analyses. Julia Cox and Chris Fleisher (University of Georgia) assisted with stable isotope and electron microprobe analyses, respectively. The authors are also indebted to Mr. Steve Ludington and Mr. Robert Schafer for their critical review of this manuscript.

References

- Bethke, P.M., and Barton, P.B., 1971, Distribution of some minor elements between coexisting sulfide minerals: *Economic Geology*, v. 66, p. 140-163.
- Christiansen, R.L., and Yeats, R.S., 1992, Post-Laramide geology of the U.S. Cordilleran region, *in* Burchfiel, B. C., Lipman, P. W., and Zoback, M. L., eds., *The Cordilleran Orogen: Conterminous U.S.*: Boulder, Colorado, Geological Society of America, *The Geology of North America*, v. G-3.
- Deer, W.A., Howie, R.A., and Zussman, J., 1999, *The rock forming minerals*: Longman, Essex, 696 p.
- Emmons, W.H., 1910, A reconnaissance of some mining districts in Lander and Eureka Counties, NV: *Geological Survey Bulletin* 408, p. 117-118.
- Field, C.W., and Fifarek, R.H., 1985, Light stable-isotope systematics in the epithermal environment, *in* Berger, B.R., and Bethke, P.M., eds., *Geology and geochemistry of epithermal systems*: Chelsea, MI, Society of Economic Geologists, *Reviews in Economic Geology*, v. 2, p. 99-128.
- Fleischer, M., 1978, New mineral names: *American Mineralogist*, v. 63, p. 1289-1291.
- Friedman, I., and O'Neil, J.R., 1977, *Data of geochemistry, Sixth Edition*: U.S. Geological Survey Professional Paper 440-KK.
- Guilbert, J.M., and Park, C.F. Jr., 1999, *The geology of ore deposits*: W.H. Freeman and Company, New York, 985 p.
- Gilluly, J., and Gates, O., 1965, Tectonic and igneous geology of the northern Shoshone Range, Nevada: U.S. Geological Survey Professional Paper 465, 153 p.
- Henley, R.W., 1985, The geothermal framework of epithermal deposits, *in* Berger, B.R., and Bethke, P.M., eds., *Geology and geochemistry of epithermal systems*: Chelsea, MI, Society of Economic Geologists, *Reviews in Economic Geology*, v. 2, p. 1-43

- Henley, R.W., and Brown, K.L., 1985, A practical guide to the thermodynamics of geothermal fluids and hydrothermal ore deposits, *in* Berger, B.R., and Bethke, P.M., eds., *Geology and geochemistry of epithermal systems*: Chelsea, MI, Society of Economic Geologists, *Reviews in Economic Geology*, v. 2, p. 25-44.
- Hewett, D.F., 1971, Coronadite – Modes of occurrence and origin: *Economic Geology*, v. 66, p. 104-177.
- Hoefs, J., 1997, *Stable isotope geochemistry*: Springer-Verlag, New York, 201 p.
- Kajiwara, Y., and Krouse, H.R., 1971, Sulfur isotope partitioning in metallic sulfide systems: *Canadian Journal of Earth Science*, v. 8, p. 1397-1408.
- Kelson, C.R., Keith, J.D., Christiansen, E.H., and Meyer, P.E., 2000, Mineral paragenesis and depositional model of the Hilltop gold deposit, Lander County, NV, *in* Cluer, J.K., Price, J.G., Struhsacker, E.M., Hardyman, R.F., and Morris, C.L., eds., *Geology and ore Deposits 2000: The Great Basin and Beyond: Geological Society of Nevada Symposium Proceedings*, Reno/Sparks, May 2000, p. 1107-1132.
- Korzinsky, M.A., Tkachenko, S.I., Shmulovich, K.I., Taran, Y.A., and Steinberg, G.S., 1994, Discovery of a pure rhenium mineral at Kudriavoy volcano: *Nature*, v. 369, p. 51-52.
- Krauskopf, K.B., and Bird, D.K., 1995, *Introduction to geochemistry*: McGraw-Hill Inc., New York, 647 p.
- Lisle, R.E., and Desrochers, G.J., 1988, Geology of the Hilltop gold deposit, Lander County, Nevada: *In* Schafer, R. W., Cooper, J. J., and Vikre, P. G. (eds.), *Bulk mineable precious metal deposits of the western United States*, p. 101-117.
- Maher, B.J., and Browne, Q.J., 1993, Constraints on the age of gold mineralization and metallogenesis in the Battle Mountain-Eureka mineral belt, Nevada: *Economic Geology*, v. 88, p. 409-478.
- Markey, R.J., Hannah, J.L., Morgan, J.W., and Stein, H.J. (2003) A double spike for osmium analysis of highly radiogenic samples: *Chemical Geology*, v. 200, p. 395-406.

- McCrea, J.M., 1950, On the isotopic chemistry of carbonates and a paleo-temperature scale: *Journal of Chemical Physics*, v. 18, p. 849-857.
- McKee, E.H., and Silberman, M.L., 1970, Geochronology of Tertiary igneous rocks in central Nevada: *Geological Society of America Bulletin*, v. 81, p. 2317-2328.
- McDougall, I., and Harrison, T.M., 1999. *Geochronology and Thermochronology by the $^{40}\text{Ar}/^{39}\text{Ar}$ method*, Oxford Univ. Press, NY, 2nd edition, 269 p.
- Smoliar, M.I., Walker, R.J., and Morgan, J.W. (1996) Re-Os isotope constraints on the age of Group IIA, IIIA, IVA, and IVB iron meteorites: *Science*, v. 271, p. 1099-1102.
- Stager, H.K., 1977, *Geology and mineral deposits of Lander County, Nevada*: Nevada Bureau of Mines and Geology Bulletin 88, 106 p.
- Stein, H.J., Morgan, J.W., Markey, R.J., and Hannah, J.L., 1998, An introduction to Re-Os: What's in it for the mineral industry?: *Society of Economic Geologists Newsletter*, no. 32, p. 1, 8-15.
- Stein, H.J., Markey, R.J., Morgan, J.W., Hannah, J.L., and Scherstén, A., 2001, The remarkable Re-Os chronometer in molybdenite: how and why it works: *Terra Nova*, v. 13, no. 6, p. 479-486.
- Stein, H., Scherstén, A., Hannah, J., and Markey, R. (2003) Sub-grain scale decoupling of Re and 187Os and assessment of laser ablation ICP-MS spot dating in molybdenite: *Geochimica et Cosmochimica Acta*, v. 67, no. 19, p. 3673-3686.
- Vanderburg, W.O., 1939, *Reconnaissance of some mining districts in Lander County, Nevada*: U.S. Bureau of Mines Information Circular 7043, p. 47-50.
- Zheng, Y-F., 1990, Carbon-oxygen isotopic covariation in hydrothermal calcite during degassing of CO_2 : *Mineralium Deposita*, v. 25, p. 246-250.

CHAPTER 3

GEOCHEMICAL AND GEOCHRONOLOGICAL CONSTRAINTS ON MINERALIZATION WITHIN THE HILLTOP, LEWIS, AND BULLION MINING DISTRICTS, BATTLE MOUNTAIN-EUREKA TREND, NEVADA¹

¹ Kelson, Chris R., Crowe, Douglas E., and Stein, Holly J. For submission to *Economic Geology*.

Abstract

The Hilltop, Lewis, and Bullion mining districts, located in the northern Shoshone Range, Lander County, Nevada, are part of the greater Battle Mountain-Eureka trend and include both vein- and porphyry-type deposits hosted within siliceous and siliciclastic upper plate rocks of the Roberts Mountains allochthon.

$^{40}\text{Ar}/^{39}\text{Ar}$ and Re-Os chronology of igneous rocks, porphyry-style Cu-Mo mineralization, and gangue minerals associated with vein-hosted mineralization elucidate the relationship between magmatic activity, hydrothermal fluid flow, and mineralization. Dominantly felsic intrusive rocks were emplaced throughout the northern Shoshone Range between 39.3 ± 0.4 and 38.1 ± 0.4 Ma along a W-NW trend, and minor Cu + Mo ± Au porphyry-style mineralization is associated with some of the intrusions. $^{40}\text{Ar}/^{39}\text{Ar}$ ages for biotite and/or hornblende from unaltered igneous rocks within and/or proximal to mineralized areas are nearly coincident with molybdenite ages (40.1 ± 0.6 Ma, average) supporting a relation between pluton emplacement and porphyry Cu-Mo mineralization. Constraints on the deposition of quartz vein-hosted gold (35.9 ± 0.1 Ma, Hilltop deposit) and base-metal mineralization (38.3 ± 0.1 Ma, Gray Eagle mine) are established via $^{40}\text{Ar}/^{39}\text{Ar}$ ages of associated gangue clay (illite, muscovite) minerals. The discrepancies between the ages of Au- and base-metal-bearing vein-hosted mineralization (younger) and nearby intrusive igneous rocks (older) suggests the vein mineralization formed during prolonged hydrothermal activity related to igneous rock emplacement or from heat associated with a second, slightly younger phase of intrusive igneous rocks at depth.

The quartz vein-hosted sulfide (ore) minerals from the northern Shoshone Range are isotopically similar ($\delta^{34}\text{S}_{\text{CDT}}$ range from -6 to +9 per mil) to other sulfide minerals from Cu-Mo porphyry deposits and Cordilleran vein-type deposits, supporting a mostly magmatic sulfur source, except hypogene melnikovite (banded, botryoidal) pyrite from the Hilltop deposit ($\delta^{34}\text{S}_{\text{CDT}}$ range from -4 to -15 per mil), which reflects biogenic influence. Carbon isotope data from vein gangue carbonate minerals ($\delta^{13}\text{C}_{\text{PDB}}$ range from -0.2 to -11.6 per mil) support mixed magmatic \pm organic matter \pm carbonate rock sources for carbon; carbonate oxygen was derived mainly from magmatic fluids ($\delta^{18}\text{O}_{\text{VSMOW}}$ range from -1.3 to +14.4 per mil). Pressure-corrected primary fluid inclusion data (salinity range from 0 to 6.4 equiv. wt. % NaCl; T_h range from 109-425°C), in conjunction with measured $\delta^{18}\text{O}_{\text{VSMOW}}$ data (-0.97 to +17.3‰), suggest the ore-bearing vein quartz formed from variable mixtures of magmatic and meteoric components (calculated $\delta^{18}\text{O}_{\text{VSMOW}}$ -16.2 to +13.3‰).

Depositional temperatures of ore (base metal) minerals, calculated using sulfur isotope fractionation between co-existing sulfides, range from 250-500°C and agree with the range of vein quartz primary fluid inclusion T_h values.

Geochronology and stable isotope data show that quartz vein-hosted precious and base metal mineralization and molybdenite (porphyry) mineralization within the Hilltop, Lewis, and Bullion mining districts are genetically related to Eocene magmatism. Sulfur isotope fractionation and fluid inclusion geothermometry indicates that some vein mineralization temperatures exceeded relatively low-temperature epithermal conditions and were more closely related to higher temperature porphyry-style processes.

Introduction

The Battle Mountain-Eureka trend, one of Nevada's major alignments of base- and precious-metal mines and deposits (Roberts, 1966), is located within the Great Basin province – one of the world's most prodigious gold-producing regions. Although metals are produced from a wide variety of deposit types within these trends, gold has been recovered mostly from sediment (carbonate)-hosted Carlin (disseminated)-type deposits since the 1960s (John et al., 2003). In 2001, Nevada accounted for nearly three quarters of United States gold production and a tenth of world gold production, behind only South Africa and Australia (Price and Meeuwig, 2002).

The Battle Mountain-Eureka trend consists of 10 mining districts, three of which (Hilltop, Lewis, and Bullion districts) are located in the northern Shoshone Range in Lander County (Figs. 3.1, 3.2). These districts, organized shortly after the 1859 Comstock Lode discovery, include over 140 mines and prospects (Stewart and McKee, 1977). Unlike Carlin-type deposits, mineralization within the northern Shoshone Range occurs mostly as vein- and fracture-fill in upper plate, early Paleozoic siliceous and siliciclastic rocks. Minor Cu + Mo ± Au porphyry-style mineralization is associated with some granitic intrusive rocks emplaced through the northern Shoshone Range along a west-northwest trend (Kelson et al., 2000).

Between 1902 and 1936, more than 33 Koz gold (placer and lode), 5 Moz silver, 53 Moz lead, and 20 Moz copper have been collectively produced from the Hilltop, Lewis, and Bullion districts accounting for 59%, 27%, 49%, and 8% (respectively) of total Au, Ag, Pb, and Cu produced from all 15 mining districts within Lander County during that time (Vanderburg, 1939). Other commodities including mercury, antimony, turquoise, fluorspar, barite, and

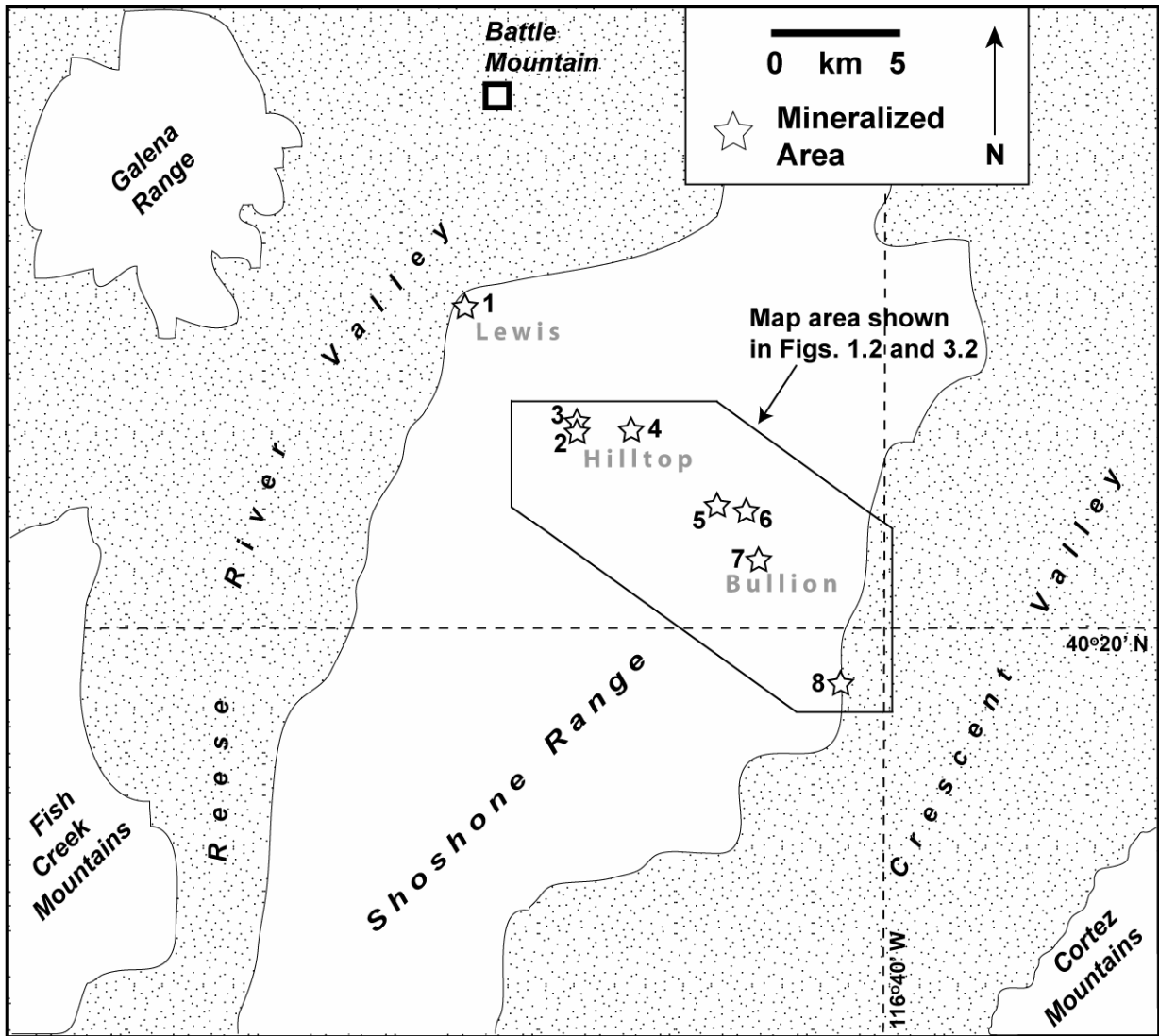
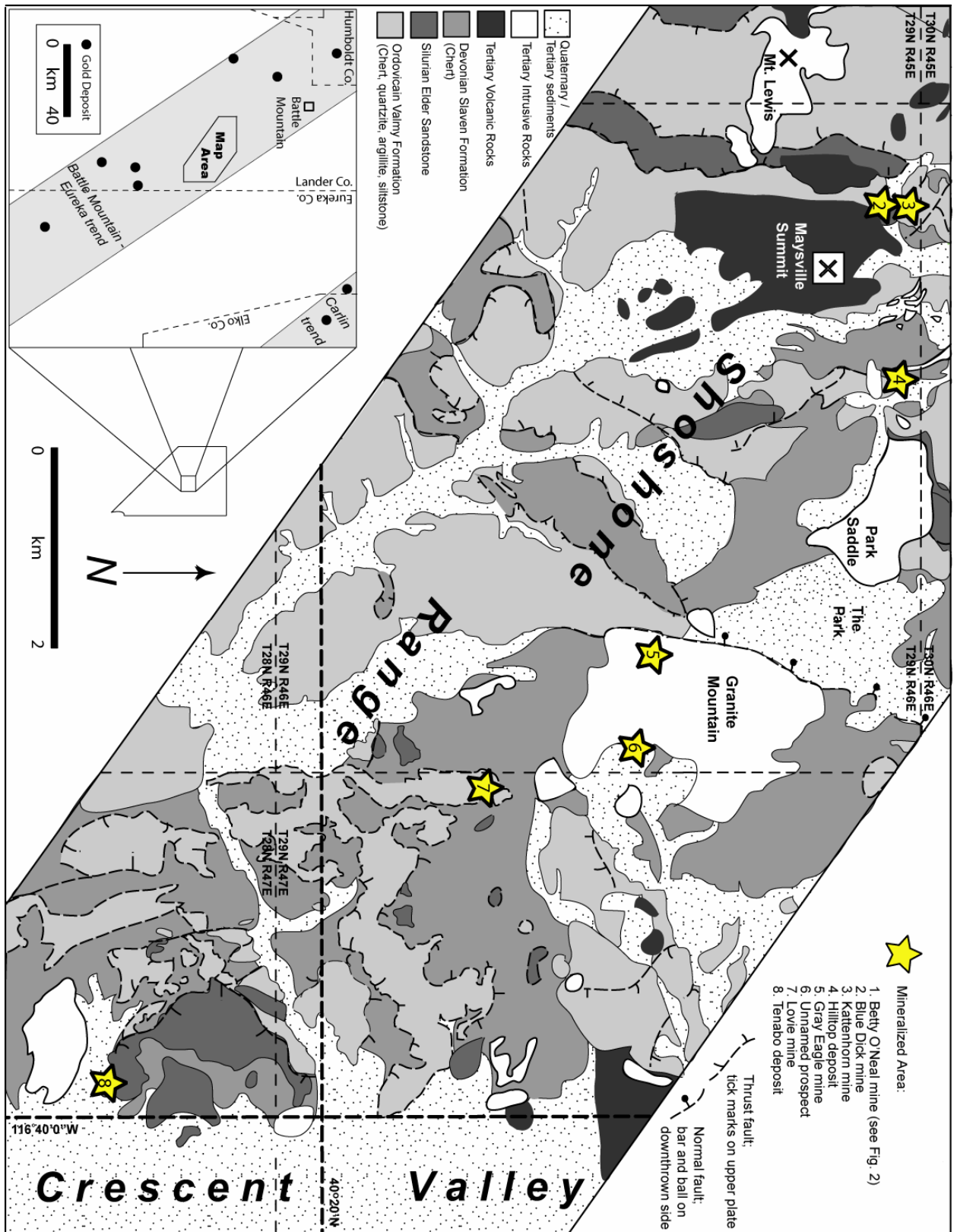


Figure 3.1: Location of the Lewis, Hilltop, and Bullion mining districts and mineralized areas studied here, northern Shoshone Range, Lander County, Nevada. See Fig. 3.1 for names of mineralized areas.

Figure 3.2 (following page): Simplified geologic map of the northern Shoshone Range study area, Lander County, Nevada. Major geographic features and mineralized areas in this study are shown. Modified from Gilluly and Gates (1965) and Cortez Joint Venture (unpublished) map.



manganese were also produced. Since 1936, mining operations in the northern Shoshone Range have largely ceased. However, considerable interest in exploring and re-evaluating the inactive mines (mostly for gold) within the Hilltop, Lewis, and Bullion districts continues to present day, due to their close proximity to other Bullion district Au deposits (Tenabo deposit, 1.5 Moz total Au (McCusker, 2004); Gold Acres, 700 Koz total Au, and the Pipeline/South Pipeline complex, > 20 Moz total Au (R. Hays, pers. comm., 2006)).

Despite the production histories of the Hilltop, Lewis, and Bullion mining districts and their close spatial association to large Au-bearing deposits (e.g. Pipeline/South Pipeline, Fortitude), there are relatively few descriptive studies (Emmons, 1910; Vanderburg, 1939; Stewart and McKee, 1977) and no detailed studies concerning mineralization within these districts, with the exception of the Hilltop deposit. The Hilltop deposit (Hilltop district) has been examined more thoroughly in recent years (Desrochers, 1984; Lisle and Desrochers, 1988; Kelson et al, 2000; Kelson et al., 2005) as it is the largest gold deposit (2 Moz gold, Kelson et al., 2000) within the silver- and base metal-dominant northern Shoshone Range.

This paper is the first in-depth examination of northern Shoshone Range mineralization. We use Re-Os and $^{40}\text{Ar}/^{39}\text{Ar}$ geochronology, stable and radiogenic isotopes, fluid inclusion data, and major and trace element data from eight mineralized areas within the Hilltop, Lewis, and Bullion districts to establish temporal-chemical relationships between intrusive igneous rocks and vein- and porphyry-type mineralization, and the conditions under which mineralization occurred.

Regional Geologic Setting

Nevada lies within the Cordillera of the North American continent. A brief history of important geologic events that have shaped this portion of north-central Nevada and the Cordillera is summarized here; see Madrid and Roberts (1991) for detailed stratigraphy and tectonic information.

The geology of Nevada records a long and complex tectonic, sedimentary, and igneous history from Precambrian to Tertiary beginning with the fragmentation and subsequent rifting of a Late Proterozoic supercontinent between 600 and 555 Ma (Armin and Mayer, 1983; Burchfiel et al., 1992). This breakup formed a north-trending passive continental margin (most of present-day Nevada) along the western edge of North America. Subsequent subsidence of this western passive edge initiated deposition of up to 5,000 m of shallow-water, carbonate-platform (miogeoclinal) sediments from Precambrian to Devonian time (Stewart and Poole, 1974; Stewart, 1980; Cook and Taylor, 1991). Simultaneously, a westward thickening wedge of deep-water, siliceous and siliciclastic (eugeoclinal) sediments was deposited west of and adjacent to the carbonate sediments.

Sedimentation along this passive margin continued until the Middle Paleozoic, when the deep-water rocks were thrust 100 to 145 km (Roberts et al., 1958; Stewart and Poole, 1974; Nilson and Stewart, 1980; Burchfiel and Royden, 1991) eastward over the coeval shallow-water (autochthonous, lower plate) rocks along the Roberts Mountains thrust during the Late Devonian-Early Mississippian Antler orogeny. The transported (allochthonous, upper plate) sequence consists mostly of Cambrian to Devonian chert, argillite, sandstone, siltstone, and

greenstone. The autochthonous (lower plate) sequence consists of limestone and dolomite with lesser shale and sandstone (Nilson and Stewart, 1980; Turner et al., 1989). Estimates for the duration of allochthon emplacement range from 8 my (Nilson and Stewart, 1980; Burchfiel and Royden, 1991) to 35 my (Carpenter et al., 1994). The exact cause(s) of the Antler orogeny are unclear (Nilson and Stewart, 1980); allochthon emplacement probably resulted from the partial closure of a small ocean basin between the continental margin and the Sierran-Klamath island arc (Burchfiel and Davis, 1972), although direct arc-continent collision is suspect (Poole, 1974; Johnson and Pendergast, 1981; Burchfiel and Royden, 1991; Carpenter et al., 1994). Imbricate thrusting and extensive folding of the allochthonous (upper plate) rocks accompanied the Antler Orogeny. Subsequent erosion of the resultant topographic high (Antler orogenic belt) during the Mississippian shed detrital material into depressions east (Chainman-Diamond Peak trough) and west (Pumpnickel-Havallah trough) of the belt (Gilluly and Gates, 1965; Roberts, 1966; Stewart, 1980). The Roberts Mountains thrust and Roberts Mountains allochthon lie ~20 km east of the study area (Fig. 1.1).

Sedimentary and tectonic patterns remained essentially unchanged until the Late Pennsylvanian-Permian Humboldt orogeny, when uplift throughout much of Nevada produced a widespread unconformity and an influx of coarse detrital material into basins east of the Antler belt (Ketner, 1977). The Humboldt orogeny probably represents a period of tectonic adjustment instead of a true mountain-building event (Snyder et al., 1991) and possibly includes reactivation of the Antler orogenic belt.

During the Late Permian-Early Triassic Sonoma orogeny another deep marine assemblage of mid Paleozoic to Permian siliceous, siliciclastic, and volcanic basinal strata (Miller et al., 1992) was thrust eastward between 70 and 100 km over coeval shallow-water

deposits on the Antler orogenic belt and erosional remnants of the Roberts Mountains allochthon along the Golconda thrust (Burchfiel and Davis, 1972; Stewart, 1980; Snyder and Brueckner, 1983). Although several theories explaining the Sonoma orogeny have been proposed, a model advocating the collision between an eastward-migrating island arc and (subsequent accretion to) the continent is the most widely accepted (Speed, 1971; Silberling, 1973; Speed, 1979; Stewart, 1980; Miller et al., 1992). The Golconda thrust and Golconda allochthon lie ~100 km west of the study area (Fig. 1.1). An active continental margin west of Nevada and the accretion of oceanic terranes onto the western edge of the continent marked the culmination of the Sonoma orogeny (Burchfiel et al., 1992).

The Early to Middle Mesozoic Cordillera was dominated by continued shallow- and deep-water marine and volcanogenic sediment deposition over central and western Nevada, east of a magmatic arc or arcs now represented by Triassic and Jurassic igneous rocks in western Nevada, eastern California, and southwest Arizona. This arc formed across all earlier paleogeographic belts, indicating a probable adjustment in the configuration and interaction of the Kula, Farallon, and North American plates and the association with the development of an active east-dipping subduction zone (Miller et al., 1992). Contractual deformation (folding and thrusting) began to affect the arc and back-arc in the Jurassic and culminated in the development of the Sevier fold-thrust belt in the Cretaceous (Burchfiel et al., 1992; Dickenson, 1992). Arc magmatism continued during the Cretaceous and was accompanied inland by felsic crustal-melt intrusions associated with the Cretaceous crustal thickening.

Widespread magmatic activity occurred throughout Nevada between 43 and 17 Ma, gradually migrating southward with time, including the eruption of extensive siliceous tuffs between 34 and 17 Ma (Stewart, 1980). Regional uplift and possible reactivation of an older, pre-

existing crustal feature – the Northern Nevada rift (John et al., 2000) - occurred during middle to late Tertiary time (Zoback and Thompson, 1978). Extension within the Great Basin has become the dominant land-shaping force since middle Miocene time and continues to present day (Thompson and Burke, 1974; Christiansen and Yeats, 1992) providing the regions' familiar Basin-and-Range topography.

Northern Shoshone Range and District Geology

The Shoshone Mountains (and their northern extension, the Shoshone Range), one of several northeast-trending mountain ranges within Lander County, extend over 300 km and rise over 1500 m (5000 ft) above the adjacent valleys. The Hilltop, Lewis, and Bullion districts (Fig. 3.2) cover approximately 200 km² of the range's northern end, and are flanked by the Battle Mountain district (Galena Range, northwest) and Cortez district (Cortez Mountains, southeast) within the greater Battle Mountain-Eureka trend.

Early geologic descriptions (King, 1876; Spurr, 1903; Emmons, 1910; Lee et al., 1916) of the northern Shoshone Range are largely reconnaissance in nature; detailed, comprehensive studies were completed by Gilluly and Gates (1965) and Stewart and McKee (1977). Emmons (1910) first documented Hilltop, Lewis, and Bullion district mineralization and included maps and descriptions of then-accessible underground mines. Vanderburg (1939) and Stager (1977) also provide comprehensive overviews of individual mine and district production histories, geology, and ore occurrences.

Paleozoic and Tertiary rocks underlie the northern Shoshone Range. The oldest and most abundant are allochthonous siliceous/siliciclastic sedimentary and volcanic rocks of the

Ordovician Valmy Formation (chert, argillite, quartzite, siltstone, and greenstone), Silurian Elder Sandstone, and Devonian Slaven Chert (Gilluly and Gates, 1965). No lower plate (autochthonous) carbonate rocks occur in this study area, although lower plate windows (i.e. Goat Ridge, Red Rock, Gold Acres, Pipeline) are exposed further south (Roberts, 1960, Foo et al., 1996) and rare, small carbonate lenses exist within the upper plate formations (Gilluly and Gates, 1965). Structural displacement and deformation of the Paleozoic strata is widespread and locally intense; these rock units are frequently in thrust fault contact with one another and commonly exhibit extreme internal folding, imbrication, and tectonic thickening due mostly to compressional stresses associated with the Antler orogeny. Ordovician Valmy Formation thickness in the northern Shoshone Range is estimated to be more than 7600 m (25,000 ft); five times its original depositional thickness (Gilluly and Gates, 1965).

Tertiary rocks include Eocene granodioritic intrusive rocks and Miocene or Pliocene felsic intrusive rocks, basalt, andesite and rhyolite flows, and tuffs. The Eocene intrusive rocks are emplaced along a west-northwest trend through the northern Shoshone Range, and are located both proximal and distal to mineralized areas (Gilluly and Gates, 1965; Stager, 1977; Kelson et al., 2000; Kelson et al., 2005). The largest Eocene intrusion in the northern Shoshone Range is Granite Mountain, which covers approximately 10 km² and rises over 600 m (2000 ft) above the adjacent valleys. Late Tertiary volcanic rocks occur throughout the range but are most abundant on its eastern flank. Basin and range faults bound the Shoshone Mountains and have tilted the range 5-15° east (Lisle and Desrochers, 1988).

The existence of a caldera centered on Mt. Lewis (western half, northern Shoshone Range) has been debated (Wrucke and Silberman, 1975, 1977; Gilluly, 1977; Stewart, 1980; White, 1985), and may have played an important role in structurally-preparing the upper plate

rocks for subsequent mineralizing fluids within at least the Lewis and Hilltop mining districts. Currently, its temporal and genetic relationship to nearby Lewis and Hilltop district mineralization is unclear.

Battle Mountain – Eureka Trend

Roberts (1966) first identified 12 mineral “belts” or trends – alignments of mines and deposits, including the Battle Mountain – Eureka trend – throughout Nevada. The origin of these mineral trends is not completely understood. Several workers (Roberts, 1966; Shawe, 1991; Zamudio and Atkinson, 1991; Grauch et al., 2003; Howard, 2003; among others) have presented geologic, isotopic, and geophysical data supporting deep-penetrating crustal structures underlying or coincident with mineral trends that may have acted as conduits for intrusive igneous rocks and/or mineralizing fluids. The Carlin and Battle Mountain-Eureka trends roughly parallel each other and the Northern Nevada rift, but neither are coincident with the western edge of the Precambrian crust as inferred by the $^{87}\text{Sr}/^{86}\text{Sr} = 0.706$ (Kistler and Peterman, 1978) and $^{208}\text{Pb}/^{204}\text{Pb} = 38$ (Tosdal et al., 2000) isopleths.

The Battle Mountain-Eureka is a northwest-trending alignment of over 30 major base and precious-metal mines and deposits (and hundreds of smaller mines and prospects), comprising 10 mining districts (Roberts, 1966) covering approximately 4400 km² of north-central Nevada. Mineralization occurs within a wide variety of deposit types (skarn, vein, stockwork, and disseminated “Carlin-type”) and is hosted by both upper and lower plate rocks. Igneous rocks within the trend delineate three separate magmatic pulses — 100-85 Ma, 40-34 Ma, and ~15 Ma (Christiansen and Yeats, 1992; Maher et al., 1993) — each associated with the deposition of

different metals or suites of metals (Maher et al., 1993). Most of the mineralization within the Battle Mountain – Eureka trend, including the Hilltop, Lewis, and Bullion mining districts, is associated with 40-34 Ma igneous rocks (Shawe, 1991; Maher et al., 1993; Kelson et al., 2005).

Northern Shoshone Range Mineral Deposits

The northern Shoshone Range contains both porphyry-style Cu-Mo±Au and vein-type mineralization. Vein-type mineralization is ubiquitous, and ore from the Hilltop, Lewis, and Bullion mining districts comes from this type. Most mines within these districts have been inactive since the 1930s; however, recent (1974-1980) reevaluation of two deposits (Hilltop and Tenabo, both historic producers of vein-hosted base- and/or precious metals) has delineated additional Au reserves. The Hilltop deposit is estimated to contain 2 Moz of near surface, bulk-mineable (non- Carlin-type) Au with appreciable (porphyry) Cu + Mo hosted within highly fractured host rocks (Lisle and Desrochers, 1988; Kelson et al., 2000; Kelson et al., 2005). Nearly 1 Moz Au was mined intermittently from Tenabo between 1974 and 1980, with another 580 Koz Au recently delineated (McCusker, 2004).

This study focuses on mostly vein-type mineralization from eight different locales within the northern Shoshone Range: the Hilltop deposit and Blue Dick and Kattenhorn mines (Hilltop district); the Betty O’Neal mine (Lewis district); the Gray Eagle and Lovie mines, Tenabo deposit, and an unnamed prospect (Bullion district) (Table 3.1).

Table 3.1: Types and orientations of ore-bearing structures and Ag:Au ratios for northern Shoshone Range vein deposits.

Mineralized area	Main ore-bearing structure(s)	Strike, Dip (°) of ore-bearing structure(s)	Ag:Au	Reference
Betty O'Neal	Vein	N30W, 20-50E	161	1
Blue Dick	Vein	N45W, 45SW	32	2
Kattenhorn	Vein	N45W, 45SW	102	2
Hilltop	Breccia bounded by two faults	Due N, 25W	10	3,4
Hilltop	Discordant quartz breccia pipe	Due N, 90	~3	3,4
Gray Eagle	Fissure vein	N70E, 70N	60	1
Unnamed prospect	Vein, shear zone	N70E, 90	15	--
Lovie	Vein	N65E, 20-50SE	109	1
Tenabo	Sheeted zones	Due W, 30S	~10	1

References: 1=Emmons, 1910; 2=Vanderburg, 1939; 3=Lisle and Desrochers, 1988; 4=Kelson et al., 2000.

Vein-type mineralization

Paleozoic siliceous/siliciclastic (upper plate) rocks of the Roberts Mountains allochthon and/or Tertiary intrusive igneous rocks host the vein deposits within the northern Shoshone Range (Fig. 3.3a – 3.3p). The Ordovician Valmy Formation, consisting of chert, argillite, quartzite, siltstone, and lesser greenstone (see Gilluly and Gates (1965) and Kelson et al. (2000) for detailed petrographic descriptions) underlies most of the northern Shoshone Range and hosts most of the mineralization. Mineralization occurs only in areas of intense structural preparation (breccias, faults, fractures, and shear zones) and decreases rapidly away from these areas. Alteration halos around veins in upper plate host rocks are largely absent; intrusive igneous host rocks adjacent to veins are locally argillized, silicified, and/or sericitized.

Vein-hosted ore and gangue mineral assemblages are generally similar between deposits. Gangue minerals include quartz (ubiquitous), calcite with Fe, Mn, and/or Mg, Ba- and/or Ca-sulfates (common), and rare clay, e.g. chlorite, illite (“sericite”), muscovite, or smectite; ore is always associated with quartz. Except for Hilltop’s discordant quartz breccia pipe (Fig. 3.3a and 3.3b), veins are comprised of massive clear or milky-white, coarsely crystalline to microcrystalline quartz. Quartz also occurs within fine-grained silica-sulfide veins (Fig. 3.3c and 3.3d) and breccia matrix (Fig. 3.3e) (e.g. Hilltop deposit, Kelson et al., 2000) and with organic carbon-rich matrix in barren Blue Dick mine pebble dikes or breccias (Fig. 3.3f). Sulfide phases include galena, sphalerite, arsenopyrite, pyrite, chalcopyrite, fahlore, and other sulfosalts (Figs. 3.3g – 3.3p). Native gold (Fig. 3.3a) and electrum are rare, and are more commonly found disseminated in pyrite, arsenopyrite, and arsenian pyrite (based on assay data) (Fig. 3.3d). Major silver-bearing minerals include fahlore and other sulfosalts, with subordinate argentiferous

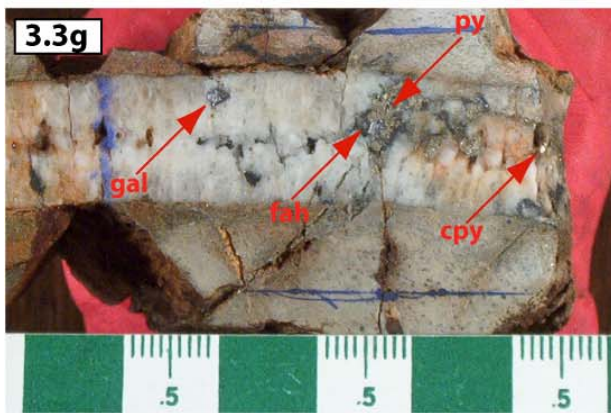
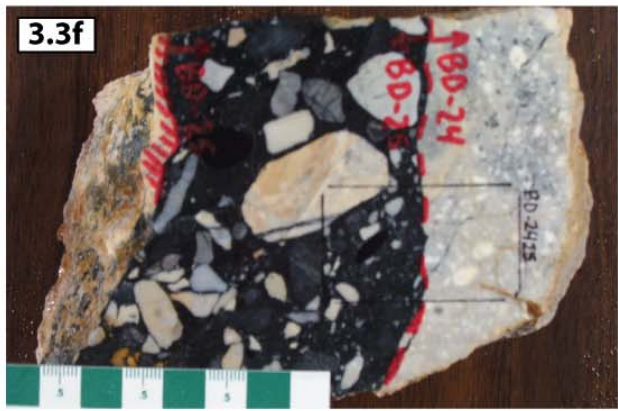
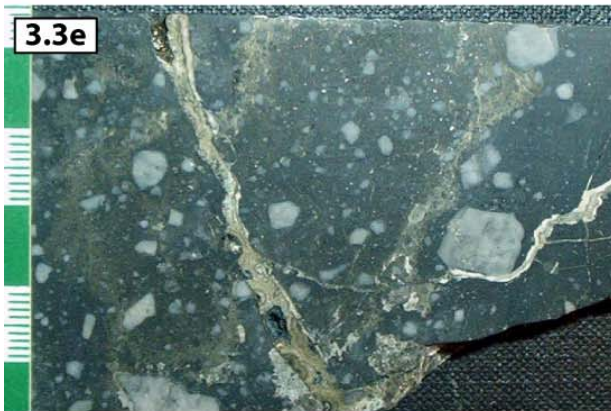
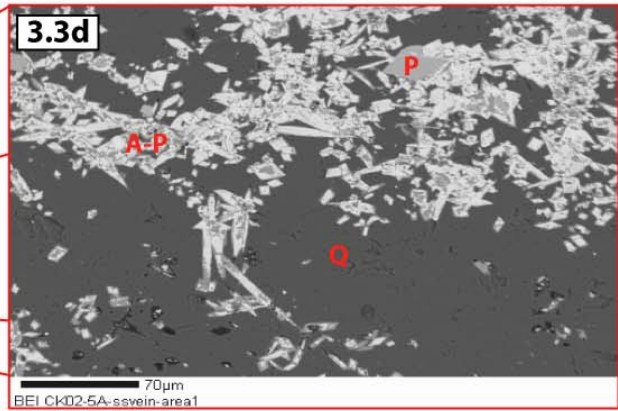
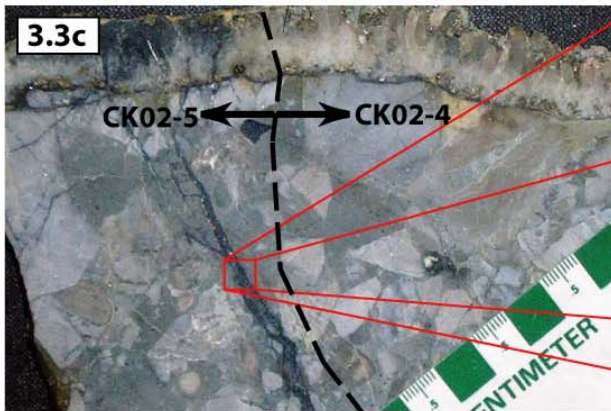
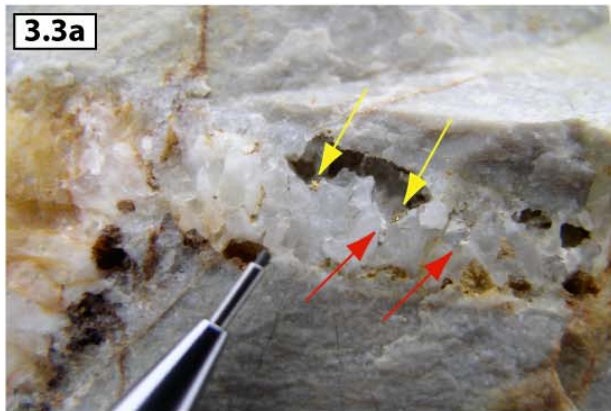
Figure 3.3 (following pages): Examples of northern Shoshone Range vein mineralization. See text for explanation of Hilltop deposit mineralization “Events”.

- A) Quartz matrix with visible gold (yellow arrows) and mixed-layered smectite/illite clay (sample DSC BXA, red arrows), discordant quartz breccia pipe, Hilltop deposit.
- B) Discordant quartz breccia pipe, Hilltop deposit. Angular clasts of altered Valmy Formation argillite (tan) and chert (gray) within gold-bearing quartz matrix.
- C) Ore sample, Hilltop deposit. Based on quartz vein morphology, this sample is similar to the discordant quartz breccia pipe. Large quartz vein contains pyrite + galena + sphalerite + fahlore + arsenopyrite + rare cassiterite, and clearly post-dates breccia formation: Note silica-sulfide veinlet cutting breccia and quartz vein, and spreading along quartz vein / breccia boundary. Assay data (CK02-4 = 3 ppm Au; CK02-5 = 11 ppm Au) supports the relationship between silica-sulfide veinlets (Event 2) and Au.
- D) Back scattered electron image of the Au-bearing silica-sulfide veinlet (Event 2). Veinlet is composed of a fine-grained mixture of quartz (Q) + pyrite (P) + arsenopyrite / arsenian pyrite (A-P). Arsenopyrite crystals frequently possess pyritic rims. Gold has not been directly observed within the silica-sulfide veins and probably occurs as sub-micron sized particles within one or more of these phases.
- E) Massive silica-sulfide (Event 2, main zone, Hilltop deposit) matrix cataclasite containing altered fragments of Valmy Formation chert, cut by younger veins of Event 5 melnikovite pyrite. Assay data: 4.8 ppm Au, 4.8 ppm Ag, > 1% As. Note finely-banded pyrite within the veins.

- F) Unmineralized pebble dike, Blue Dick mine. Variably-sized, sub-angular fragments of siliceous and siliciclastic rocks and altered feldspar porphyry wall rock in a fine-grained quartz + organic carbon matrix. This pebble dike was not observed in other northern Shoshone Range vein deposits.
- G) Galena + chalcopyrite + fahlore + arsenopyrite + pyrite – bearing quartz vein, Lovie mine.
- H) Molybdenite-bearing quartz vein (sample 97-10 106.1), porphyry mineralization, Hilltop deposit.
- I) Ore-bearing quartz vein, Betty O’Neal mine. Note secondary Cu-oxide minerals within larger patches of fahlore. Assay data: 21 ppb Au, 602 ppm Ag.
- J) Back scattered electron image of Betty O’Neal mine ore. Sulfide phases include bournonite (B), Ag-bearing fahlore (F), galena (G), and argentite (A). Ox = oxidized bournonite.
- K) Gray Eagle mine ore. Pyrite + galena + fahlore + arsenopyrite ± chalcopyrite ± sphalerite ± electrum – bearing quartz vein hosted by Granite Mountain granite. Wall rock adjacent to veins is argillized ± silicified ± sericitized.
- L) Galena + sphalerite (part of Event 1 assemblage, Hilltop deposit) as matrix within Hilltop fault zone (main zone lower boundary) clast-supported breccia. Note presence of both altered (bleached) and unaltered (i.e. organic-carbon bearing), sub-rounded fragments of Valmy Formation chert, indicating significant clast movement and the close proximity of unaltered (and unmineralized) footwall rocks of the Hilltop fault (and main zone).
- M) Back scattered electron image of Betty O’Neal mine ore (hand sample = black / purple gossan between drusy quartz veins). Electron microprobe reveals alternating bands of Pb- (light) and Mn- (dark) oxide (e.g. coronadite; Ramdohr, 1969) between / within

quartz veins. Vugs within the banded material contain small, euhedral crystals of the same material.

- N) Back scattered electron image of the same sample in Figure 3M. Raft (?) of chlorargyrite within alternating Pb- and Mn-oxide bands. Assay data: 172 ppb Au, 2891 ppm Ag (~87 oz/t, Ag).
- O) Melnikovite (banded) pyrite (Event 5, main zone, Hilltop deposit). Late-stage, post-Au mineralization banded pyrite and marcasite surrounding clasts of altered intrusive igneous rock and altered Valmy Formation chert and quartzite. Some Event 5 mineralization contains very high Sb and As concentrations (with lesser Co and Ni) and formed under alternating magmatic and biologic influences (see sulfur isotope data).
- P) “Massive” pyrite (Event 5, main zone, Hilltop deposit) as matrix surrounding clasts of altered intrusive igneous rocks and Valmy Formation argillite, chert, and quartzite. Thin, black silica-sulfide veinlets at upper right represent Event 2 mineralization (main Au-bearing event).



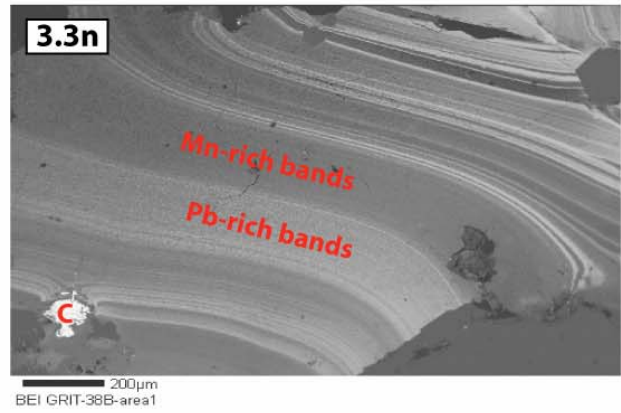
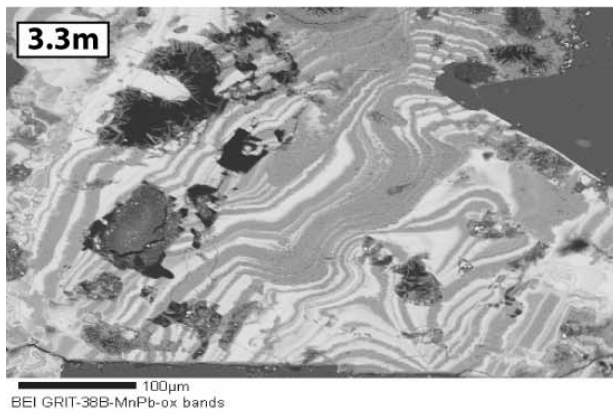
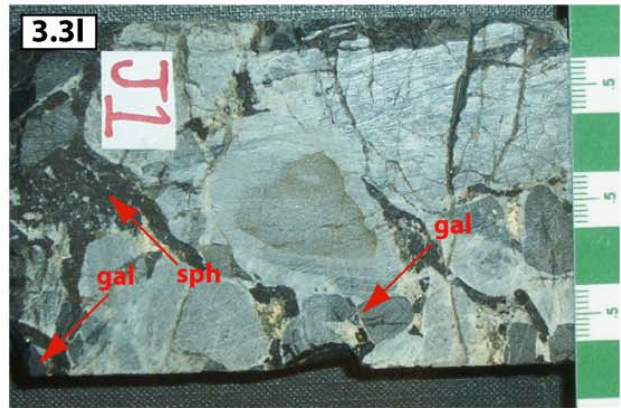
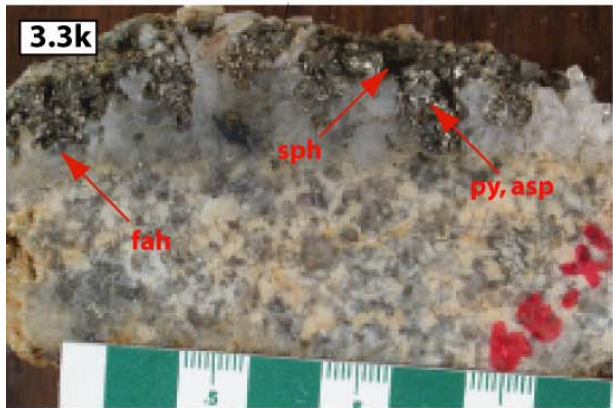
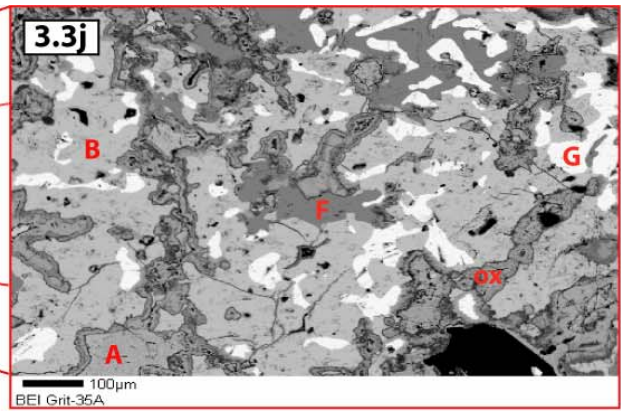
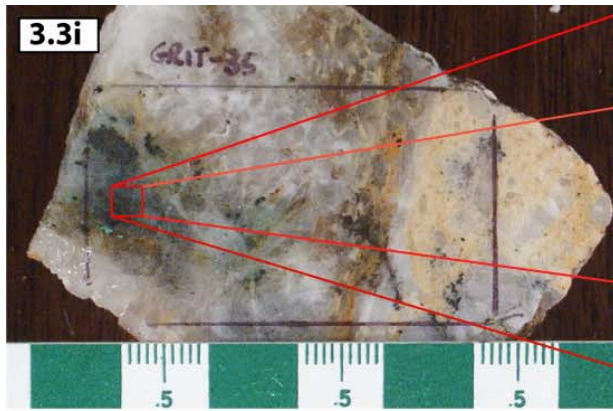


Table 3.2 (following two pages): Electron microprobe analyses of sulfide minerals from northern Shoshone Range vein deposits. Data from Kelson et al. (2005).

Hilltop mine and immediate area (Hilltop district)

	py	fah	mia	asp	sph	gal	cpy	stib	bn	cst	elec
Fe	44.84	3.88	0.00	34.10	7.94	0.21	29.22	0.04	0.04	3.09	--
S	51.03	27.16	20.77	20.49	32.93	11.88	33.49	27.51	19.43	26.08	--
Sb	0.04	17.58	40.38	0.46	0.02	0.21	0.03	70.83	24.29	25.85	--
As	0.34	1.36	0.35	43.51	0.00	0.00	0.00	0.56	1.16	2.79	--
Zn	0.08	13.30	0.06	0.05	55.56	0.31	0.21	0.02	0.26	5.26	--
Pb	0.84	0.00	0.00	0.06	0.00	83.44	0.00	0.00	43.41	0.01	--
Si	0.25	0.03	0.04	0.03	0.07	0.04	0.02	0.04	0.02	0.00	--
Ag	0.01	1.14	39.26	0.01	0.03	0.42	0.02	0.05	0.03	1.58	13.40
Cu	0.10	30.20	0.11	0.10	0.76	0.23	33.23	0.06	13.39	35.59	--
Mn	0.02	0.07	0.03	0.04	0.78	0.03	0.01	0.02	0.02	0.04	--
Au	0.02	0.03	0.00	0.03	0.03	0.01	0.01	0.02	0.00	0.00	85.07
Sn	0.00	4.91	0.00	0.00	0.06	0.00	0.05	0.26	0.04	0.15	--
Se	0.01	0.02	0.72	0.00	0.02	2.15	0.01	0.24	0.09	0.00	--
Cd	0.01	0.12	0.01	0.02	1.21	0.04	0.01	0.00	0.00	0.00	--
Ge	0.00	0.00	0.00	0.00	0.01	0.01	0.02	0.00	0.05	0.00	--
Cl	0.00	0.00	0.03	0.01	0.01	0.07	0.00	0.01	0.03	0.01	--
Te	0.01	0.00	0.00	0.02	0.02	0.08	0.01	0.00	0.00	0.00	--
Hg	0.01	0.11	--	0.00	0.01	0.01	0.04	0.01	0.00	--	--
Total	97.61	99.85	101.51	98.89	99.44	99.13	96.37	99.61	102.25	100.45	98.46
n	22	9	3	13	11	14	7	5	3	1	10

Lovie mine (Bullion district)

	py	fah	asp	sph	gal
Fe	45.61	4.48	36.23	7.80	0.23
S	52.59	23.36	21.11	33.27	13.46
Sb	0.01	21.45	0.03	0.01	0.24
As	0.09	0.48	44.95	0.00	0.00
Zn	0.06	11.60	0.11	56.69	0.09
Pb	0.00	0.00	0.14	0.00	85.96
Si	0.05	0.03	0.00	0.01	0.01
Ag	0.01	19.33	0.02	0.02	0.22
Cu	0.02	17.78	0.03	0.14	0.15
Mn	0.02	0.10	0.02	1.59	0.02
Au	0.02	0.02	0.00	0.05	0.03
Sn	0.00	0.93	0.00	0.00	0.01
Se	0.00	0.01	0.00	0.00	0.01
Cd	0.04	0.11	0.02	1.01	0.03
Ge	0.00	0.01	0.00	0.00	0.01
Cl	0.00	0.03	0.00	0.01	0.06
Te	0.04	0.00	0.02	0.07	0.05
Hg	0.01	0.00	0.10	--	0.01
Total	98.56	99.69	102.73	99.84	100.55
n	5	6	2	4	8

Kattenhorn mine (Hilltop district)

	py	fah	gal	chl
Fe	44.12	1.21	0.00	0.14
S	49.48	15.33	12.62	0.08
Sb	0.06	7.69	0.16	0.00
As	0.00	0.16	0.00	0.00
Zn	0.07	19.28	0.06	0.00
Pb	0.00	0.17	84.27	0.00
Si	0.55	1.17	0.96	6.62
Ag	0.04	16.82	0.16	65.75
Cu	0.06	30.01	0.03	0.00
Mn	0.02	0.36	0.01	0.00
Au	0.01	0.06	0.02	0.18
Sn	0.00	4.58	0.01	0.00
Se	0.01	0.84	1.41	0.06
Cd	0.00	0.14	0.04	0.32
Ge	0.00	0.01	0.00	0.00
Cl	0.01	0.05	0.08	4.50
Te	0.03	0.25	0.01	0.18
Hg	0.01	0.13	0.00	0.02
Total	94.47	98.26	99.86	77.84
n	2	5	2	1

Notes: Py, pyrite; fah, fahlore; mia, miargyrite; asp, arsenopyrite; sph, sphalerite; gal, galena; cpy, chalcopyrite; chl, chlorargyrite-bromargyrite; stib, stibnite; bn, bournonite; cst, chalcostibnite; ac, acanthite; elec, electrum; geo, geffroyite; hes, hessite

n = number of analyses

All data in average wt. %

-- = not analyzed

Minerals not listed in tables = not present in samples analyzed.

Blue Dick mine (Hilltop district)						Betty O'Neal mine (Lewis district)								
	py	fah	ac	mia	asp		py	fah	ac	sph	gal	cpy	chl	bn
Fe	46.03	1.77	0.26	0.01	31.72	Fe	44.83	2.36	0.06	2.21	0.20	27.81	0.04	0.08
S	51.87	23.21	13.60	18.59	18.87	S	52.15	22.73	15.40	32.34	13.42	33.87	0.01	19.83
Sb	0.02	25.85	0.56	37.12	0.77	Sb	0.01	25.54	0.00	0.02	0.09	0.05	0.02	25.31
As	0.00	0.89	0.02	0.40	43.10	As	0.16	1.05	0.00	0.00	0.00	0.00	0.01	0.53
Zn	0.04	5.13	0.07	0.02	0.00	Zn	0.06	4.68	0.22	61.85	0.76	0.08	0.05	0.02
Pb	0.01	0.01	0.02	0.17	0.11	Pb	0.00	0.01	0.00	0.01	88.29	0.00	0.04	41.69
Si	0.09	0.04	0.24	0.07	3.84	Si	0.03	0.03	0.03	0.10	0.04	0.05	0.19	0.01
Ag	0.01	17.23	84.45	39.97	0.04	Ag	0.04	21.91	86.40	0.57	0.07	0.08	88.23	0.03
Cu	0.04	25.94	0.06	0.00	0.09	Cu	0.06	22.52	2.21	0.09	0.31	32.78	0.05	13.12
Mn	0.03	0.05	0.04	0.00	0.00	Mn	0.05	0.05	0.00	0.43	0.00	0.03	0.41	0.00
Au	0.00	0.00	0.00	0.00	0.00	Au	0.06	0.02	0.08	0.00	0.02	0.02	0.02	0.00
Sn	0.00	0.06	0.00	0.00	0.00	Sn	0.00	0.03	0.00	0.00	0.01	0.00	0.00	0.02
Se	0.01	0.05	0.10	1.36	0.00	Se	0.01	0.00	1.03	0.00	0.17	0.00	0.00	0.18
Cd	0.03	0.10	0.43	0.00	0.00	Cd	0.02	0.20	0.46	0.62	0.05	0.01	0.41	0.00
Ge	0.00	0.00	0.01	0.00	0.00	Ge	0.00	0.00	0.00	0.01	0.02	0.00	0.04	0.00
Cl	0.00	0.03	0.08	0.03	0.01	Cl	0.01	0.02	0.08	0.00	0.05	0.00	3.41	0.01
Te	0.00	0.00	0.13	0.00	0.00	Te	0.02	0.00	0.15	0.02	0.05	0.04	0.09	0.00
Hg	0.02	0.12	0.04	0.32	0.00	Hg	0.00	0.02	0.00	0.00	0.01	0.01	0.01	0.03
Total	98.17	100.43	100.10	98.06	98.56	Total	96.75	101.19	106.11	98.25	103.57	94.81	91.55	100.87
n	11	3	3	1	1	n	6	10	1	5	10	2	11	1

Grey Eagle mine (Bullion district)									Unnamed prospect (Bullion district)						
	py	fah	asp	sph	gal	cpy	hes	elec		py	fah	asp	sph	gal	geo
Fe	45.58	3.43	35.04	9.63	0.19	28.70	--	0.00	Fe	45.25	3.10	34.76	6.24	0.04	24.62
S	52.35	24.06	21.92	32.76	13.58	34.05	--	0.17	S	53.84	25.84	21.80	34.18	14.42	32.77
Sb	0.02	28.10	0.17	0.02	0.02	0.04	--	0.00	Sb	0.01	27.33	0.04	0.03	0.19	0.00
As	0.19	0.88	43.54	0.00	0.00	0.00	--	0.00	As	0.00	1.06	43.63	0.00	0.00	0.00
Zn	0.14	4.09	0.01	54.99	0.10	0.04	--	0.00	Zn	0.01	4.20	0.00	58.01	0.06	0.12
Pb	0.00	0.01	0.00	0.00	85.44	0.00	--	0.00	Pb	0.00	0.00	0.01	0.02	87.71	0.00
Si	0.07	0.04	0.01	0.04	0.03	0.08	--	0.04	Si	0.01	0.01	0.01	0.01	0.05	0.00
Ag	0.02	5.22	0.02	0.01	0.96	0.02	60.39	22.83	Ag	0.03	8.02	0.01	0.01	0.08	12.79
Cu	0.05	34.72	0.04	0.04	0.07	34.66	--	0.12	Cu	0.04	33.50	0.06	0.09	0.07	27.26
Mn	0.01	0.04	0.02	0.22	0.02	0.01	--	0.04	Mn	0.02	0.00	0.01	0.21	0.02	0.00
Au	0.04	0.03	0.05	0.03	0.00	0.02	--	77.29	Au	0.02	0.00	0.05	0.00	0.03	0.07
Sn	0.00	0.08	0.00	0.00	0.00	0.00	--	0.00	Sn	0.00	0.03	0.00	0.00	0.01	0.00
Se	0.01	0.01	0.00	0.01	0.00	0.01	--	0.02	Se	0.00	0.00	0.00	0.01	0.00	0.00
Cd	0.00	0.06	0.00	1.34	0.06	0.02	--	0.10	Cd	0.00	0.00	0.00	1.05	0.08	0.05
Ge	0.00	0.00	0.00	0.00	0.05	0.00	--	0.00	Ge	0.00	0.00	0.00	0.00	0.00	0.00
Cl	0.01	0.01	0.00	0.01	0.05	0.01	--	0.03	Cl	0.00	0.01	0.01	0.01	0.05	0.04
Te	0.03	0.00	0.02	0.02	0.12	0.00	37.99	0.03	Te	--	--	--	--	--	--
Hg	0.04	0.00	0.02	0.05	0.03	0.00	--	0.00	Hg	--	--	--	--	--	--
Total	98.54	100.78	100.88	99.16	100.74	97.66	98.38	100.67	Total	99.23	103.10	100.38	99.85	102.80	97.72
n	5	5	4	4	5	3	2	1	n	3	2	3	5	3	1

Notes: Py, pyrite; fah, fahlore; mia, miargyrite; asp, arsenopyrite; sph, sphalerite; gal, galena; cpy, chalcopyrite; chl, chlorargyrite-bromargyrite; stib, stibnite; bn, bournonite; cst, chalcostibnite; ac, acanthite; elec, electrum; geo, geffroyite; hes, hessite
n = number of analyses
All data in average wt. %
-- = not analyzed
Minerals not listed in tables = not present in samples analyzed.

6. Sphalerite/wurtzite (youngest)

Event No. Betty O'Neal mine (Kelson et al., 2005):

1. Quartz (oldest)
2. Carbonate ± Ca-sulfate + epidote ± sericite ± chlorite ± pyrite ± fahlore
3. Quartz + fahlore ± carbonate + sphalerite + galena + chalcopyrite +
 bournonite (Fig. 3.3i and 3.3j).
4. Quartz + barite
5. Quartz ± pyrite ± sericite
6. Sericite ± quartz ± pyrite ± clay
7. Quartz (youngest)

Intergrown fahlore (the primary Ag-bearing phase), galena, and bournonite in Betty O'Neal mine ore (Event 3, Fig. 3.3j) is unique among northern Shoshone Range vein deposits, but is texturally and mineralogically similar to ore from the Coeur d'Alene and Julcani mining districts (Sack and Goodell, 2002; Sack et al., 2002). This texture may indicate retrograde Ag-enrichment in fahlore occurred during cooling of a miargyrite-bearing galena; since Sack and Goodell (2002) estimate fahlore compositions are unaffected below ~220°C via this method, a minimum temperature of Betty O'Neal mine Event 3 mineralization may be inferred.

Porphyry-type mineralization

Weak Cu+Mo±Au porphyry-type mineralization is associated with some of the Tertiary granitic intrusions emplaced throughout the northern Shoshone Range, but typical alteration

halos associated with porphyry-type mineralization are largely absent due to the chemically unreactive nature of the siliciclastic and siliceous host rocks. Molybdenite spatially associated with felsic intrusive igneous rocks at the Hilltop and Tenabo deposits and Park Saddle area occurs as vein material or is disseminated throughout the host rock. Molybdenite-bearing veins always contain quartz and commonly carbonate minerals. Other associated phases include chalcopyrite, pyrite, and an unidentified mineral (avg. wt. %: S = 4.6, Sb = 0.2, Pb = 5.4, Se = 2.4, Bi = 56.5, Te = 28.2, O = 1.9, U = 1.1; total 100.3%, n = 44) commonly intergrown with Hilltop molybdenite (Kelson et al., 2005).

Methods

Samples of intrusive igneous rocks and vein ore from eight mineralized areas were collected throughout the northern Shoshone Range to investigate the mineralogy, geochemistry, and geochronology. Samples were collected in situ where possible (underground workings, surface outcrop, prospect pits, or drill holes) to note original field relationships; however, due to the inaccessibility of most underground workings, vein ore and gangue samples were collected from mine dumps and waste piles.

BSI Inspectorate Precious Metals and ALS Chemex provided thirty-one element analyses for each sample via fire assay (Au) and ICP (Ag, Al, As, B, Ba, Bi, Ca, Cd, Co, Cr, Cu, Fe, Hg, K, La, Mg, Mn, Mo, Na, Ni, P, Pb, Sb, Se, Sr, Tl, Th, V, W, Zn) (Appendix A). ALS Chemex also provided major- and rare earth- element analyses (via XRF and ICP, respectively) for intrusive igneous rocks (Table 3.3).

Table 3.3 (following page): Major and trace element chemical data for northern Shoshone Range igneous rocks.

No. on Fig. 5	1	2	3	4	5	6	7	8	9	10	11
Sample	HT02-5	CK02-8	CK02-14	GM-3	GM-4	GM-6	GM-10	GM-15	T99413-570	GRIT-53	PH-156-260
Rock type	granite	aplite	granite	granodiorite	amphibolite inclusion	granite	rhyolite dike	granite	granodiorite	basaltic andesite	silicified granite
Sample Location	Hilltop	Granite Mountain	Maysville Summit	Granite Mountain	Granite Mountain	Granite Mountain	Granite Mountain	Granite Mountain	Tenabo	Betty O'Neal	Hilltop
SiO ₂	78.18	87.20	79.18	70.87	54.77	78.25	74.75	79.95	66.07	54.19	86.70
TiO ₂	0.30	0.03	0.34	0.48	0.66	0.25	0.49	0.26	0.58	0.58	0.08
Al ₂ O ₃	9.06	7.84	9.16	8.73	14.59	10.56	8.25	9.31	16.16	13.61	4.97
Fe ₂ O ₃	0.58	0.07	0.56	1.50	1.57	0.46	0.66	0.53	0.51	0.98	0.45
FeO	3.31	0.37	3.19	8.47	8.92	2.59	3.74	3.02	2.92	5.56	2.52
MnO	0.01	0.01	0.05	0.26	0.30	0.05	0.04	0.04	0.03	0.10	0.05
MgO	1.67	0.07	1.55	3.73	5.12	1.06	2.18	1.07	2.38	6.84	3.17
CaO	1.33	0.02	1.45	2.71	7.78	1.68	1.41	1.75	4.24	8.73	1.21
Na ₂ O	1.58	1.54	2.34	2.35	3.22	2.48	1.66	2.03	3.01	1.52	0.03
K ₂ O	1.14	2.50	1.15	0.64	1.30	1.38	0.90	1.15	1.83	1.95	0.72
P ₂ O ₅	0.10	0.01	0.11	0.20	0.19	0.09	0.17	0.07	0.16	0.13	0.11
LOI	2.90	0.56	2.15	0.35	0.98	0.70	4.80	0.00	2.04	5.32	3.00
ox.tot (%)	100.16	100.22	101.23	100.29	99.40	99.55	99.05	99.18	99.93	99.51	103.00
Ag	0.0	1.9	0.2	0.0	0.0	0.0	0.0	0.1	0.1	12.1	0.8
As	9.0	36.0	0.0	11.0	NA	5.0	12.0	0.0	66.5	2.0	14.0
Au ppb	63.0	26.0	35.0	12.0	NA	11.0	2.0	16.0	68.5	20.0	310.0
B	14.0	5.0	10.0	12.0	NA	11.0	17.0	14.0	NA	8.0	NA
Ba	1520.0	341.0	1370.0	1015.0	362.0	1085.0	1390.0	1120.0	1175.0	1080.0	260.0
Be	2.2	2.5	1.8	2.2	2.3	2.5	1.7	2.1	2.0	1.3	NA
Bi	5.0	6.0	4.0	3.0	NA	4.0	10.0	2.0	0.1	3.0	6.0
Cd	1.5	0.0	0.6	0.6	NA	0.5	1.0	0.0	0.1	1.1	0.0
Ce	44.1	18.0	50.9	40.0	57.2	31.1	76.9	45.8	35.0	32.6	NA
Co	9.8	1.0	11.1	8.1	18.1	7.0	21.4	9.0	8.7	35.3	10.0
Cr	90.0	120.0	110.0	140.0	320.0	120.0	190.0	130.0	450.0	840.0	186.0
Cs	3.2	2.8	3.0	4.7	15.2	4.7	6.0	3.8	3.4	3.6	NA
Cu	310.0	3.0	8.0	2.0	2.0	3.0	16.0	1.0	9.0	37.0	655.0
Dy	2.3	2.6	2.7	2.6	8.5	2.4	3.2	2.4	1.9	2.5	NA
Er	1.4	2.0	1.6	1.5	4.6	1.4	1.7	1.5	1.1	1.5	NA
Eu	0.9	0.2	1.1	0.9	2.0	0.9	1.5	1.0	0.8	0.9	NA
Ga	18.0	12.0	21.0	20.0	21.0	20.0	19.0	20.0	18.0	17.0	NA
Gd	3.2	2.4	3.8	3.4	9.1	2.9	5.7	3.4	2.6	3.0	NA
Ge	0.2	0.1	0.1	0.1	0.2	0.1	0.2	0.2	0.1	0.2	NA
Hf	3.0	4.0	4.0	4.0	3.0	3.0	5.0	4.0	3.0	3.0	NA
Hg ppb	24.0	54.0	0.0	0.0	0.0	0.0	27.0	39.0	0.0	0.0	0.0
Ho	0.5	0.6	0.5	0.5	1.6	0.5	0.6	0.5	0.4	0.5	NA
In	0.1	0.0	0.0	0.0	0.2	0.0	0.1	0.0	0.0	0.0	NA
La	22.2	6.9	25.7	19.6	17.3	15.3	41.6	22.9	17.2	16.0	10.0
Li	27.3	7.8	19.1	44.2	27.2	72.6	46.2	41.4	13.8	51.9	NA
Lu	0.2	0.5	0.2	0.2	0.7	0.2	0.2	0.2	0.2	0.2	NA
Mo	11.0	3.0	2.0	3.0	0.0	2.0	2.0	0.0	3.0	0.0	87.0
Nb	8.0	14.0	9.0	10.0	13.0	10.0	16.0	10.0	7.0	6.0	NA
Nd	19.3	9.4	22.2	18.8	42.6	15.0	34.2	20.4	15.8	15.4	NA
Ni	10.0	3.0	13.0	8.0	62.0	11.0	60.0	10.0	13.0	164.0	52.0
P	353.0	64.0	480.1	437.0	829.2	368.0	850.0	377.0	710.0	228.0	470.0
Pb	69.0	53.0	43.0	22.0	12.0	20.0	23.0	18.0	11.0	14.0	28.0
Pr	5.4	2.5	6.3	5.1	9.5	4.1	9.6	5.5	4.0	4.1	NA
Rb	91.8	136.0	84.9	106.5	47.3	122.0	72.4	105.5	92.6	48.0	NA
Re	0.0	0.0	0.0	0.0	0.0	0.0	0.0	0.0	0.0	0.0	NA
S	177.3	NA	139.5	100.0	NA	23.5	NA	165.1	400.0	NA	NA
Sb	0.0	0.0	34.0	0.0	NA	0.0	0.0	0.0	0.4	0.0	0.0
Se	0.0	0.0	0.0	0.0	NA	0.0	0.0	0.0	1.0	0.0	NA
Sm	3.6	2.6	4.1	3.9	11.2	3.3	6.1	3.8	2.9	3.3	NA
Sn	2.0	0.0	0.0	3.0	5.0	1.0	5.0	5.0	1.0	2.0	NA
Sr	425.0	80.8	677.0	521.0	420.0	524.0	443.0	553.0	452.0	450.0	19.0
Ta	0.7	4.2	0.7	0.9	0.8	1.1	1.0	0.8	0.5	0.5	NA
Tb	0.4	0.4	0.5	0.4	1.5	0.4	0.6	0.5	0.4	0.4	NA
Te	0.2	0.1	0.0	0.0	0.0	0.0	0.0	0.0	0.1	0.0	NA
Th	7.0	22.0	8.0	7.0	6.0	6.0	11.0	9.0	7.0	5.0	NA
Ti	0.6	0.0	0.0	0.0	0.0	0.0	0.0	0.0	0.0	0.0	NA
Tm	0.2	0.4	0.2	0.2	0.7	0.2	0.2	0.2	0.1	0.2	NA
U	2.3	8.6	2.4	2.3	2.4	3.6	2.7	2.4	2.5	2.7	0.0
V	84.0	0.0	67.0	72.0	174.0	67.0	122.0	79.0	58.0	141.0	67.0
W	1.0	3.0	1.0	1.0	1.0	2.0	4.0	2.0	3.0	1.0	0.0
Y	13.6	19.4	16.3	16.2	49.3	15.4	19.2	15.9	11.2	15.4	67.0
Yb	1.2	2.7	1.4	1.5	4.6	1.5	1.3	1.4	1.1	1.4	NA
Zn	110.0	10.0	87.0	73.0	148.0	66.0	112.0	73.0	43.0	78.0	58.0
Zr	121.5	53.4	132.5	129.0	99.9	94.1	177.5	130.5	107.0	94.1	NA
tr.tot (%)	0.4	0.1	0.3	0.3	0.3	0.3	0.4	0.3	0.4	0.3	0.2
TOTAL	100.5	100.3	101.6	100.6	99.7	99.8	99.4	99.5	100.3	99.8	103.2

Notes: NA = not analyzed. All oxide data in wt. %; all trace element data in ppm unless noted otherwise.

The amount and stable isotopic signatures of organic carbon in carbonaceous fault gouge and unaltered and altered Ordovician Valmy Formation (upper plate) host rocks were determined at the Savannah River Ecology Laboratory (SREL). Each sample was powdered, weighed, and subjected to fuming HCl digestion for 24 hours at room temperature to remove all inorganic (carbonate) material. After rinsing and drying, the acid-insoluble residue was weighed again and sealed in clean tin capsules; the resulting $\delta^{13}\text{C}$ isotopic analysis follows the procedure outlined by Graves et al. (2002). The amount and isotopic signature of organic carbon in pebble dike/breccia matrix were determined at the Stable Isotope/Soil Biology Laboratory, University of Georgia Institute of Ecology, utilizing a Carlo Erba NA1500, CHN, Elemental Analyzer coupled to a Finnigan Delta C Mass Spectrometer via a Finnigan Conflo II Interface following similar methods (outlined above) and described by Coleman and Fry (1991) (Table 3.4).

Vein ore and gangue mineral identification, homogeneity (for isotope analysis), and composition were verified using transmitted and reflected light microscopy and a JEOL 8600 Electron Microprobe (Department of Geology, University of Georgia).

Carbon, oxygen, and sulfur stable isotope analyses from carbonate rocks and vein carbonate, sulfide, and sulfate minerals were conducted using vacuum extraction lines and a dual inlet Finnigan MAT 252 mass spectrometer (Stable Isotope Laboratory, Department of Geology, University of Georgia). Electron microprobe software, standards, operating conditions, and routines and techniques and standards associated with the stable isotope analyses are described in Kelson et al. (2005). Oxygen from vein quartz samples was analyzed at the Department of Earth and Planetary Sciences, University of New Mexico, using the laser fluorination technique of Sharp (1995) with a 25W Merchatek laser and BrF_5 as the fluorinating agent. The liberated O_2 , frozen directly into a Finnigan MAT 251 mass spectrometer inlet system after passing through

Table 3.4: $\delta^{13}\text{C}$ data for organic carbon-bearing rocks, breccias, and fault gouge, northern Shoshone Range.

Deposit	Sample	Description	% organic carbon in sample	$\delta^{13}\text{C}_{\text{PDB}}$
HT	CK98-01	Unaltered Valmy Formation quartzite	0.07	-27.3
HT	CK98-02	Unaltered Valmy Formation argillite	0.49	-28.0
HT	CK98-03	Unaltered Valmy Formation chert	0.27	-29.1
HT	CK98-05	Bleached and recrystallized Valmy chert near contact with intrusion	0.02	-30.1
HT	CK98-13	Partially bleached Valmy chert above Hilltop's Main Zone	0.06	-22.9
HT	CK98-15	Unaltered Valmy Formation siltstone	0.09	-25.9
HT	CK98-16	Unaltered Valmy Formation siltstone	0.4	-28.7
HT	97-15-590.5	2"-wide carbonaceous fault gouge	3.78	-30.2
HT	97-16-529.3	1"-wide carbonaceous fault gouge	0.76	-28.7
HT	97-16-550	≤ 3 "-wide carbonaceous "dike" / fault gouge	3.91	-29.8
HT	BURNS-01	Unaltered Valmy Formation chert directly below Main Zone	0.08	-29.4
BON	GRIT-08	Black fault gouge	0.25	-28.7
BON	GRIT-12	Black argillite with disseminated pyrite	0.47	-27.8
BD	BD-17*	Black matrix in unmineralized pebble dike / breccia	0.38	-29.1
BD	BD-23*	Black matrix in unmineralized pebble dike / breccia	0.63	-28.4
BD	BD-25*	Black matrix in unmineralized pebble dike / breccia	0.98	-29.5

Notes:

HT = Hilltop mine; BON = Betty O'Neal mine; BD = Blue Dick mine.

For all carbon and oxygen isotope values $\sigma = 0.19$ per mil; samples analyzed at Savannah River Ecology Lab (SREL).

* For all carbon isotope values $\sigma = 0.09$ per mil; samples analyzed at The Stable Isotope/Soil Biology Lab, University of Georgia Institute of Ecology.

NaCl to eliminate any remaining traces of F₂ gas, was desorbed from 5A molecular sieve by heating to 90°C for 10 minutes.

Salinity and homogenization temperatures of primary fluid inclusions within vein quartz were measured with a Fluid Inc. gas-flow heating/freezing system attached to a Leitz Laborlux S transmitted light microscope. Homogenization temperature accuracy is better than 1% of the measured value, and freezing point depressions are accurate within 1°C.

Geochronology of intrusive igneous rocks and vein mineralization was established using ⁴⁰Ar/³⁹Ar analyses of primary, unaltered (verified by transmitted light microscopy) biotite and/or amphibole separates handpicked from crushed rocks, and K-bearing gangue clay minerals separated from mineralized veins. Analyses were performed at the Radiogenic Isotope Laboratory (RIL, Department of Geological Sciences, The Ohio State University), the New Mexico Geochronological Research Laboratory (NMGRL, New Mexico Bureau of Geology and Mineral Resources), and the Pacific Centre for Isotopic and Geochemical Research (PCIGR, Department of Earth and Ocean Sciences, University of British Columbia). Sample GM-3 was used as an inter-laboratory standard. Ages for molybdenite were determined by the Re-Os method at AIRIE, Colorado State University.

⁴⁰Ar/³⁹Ar analyses of CK02-8 (potassium feldspar and muscovite), GM-10 (potassium feldspar), and GM-3 (biotite) were performed at PCIGR. Mineral separates were wrapped in aluminum foil and stacked in an irradiation capsule with similar-aged samples and neutron flux monitors (Fish Canyon Tuff sanidine, 28.02 Ma (Renne et al., 1998)). The samples were irradiated on October 20, 2005 at the McMaster Nuclear Reactor in Hamilton, Ontario, for 24 MWH, with a neutron flux of approximately 3×10^{16} neutrons/cm². Analyses (n=56) of 14 neutron flux monitor positions produced errors of <0.5% in the J value. The samples were baked

at ~120°C for four days prior to analysis on November 14 and 15 and December 7 and 8, 2005, at the Noble Gas Laboratory, PCIGR. The separates were step-heated at incrementally higher powers in the defocused beam of a 10W CO₂ laser (New Wave Research MIR10) until fused. The gas evolved from each step was analyzed by a VG5400 mass spectrometer equipped with an ion-counting electron multiplier. All measurements were corrected for total system blank, mass spectrometer sensitivity, mass discrimination, radioactive decay during and subsequent to irradiation, as well as interfering Ar from atmospheric contamination and the irradiation of Ca, Cl and K (isotope production ratios: (⁴⁰Ar/³⁹Ar)_K=0.0302, (³⁷Ar/³⁹Ar)_{Ca}=1416.4306, (³⁶Ar/³⁹Ar)_{Ca}=0.3952, Ca/K=1.83(³⁷ArCa/³⁹ArK).

All other geochronology methodologies are detailed in Kelson et al. (2005).

Intrusive Igneous Rocks

Northern Shoshone Range igneous rocks are part of the greater Tuscarora magmatic belt; a west-northwest-trending swath of 43-37 Ma, predominantly calc-alkalic, intermediate to felsic igneous rocks erupted or emplaced across northern and northeastern Nevada and west-central Utah (Armstrong, 1970; Stewart and McKee, 1977; Silberman, 1985; White, 1985; Christiansen and Yeats, 1992; Kelson et al., 2005; and this study). Coeval volcanic equivalents of northern Shoshone Range intrusive igneous rocks have not been identified (Gilluly and Gates, 1965).

Petrography and mineralogy

Intrusive igneous rocks are emplaced along a west-northwest trend throughout the northern Shoshone Range (Gilluly and Gates, 1965; Kelson et al., 2000; Kelson et al, 2005) and underlie most of the area (Fig. 3.4). Samples of unaltered, subalkaline igneous rocks collected for this study include granite, granodiorite, and basaltic andesite (Fig. 3.5) (Le Maitre, 2002). These rocks occur as variably sized stocks, plugs, or dikes located both distal and proximal to (or host) base- and precious-metal bearing vein deposits; others are associated with molybdenite (porphyry)-type mineralization and others are completely barren.

The Granite Mountain stock is the largest (~10 km²) exposed intrusion in the northern Shoshone Range. It consists mostly of granodiorite (GM-3) with variably sized inclusions of amphibolite (GM-4) (oldest), quartz diorite porphyry, and granodiorite porphyry (youngest); granitic components (GM-6) are also present. Quartz diorite porphyry (GM-15) occurs peripherally to the stock, and aplite (CK02-8) and rhyolite dikes (GM-10) post-date all other phases. The granodiorite is light gray in color and is mineralogically similar to the intrusive rocks at Tenabo and Hilltop; major phases include equigranular quartz, hornblende, biotite, plagioclase, and K-feldspar. Accessory phases include magnetite, apatite, and sphene (Gilluly and Gates, 1965; and this study). Fragments of country rocks within the stock are rare, suggesting passive emplacement.

Aplite dikes are white-light tan, rarely more than 20 cm wide, and contain essentially no macroscopic minerals; electron microprobe analysis reveals ≤1 mm-long grains of mostly K-feldspar, muscovite, and quartz with minor amounts of hematite and thorite. Dark brown, fine-grained rocks originally described as lamprophyre dikes by Gilluly and Gates (1965) are in fact

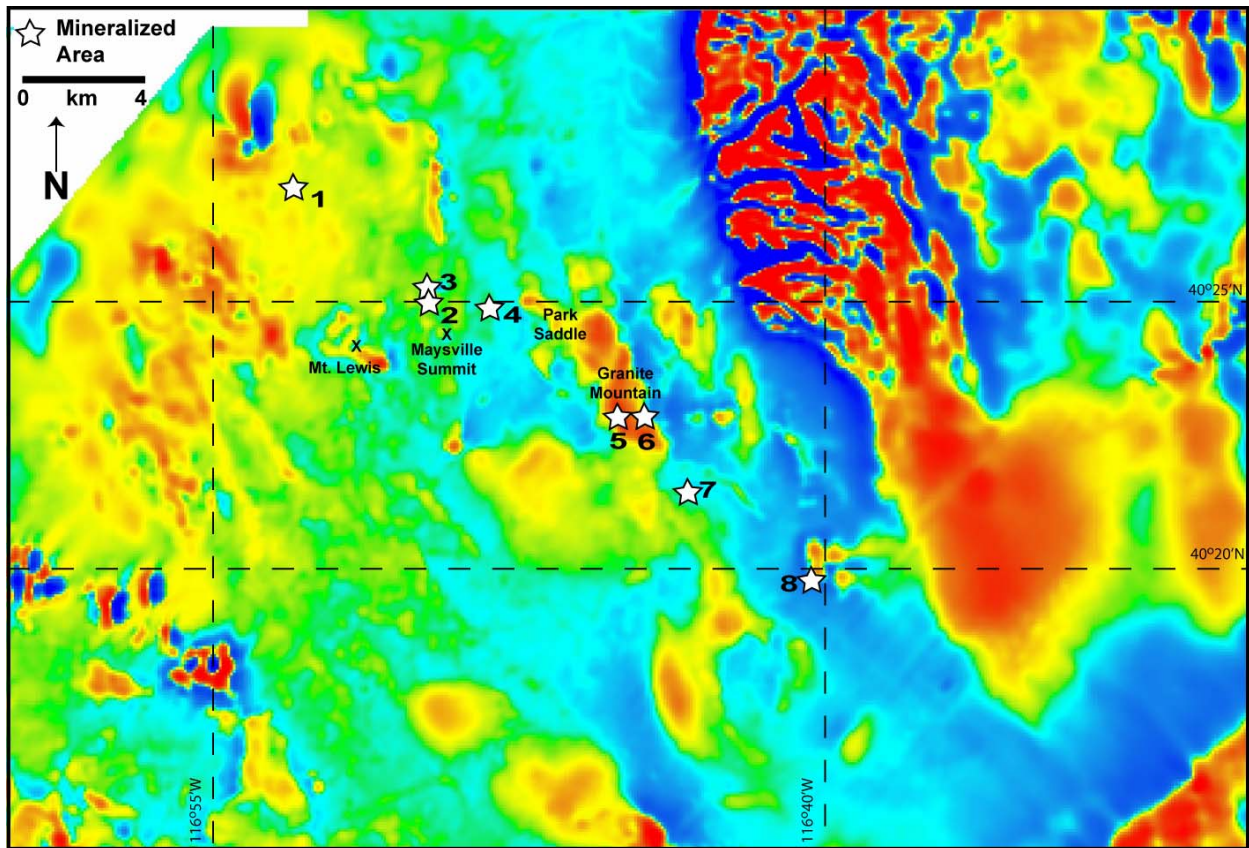


Figure 3.4: Aeromagnetic map of the northern Shoshone Range study area and adjacent areas, band pass filtered to emphasize magnetic structures and bodies between the surface and 500 m. Red colors indicate magnetic “highs” (e.g. igneous rocks); blue colors indicate magnetic “lows” (e.g. limestone). Courtesy of Placer Dome U.S., Inc. See Fig. 3.2 for mineralized area (stars) legend.

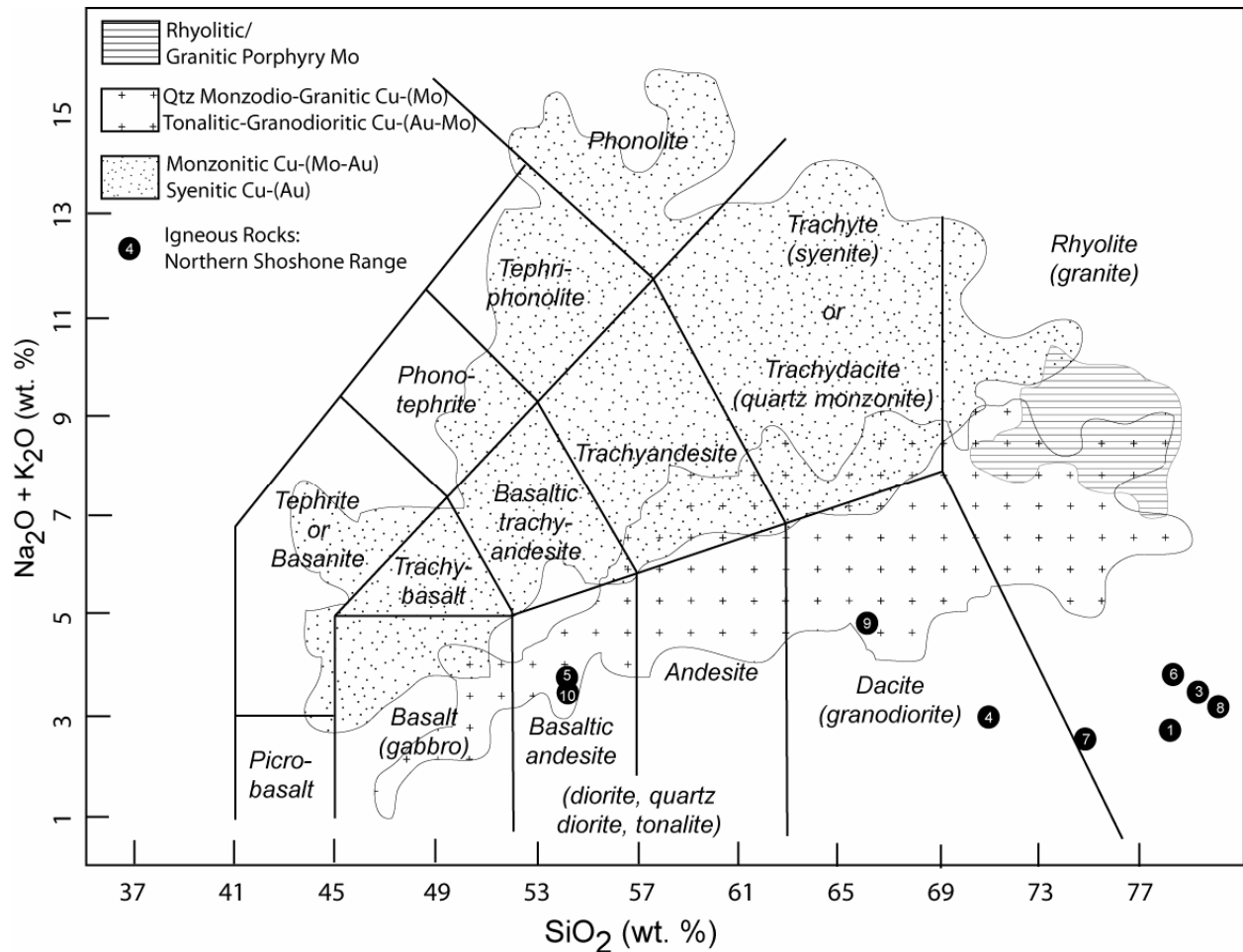


Figure 3.5: Whole rock chemical data plot for least altered northern Shoshone Range igneous rocks compared to igneous rocks related to porphyry systems (modified from Le Maitre, 2002; Seedorff et al., 2005). See Table 3.3 for sample number identification.

rhyolites (GM-10), composed of quartz, ilmenite, K-feldspar (fresh cores with argillized rims), chlorite, barite, dolomite (\pm Fe), apatite, hematite, and rare fresh biotite. The abundance of chlorite (as groundmass and biotite replacement), carbonate, and argillized feldspars probably indicate pneumatolytic alteration of the rock's original minerals by volatile-rich fluids. Based on $^{40}\text{Ar}/^{39}\text{Ar}$ data, the aplite and rhyolite dikes are essentially contemporaneous.

None of the phases within the Granite Mountain stock are mineralized or exhibit large-scale, pervasive, hydrothermal alteration indicative of porphyry-type mineralization. Alteration halos between the granitic host rock and all other phases and inclusions are absent; only country rocks in contact with the stock exhibit minimal and limited alteration (bleaching, hornfels). However, the Granite Mountain stock hosts two base- and precious-metal-bearing veins (the Gray Eagle mine and an unnamed prospect) and several isolated groups of barren quartz + barite \pm carbonate veins.

The Hobo Gulch intrusion, located 0.5 km south of the Hilltop gold deposit, is a small ($< 0.5 \text{ km}^2$) granitic stock and probably represents the westernmost extension of the larger, mostly-buried Park Saddle – Granite Mountain pluton (Fig. 3.4). The relationship of the Hobo Gulch intrusion to four coextensive, cospatial, and rootless felsic dikes (oldest to youngest, based on cross-cutting relationships: diorite, feldspar porphyry, quartz feldspar porphyry, granodiorite) within the Hilltop deposit (Kelson et al., 2000) is difficult to establish. These felsic dikes are locally fractured or sheared and mineralized.

Unlike the Granite Mountain stock, portions of the Hobo Gulch intrusion and all of Hilltop's felsic dikes exhibit varying degrees of phyllic, propylitic, and/or argillic alteration. Ordovician Valmy Formation rocks are frequently bleached and recrystallized adjacent to the

Hobo Gulch intrusion; organic carbon-rich chert and argillite beds are commonly recrystallized into a featureless, amorphous white rock near the contact (Kelson et al., 2000) (Table 4.4). Alteration of country rocks near the felsic dikes is minimal. The upper portion of the Hobo Gulch intrusion and Hilltop's felsic dikes contain fragments of altered (bleached) Valmy Formation rocks in varying amounts (up to 90% of the total igneous rock, locally), sizes (\leq 0.5m), and angularity. An unmineralized, rock flour-matrix breccia pipe containing clasts of altered Valmy Formation rocks and altered intrusive igneous rocks mantles the Hobo Gulch intrusion. Molybdenite + chalcopyrite-bearing quartz veins occur along the periphery and in the cupola of the Hobo Gulch intrusion, within adjacent country rocks, and within Hilltop's felsic dikes.

An unmineralized, dark gray basaltic andesite (GRIT-53) is exposed only on the northwest flank of the northern Shoshone Range near the Betty O'Neal mine, and is interpreted as a hypabyssal intrusion. This rock contains macroscopic phenocrysts of feldspar, biotite, clinopyroxene, pyrite, and abundant \leq 2 cm, white/clear quartz xenocrysts in a groundmass of carbonate, clinopyroxene, feldspar, and minor pyrite/ilmenite/magnetite. Biotite phenocrysts are partially or completely altered to epidote \pm chlorite \pm pyrite; feldspars contain fresh cores surrounded by a thin argillized rim, and clinopyroxene phenocrysts are completely altered to carbonate \pm pyrite. The quartz xenocrysts have a sub-rounded to rounded morphology and exhibit evidence of chemical disequilibrium (embayments and rims altered to fine-grained pyroxene) with the surrounding groundmass. The quartz xenocrysts closely resemble pieces of Betty O'Neal mine quartz veins, suggesting the intrusion post-dates vein mineralization. Classification of this rock (basaltic andesite) based on whole-rock geochemistry is difficult due to the SiO₂ contributed by the quartz xenocrysts.

Eocene basaltic andesites are uncommon within the northern Carlin trend, and pre-date gold mineralization within the Carlin trend (Ressel and Henry, in review).

Major and trace element geochemistry

Although detailed geochemical analysis of northern Shoshone Range igneous rocks is not the main focus of this study, major and trace element data were collected to identify any geochemical differences between barren igneous rocks (CK02-8, CK02-14, GM-3, GM-4, GM-6, GM-10, GM-15, and GRIT-53) and igneous rocks more closely associated with mineralization (HT02-5, T99413-570, PH-156-260). Major element geochemical data show that igneous rocks collected throughout the northern Shoshone Range have variable alkali contents ($\text{Na}_2\text{O} + \text{K}_2\text{O}$ range from 2.56% to 4.84%) and mostly plot as granodiorites and granites on a total alkali-silica diagram (Le Maitre, 2002) (Fig. 3.5). Two samples (CK02-8 and PH-156-260) are not plotted; each contains ~87 wt % SiO_2 representing late-stage, silica-rich aplite and altered (silicified) granite, respectively.

All least-altered igneous rocks are plotted on chondrite-normalized REE diagrams using values from Sun (1980) and Sun and McDonough (1989) and MORB-normalized spider diagrams using values from Pearce (1983). The five igneous phases present within the Granite Mountain stock are shown together (Figs. 3.6 and 3.7). Samples GM-3, GM-6, and GM-15 (granodiorite-granite) are enriched in LREE relative to the HREE, typical of felsic liquids containing feldspar, hornblende, apatite, and sphene; GM-10 (brown rhyolite dike) and the other igneous rocks exhibit similar LREE-enriched patterns. The negative Eu anomaly in GM-4 (amphibolite inclusion) supports the paucity of feldspar in the sample and/or an Eu-depleted (or

Figure 3.6 (following page): Chondrite-normalized REE diagrams for least altered igneous rocks, northern Shoshone Range, compared to other Eocene igneous rocks associated with mineralization in the Carlin trend (data from Ressel et al., in review). Normalization values from Sun (1980). See Table 3.3 for sample data.

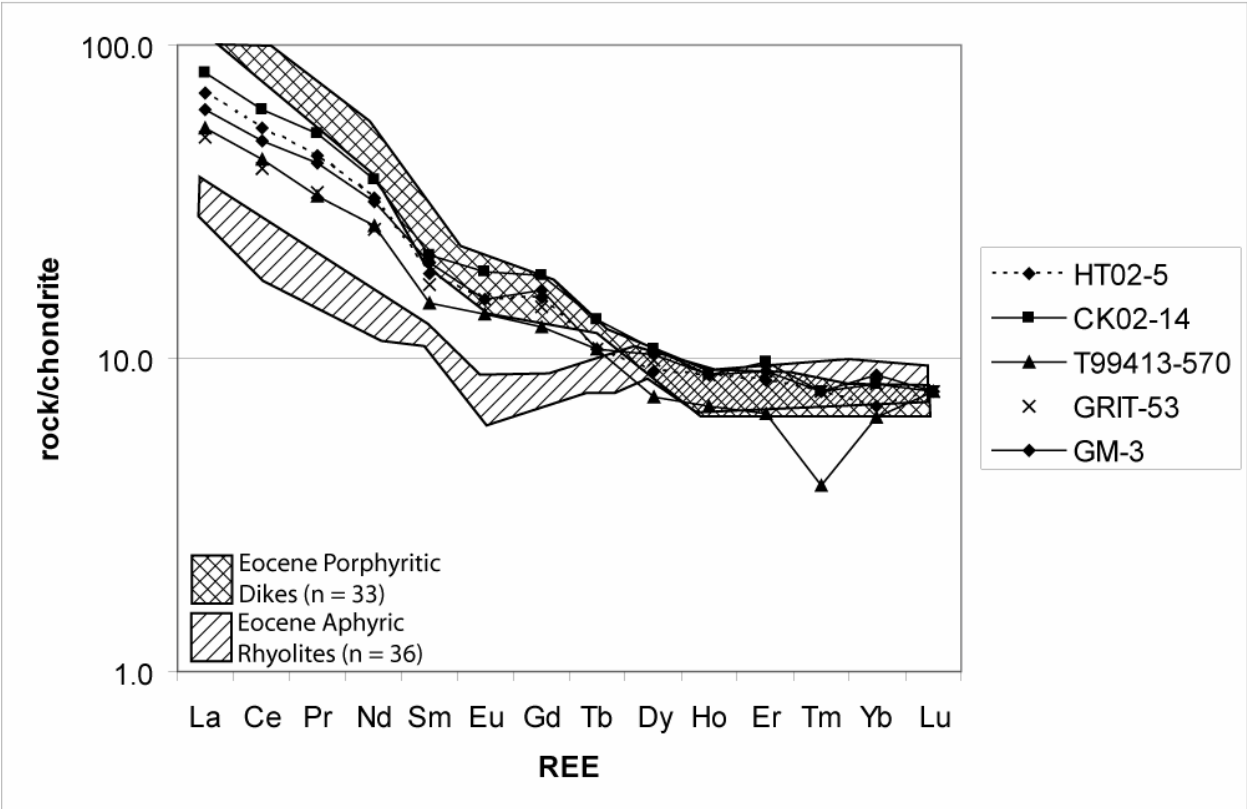
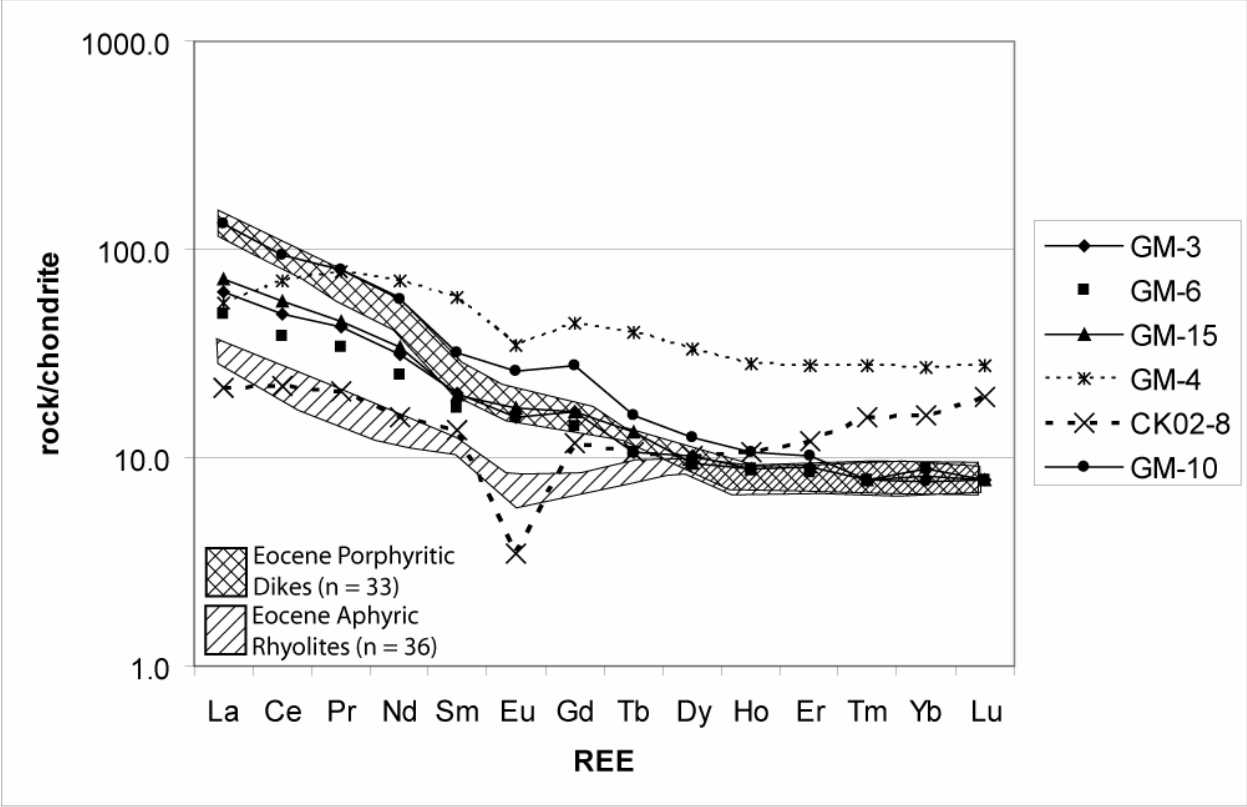
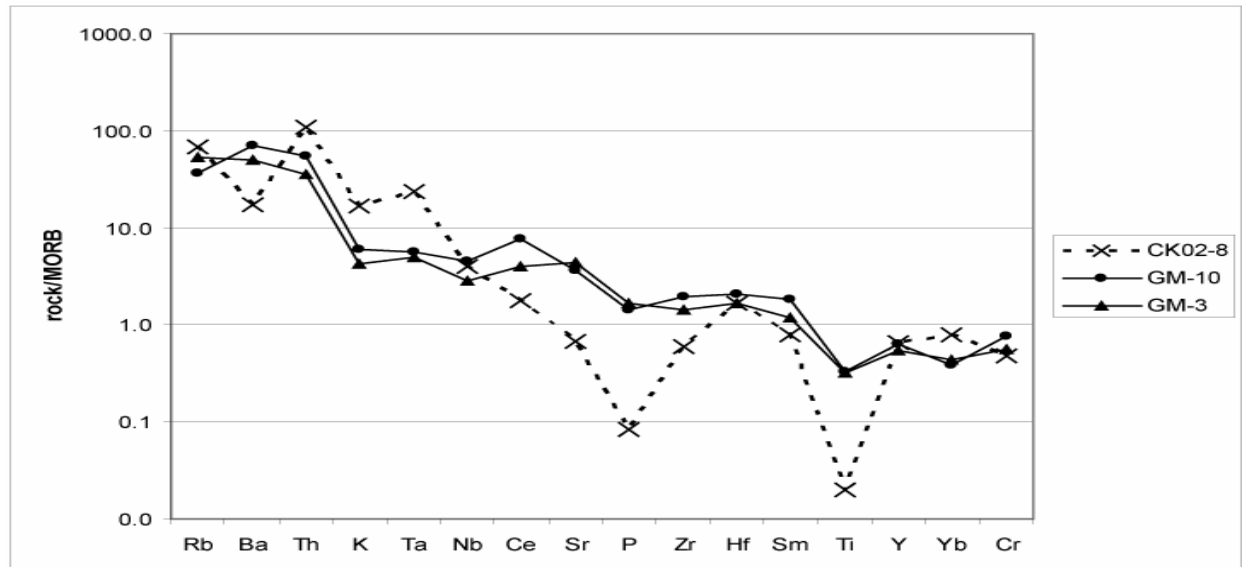
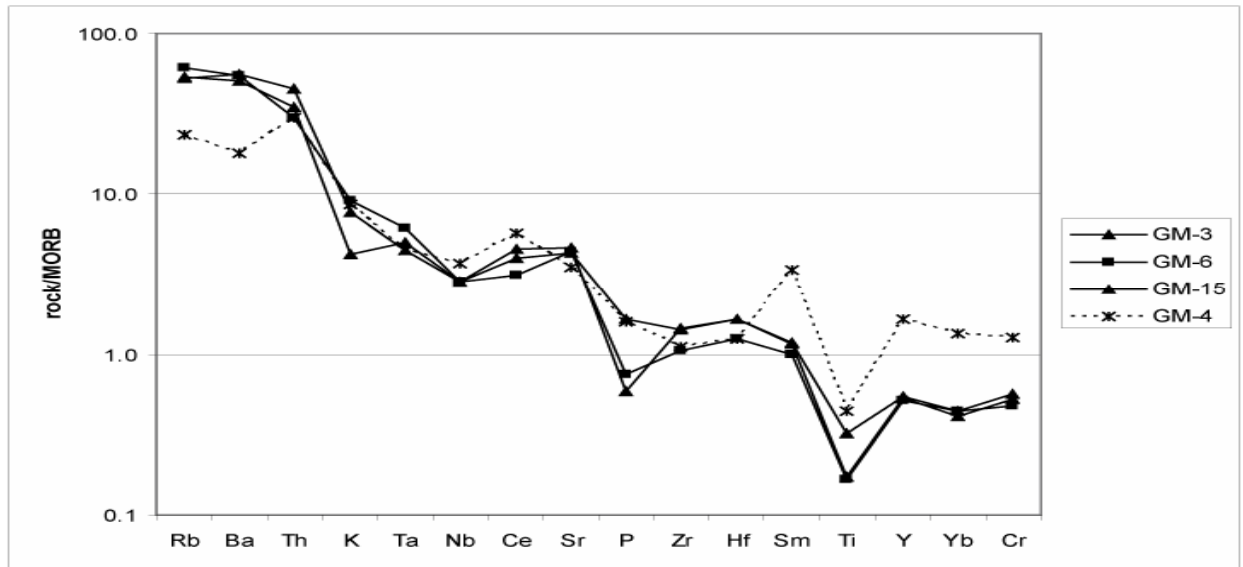
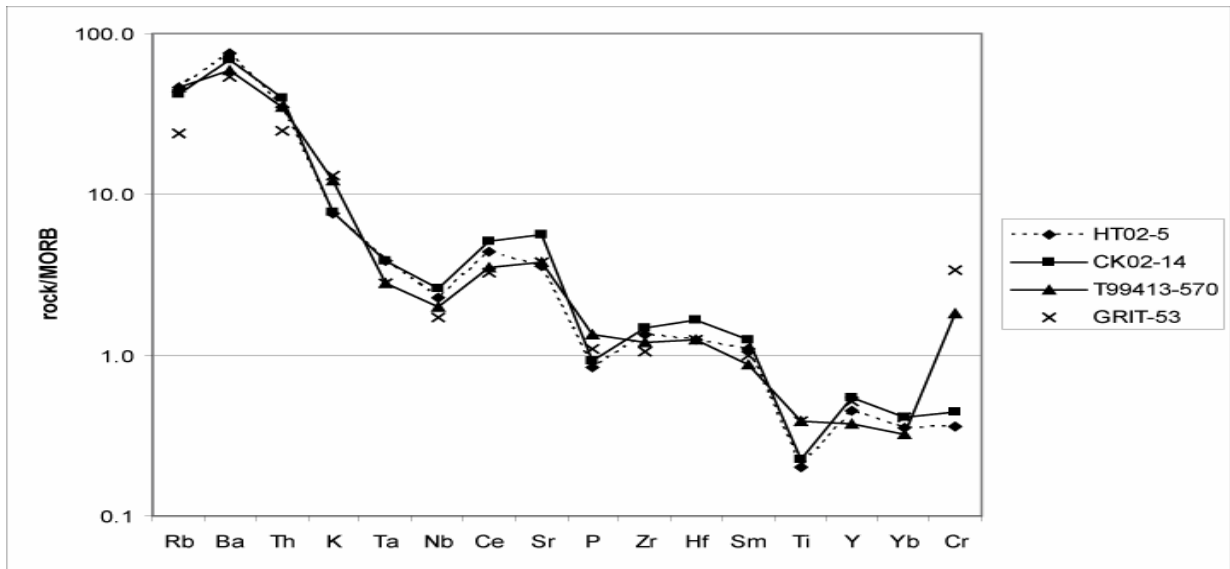


Figure 3.7 (following page): MORB-normalized spider diagrams for least altered igneous rocks, northern Shoshone Range. Normalization values from Pearce (1983). See Table 3.3 for sample data.



Eu-retaining) magma source (Rollinson, 1995); the large negative Eu anomaly in the aplite dike (CK02-8) is probably due to the extensive removal of plagioclase or residual plagioclase in the source material. Rare earth element patterns for northern Shoshone Range igneous rocks are similar to Eocene porphyritic dikes and aphyric rhyolites (n = 39) associated with gold mineralization within the Carlin trend (Ressel and Henry, in review). The spider diagram patterns (Fig. 3.7) are typical of felsic igneous rocks, except for the exaggerated patterns of CK02-8 (aplite dike) and GM-4 (amphibolite inclusion). Elevated Cr concentrations in GRIT-53 and T99413-570 probably reflect contamination from the laboratories' sample preparation (e.g. crushing) equipment. Discrimination diagrams [Rb-(Y+Nb)] classify all igneous rocks studied here as volcanic arc granites (after Pearce et al., 1984) but do not delineate any major differences between mineralized and unmineralized samples.

Geochronology

Kelson et al. (2005) and this study utilized $^{40}\text{Ar}/^{39}\text{Ar}$ and Re-Os to determine the ages of northern Shoshone Range igneous rocks and mineralization. Previous workers (Silberman and McKee, 1971) obtained ages via K-Ar for some northern Shoshone Range igneous rocks; however, the $^{40}\text{Ar}/^{39}\text{Ar}$ method offers more precise analyses and is more resistant to subsequent thermal disturbances than K-Ar. The Re-Os chronometer in molybdenite has been shown to endure thermal overprints (Stein et al., 1998; 2001; 2003; Selby and Creaser, 2001). Mineral separates analyzed include biotite, amphibole, muscovite, potassium feldspar, illite, and molybdenite; no whole rock analyses were performed.

Fifteen of the seventeen samples analyzed via $^{40}\text{Ar}/^{39}\text{Ar}$ from Kelson et al. (2005) and this study yielded plateau ages, each plateau represents more than 61% of the total ^{39}Ar released from similar-age adjacent portions of the release spectra. Two samples (DSC BXA, PH-156 260) yield no plateau, probably indicating sample disturbance and excess or loss of ^{40}Ar (Lanphyre and Dalrymple, 1976). Construction of $^{36}\text{Ar}/^{40}\text{Ar}$ vs. $^{40}\text{Ar}/^{39}\text{Ar}$ plots (utilizing all steps) and calculation of isochron ages were done for samples yielding no age plateau. Isochron ages are determined by the slope and intercept of a line drawn through points representing $^{36}\text{Ar}/^{40}\text{Ar}$ and $^{40}\text{Ar}/^{39}\text{Ar}$ ratios measured from each released gas fraction, and indicate sample age and excess or loss of radiogenic Ar relative to atmosphere (York, 1969; Steiger and Jäger, 1977). Previous age data for igneous rocks obtained via conventional K-Ar analysis are compiled with $^{40}\text{Ar}/^{39}\text{Ar}$ and Re-Os age data from Kelson et al. (2005) and this study and summarized in Table 3.5 and Figure 3.8. All previous and present $^{40}\text{Ar}/^{39}\text{Ar}$ ages reported in Table 3.5 and Figure 3.8 have been normalized relative to 28.02 Ma Fish Canyon sanidine (Renne et al., 1998).

$^{40}\text{Ar}/^{39}\text{Ar}$ age spectra; igneous rocks

Northern Shoshone Range igneous rocks yield ages between 39.7 and 38.5 Ma. Most sample ages are calculated from gas released from at least three contiguous steps (plateaus); total gas ages are used when no plateau is defined. Early heating steps of biotite and hornblende separates typically exhibit anomalous K/Ca values and low amounts of released radiogenic gas, probably indicating alteration or small amounts of contaminants in the minerals' rims (see Appendix B for all $^{40}\text{Ar}/^{39}\text{Ar}$ age spectra and associated data). The spectrum for GRIT-53 biotite yields a plateau containing > 87% of the gas released, not including step H (inaccurate due to

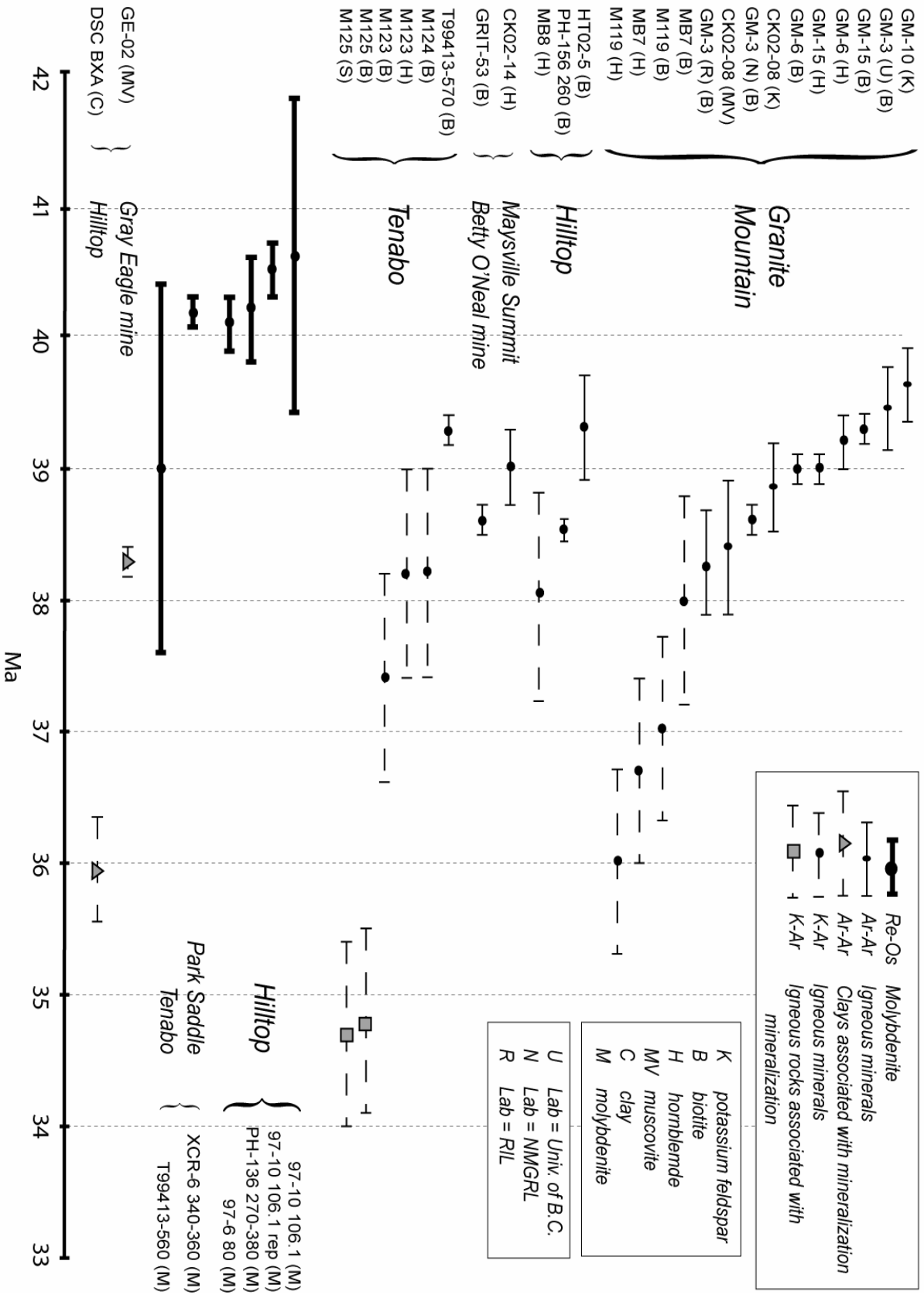
Table 3.5 (following page): Summary of all K-Ar, Ar/Ar, and Re-Os geochronology data for northern Shoshone Range igneous rocks, molybdenite (porphyry) mineralization, and vein-hosted mineralization.

Sample No.	Sample Location	Mineral Analyzed	Re. ppm	¹⁸⁷ Os, ppb	% K ₂ O	Plateau Steps	Plateau % ³⁹ Ar	Plateau Age (Ma)	⁴⁰ Ar/ ³⁹ Ar Isochron Age (Ma)	Total Gas Age (Ma)	K-Ar Age (Ma)	Re-Os Age (Ma)	Reference	Host Rock / Comments
M-125	Tenabo	biotite			8.24						34.8 ± 0.7		1	Dikes that intrude the Tenabo stock and are spatially associated with gold-quartz veins.
M-124	Tenabo	sanidine			11.6						34.7 ± 0.7		1	
M-123	Tenabo	biotite			8.79						38.2 ± 0.8		1	Tenabo stock.
199413-570	Tenabo	hornblende			1.08						37.4 ± 0.8		1	
199413-560	Tenabo	biotite			8.04	8	85.6	39.3 ± 0.1			38.2 ± 0.8		2	Tenabo stock.
(MIDD-49)												39.0 ± 1.4	2	Quartz vein within the Tenabo stock.
XCR-6 340-380 (MIDD-291)	Park Sdile	molybdenite	0.5769 (2)	0.2432 (2)								40.2 ± 0.1	2	Molybdenite + pyrite disseminated in feldspar porphyry.
MB7	Gr Min	biotite			7.66						38.0 ± 0.8		1	Granodiorite.
M119	Gr Min	hornblende			0.95						36.7 ± 0.7		1	Granodiorite.
		biotite			7.25						37.0 ± 0.7		1	Granodiorite.
		hornblende			0.89						36.0 ± 0.7		1	Granodiorite.
GM-3 (R)	Gr Min	biotite			7.9	19	96	38.3 ± 0.4	37.8 ± 0.2				2	Granodiorite. STANDARD
GM-3 (N)	Gr Min	biotite			7.73	7	97.1	38.6 ± 0.1	39.5 ± 0.3				2	Granodiorite. STANDARD
GM-3 (U)	Gr Min	biotite			NR	5	90.8	39.5 ± 0.2	38.5 ± 0.6				3	Granodiorite. STANDARD
CK02-08	Gr Min	muscovite			NR	5	97.4	38.4 ± 0.5	38.9 ± 2.1				3	Aplitic dike hosted by Granite Mountain stock.
GM-10	Gr Min	k-feldspar			NR	4	84.1	38.8 ± 0.5	39.6 ± 0.6				3	Rhyolite dike hosted by Granite Mountain stock.
GM-6	Gr Min	k-feldspar			NR	3	75	39.6 ± 0.3	39.6 ± 0.6				2	Granite.
		biotite			7.97	5	63	39.0 ± 0.1					2	
		hornblende			1.29	6	61.3	39.2 ± 0.2					2	Granite
GM-15	Gr Min	biotite			8.31	7	86.5	39.3 ± 0.1					2	Granite
GE-02	Gray Eagle	hornblende			1.09	7	71.9	39.0 ± 0.1					3	Sulfide-bearing quartz vein.
CK02-14	May. Sum.	hornblende			4.36	15	100	38.3 ± 0.1					3	Granite.
MB8	Hilltop	hornblende			0.23	8	95.4	39.0 ± 0.3			38.1 ± 0.8		1	Hilltop stock (Hobo Gulch intrusion?)
PH-156 280	Hilltop	biotite			1.02								3	Hobo Gulch intrusion.
HT02-5	Hilltop	biotite			8.36								3	Hobo Gulch intrusion.
DSC BXA	Hilltop	biotite			3.2	6	84.4	39.3 ± 0.4	35.9 ± 0.4	42.4 ± 0.4			2	Mixed muscovite/smectite clay from gold-bearing discordant quartz breccia pipe.
		muscovite			3.3								2	Quartz vein within Hobo Gulch intrusion.
97-6 80	Hilltop	molybdenite	142.34 (3)	59.7 (2)							40.1 ± 0.2		2	Quartz vein within Hobo Gulch intrusion.
(MIDD-63)													2	Quartz vein hosted by Ordovician Valmy argillite.
97-10 106.1	Hilltop	molybdenite	51 (2)	21.88 (3)							40.6 ± 1.2		2	Quartz vein hosted by Ordovician Valmy argillite.
(MIDD-51)													2	Quartz vein hosted by Ordovician Valmy argillite.
97-10 106.1	Hilltop	molybdenite	49.59 (3)	21.06 (4)							40.5 ± 0.2		2	Replicate analysis to improve spiking.
(MIDD-64)													2	Replicate analysis to improve spiking.
PH-136 270-380 (MIDD-290)	Hilltop	molybdenite	18.5 (2)	7.79 (5)							40.2 ± 0.4		2	Molybdenite + chalcopyrite-bearing quartz vein in brecciated Ordovician Valmy Formation rocks.
GRT-53	Betty O'Neal	biotite			8.31	6	87.7	38.6 ± 0.1					3	Hyabys'sal basaltic andesite.

Notes:

References: 1) Silberman and McKee (1971); 2) Kelson et al. (2005); 3) This study.
(R) = Standard analyzed at the Radiogenic Isotope Laboratory, The Ohio State University.
(N) = Standard analyzed at the New Mexico Geochronological Research Laboratory, New Mexico Institute of Mining and Technology.
(U) = Standard analyzed at the Argon Geochronology Laboratory, Pacific Centre for Isotopic and Geochemical Research, University of British Columbia
For Re and ¹⁸⁷Os concentration data, absolute uncertainties shown, all at two sigma level, for last digit indicated.
Uncertainties for all ⁴⁰Ar/³⁹Ar ages are listed in Appendix B
All ⁴⁰Ar/³⁹Ar ages for samples reported in Kelson et al. (2005) and in this study have been normalized relative to 28.02 Ma Fish Canyon Sanidine.
Park Sdile = Park Saddle; Gr Min = Granite Mountain; May Sum = Maysville Summit
See Kelson et al. (2005) for all other information regarding Re-Os analyses and methodologies.

Figure 3.8 (following page): Summary of all geochronology (K-Ar, Ar/Ar, Re-Os) data for igneous rocks and molybdenite mineralization and vein-associated minerals, northern Shoshone Range. See Table 3.5 for sample descriptions and references.



mass spectrometer problem during analysis). Plateaus comprised of at least 5-steps and 83% gas released define the ages of most samples. The age of PH-156 260 biotite is based on the total amount of gas released, as step heating did not yield a definable plateau.

Biotite and hornblende separates were analyzed from GM-6 and GM-15 and subsequent plateau ages calculated from at least 61% released gas over five to eight contiguous steps. Since the plateau ages represent the time of closure to Ar loss associated with magma cooling below 550°C (hornblende) and 350°C (biotite) (McDougall and Harrison, 1999), a maximum cooling rate of 200°C / 480 k years for GM-3 (northern tip of the Granite Mountain stock) may be estimated. However, due to the similar plateau ages of biotite and hornblende from both samples, the Granite Mountain stock probably cooled quickly implying a relatively shallow level of emplacement.

Potassium feldspar from GM-10 (rhyolite dike) yields an $^{40}\text{Ar}/^{39}\text{Ar}$ age of 39.6 ± 0.3 Ma (older than the host granite) based on a hump-shaped release spectra with a 3-step plateau accounting for 75% of released ^{39}Ar , and represents a maximum sample age.

$^{40}\text{Ar}/^{39}\text{Ar}$ age spectra; clay minerals

Two clay minerals were analyzed to constrain ages of base and precious-metal mineralization. DSC BXA (mixed-layered muscovite/smectite) required no separation and was identified via X-ray diffraction (XRD) prior to encapsulation and $^{40}\text{Ar}/^{39}\text{Ar}$ analysis (Kelson et al., 2005). Sample GE-02 (muscovite) was identified via microscopy and did not require encapsulation after separation. DSC BXA (muscovite/smectite) was recovered from the gold-

bearing matrix of the Hilltop deposits' discordant quartz breccia pipe, and GE-02 (muscovite) was separated from an ore-bearing quartz vein from the Gray Eagle mine.

Sample DSC BXA did not yield a plateau age; however, corrected ages of 35.9 ± 0.4 Ma (isochron) and 42.4 ± 0.4 Ma (total gas) are calculated based on three heating steps. Although the data are poorly resolved, the isochron age is probably more accurate. The source of excess ^{40}Ar (isochron intercept $^{36}\text{Ar}/^{40}\text{Ar} = 0.0031$; atmosphere = 0.0034) is unclear.

Sample GE-02 (muscovite) yielded a well-behaved, 15-step plateau age of 38.3 ± 0.1 Ma. See Appendix B for all $^{40}\text{Ar}/^{39}\text{Ar}$ data for igneous rocks and mineralized samples from the northern Shoshone Range.

Re-Os data; molybdenite (porphyry mineralization)

Five molybdenites from four samples from the Hilltop district yield ages from 40.1 ± 0.2 to 40.6 ± 1.2 Ma with a weighted mean of 40.2 ± 1.7 Ma (MSWD = 2.4, 95% CL). A single molybdenite sample from the Tenabo deposit yields a 39.0 ± 1.4 Ma age (Kelson et al., 2005).

Relationship between Magmatism and Mineralization

$^{40}\text{Ar}/^{39}\text{Ar}$ and Re-Os data

Rhenium-osmium ages of molybdenite from the Hilltop district and Tenabo deposit are systematically slightly older than $^{40}\text{Ar}/^{39}\text{Ar}$ ages for primary biotite and hornblende from nearby intrusive igneous rocks. The age difference is interpreted here as the delay in isotopic closure of

argon-based systematics in a thermally perturbed regime (e.g. Stein et al., 2001). Thus, the Re-Os and $^{40}\text{Ar}/^{39}\text{Ar}$ ages both record an association between pluton emplacement and molybdenite mineralization (Table 3.5).

Fluid inclusion data from vein deposits

Primary fluid inclusion homogenization temperature and salinity measurements were made from fifteen quartz vein samples from six separate deposits (Table 3.6). Secondary and pseudosecondary fluid inclusions were not considered. Primary fluid inclusions were frozen before being subjected to heating tests; homogenization temperatures (i.e. *minimum* fluid trapping temperatures) range from 109°C to 425°C (n = 179) and salinities from six deposits range from 0 to 6.4 equiv wt % NaCl. Primary fluid inclusion homogenization temperatures and salinities also vary within the same vein, yielding a range of calculated vein quartz source fluid ($\delta^{18}\text{O}$) signatures. Primary fluid inclusion data are pressure corrected assuming quartz deposition at one km depth under lithostatic pressure (25 MPa; Potter, 1977; Ehlers and Blatt, 1980) as no evidence of boiling was observed. All measured inclusions homogenized by disappearance of the vapor bubble and contained no daughter salts. Variations in vein quartz opacity, color (clear to milky white), and morphology affected the number of measurable fluid inclusions. Earlier fluid inclusion measurements (Lisle and Desrochers, 1988) from Hilltop's discordant quartz breccia pipe generally agree with data presented here, although Lisle and Desrochers (1988) also noted vapor-dominated inclusions.

Table 3.6: Salinity and homogenization temperatures for primary fluid inclusion as well as oxygen isotope compositions of host vein quartz, northern Shoshone Range vein deposits.

Deposit	Sample	Number of Inclusions Measured	Measured $\delta^{18}\text{O}$	Th ($^{\circ}\text{C}$)	Salinity		$\delta^{18}\text{O}$ source fluid (calculated)
					Range eq.wt% NaCl	$10^3 \ln \alpha$ Quartz-Water	
Gray Eagle	GE-X1-B	30	13.89	295 - 380	4.2 - 6.2	7.7 - 5	6.2 - 8.9
Gray Eagle	GE-02	3	13.32	275 - 327	0 - 1.7	8.4 - 6.4	4.9 - 6.9
		18		336 - 393	0 - 4.5	6.3 - 4.7	7.0 - 8.6
Hilltop	DSC BXA	13	6.99	109 - 175	0 - 0.2	18.8 - 13.8	-11.8 to -6.8
		3		270	nm	8.6	-1.6
Hilltop	97-10-106.1	15	14.66	306 - 350	1.9 - 2.9	7.3 - 6.7	7.4 - 8
Hilltop	CK02-4A	23	2.14	228 - 314	0 - 1.9	10.5 - 6.9	-8.4 to -4.8
Hilltop	97-10-841	4	11.1	195 - 259	nm	12.5 - 12.2	-1.4 - 2.1
Betty O'Neal	GRIT-38B	4	-0.26	270 - 280	0 - 3.4	8.6 - 8.2	-8.9 to -8.5
Betty O'Neal	GRIT-26B	8	-0.97	156 - 206	1.6 - 2.2	15.2 - 11.9	-16.2 to -12.9
Blue Dick	BD-21B lite	0	5.46	nm	nm	nm	nm
Blue Dick	BD-21B dark	0	6.14	nm	nm	nm	nm
Kattenhorn	KATT-1B	12	8.54	181 - 218	0.5 - 2.2	13.4 - 11	-4.9 to -2.5
Kattenhorn	KATT-10	1	0.79	335	nm	6.2	-5.4
Lovie	LOVIE-31	4	17.34	300 - 310	nm	7.4 - 7	9.9 - 10.3
		11		325 - 383	nm	6.6 - 4.9	10.7 - 12.4
		2		425	nm	4	13.3
Lovie	LOVIE-22A	3	16.17	272	2.1	8.5	7.67
		4		205 - 230	nm	11.9 - 10.4	4.27 - 5.77
Lovie	LOVIE-35B	21	16.7	300 - 377	4 - 6.4	7.4 - 5.1	9.3 - 11.6

Notes:

1. Data only for primary fluid inclusions.
2. All oxygen isotope values relative to VSMOW.
3. nm = not measured.
4. All Th values pressure corrected (1 km depth, lithostatic conditions) using data from Potter (1977).

Stable isotope data from vein deposits

$\delta^{18}\text{O}$ data indicate variable and mixed vein quartz source fluids. Source fluid signatures were calculated using the quartz-water fractionation equation of Clayton et al. (1972) with data from vein quartz $\delta^{18}\text{O}$ (measured) and primary fluid inclusion homogenization temperatures. Calculated $\delta^{18}\text{O}$ vein quartz source fluid compositions from six deposits range from nearly pure meteoric (e.g. Betty O'Neal mine) to nearly pure magmatic (e.g. Lovie mine); other deposits formed from variable mixtures of meteoric and magmatic fluids (Figs. 3.9, 3.10, and 3.11). $\delta^{18}\text{O}$ reference values for primary granodioritic magmatic water and north-central Nevada meteoric water (ca. 40 Ma) are extrapolated from Beck (1992), Field and Fifarek (1985) and Ressel and Henry (in review).

$\delta^{13}\text{C}$ and $\delta^{18}\text{O}$ data from vein carbonate minerals and upper plate limestone range from –11.7 to –0.2 per mil ($\delta^{13}\text{C}$) and –4.7 to 17.0 per mil ($\delta^{18}\text{O}$), indicating a mostly magmatic source ($\delta^{13}\text{C}$ range –4 to –7 per mil; $\delta^{18}\text{O}$ range –5 to 5 per mil) (Field and Fifarek, 1985). Relatively depleted $\delta^{13}\text{C}$ values may indicate an organic carbon component ($\delta^{13}\text{C}$ –27.8 per mil, average) from the upper plate host rocks (Table 3.7). Isotopically similar carbonaceous matter also occurs as unmineralized fault gouge ($\delta^{13}\text{C}$ –29.3 per mil, average, Hilltop mine) and unmineralized pebble dike matrix ($\delta^{13}\text{C}$ –29.0 per mil, average, Blue Dick mine). Upper plate carbonate lenses ($\delta^{13}\text{C}$ –4.7 and $\delta^{18}\text{O}$ 16.5 per mil, average) occur in the Lovie mine area and may have isotopically influenced Lovie mine vein carbonate minerals (Table 3.7, Fig. 3.12).

The $\delta^{34}\text{S}$ values for vein sulfide minerals (n = 94) range from –19 to 22 per mil; vein barite (n = 25) values range from 5.9 to 21.9 per mil (Table 3.8). Most (95%) sulfide sulfur values coincide with other sulfide data from Cu-porphyry deposits (–3 to 9 per mil) and zoned

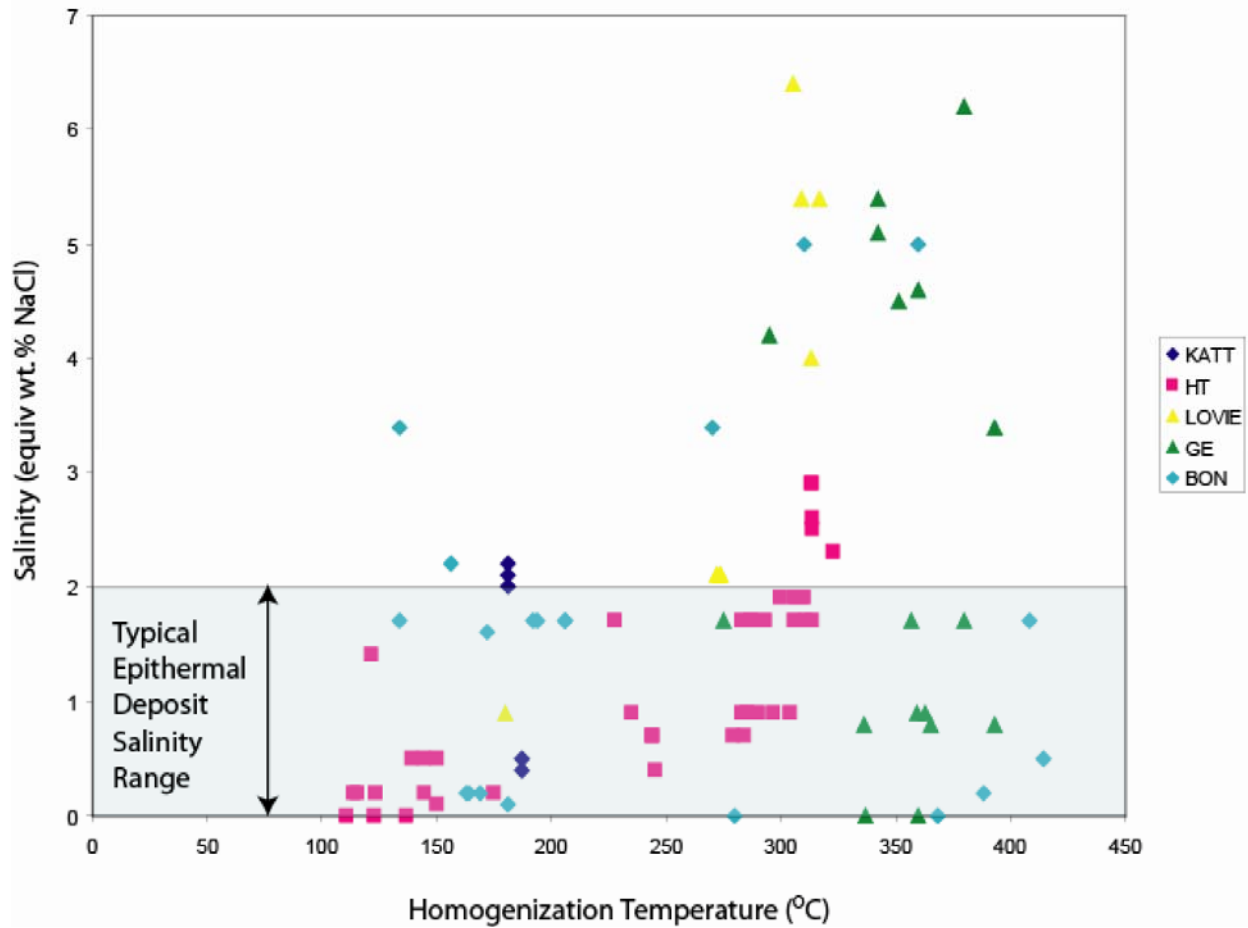


Figure 3.9: Salinity vs. homogenization temperature plot of primary fluid inclusion data from northern Shoshone Range ore-bearing quartz veins. KATT = Kattenhorn mine; HT = Hilltop deposit; LOVIE = Lovie mine; GE = Grey Eagle mine; BON = Betty O’Neal mine.

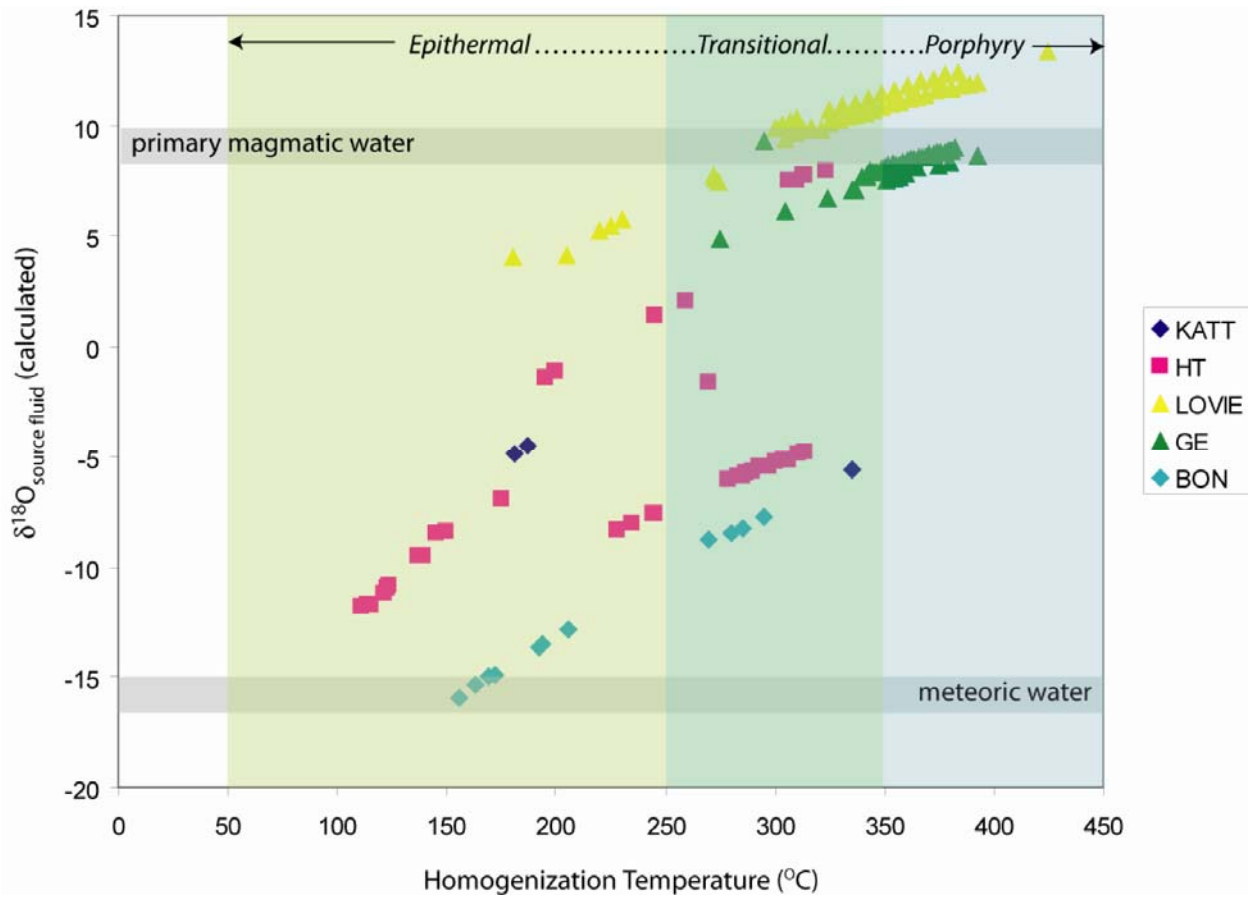


Figure 3.11: Plot of primary fluid inclusion homogenization temperatures vs. calculated $\delta^{18}\text{O}$ for fluids associated with vein quartz carrying epithermal – porphyry-type base- and precious metal mineralization. Figure 3.10: Plot of salinity vs. calculated $\delta^{18}\text{O}$ for fluids associated with ore-bearing vein quartz. KATT = Kattenhorn mine; HT = Hilltop deposit; LOVIE = Lovie mine; GE = Grey Eagle mine; BON = Betty O’Neal mine.

Table 3.7: $\delta^{13}\text{C}$ and $\delta^{18}\text{O}$ data for carbonate gangue minerals and upper plate (?) limestone, northern Shoshone Range vein deposits. Data from Kelson et al. (2005).

Deposit	Sample	Description	Host Rock	$\delta^{13}\text{C}_{\text{PDB}}$	$\delta^{18}\text{O}_{\text{VSMOW}}$
HT	97-8-106.8-1	1/2"-wide qtz vein with carb + py +cpy in center	Phyl. altered Tgd	-6.1	2.9
HT	97-8-136-1	F.g. carb in center of 3/4"-wide euhedral qtz vein	Prop. altered Tgd	-8.8	3.3
HT	97-8-136-2	1/4"-wide envelope of euhedral carb bordering 97-8-136-1 vein	Prop. altered Tgd	-11.7	6.0
HT	97-10-305.8	1/8"-wide envelope of carb+bar+kaol bordering qtz vein	Prop. altered Tfp	-2.5	3.3
HT	97-11-168	1/2"-wide cal veinlet	Valmy siliciclastics	-8.7	9.3
HT	97-11-700-2	1/8"-wide envelope of carb+bar bordering 97-11-700-3 vein	Valmy siliciclastics	-6.0	12.8
HT	97-11-700-3	1/2" -wide carb+qtz+bar+rock frag vein	Valmy siliciclastics	-5.2	7.9
HT	97-13-221-1	Euhedral cal xtals in f.g. groundmass (97-13-221-3)	Phyl-prop alt Tgd	-5.4	2.4
HT	97-13-221-3	F.g. carb+ser groundmass	Phyl-prop alt Tgd	-4.9	2.7
HT	97-13-92.5	$\leq 1/2"$ -wide carb vein	Phyl. altered Tfp	-5.9	14.4
HT	97-13-390-1	Carb crystals along fracture	GRDR	-3.2	4.2
BON	1-8S-B-2	$\leq 3/4"$ -wide carb vein between massive qtz and wall rock	Carb vein	-3.4	8.7
BON	05A-1	Carb+qtz matrix between rock clasts	Breccia	-4.5	7.3
BON	06A-1	Carb matrix between rock clasts w/ gal+fah+sph	Breccia	-3.4	0.1
BON	29A-1	1/2"-wide cal vein (with rock clasts)	Massive qtz vein	-3.7	-0.6
BON	32-1	Massive carb	Massive carb vein	-2.9	-1.3
BON	55-1	Massive carb	Massive carb vein	-3.4	2.9
BON	10-1	Piece of qtz+carb+bar with py+sph	Breccia	-7.4	11.7
BON	64-1	Massive carb	Massive carb vein	-2.9	-4.7
BON	34-2	qtz+carb matrix breccia with black siltstone(?) clasts	Breccia	-2.4	-1.6
BON	07-2	1/2" -wide area of py+carb stockwork veinlets	Silicified siltstone(?)	-3.2	3.2
Lovie	37-1	Black and white carb breccia with silicified rock clasts	Breccia	-1.6	16.7
Lovie	42-2	Massive cal cut by chl+ep veins	Massive cal vein	-0.2	17.0
Lovie	46-1	Unaltered limestone float	Limestone	-4.7	18.8
Lovie	46-2	Unaltered limestone float	Limestone	-4.7	14.1
UN	CK02-13-1	Piece of carb+py+cpy+sph+qtz vein (float)	Vein	-3.8	-2.5
UN	CK02-11-1	Qtz+cal vein with ser+py+gal+sph+fah+asp	Phyl-arg. altered Tgd	-2.3	2.6

Notes:

HT = Hilltop mine; BON = Betty O'Neal mine; Lovie = Lovie mine; UN = unnamed prospect.

Alteration: Phyl = phyllic; Prop = propylitic; Arg = argillic.

Tgd = Tertiary granodiorite; Tfp = Tertiary feldspar porphyry; GRDR = Granodiorite.

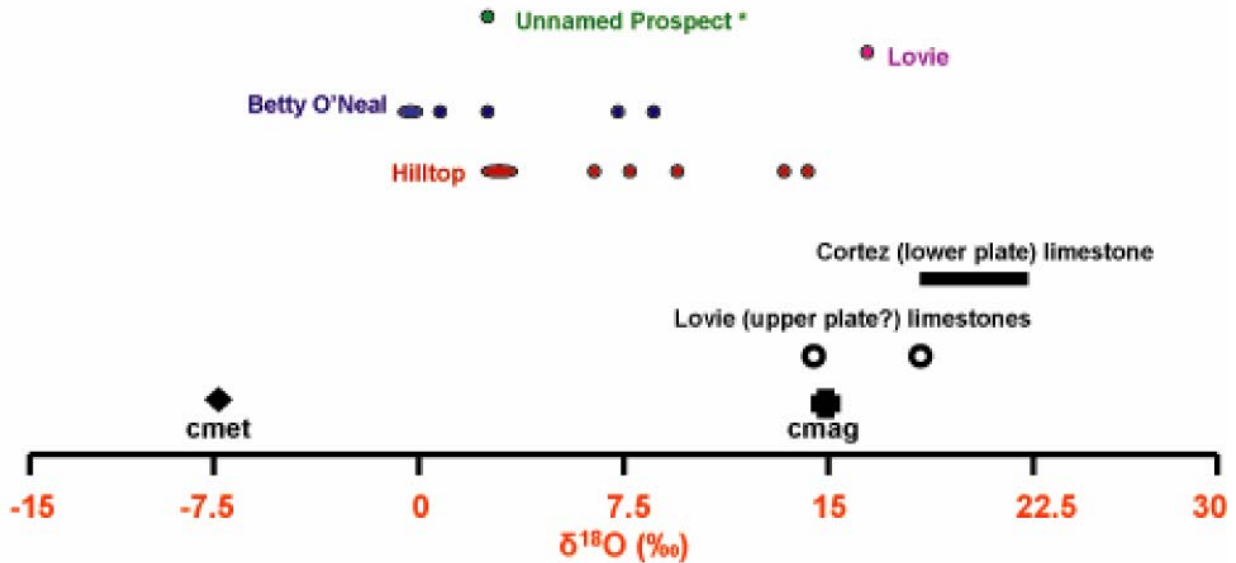
Carb = carbonate; py = pyrite; cpy = chalcopyrite; qtz = quartz; kaol = kaolinite; bar = barite; gal = galena; fah = fahlore; sph = sphalerite; asp = arsenopyrite; ser = sericite; chl = chlorite; cal = calcite; ep = epidote.

All data corrected using the fractionation factor of calcite at 50°C = 1.00922525

Unless specified, "carb" refers to CaCO_3 with small impurities of Fe, Mg, and/or Mn.

For all carbon and oxygen isotope values $\sigma = 0.1$ per mil; analyses performed at the Stable Isotope Laboratory, University of Georgia.

Oxygen isotopes (carbonate minerals)



Carbon isotopes (carbonate minerals)

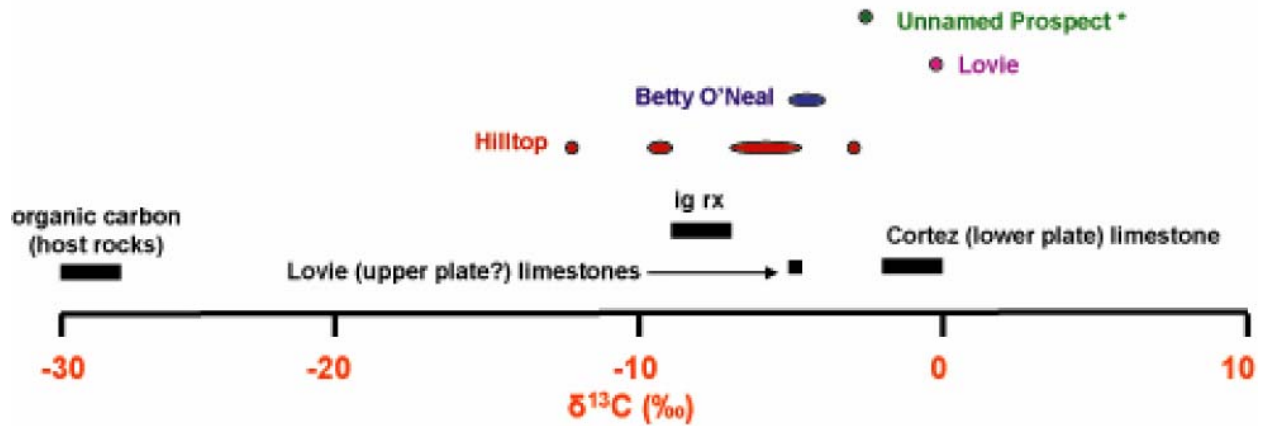


Figure 3.12: Plot of carbon and oxygen isotope data from carbonate gangue minerals associated with mineralization. Cortez Range (lower plate) carbonate rocks (Field and Fifarek, 1985) are compared with Lovie (upper plate?) limestones and organic carbon (this study). Calcite in equilibrium with meteoric water (cmet) and primary granodioritic magmatic water (cmag) at 250°C (Kelson et al., 2005).

Table 3.8 (next page): $\delta^{34}\text{S}$ data for sulfide and sulfate minerals from northern Shoshone Range
vewin deposits. Data from Kelson et al. (2005).

Deposit	Sample	Mineral	$\delta^{34}\text{S}_{\text{CDT}}$	Deposit	Sample	Mineral	$\delta^{34}\text{S}_{\text{CDT}}$
BON	49-1	bar	19.3	HT	97-6-80-1	moly	5.6
BON	04B-1	py	4.9	HT	97-6-80-3	py	5.4
BON	52	bar	18.2	HT	97-7-365-PY3	py	2
BON	56A-1	py	5.9	HT	97-7-365-PY4	py	2.3
BON	51SB-1	bar	19.5	HT	97-7-365-PY2	py	-2.6
BON	07-1	py	4.7	HT	97-8-436-1	py	-2.7
BON	08-1	py	4.9	HT	97-8-380.6-B7	mel py	-0.4
BON	35-4	bar	18.2	HT	97-8-380.6-B6	mel py	-12.1
BON	27-3	fah	4.5	HT	97-8-380.6-B4	mel py	-7.2
BON	35-5	fah	4.6	HT	97-8-380.6-B5	mel py	-7.6
BON	27-3	fah	4.4	HT	97-8-466	bar	15.2
Lovie	22-2	py	7	HT	97-8-380.6-B8	mel py	5.6
Lovie	22-3	gal	3.6	HT	97-8-416	stib	5.5
Lovie	29-2	py	6.3	HT	97-8-106.8-2	py	5.5
Lovie	03B-2	sph	6.2	HT	97-8-380.6-C	mel py	2
Lovie	05-1	sph	5	HT	97-8-380.6-B3	mel py	-5.4
Lovie	35A-1	gal	5.6	HT	97-8-380.6-B1	mel py	4.6
Lovie	09-1	bar	20.9	HT	97-8-380.6-B2	mel py	1.1
Lovie	27-1	py	7.1	HT	97-9-358-1	py/asp	5.8
Lovie	03A-1	py	5.1	HT	97-10-1084.5-2	py	5.1
KATT	27A-1	bar	13.6	HT	97-10-1084.5-1	sph	4.9
KATT	31-1	bar	11	HT	97-10-106.1-1	moly	4.3
KATT	12-1	bar	16.3	HT	97-10-1181.5-2	py	6
KATT	09-1	bar	21.5	HT	97-10-1161.7	py	6.4
KATT	3-4-5-S-1	bar	11.3	HT	97-10-1160.6-2	py	5.4
GE	08-1	py	7.1	HT	97-10-1160.6-1	gal	3.2
GE	05-1	sph	6.7	HT	97-10-1134.2-1	gal	3.5
GE	04-2	py	6.6	HT	97-10-1206.4-1	py	5.5
GE	X1-1	py	6.3	HT	97-11-665.3-1	bar	10.4
GE	10-1	py	6.2	HT	97-11-700-1	bar	5.9
GE	05-2	py	5.8	HT	97-11-665.3-4	py	5.8
GE	09-2	py	6.8	HT	97-11-1232.5-1	py	22
GE	07-2	py	6.5	HT	97-11-1235.4-1	bar	16.3
GE	04-4	sph	7.1	HT	97-11-1106-1	bar	10.9
GE	04-1	gal	5.8	HT	97-11-665.3-3	sph	5.2
GM	18	bar	17.7	HT	97-11-1027.5-1	py	4.4
GM	13-1	bar	18.7	HT	97-11-991	py	6.2
HT	HT02-12-SITE	stib	3.8	HT	97-11-1235.4-2	py	14.4
HT	HT02-14-1	py	4.3	HT	97-11-1168-1	bar	13.9
HT	HT02-8-1	stib	3.9	HT	97-13-221-2	py	5.8
HT	CK02-4/5-1	py	-2.1	HT	97-13-373-1	py	4.8
HT	CK02-4/5-2	py	4.5	HT	97-14-212	stib	2.9
HT	CK02-4/5-3	py/asp	3.5	HT	97-15-488.5-3	py	5.3
HT	CK02-22	bar	18	HT	97-15-488.5-1	py	-2.7
HT	CKO2-31	gal	3.1	HT	97-15-488.5-2	py	6.9
HT	CKO2-28	py	4.1	HT	97-15-488.5-5	py	7.1
HT	CKO2-29-1	py	4.4	HT	97-15-567-1	py	-18.9
HT	CKO2-21	bar	17.7	HT	97-16-484-1	py	-15.6
UN	CK02-11-3	py	7	HT	97-16-484-2	py	5.3
UN	CK02-11-2	sph	6.2	HT	97-16-503.3-3	py	-1.9
UN	CK02-11	py	6.9	HT	97-16-503.3-1	py	-15.9
HT	CK02-1-2	asp	5.1	HT	97-16-339	py	4.1
HT	CK02-2-2	asp/py	4.9	HT	97-16-430.9-2	py	-1.0
HT	CK02-32	gal	3.6	HT	97-16-503.3-2	py	-10.6
HT	Sb-P-1	bar	14.8	HT	97-16-430.9-1	py	-2.1
HT	Sb-P-2-2	bar	21.3	HT	97-16-430.9-3	py	4.2
HT	Sb-P-2-1	stib	3.3	HT	BURNS-05	bar	16
HT	97-1-497B-1	bar	12.7	HT	BURNS-05-3	py	-2.3
HT	97-5-473.5-1	bar	14.3	HT	IND. N. ADIT-1	py	4.9
HT	97-6-434	stib	3.3				

BON = Betty O'Neal mine; Lovie = Lovie mine; KATT = Kattenhorn mine; GE = Grey Eagle mine; GM = Granite Mountain; HT = Hilltop deposit / area; UN = Unnamed prospect.

bar = barite; py = pyrite; sph = sphalerite; gal = galena; stib = stibnite; asp = arsenopyrite; moly = molybdenite; mel py = melnikovite pyrite (b=band; c=center band); fah = fahlore.

For all sulfur isotope data $\sigma = 0.1$.

polymetallic veins (-6.3 to 4.9 per mil) (gray box, Fig. 3.13) – mineralization widely accepted as being magmatic in origin (Field and Fifarek, 1985; Hedenquist and Lowenstern, 1994). Sulfides with relatively depleted (<-6.3 per mil) sulfur isotope values probably derived their sulfur from a biogenic source; enriched (> 10 per mil) sulfur isotope values probably indicate fluid interaction with diagenetic pyrite or hydrothermal sulfate (Field and Fifarek, 1985).

Calculated depositional temperatures (Table 3.9) of nine co-existing sulfide mineral pair from four deposits using sulfur isotope fractionation equations of Kajiwara and Krouse (1971) (Kelson et al., 2005) mostly agree with primary fluid inclusion homogenization temperatures (this study).

Discussion: Northern Shoshone Range Vein-Hosted Mineralization

Mineralogical, fluid inclusion, and stable isotope data suggest ore-bearing veins within the northern Shoshone Range formed from fluids with a wide range of temperatures and compositions. Some veins (i.e. Betty O’Neal mine, Hilltop’s discordant quartz breccia pipe) formed from relatively low temperature, low salinity, meteoric fluids (<300°C, <2 equiv wt % NaCl); others (i.e. Lovie mine, Gray Eagle mine) formed from higher temperature, more saline, magmatic fluids (300-425°C, 4-6.4 equiv wt % NaCl). Other veins formed under intermediate conditions.

A shallow depositional depth (~ 1 km) is assumed for northern Shoshone Range vein deposits based on high vein densities and large vein widths (up to 3 m; Emmons, 1910, Guilbert and Park, 1986). Fractures within siliceous and siliciclastic host rocks served as both pathways

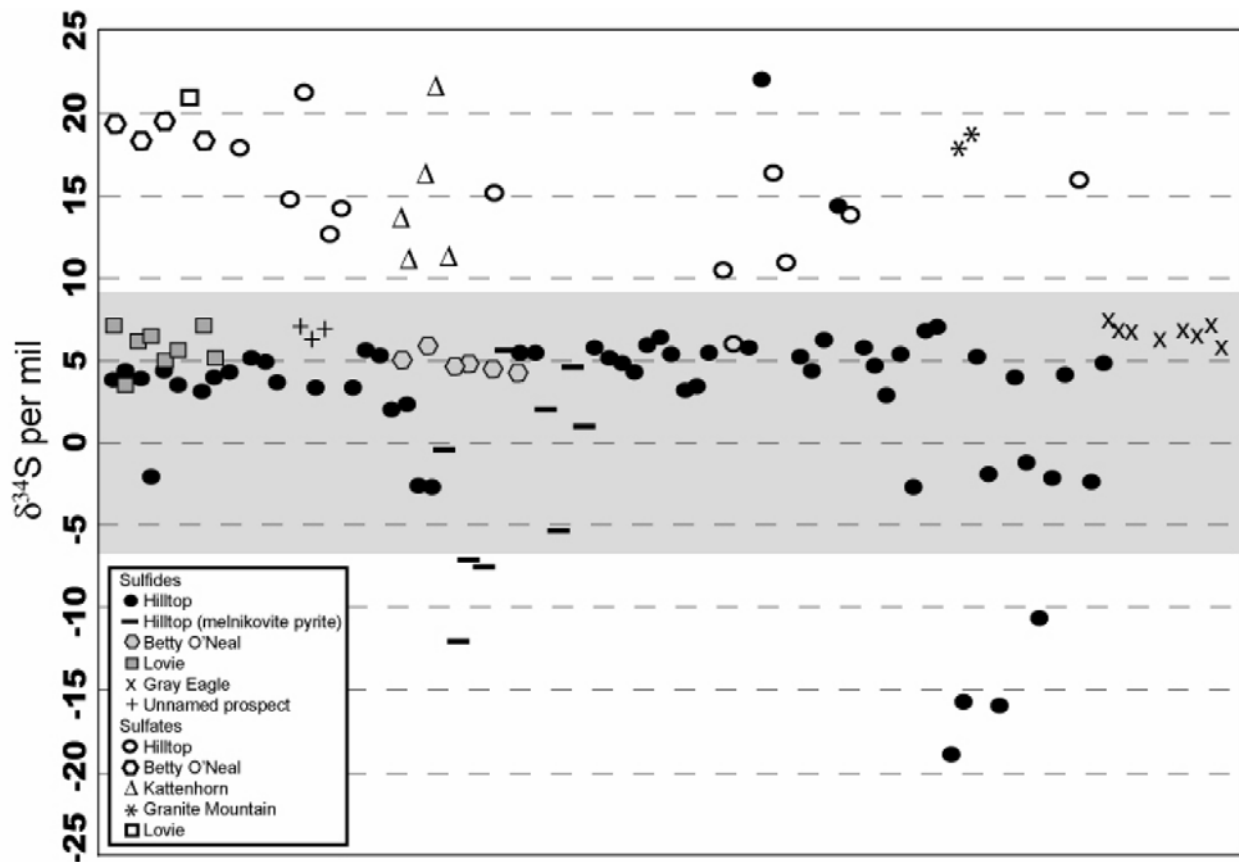


Figure 3.13: Sulfide and sulfate (barite) sulfur isotope data from northern Shoshone Range vein deposits (data from Kelson et al. (2005) and this study). Gray box incorporates range of sulfide sulfur values from Cu-porphyry deposits (-3 to 9 ‰; Hedenquist and Lowenstern, 1994), magmatic sulfur (-3 to 3 ‰) and sulfide sulfur values from zoned polymetallic vein deposits (-6.3 to 4.9 ‰) (Field and Fifarek, 1985).

Table 3.9: Calculated depositional temperatures based on sulfur isotope fractionation between two co-existing mineral phases using fractionation equations of Kajiwara and Krause (1971).

Data from Kelson et al. (2005).

Deposit	Sample Pair	Mineral pair	Δ per mil	Temp °C
Lovie	03A, B	sph-py	1.1	249
GE	05-1,2	sph-py	0.9	304
GE	04-1,2	gal-py	0.8	900
GE	04-1,4	gal-sph	1.3	511
GE	04-2,4	py-sph	0.5	502
UN	CK02-11-2,3	sph-py	0.8	339
Hilltop	97-10-1084.5-1,2	sph-py	0.2	952
Hilltop	97-10-1160.6-1,2	gal-py	2.2	434
Hilltop	97-11-665.3-3,4	sph-py	0.6	434
Hilltop	97-6-80-1,3	mo-py	0.2	653

and depositional sites for ore-bearing fluids as the siliciclastic host rocks' poor primary permeability limited fluid flow to the open fracture spaces.

Changes in fluid temperature and/or pH probably initiated ore mineral precipitation within the vein deposits. The lack of alteration halos around veins and the presence of unaltered wall rock clasts within vein material testify to the inability of ore-bearing fluid to chemically react with the host rocks and preclude a change in fluid pH via this method (Kelson et al., 2000). The paucity of vapor-dominated fluid inclusions in vein quartz suggests fluid boiling was probably not a significant ore-depositing mechanism. However, the presence of multiple generations of quartz veins within most deposits support repeated fracturing and healing (throttling) of the individual hydrothermal systems, and very few base- or precious-metal deposits actually exhibit uncontested evidence supporting fluid boiling coincident with metal deposition (Hayba et al., 1985).

Nearly coincident $^{40}\text{Ar}/^{39}\text{Ar}$ and Re-Os ages support a relationship between intrusive igneous rocks and molybdenite mineralization, and stable isotope data support a magmatic source for most vein ore and gangue minerals. The emplacement of numerous Eocene stocks, plugs, and dikes probably supplied the heat necessary to generate and maintain meteoric and/or magmatic fluid convection through the adjacent fractured upper plate host rocks. Since no single intrusion centrally underlies the entire northern Shoshone Range (Fig. 3.4), most vein deposits probably represent individual hydrothermal systems that operated adjacent to separate intrusive igneous stocks. The age discrepancies between base- and precious-metal-bearing veins and nearby intrusive igneous rocks may suggest active individual hydrothermal systems of variable duration subsequent to pluton emplacement; sulfide-bearing quartz veins from the Gray Eagle mine are at least 0.5 m.y. younger than the Granite Mountain host rock, and the gold-bearing

discordant quartz breccia pipe (Hilltop deposit) may be about 3 m.y. younger than the nearby Hobo Gulch intrusion. These data coincide with hydrothermal system lifetimes calculated by previous workers (Whalen et al., 1982; Silberman et al., 1979; Silberman, 1985), who describe hydrothermal convection cells associated with porphyry copper, epithermal Au-Ag, hot spring, and polymetallic vein deposits which operate up to 3 m.y. after initial igneous stock emplacement, with hydrothermal activity and ore-deposition occurring in episodic pulses (Silberman, 1983). However, it is doubtful if the northern Shoshone Ranges' relatively small, individual intrusive igneous plugs and stocks, emplaced at shallow depth and cooling rapidly within relatively impermeable siliciclastic host rocks, could generate enough heat to maintain such long-lived hydrothermal systems subsequent to emplacement. Hydrothermal convection resulting from the cooling and crystallization of these small (<2 km-wide) individual plutons would cease after 100,000 yrs (Norton and Cathles, 1979). However, subsequent, younger pulses of magmatism could provide the heat necessary to maintain an already active, ore-forming hydrothermal system (Silberman, 1983). This scenario may have occurred at Tenabo, as K-Ar ages for dikes "spatially associated with gold-quartz veins" are at least 1.1 m.y. younger than the K-Ar age of the Tenabo stock (Silberman and McKee, 1971). Similarly aged, younger intrusive igneous rocks have not been recognized elsewhere in the northern Shoshone Range.

The variable fluid sources, depositional temperatures, and salinities of each northern Shoshone Range vein deposit may indicate its formation relative to a cooling and crystallizing pluton and associated hydrothermal system (Hedenquist and Lowenstern, 1994). Early, high temperature (~500-600°C), magmatic, and relatively saline fluids emanating from a pluton could have formed the Lovie and Grey Eagle vein deposits and Hilltop's porphyry veins. In contrast, the Betty O'Neal mine could have formed from the lower temperature (~200°C), less saline

meteoric fluids that would have been more abundant further away from a cooling pluton.

Variable vein quartz source fluid salinities within each deposit and even within the same vein (Table 6) may also result from fluid boiling, evaporation, and/or mixing (Simmons et al., 2005).

Considering the extent of base- and precious-metal mineralization hosted by the chemically-inert siliciclastic upper plate rocks of the northern Shoshone Range, the depth of the Roberts Mountains thrust and the underlying lower plate carbonate assemblage is of considerable exploration interest. Did the ore-bearing fluids interact with the lower plate carbonate rocks as they ascended toward the surface? Were the ore-bearing fluids localized or channeled along the Roberts Mountains thrust? Insight to these questions may be provided by comparing carbon and oxygen isotope signatures between carbonate gangue minerals from four vein deposits, upper plate limestones (Lovie mine area), and lower plate carbonate rocks (Cortez area; Field and Fifiarek, 1985). Although the oxygen isotope data are inconclusive, carbon isotope data from the unnamed prospect, Lovie mine, and some Hilltop vein carbonate minerals suggest carbon was at least partially derived from a source isotopically similar to Cortez (lower plate) limestone (Fig. 3.12).

Classification of northern Shoshone Range vein deposits

It is problematic to categorize northern Shoshone Range vein deposits as solely low or high sulfidation epithermal- or porphyry-type. Essential identification and classification criteria, i.e. coeval volcanic host rocks and traditional alteration types and mineral assemblages (White and Hedenquist, 1990; Simmons et al., 2005) associated with epithermal and porphyry deposit types are almost or wholly lacking. Additionally, fluid inclusion, stable isotope, and

geothermometry data support a range of fluid sources and depositional temperatures spanning the continuum between low temperature (epithermal) and higher-temperature (porphyry) regimes (Kelson et al., 2005; and this study).

Based on Ag:Au ratios (range from 10 to 161), ore minerals (base metal sulfide- and Ag-rich), gangue minerals (quartz, carbonate, barite), sulfide sulfur isotope ratios (mostly between +2 and +8 per mil), and vein quartz salinities (0-6.4 equiv wt % NaCl), most northern Shoshone Range vein deposits share similarities with Cordilleran vein-type deposits, porphyry-related base metal veins, and/or higher-temperature analogues of intermediate-sulfidation epithermal deposits.

Cordilleran vein-type deposits (e.g. Magma Vein, Casapalca, Coeur d'Alene; Guilbert and Park, 1986) form in compressive margin settings and may not be obviously related to nearby igneous activity. Features of Cordilleran vein deposits include: 1) spatial and temporal association with calc-alkaline igneous rocks; 2) hydrothermally-transported ore elements deposited from solutions in separate stages; 3) ore minerals occur as open-space or fracture fill material in siliceous/siliciclastic host rocks or as replacements in carbonate host rocks; 4) shallow (<1 km) deposition of the surface; 5) metal zonation in veins; Sn-W-Mo (high temperature) through Cu-Zn to Zn-Pb-Mn-Ag (low temperature); and 6) sulfide sulfur isotope ratios close to zero per mil (Sawkins, 1972; Guilbert and Park, 1986). Northern Shoshone Range vein deposits share most of these features, differing only by the lack of W-bearing minerals and an average sulfide sulfur isotope ratio of 3.5 per mil.

Porphyry-related base metal veins are similar to Cordilleran veins, but possess a stronger spatial and genetic link to intrusive igneous rocks associated with porphyry-type deposits (Guilbert and Park, 1986). The common association with underlying bulk-tonnage ore bodies (in

addition to their own mineable potential) make base-metal veins attractive exploration targets (Seedorff et al., 2005). The oldest, highest-temperature stage (Event 1) of the Hilltop deposit's main zone mineralization may represent a porphyry-related base metal vein assemblage; Event 1 minerals (galena + sphalerite + fahlore + pyrite + stannite + chalcopyrite + jamesonite; Kelson et al., 2000) derived their sulfur from a magmatic source ($\delta^{34}\text{S}_{\text{CDT}}=3.2$ to 5.4 per mil) and were probably deposited during the waning stages of granitic pluton emplacement responsible for Hilltop's Mo-bearing, Au-poor porphyry-type mineralization (Kelson et al., 2005). An association between Cu, Zn, Pb, and Ag-rich mineral suites and Mo-bearing, Au-poor porphyries is typical of porphyry-related base metal veins (Einaudi et al., 2003).

Northern Shoshone Range vein deposits also share similarities with intermediate sulfidation deposits (e.g. Creede, Comstock; John, 2001) which are associated with calc-alkaline intermediate to felsic igneous rocks and form in neutral stress to mildly extensional arcs and compressive back arcs during arc volcanism. Intermediate sulfidation deposits commonly contain carbonate and barite gangue minerals and Ag-Au, Zn, Pb, Cu \pm Mo, As, and Sb-bearing ore minerals (especially fahlore, which is ubiquitous in all northern Shoshone Range vein deposits and is the dominant ore mineral) within quartz veins (Einaudi et al., 2003; Sillitoe and Hedenquist, 2003; Simmons et al., 2005). Vein quartz salinities range from 0 to 12 equiv wt % NaCl (see compilation by Sillitoe and Hedenquist, 2003), similar to the northern Shoshone Range vein deposits studied here. At the Hilltop deposit, younger, lower-temperature (and Au-bearing) episodes of main zone mineralization (Events 2-4) most closely resemble intermediate-sulfidation mineral assemblages (Kelson et al., 2000).

Summary and Conclusions

Northern Shoshone Range vein deposits, part of the greater Battle Mountain-Eureka trend, are historic producers of copper, lead, silver, and gold. Collectively, these veins most closely resemble Cordilleran vein-type, porphyry related base metal vein-type, or high-temperature analogues of intermediate sulfidation epithermal deposits. We conclude that:

1. All igneous rocks within the study area are Eocene age;
2. Molybdenite mineralization is essentially contemporaneous with Eocene granitic intrusive rocks;
3. No definitive geochemical difference exists between barren intrusive igneous rocks and those associated with porphyry (molybdenite) mineralization;
4. Vein-hosted mineralization is younger than the oldest igneous rocks within the study area based on samples from the Gray Eagle mine (at least 0.5 m.y. younger than the Granite Mountain host rock) and the discordant quartz breccia pipe at Hilltop (at least 2.8 m.y. younger than the nearby Hobo Gulch intrusion). The age differences may reflect active hydrothermal systems associated with individual igneous intrusions or a secondary pulse of heat and/or fluids associated with slightly younger magmatism (e.g. Tenabo);
5. A magmatic source for most vein-hosted sulfide minerals and variable sources (mostly meteoric and/or magmatic, with lesser organic carbon and carbonate rock sources) for carbonate minerals' carbon and oxygen. Oxygen isotope data support variably-mixed meteoric and/or magmatic source fluids for vein quartz;
6. Vein quartz source fluids possessed variable salinities, even within the same deposit;

7. Ore mineral and ore-bearing vein quartz deposition occurred over a wide temperature range (based on geothermometry data from fluid inclusions and stable isotope partitioning) spanning the epithermal-porphyry continuum, probably representing the transitional zone between the two regimes.

Acknowledgements

This paper represents part of a Ph.D. dissertation completed at the University of Georgia in Athens, Georgia. This research would not have been possible without the generous support of the Cortez Joint Venture, and very special thanks to Mr. Robert C. Hays, Jr., Technical Services Superintendent, Cortez Joint Venture. This research was also funded by the Society of Economic Geologists (Hugh E. McKinstry Grant), the Geological Society of America (Grant No. 7180-02), the Department of Geology, University of Georgia, and the Graduate School (Dissertation Completion Award), University of Georgia. Permission of the Cortez Joint Venture to publish this investigation is gratefully acknowledged. Thanks to: Dr. Kenneth A. Foland (RIL), Dr. Matthew T. Heizler (NMGRL), and Mr. Thomas D. Ullrich (UBC) for their assistance and insight with the $^{40}\text{Ar}/^{39}\text{Ar}$ data. Dr. Chris Romanek (SREL) and Mr. Tom Maddux (UGA) assisted with the carbon isotope data. Dr. Zachary D. Sharp (UNM) provided the silicate oxygen isotope analyses. Richard Markey and Aaron Zimmerman (AIRIE, Colorado State University) provided the Re-Os analyses. Ms. Julia Cox and Mr. Chris Fleisher (UGA) assisted with stable isotope and electron microprobe analyses, respectively.

References

- Armin, R.A., and Mayer, L., 1983, Subsidence analysis of the Cordilleran miogeocline: Implications for timing of late Proterozoic rifting and amount of extension: *Geology*, v. 11, p. 702-705.
- Armstrong, R.L., 1970, Geochronology of Tertiary igneous rocks, eastern Basin and Range Province, western Utah, eastern Nevada, and vicinity, U.S.A.: *Geochimica et Cosmochimica Acta*, v. 34, p. 203-232.
- Beck, Jr., M.E., 1992, Tectonic significance of paleomagnetic results for the western conterminous United States, *in* Burchfiel, B.C., Lipman, P.W., and Zoback, M.L. eds., *The Cordilleran Orogen: Conterminous U.S.*: Boulder, Colorado, Geological Society of America, *The Geology of North America*, v. G-3, p. 683-697.
- Burchfiel, B.C, and Davis, G.A., 1972, Structural framework and evolution of the southern part of the Cordilleran orogen, western United States: *American Journal of Science*, v. 275-A, p. 363-396.
- Burchfiel, B.C, and Royden, L.H., 1991, Antler orogeny: A Mediterranean-type orogeny: *Geology*, v. 19, p. 66-69.
- Burchfiel, B.C., Cowan, D.S., and Davis, G.A., 1992, Tectonic overview of the Cordilleran orogen in the western United States, *in* Burchfiel, B.C., Lipman, P.W., and Zoback, M.L. eds., *The Cordilleran Orogen: Conterminous U.S.*: Boulder, Colorado, Geological Society of America, *The Geology of North America*, v. G-3, p. 407-480.
- Carpenter, J.A., Carpenter, D.G., and Dobbs, S.W., 1994, Antler orogeny: Paleostuctural analysis and constraints on plate tectonic models with a global analogue in southeast Asia, *in* Dobbs, S.W., and Taylor, W.J., eds., *Structural and stratigraphic investigations and petroleum potential of Nevada, with special emphasis south of the Railroad Valley Producing Trend: Nevada Petroleum Society Conference Volume II*, p. 187-240.
- Christiansen, R.L., and Yeats, R.S., 1992, Post-Laramide geology of the U.S. Cordilleran region, *in* Burchfiel, B.C., Lipman, P.W., and Zoback, M.L. eds., *The Cordilleran Orogen: Conterminous U.S.*: Boulder, Colorado, Geological Society of America, *The Geology of North America*, v. G-3, p. 261-406.

- Clayton, R.N., O'Neil, J.R., and Mayeda, T.K., 1972, Oxygen isotope exchange between quartz and water: *Journal of Geophysical Research*, v. 77, no. 17, p. 3057-3067.
- Cook, H.E., and Taylor, M.E., 1991, Paleozoic carbonate passive-margin evolution and resulting petroleum reservoirs – Great Basin, western United States, *in* Raines, G.L., Lisle, R.E., Schafer, R. W., and Wilkenson, W.H., eds., *Geology and ore deposits of the Great Basin*: Geological Society of Nevada, p. 927-939.
- Coleman, D., and Fry, B., 1991, *Carbon Isotope Techniques*. Academic Press/Harcourt Brace Jovanovich, New York.
- Desrochers, G.J., 1984, *Geology of part of the Hilltop district, Lander County, Nevada*: M.S. thesis, University of Nevada, Reno, 97 p.
- Dickenson, W.R., 1992, Cordilleran sedimentary assemblages, *in* Burchfiel, B.C., Lipman, P.W., and Zoback, M.L. eds., *The Cordilleran Orogen: Conterminous U.S.*: Boulder, Colorado, Geological Society of America, *The Geology of North America*, v. G-3, p. 539-552.
- Ehlers, E.G., and Blatt, H., 1982, *Petrology: Igneous, sedimentary and metamorphic*: W.H. Freeman and Company, San Francisco, 732 p.
- Einaudi, M.T., Hedenquist, J.W., and Inan, E.E., 2003, Sulfidation state of fluids in active and extinct hydrothermal systems: Transitions from porphyry to epithermal environments: *Society of Economic Geologists Special Publication 10*, p. 285-313.
- Emmons, W.H., 1910, A reconnaissance of some mining camps in Elko, Lander, and Eureka Counties, Nevada: *U. S. Geological Survey Bulletin 408*, 130 p.
- Field, C.W., and Fifarek, R.H., 1985, Light stable-isotope systematics in the epithermal environment, *in* Berger, B.R., and Bethke, P.M., eds., *Geology and geochemistry of epithermal systems*: Chelsea, MI, Society of Economic Geologists, *Reviews in Economic Geology*, v. 2, p. 99-128.
- Foo, S.T., Hays, Jr., R.C., and McCormack, J.K., 1996, Geology and mineralization of the South Pipeline Gold Deposit, Lander County, Nevada, *in* Coyner, A.R., and Fahey, P.L., eds., *Geology and Ore Deposits of the American Cordillera: Geological Society of Nevada Symposium Proceedings, Reno/Sparks, Nevada, April 1995*, p. 111-121.

- Gilluly, J., 1977, Cauldron subsidence near Mount Lewis, Nevada; a misconception: *Journal of Research of the U.S. Geological Survey*, vol. 5, no. 3, p. 325-329.
- Gilluly, J., and Gates, O., 1965, Tectonic and igneous geology of the northern Shoshone Range, Nevada: U.S. Geological Survey Professional Paper 465, 153 p.
- Grauch, V.J.S., Rodriguez, B.D., and Wooden, J.L., 2003, Geophysical and isotopic constraints on crustal structure related to mineral trends in north-central Nevada and implications for tectonic history: *Economic Geology*, v. 98, p. 269-286.
- Graves, G.R., Romanek, C.S., and Navarro, A.R., 2002, Stable isotope signature of philopatry and dispersal in a migratory songbird: *Proceedings of the National Academy of Sciences USA*, vol. 99, no. 12, p. 8096-8100.
- Guilbert, J.M., and Park, C.F. Jr., 1986, *The geology of ore deposits*: W.H. Freeman and Company, New York, 985 p.
- Hayba, D.O., Bethke, P.M., Heald, P., and Foley, N.K., 1985, Geologic, mineralogic, and geochemical characteristics of volcanic-hosted epithermal precious-metal deposits, *in* Berger, B.R., and Bethke, P.M., eds., *Geology and geochemistry of epithermal systems*: Chelsea, MI, Society of Economic Geologists, *Reviews in Economic Geology*, v. 2, p. 129-169.
- Hedenquist, J.W., and Lowenstern, J.B., 1994, The role of magmas in the formation of hydrothermal ore deposits: *Nature*, v. 370, no. 6490, p. 519-527.
- Howard, K.A., 2003, Crustal structure in the Elko-Carlin region, Nevada during Eocene gold mineralization: Ruby-East Humboldt metamorphic core complex as a guide to the deep crust: *Economic Geology*, v. 98, p. 249-268.
- John, D.A., 2001, Miocene and Early Pliocene Epithermal Gold-Silver Deposits in the Northern Great Basin, Western United States: Characteristics, Distribution, and Relationship to Magmatism: *Economic Geology*, v. 96, p. 1827-1854.

- John, D.A., Wallace, A.R., Ponce, D.A., Fleck, R.B., and Conrad, J.E., 2000, New perspectives on the geology and origin of the northern Nevada rift, *in* Cluer, J.K., Price, J.G., Struhsacker, E.M., Hardyman, R.F., and Morris, C.L., eds., *Geology and ore Deposits 2000: The Great Basin and Beyond: Geological Society of Nevada Symposium Proceedings*, Reno/Sparks, May 2000, p. 127-154.
- John, D.A., Hofstra, A.H., and Theodore, T.G., 2003, Preface, *in* A Special Issue Devoted to Gold Deposits in Northern Nevada: Part 1. Regional Studies and Epithermal Deposits: *Economic Geology*, v. 98, p. 225-234.
- Johnson, J.G., and Pendergast, A., 1981, Timing and mode of emplacement of the Roberts Mountains allochthon, Antler orogeny: *Geological Society of America Bulletin*, Part 1, v. 92, p. 648-658.
- Kajiwara, Y., and Krause, H.R., 1971, Sulfur isotope partitioning in metallic sulfide systems: *Canadian Journal of Earth Science*, v. 8, no. 11, p. 1397-1408.
- Kelson, C.R., Keith, J.D., Christiansen, E.H., and Meyer, P.E., 2000, Mineral paragenesis and depositional model of the Hilltop gold deposit, Lander County, NV, *in* Cluer, J.K., Price, J.G., Struhsacker, E.M., Hardyman, R.F., and Morris, C.L., eds., *Geology and ore Deposits 2000: The Great Basin and Beyond: Geological Society of Nevada Symposium Proceedings*, Reno/Sparks, May 2000, p. 1107-1132.
- Kelson, C.R., Crowe, D.E., and Stein, H.J., 2005, Geochronology and geochemistry of the Hilltop, Lewis, and Bullion mining districts and surrounding area, Battle Mountain-Eureka trend, Nevada, *in* Rhoden, H.N., Steininger, R.C., and Vikre, P.G., eds., *Geological Society of Nevada Symposium 2005: Window to the World*, Reno, Nevada, May 2005.
- Ketner, B.K., 1977, Late Paleozoic orogeny and sedimentation, southern California, Nevada, Idaho, and Montana, *in* Stewart, J.H., Stevens, C.H., and Fritsche, A.E., eds., *Paleozoic paleogeography of the western United States, Pacific Coast Paleogeography Symposium I: Society of Economic Paleontologists and Mineralogists, Pacific Section*, p. 363-364.
- King, C., 1876, *Geological and topographical atlas accompanying the report of the Geological Exploration of the Fortieth Parallel*.

- Kistler, R.W. and Peterman, Z.E., 1978, Reconstruction of crustal blocks of California on the basis of initial strontium isotopic compositions of Mesozoic granite rocks: U.S. Geological Survey Professional Paper 1071, 17p.
- Lanphere, M.A., and Dalrymple, G.B., 1976, Identification of excess ^{40}Ar by the $^{40}\text{Ar}/^{39}\text{Ar}$ age spectrum technique: *Earth and Planetary Science Letters*, v. 32, p. 141-148.
- Le Maitre, R.M., 2002, *Igneous rocks: A classification and glossary of terms – recommendations of the International Union of Geological Sciences Subcommittee on the systematics of igneous rocks*: Cambridge, United Kingdom, Cambridge University Press, 236 p.
- Lee, W.T., Stone, R.W., Gale, H.S., and others, 1916, *The Overland Route, with a side trip to Yellowstone Park, Pt. B of Guidebook of the western United States*: U.S. Geological Survey Bulletin 612.
- Lisle, R.E., and Desrochers, G.J., 1988, Geology of the Hilltop gold deposit, Lander County, Nevada, *in* Schafer, R.W., Cooper, J.J., and Vikre, P.G., eds., *Bulk mineable precious metal deposits of the western United States*, p. 101-117.
- Madrid, R.J., and Roberts, R.J., 1991, Origin of gold belts in north-central Nevada, *in* Raines, G.L., Lisle, R.E., Schafer, R. W., and Wilkenson, W.H., eds., *Geology and ore deposits of the Great Basin*: Geological Society of Nevada, p. 927-939.
- Maher, B.J., and Browne, Q.J., 1993, Constraints on the age of gold mineralization and metallogenesis in the Battle Mountain-Eureka mineral belt, Nevada: *Economic Geology*, v. 88, p. 409-478.
- McCusker, R.T., 2004, Geological report on the Robertson property, Lander County, Nevada, U.S.A.: Coral Gold Corporation unpublished in-house report.
- McDougall, I., and Harrison, T.M., 1999, *Geochronology and thermochronology by the $^{40}\text{Ar}/^{39}\text{Ar}$ method*, 2nd ed., Oxford University Press, New York, 269p.

- Miller, E.L., Miller, M.M., Stevens, C.H., Wright, J.E., and Madrid, R., 1992, Late Paleozoic paleographic and tectonic evolution of the western U.S. Cordillera, *in* Burchfiel, B.C., Lipman, P.W., and Zoback, M.L. eds., *The Cordilleran Orogen: Conterminous U.S.*: Boulder, Colorado, Geological Society of America, *The Geology of North America*, v. G-3, p. 57-106.
- Nilson, T.H., and Stewart, J.H., 1980, The Antler Orogeny – Mid-Paleozoic tectonism in western North America: *Geology*, v. 8, p. 298-302.
- Norton, D., and Cathles, L.M., 1979, Thermal aspects of ore deposition, *in* Barnes, H.L., ed., *Geochemistry of hydrothermal ore deposits*, 2nd ed.: New York, John Wiley and Sons, p. 611-683.
- Pearce, J.A., 1983, Role of the sub-continental lithosphere in magma genesis at active continental margins, *in* Hawkesworth, C.J., and Norry, M.J., eds., *Continental basalts and mantle xenoliths*. Shiva, Nantwich, p. 230-249.
- Pearce, J.A., Harris, N.B.W., and Tindle, A.G., 1984, Trace element discrimination diagrams for the tectonic interpretation of granitic rocks. *Journal of Petrology*, vol. 25, p. 956-983.
- Poole, F.G., 1974, Flysch deposits of Antler foreland basin, western United States: *Society of Economic Paleontologists and Mineralogists Special Publication 22*, p. 58-82.
- Potter, II, R.W., 1977, Pressure-correction for fluid inclusion homogenization temperatures based on the volumetric properties of the system NaCl-H₂O: *U.S. Geological Survey Journal of Research*, v. 5, p. 603-607.
- Price, J.G., and Meeuwig, R.O., 2002, Overview, *in* *The Nevada Mineral Industry 2001*: Nevada Bureau of Mines and Geology Special Publication MI-2001, p. 3-12.
- Renne, P.R., Swisher, C.C., Diano, A.L., Karner, D.B., Owens, T.L., and DePaulo, D.J., 1998, Intercalibration of standards, absolute ages and uncertainties in ⁴⁰Ar/³⁹Ar dating: *Chemical Geology*, 145, p. 117-152.
- Ressel, M.W., and Henry, C.D., in review, Igneous geology of the Carlin trend, Nevada: Evolution of the Eocene plutonic complex and significance for Carlin-type gold deposits.

- Roberts, R.J., Hotz, P.E., Gilluly, J., and Furgusan, H.G., 1958, Paleozoic rocks of north central Nevada: American Association of Petroleum Geologists Bulletin, v. 42, p. 2813-2857.
- Roberts, R.J., 1960, Alinement of mining districts in north-central Nevada: U.S. Geological Survey Professional Paper 400-B, p. B17-B19.
- Roberts, R.J., 1966, Metallogenic provinces and mineral belts in Nevada: Nevada Bureau of Mines and Geology Report 13, part A, p. 47-72.
- Rollinson, H., 1995, Using geochemical data: Evaluation, presentation, interpretation. Singapore, Longman Group UK Limited, 352 p.
- Sack, R.O., and Goodell, P.C., 2002, Retrograde reactions involving galena and Ag-sulfosalts in a zoned ore deposit, Julcani, Peru: Mineralogical Magazine, v. 66, no. 6, p. 1043-1062.
- Sack, R.O., Kuehner, S.M., and Hardy, L.S., 2002, Retrograde Ag-enrichment in fahlores from the Coeur d'Alene mining district, Idaho, USA: Mineralogical Magazine, v. 66, no. 1, p. 215-229.
- Sack, R.O., Lynch, J.V.G., and Foit, Jr., F., 2003, Fahlore as a petrogenetic indicator: Keno Hill Ag-Pb-Zn district, Yukon, Canada: Mineralogical Magazine, v. 67, no. 5, p. 1023-1038.
- Sawkins, F.J., 1972, Sulfide ore deposits in relation to plate tectonics: Journal of Geology, vol. 80, p. 377-396.
- Seedorff, E., Dilles, J.H., Proffett, Jr., J.M., Einaudi, M.T., and four others, 2005, Porphyry Deposits: Characteristics and origin of hypogene features, *in* Hedenquist, J.W., Thompson, J.F.H., Goldfarb, R.J., and Richards, J.P., eds., Society of Economic Geologists, Economic Geology 100th Anniversary Volume, p. 485-522.
- Selby, D., and Creaser, R.A., 2001, Re-Os geochronology and systematics in molybdenite from the Endako porphyry molybdenum deposit, British Columbia, Canada. Economic Geology, vol 96, p. 197-204.
- Sharp, Z. D., 1995, Oxygen isotope geochemistry of the Al₂SiO₅ polymorphs: American Journal of Science, v. 295, p. 1058-1076.

- Shawe, D.R., 1991, Structurally controlled gold trends imply large gold resources in Nevada: In Raines, G.L., Lisle, R.E., Schafer, R. W., and Wilkenson, W.H.. (eds.), *Geology and ore deposits of the Great Basin: Geological Society of Nevada*, p. 199-212.
- Silberling, N.J., 1973, Geologic events during Permian-Triassic time along the Pacific margin of the United States, *in* Logan, A., and Hills, L.V., eds., *The Permian and Triassic systems and their mutual boundary: Alberta Society of Petroleum Geology*, Calgary, Alberta, Canada, p. 345-362.
- Silberman, M.L., 1983, Geochronology of hydrothermal alteration and mineralization: Tertiary epithermal precious metal deposits in the Great Basin: Geothermal Resources Council Special Report No. 13, p. 287-303.
- Silberman, M.L., 1985, Geochronology of hydrothermal alteration and mineralization: Tertiary epithermal precious-metal deposits in the Great Basin, *in* Tooker, E.W., ed., *Geologic characteristics of sediment- and volcanic-hosted disseminated gold deposits – Search for an occurrence model: U.S. Geological Survey Bulletin 1646*, p. 55-71.
- Silberman, M.L., and McKee, E.H., 1971, K-Ar ages of granitic plutons in north-central Nevada: *Isochron/West*, no. 71-1, p. 15-32.
- Silberman, M.L., White, D.E., Keith, T.E.C., and Docktor, R.D., 1979, Duration of hydrothermal activity at Steamboat Springs, Nevada, from ages of spatially associated volcanic rocks: *U.S. Geological Survey Professional Paper 458-D*, p. D1-D14,
- Sillitoe, R.H., and Hedenquist, J.W., 2003, Linkages between volcanogenic settings, ore-fluid compositions, and epithermal precious metal deposits: *Society of Economic Geologists Special Publication 10*, p. 315-343.
- Simmons, S.F., White, N.C., and John, D.A., 2005, Geological characteristics of epithermal precious and base metal deposits, *in* Hedenquist, J.W., Thompson, J.F.H., Goldfarb, R.J., and Richards, J.P., eds., *Society of Economic Geologists, Economic Geology 100th Anniversary Volume*, p. 485-522.
- Snyder, W.S., Brueckner, H.K., 1983, Tectonic evolution of the Golconda allochthon, Nevada: Problems and perspectives, *in* Stevens, C.H., ed., *Pre-Jurassic rocks in western North American suspect terranes: Society of Economic Paleontologists and Mineralogists, Pacific Section*, p. 103-123.

- Snyder, W.S., Spinosa, C., and Gallegos, D.M., 1991, Pennsylvanian-Permian tectonism on the western U.S. continental margin, *in* Raines, G.L., Lisle, R.E., Schafer, R. W., and Wilkenson, W.H., eds., *Geology and ore deposits of the Great Basin: Geological Society of Nevada*, p. 5-19.
- Speed, R.C., 1971, Golconda thrust, western Nevada – Regional extent: *Geological Society of America Abstracts with Programs*, v. 3, no. 2, p. 199-200.
- _____, 1979, Collided Paleozoic microplate in the western United States: *Jour. Geology*, v. 87, no. 2, p. 279-292.
- Spurr, J.E., 1903, Descriptive geology of Nevada south of the 40th Parallel and adjacent portions of California: *U.S. Geological Survey Bulletin* 208.
- Stager, H.K., 1977, *Geology and Mineral Deposits of Lander County, Nevada: Nevada Bureau of Mines and Geology Bulletin* 88, 106 p.
- Stewart, J.H., 1980, *Geology of Nevada: Nevada Bureau of Mines and Geology Special Publication* 4, 104 p.
- Stewart, J.H., and Poole, F.G., 1974, Lower Paleozoic and uppermost Precambrian Cordilleran miogeocline, Great Basin, western United States, *in* Dickenson W.R., ed., *Tectonics and sedimentation: Society of Economic Paleontologists and Mineralogists Special Publication* 22, p. 28-57.
- Stewart, J.H., and McKee, E.H., 1977, *Geology and Mineral Deposits of Lander County, Nevada: Nevada Bureau of Mines and Geology Bulletin* 88, 106 p.
- Steiger, R.H., and Jäger, E., 1977, Subcommittee on geochronology: Convention on the use of decay constants in geo- and cosmo-chronology: *Earth and Planetary Science Letters*, v. 36, p. 359-362.
- Stein, H.J., Morgan, J.W., Markey, R.J., and Hannah, J.L., 1998, An introduction to Re-Os: What's in it for the mineral industry?: *Society of Economic Geologists Newsletter*, no. 32, p. 1, 8-15.

- Stein, H.J., Markey, R.J., Morgan, J.W., Hannah, J.L., and Scherstén, A., 2001, The remarkable Re-Os chronometer in molybdenite: how and why it works: *Terra Nova*, v. 13, no. 6, p. 479-486.
- Stein, H., Scherstén, A., Hannah, J., and Markey, R., 2003, Sub-grain scale decoupling of Re and ¹⁸⁷Os and assessment of laser ablation ICP-MS spot dating in molybdenite: *Geochimica et Cosmochimica Acta*, v. 67, no. 19, p. 3673-3686.
- Stewart, J.H., 1980, *Geology of Nevada: Nevada Bureau of Mines and Geology Special Publication 4*, 136 p.
- Sun, S.S., 1980, Lead isotopic study of young volcanic rocks from mid-ocean ridges, ocean islands and island arcs: *Philosophical Transactions Royal Society*, A297, 409-445.
- Sun, S.S., and McDonough, W.F., 1989, Chemical and isotopic systematics of oceanic basalts: Implications for mantle composition and processes, *in* Saunders, A.D., and Norry, M.J., eds., *Magmatism in ocean basins*. Geological Society of London Special Publication 42, p. 313-345.
- Thompson, G.A., and Burke, D.B., 1974, Regional geophysics of the Basin and Range Province: *Annual Reviews of Earth and Planetary Sciences*, v. 2, p. 213-238.
- Tosdal, R.M., Wooden, J.L., and Kistler, R.W., 2000, Geometry of the Neoproterozoic continental break-up, and implications for location of Nevadan mineral belts, *in* Cluer, J.K., Price, J.G., Struhsacker, E.M., Hardyman, R.F., and Morris, C.L., eds., *Geology and ore Deposits 2000: The Great Basin and Beyond: Geological Society of Nevada Symposium Proceedings, Reno/Sparks, May 2000*, p. 451-466.
- Turner, R.J.W., Madrid, R.J., and Miller, E.L., 1989, Roberts Mountains allochthon: Stratigraphic comparison with lower Paleozoic outer continental margin strata of the northern Canadian Cordillera: *Geology*, v. 17, p. 341-344.
- Vanderburg, W.O., 1939, *Reconnaissance of some mining districts in Lander County, Nevada: U.S. Bureau of Mines Information Circular 7043*, p. 47-50.

- Whalen, J.B., Britten, R.M., and McDougall, I., 1982, Geochronology and geochemistry of the Frieda River prospect area, Papua New Guinea: *Economic Geology*, v. 77, no. 3, p.592-616.
- White, D.E., 1985, Vein and disseminated gold-silver deposits of the Great Basin through space and time, *in* Tooker, E.W., ed., *Geologic characteristics of sediment- and volcanic-hosted disseminated gold deposits – Search for an occurrence model: U.S. Geological Survey Bulletin 1646*, p. 5-34.
- White, N.C., and Hedenquist, J.W., 1990, Epithermal environments and styles of mineralization: variations and their causes, and guidelines for exploration: *Journal of Geochemical Exploration*, vol. 36, p. 445-474.
- Wrucke, C.T. and Silberman, M.L., 1975, Cauldron subsidence of Oligocene age at Mount Lewis, Shoshone Range, Nevada: *U.S. Geological Survey Professional Paper 876*, 20p.
- _____, 1977, Cauldron subsidence of Oligocene age at Mount Lewis, Shoshone Range, Nevada – A reasonable interpretation: *Jour. Research U.S. Geological Survey*, v. 5, no.3, p. 331-335.
- Wu, I., and Petersen, U., 1977, Geochemistry of tetrahedrite and mineral zoning at Casapalca, Peru: *Economic Geology*, v. 72, p. 993-1016.
- York, D., 1969, Least squares fitting of a straight line with correlated errors: *Earth and Planetary Science Letters*, v. 5, p. 320-324.
- Zamudio, J.A., and Atkinson, Jr., W.W., 1991, Igneous rocks of the northeastern Great Basin and their relation to tectonic activity and ore deposits, *in* Buffa, R.H., and Coyner, A.R., eds., *Geology and ore deposits of the Great Basin, Field Trip Guidebook Compendium*, v. 1: Geological Society of Nevada, p. 229-242.
- Zoback, M.L., and Thompson, G.A., 1978, Basin and Range rifting in northern Nevada; Clues from a mid-Miocene rift and its subsequent offsets: *Geology*, v. 6, p. 111-116.

CHAPTER 4

CONCLUSION

The vein deposits of the northern Shoshone Range, part of the greater Battle Mountain-Eureka trend, have collectively produced almost 70 million ounces (Moz) of copper, lead, silver, and gold mostly between the 1860s and 1930s. The vein deposits are hosted within Paleozoic siliciclastic and siliceous upper plate rocks and/or Tertiary intrusive igneous rocks, and mostly felsic intrusive igneous rocks are emplaced along a west-northwest trend through the northern Shoshone Range and located both proximal and distal to mineralized areas.

Analysis of vein-hosted ore and gangue minerals and intrusive igneous rocks via various geochronological and geochemical methods, this study has established:

1. All radiogenically dated igneous rocks within the study area are Eocene in age;
2. Molybdenite mineralization is essentially contemporaneous with Eocene granitic intrusive rocks;
3. No definitive geochemical difference exists between barren intrusive igneous rocks and those associated with porphyry (molybdenite) mineralization;
4. Vein-hosted mineralization is younger than the youngest igneous rocks within the study area based on samples from the Gray Eagle mine (at least 0.5 m.y. younger than the Granite Mountain host rock) and the discordant quartz breccia pipe at Hilltop (at least 2.8 m.y. younger than the nearby Hobo Gulch intrusion). The age differences may reflect active hydrothermal systems associated with individual igneous intrusions or a secondary pulse of heat and/or fluids associated with slightly younger magmatism (e.g. Tenabo);

5. A magmatic source for most vein-hosted sulfide minerals and variable sources (mostly meteoric and/or magmatic, with lesser organic carbon and carbonate rock sources) for carbonate minerals' carbon and oxygen. Oxygen isotope data support variably-mixed meteoric and/or magmatic source fluids for vein quartz;
6. Vein quartz source fluids possessed variable salinities, even within the same deposit;
7. Ore mineral and ore-bearing vein quartz deposition occurred over a wide temperature range (based on geothermometry data from fluid inclusions and stable isotope partitioning) spanning the epithermal-porphyry continuum, probably representing the transitional zone between the two regimes.

Based on data from this study, it is problematic to classify the northern Shoshone Range vein deposits as strictly one deposit type, as they collectively exhibit characteristics indicative of low- and intermediate sulfidation epithermal deposits, Cordilleran vein-type deposits, and base metal veins associated with Cu-Mo porphyry deposits.

APPENDIX A

Geochemical (assay) data and location information for northern Shoshone Range study area samples.

N = Not present in concentrations above detection limits.

Sample	Mine / Area	UTMX	UTMY
HT02-1	Hilltop	516562	4473457
HT02-2	Hilltop	516554	4473454
HT02-3	Hilltop	515558	4473801
HT02-4	Hilltop	516812	4473231
HT02-5	Hilltop	516823	4473350
HT02-6	Hilltop	516200	4472989
HT02-7	Hilltop	516200	4472989
HT02-8	Hilltop	516200	4472989
HT02-9	Hilltop	516200	4472989
HT02-10	Hilltop	516174	4473000
HT02-11	Hilltop	516174	4473000
HT02-12	Hilltop	516087	4473065
HT02-13	Hilltop	516174	4473000
HT02-14	Hilltop	516478	4473264
HT02-15	Hilltop	515888.55	4474810.82
HT02-16	Hilltop	516127.3	4474328.2
HT02-17	Hilltop	516127.4	4474328.3
CK02-1	Hilltop	516707	4473757
CK02-2	Hilltop	516707	4473757
CK02-3	Granite Mountain	521621.37	4471992.81
CK02-4	Hilltop	516707	4473757
CK02-5	Hilltop	516707	4473757
CK02-6	Granite Mountain	521664.51	4471529.61
CK02-7	Granite Mountain	521416.55	4471527.27
CK02-8	Granite Mountain	521409.69	4471383.19
CK02-9	Granite Mountain	521433.22	4471406.16
CK02-10	Granite Mountain	522187.14	4469888.68
CK02-11	Granite Mountain	522187.14	4469888.68
CK02-12	Granite Mountain	522002.33	4469815.75
CK02-13	Granite Mountain	521956.41	4469819.19
CK02-14	Hilltop	515389.75	4473038.91
CK02-15	Hilltop	515417.43	4473220.11
CK02-16	Hilltop	515151.91	4473429.52
CK02-17	Hilltop	515586.75	4472859.76
CK02-18	Hilltop	515586.75	4472859.76
CK02-19	Hilltop	515586.75	4472859.76
CK02-20	Hilltop	515563.49	4473253.03
CK02-21	Hilltop	517446.67	4473878.91

Sample	Au ppb	Hg ppb	Ag ppm	Al %	As ppm
HT02-1	66.0	89.0	0.9	0.1	22.0
HT02-2	191.0	14.0	0.8	0.1	729.0
HT02-3	1987.0	13.0	25.5	0.2	186.0
HT02-4	143.0	14.0	0.5	2.7	24.0
HT02-5	63.0	24.0	N	2.2	9.0
HT02-6	704.0	87.0	13.9	0.2	221.0
HT02-7	41.0	45.0	0.3	0.2	6.0
HT02-8	778.0	N	326.8	0.1	432.0
HT02-9	282.0	26.0	10.6	0.1	113.0
HT02-10	53.0	374.0	2.7	0.1	22.0
HT02-11	13.0	1030.0	0.2	0.2	16.0
HT02-12	929.0	35.0	135.0	0.1	523.0
HT02-13	49.0	680.0	2.5	0.2	21.0
HT02-14	1826.0	12.0	24.4	0.1	2321.0
HT02-15	75.0	283.0	3.0	0.0	21.0
HT02-16	32390.0	910.0	85.3	0.1	7669.9
HT02-17	5.0	200.0	0.0	0.1	0.2
CK02-1	13836.0	1770.0	35.3	0.2	10000.0
CK02-2	26173.0	15000.0	48.0	0.0	10000.0
CK02-3	596.0	2160.0	1.1	0.5	2501.0
CK02-4	3011.0	760.0	5.1	0.2	1037.0
CK02-5	11233.0	570.0	18.4	0.1	6132.0
CK02-6	743.0	204.0	36.4	0.3	2324.0
CK02-7	69.0	3160.0	0.3	0.5	104.0
CK02-8	26.0	54.0	1.9	0.2	36.0
CK02-9	33.0	126.0	0.1	0.3	33.0
CK02-10	81.0	17.0	3.8	1.1	354.0
CK02-11	2532.0	390.0	38.6	0.1	10000.0
CK02-12	2544.0	187.0	27.2	0.2	10000.0
CK02-13	1160.0	11.0	4.3	0.0	6928.0
CK02-14	35.0	N	0.2	1.2	N
CK02-15	19.0	18.0	N	3.2	N
CK02-16	34.0	275.0	1.3	0.2	49.0
CK02-17	8.0	16.0	0.1	5.4	N
CK02-18	10.0	13.0	0.1	0.9	4.0
CK02-19	10.0	N	N	0.8	4.0
CK02-20	8.0	N	N	0.2	5.0
CK02-21	336.0	188.0	54.0	0.1	6599.0

Sample	B ppm	Ba ppm	Bi ppm	Ca %	Cd ppm	Co ppm	Cr ppm
HT02-1	4.0	21.0	10.0	0.1	N	N	55.0
HT02-2	6.0	28.0	5.0	0.1	N	N	44.0
HT02-3	8.0	64.0	50.0	1.1	114.4	10.0	73.0
HT02-4	15.0	230.0	6.0	0.8	1.5	7.0	31.0
HT02-5	14.0	57.0	5.0	1.0	1.5	9.0	41.0
HT02-6	8.0	106.0	5.0	0.2	1.5	N	5.0
HT02-7	4.0	797.0	2.0	0.2	N	N	6.0
HT02-8	3.0	22.0	N	0.0	N	N	7.0
HT02-9	3.0	519.0	8.0	0.1	N	N	16.0
HT02-10	3.0	806.0	N	0.0	N	N	14.0
HT02-11	3.0	785.0	N	0.1	N	N	10.0
HT02-12	4.0	55.0	2.0	0.0	N	N	28.0
HT02-13	3.0	1080.0	1.0	0.0	N	N	13.0
HT02-14	65.0	12.0	42.0	0.0	61.5	8.0	17.0
HT02-15	4.0	166.0	1.0	0.0	N	N	33.0
HT02-16	35.0	39.2	143.0	0.0	85.1	20.5	18.3
HT02-17	3.0	0.0	0.0	0.0	0.0	0.1	0.2
CK02-1	17.0	19.0	39.0	0.0	40.6	11.0	82.0
CK02-2	42.0	10.0	65.0	0.0	3.6	33.0	36.0
CK02-3	7.0	147.0	3.0	0.1	N	6.0	52.0
CK02-4	10.0	44.0	6.0	0.0	6.7	8.0	91.0
CK02-5	11.0	36.0	25.0	0.0	24.5	10.0	85.0
CK02-6	34.0	60.0	47.0	0.1	8.9	1.0	35.0
CK02-7	10.0	459.0	3.0	0.1	0.6	6.0	36.0
CK02-8	5.0	44.0	6.0	0.1	N	N	46.0
CK02-9	5.0	68.0	N	0.0	N	1.0	114.0
CK02-10	11.0	81.0	4.0	0.5	2.5	6.0	32.0
CK02-11	23.0	12.0	43.0	1.8	132.4	4.0	27.0
CK02-12	16.0	26.0	20.0	0.3	22.9	3.0	61.0
CK02-13	10.0	16.0	10.0	10.0	1.6	1.0	15.0
CK02-14	10.0	58.0	4.0	0.5	0.6	8.0	37.0
CK02-15	36.0	239.0	18.0	0.3	2.4	7.0	29.0
CK02-16	4.0	755.0	3.0	0.0	N	N	16.0
CK02-17	40.0	211.0	18.0	2.9	3.0	8.0	48.0
CK02-18	6.0	128.0	1.0	1.4	N	7.0	45.0
CK02-19	7.0	58.0	3.0	0.9	N	5.0	27.0
CK02-20	4.0	442.0	N	0.1	N	N	7.0
CK02-21	9.0	417.0	8.0	0.1	1.1	N	22.0

Sample	Cu ppm	Fe %	K %	La ppm	Mg %	Mn ppm	Mo ppm	Na %
HT02-1	13.0	0.1	0.1	N	0.0	18.0	6.0	0.0
HT02-2	12.0	0.2	0.1	N	0.0	24.0	7.0	0.0
HT02-3	436.0	1.1	0.1	4.0	0.4	537.0	4.0	0.0
HT02-4	697.0	3.2	0.2	10.0	1.2	206.0	2.0	0.0
HT02-5	342.0	2.9	0.1	6.0	1.3	205.0	9.0	0.2
HT02-6	23.0	1.1	0.2	4.0	0.0	6.0	2.0	0.0
HT02-7	5.0	0.2	0.2	N	0.0	9.0	N	0.0
HT02-8	96.0	0.3	0.1	N	0.0	5.0	N	0.0
HT02-9	3.0	0.2	0.1	N	0.0	5.0	3.0	0.0
HT02-10	5.0	0.2	0.1	N	0.0	3.0	1.0	0.0
HT02-11	1.0	0.2	0.2	4.0	0.0	4.0	N	0.0
HT02-12	16.0	0.4	0.0	N	0.0	4.0	1.0	0.0
HT02-13	6.0	0.2	0.1	N	0.0	4.0	1.0	0.0
HT02-14	207.0	16.3	0.0	N	0.0	N	N	0.0
HT02-15	6.0	0.3	0.0	N	0.0	7.0	3.0	0.0
HT02-16	1082.6	6.8	0.0	0.8	0.0	139.8	34.3	0.0
HT02-17	0.1	2.0	0.0	0.1	0.0	0.1	0.9	0.0
CK02-1	1439.0	3.3	0.0	N	0.0	63.0	37.0	0.0
CK02-2	249.0	10.2	0.0	N	0.0	123.0	1.0	0.0
CK02-3	17.0	0.9	0.1	10.0	0.0	132.0	8.0	0.0
CK02-4	199.0	1.4	0.1	3.0	0.0	38.0	29.0	0.0
CK02-5	545.0	1.6	0.0	2.0	0.0	58.0	24.0	0.0
CK02-6	70.0	8.0	0.0	5.0	0.0	141.0	3.0	0.0
CK02-7	5.0	1.7	0.1	16.0	0.0	221.0	5.0	0.0
CK02-8	3.0	0.2	0.2	6.0	0.0	41.0	2.0	0.1
CK02-9	4.0	0.3	0.1	4.0	0.0	47.0	5.0	0.1
CK02-10	34.0	2.1	0.2	9.0	0.4	137.0	1.0	0.1
CK02-11	337.0	5.7	0.1	2.0	0.2	580.0	N	0.0
CK02-12	76.0	3.5	0.2	3.0	0.0	222.0	1.0	0.0
CK02-13	8.0	2.7	0.1	4.0	0.3	5138.0	N	0.0
CK02-14	7.0	1.8	0.1	7.0	0.9	367.0	N	0.1
CK02-15	3.0	9.9	0.0	7.0	0.4	3128.0	N	0.0
CK02-16	9.0	0.3	0.1	4.0	0.0	22.0	5.0	0.0
CK02-17	2.0	11.4	0.0	9.0	1.1	2588.0	N	0.0
CK02-18	6.0	1.0	0.1	7.0	0.3	381.0	N	0.1
CK02-19	5.0	1.0	0.1	5.0	0.2	253.0	N	0.0
CK02-20	3.0	0.3	0.2	15.0	0.0	11.0	2.0	0.0
CK02-21	139.0	1.5	0.0	N	0.0	76.0	8.0	0.0

Sample	Ni ppm	P ppm	Pb ppm	Sb ppm	Se ppm
HT02-1	4.0	226.0	3.0	N	N
HT02-2	4.0	208.0	6.0	7.0	4.0
HT02-3	26.0	415.0	3981.0	64.0	84.0
HT02-4	7.0	491.0	34.0	N	N
HT02-5	8.0	353.0	60.0	N	N
HT02-6	2.0	N	714.0	352.0	22.0
HT02-7	1.0	N	8.0	7.0	N
HT02-8	N	N	59.0	10000.0	856.0
HT02-9	N	N	42.0	1395.0	5.0
HT02-10	2.0	N	14.0	595.0	4.0
HT02-11	N	N	8.0	154.0	N
HT02-12	N	N	11.0	10000.0	99.0
HT02-13	2.0	N	15.0	217.0	N
HT02-14	15.0	N	6599.0	133.0	311.0
HT02-15	4.0	N	22.0	180.0	2.0
HT02-16	127.9	185.8	2665.8	232.4	97.1
HT02-17	0.1	0.5	0.1	0.1	0.3
CK02-1	16.0	49.0	1356.0	335.0	38.0
CK02-2	25.0	90.0	42.0	375.0	N
CK02-3	8.0	246.0	16.0	10.0	N
CK02-4	19.0	45.0	242.0	69.0	5.0
CK02-5	16.0	122.0	2276.0	706.0	22.0
CK02-6	3.0	385.0	5249.0	16.0	N
CK02-7	5.0	255.0	59.0	8.0	N
CK02-8	3.0	64.0	45.0	N	N
CK02-9	6.0	30.0	12.0	N	N
CK02-10	3.0	362.0	515.0	N	N
CK02-11	3.0	180.0	5943.0	121.0	N
CK02-12	4.0	196.0	1895.0	45.0	N
CK02-13	1.0	34.0	157.0	5.0	N
CK02-14	7.0	N	30.0	34.0	N
CK02-15	11.0	N	17.0	10.0	N
CK02-16	1.0	N	21.0	13.0	N
CK02-17	12.0	N	11.0	6.0	N
CK02-18	13.0	N	12.0	11.0	N
CK02-19	8.0	N	11.0	3.0	N
CK02-20	N	N	14.0	6.0	N
CK02-21	1.0	N	10000.0	319.0	9.0

Sample	Sr ppm	Ti %	Th ppm	V ppm	W ppm	Zn ppm
HT02-1	3.0	0.0	N	4.0	N	6.0
HT02-2	9.0	0.0	N	3.0	N	2.0
HT02-3	21.0	0.0	N	6.0	N	4559.0
HT02-4	38.0	0.0	N	61.0	N	75.0
HT02-5	23.0	0.1	N	49.0	N	88.0
HT02-6	8.0	0.0	N	5.0	N	152.0
HT02-7	18.0	0.0	N	5.0	N	5.0
HT02-8	N	0.0	N	N	9.0	20.0
HT02-9	N	0.0	N	3.0	N	2.0
HT02-10	N	0.0	N	5.0	N	2.0
HT02-11	N	0.0	N	N	N	2.0
HT02-12	N	0.0	N	N	N	11.0
HT02-13	N	0.0	N	5.0	N	2.0
HT02-14	N	0.0	1.1	5.0	N	3494.0
HT02-15	N	0.0	N	3.0	N	15.0
HT02-16	17.2	0.0	N	5.3	3.5	2197.7
HT02-17	1.0	0.0	0.1	0.1	0.1	0.1
CK02-1	9.0	0.0	5.4	4.0	N	2053.0
CK02-2	22.0	0.0	19.7	3.0	N	59.0
CK02-3	11.0	0.0	0.7	13.0	N	23.0
CK02-4	11.0	0.0	N	6.0	N	350.0
CK02-5	11.0	0.0	1.5	4.0	N	1126.0
CK02-6	22.0	0.0	1.2	16.0	N	347.0
CK02-7	10.0	0.0	N	11.0	N	25.0
CK02-8	4.0	0.0	N	N	N	6.0
CK02-9	2.0	0.0	N	2.0	N	5.0
CK02-10	28.0	0.0	N	29.0	N	583.0
CK02-11	84.0	0.0	0.9	N	N	8097.0
CK02-12	14.0	0.0	N	2.0	N	1249.0
CK02-13	999.0	0.0	1.8	N	N	71.0
CK02-14	12.0	0.1	N	26.0	N	47.0
CK02-15	21.0	0.0	1.3	39.0	N	38.0
CK02-16	2.0	0.0	N	5.0	N	2.0
CK02-17	66.0	0.0	1.4	52.0	N	99.0
CK02-18	49.0	0.1	N	18.0	N	25.0
CK02-19	22.0	0.1	N	17.0	N	36.0
CK02-20	8.0	0.0	N	N	N	2.0
CK02-21	17.0	0.0	N	5.0	N	10.0

Sample	Mine / Area	UTMX	UTMY
CK02-22	Hilltop	517446.67	4473878.91
CK02-23	Hilltop	517642.09	4473891.46
CK02-24	Hilltop	517650.34	4473961.63
CK02-25	Hilltop	517650.34	4473961.63
CK02-26	Hilltop	517650.34	4473961.63
CK02-27	Hilltop	517690.66	4473966.95
CK02-28	Hilltop	517832.73	4473656.17
CK02-29	Hilltop	517832.73	4473656.17
CK02-30	Hilltop	517832.73	4473656.17
CK02-31	Hilltop	517987.24	4474212.26
CK02-32	Hilltop	517987.24	4474212.26
CK02-33	Hilltop	517987.24	4474212.26
CK02-34	Hilltop	518042.78	4474207.13
CK02-35	Hilltop	518144.16	4474351.36
CK02-36	Hilltop	518144.16	4474351.36
CK02-37	Hilltop	517942.78	4474235.05
CK02-38	Hilltop	517942.78	4474235.05
CK02-39	Hilltop	517942.78	4474235.05
CK02-40	Hilltop	519159.83	4473622.13
CK02-41	Hilltop	519159.83	4473622.13
CK02-42	Hilltop	519118.96	4473222.43
CK02-43	Hilltop	519124.19	4473163.19
CK02-44	Hilltop	518468.73	4473350.5
CK02-45	Hilltop	518468.73	4473350.5
CK02-46	Hilltop	518468.73	4473350.5
CK02-47	Hilltop	518451.38	4473291.97
CK02-48	Hilltop	517804.2	4473555.56
CK02-49	Hilltop	517804.2	4473555.56
CK02-50	Hilltop	517845.29	4473053.54
CK02-51	Hilltop	517845.29	4473053.54
CK02-52	Hilltop	517856.04	4473135.3
CK02-53	Hilltop	517571.07	4473302.03
CK02-54	Hilltop	517493.76	4473216.29
CK02-55	Hilltop	517493.76	4473216.29
CK02-56	Hilltop	517553.38	4473577.45
GM-1	Granite Mountain	521468.05	4472356.11
GM-2	Granite Mountain	521476.09	4472334.3
GM-3	Granite Mountain	521484.13	4472313.64

Sample	Au ppb	Hg ppb	Ag ppm	Al %	As ppm
CK02-22	5205.0	1660.0	106.0	0.3	10000.0
CK02-23	479.0	192.0	54.0	0.6	1840.0
CK02-24	183.0	14.0	62.0	0.3	3314.0
CK02-25	30.0	10.0	1.0	0.4	113.0
CK02-26	43.0	28.0	56.0	0.1	146.0
CK02-27	7.0	N	0.2	1.6	20.0
CK02-28	3425.0	38.0	21.8	0.0	10000.0
CK02-29	27960.0	20.0	99.0	0.2	10000.0
CK02-30	7382.0	39.0	6.9	0.8	10000.0
CK02-31	3219.0	56.0	146.0	0.2	10000.0
CK02-32	764.0	112.0	41.7	0.2	9138.0
CK02-33	72.0	55.0	1.4	0.3	488.0
CK02-34	1986.0	352.0	147.0	0.2	10000.0
CK02-35	334.0	101.0	41.1	0.3	1635.0
CK02-36	603.0	35.0	38.4	0.4	4292.0
CK02-37	359.0	3730.0	90.0	0.1	1513.0
CK02-38	25.0	25.0	1.3	1.2	129.0
CK02-39	21.0	18.0	0.5	2.7	53.0
CK02-40	27.0	N	N	0.7	50.0
CK02-41	14.0	N	N	1.0	35.0
CK02-42	28.0	N	0.2	1.2	32.0
CK02-43	544.0	10.0	0.4	4.3	13.0
CK02-44	2283.0	N	4.8	0.5	43.0
CK02-45	136.0	14.0	2.1	5.6	21.0
CK02-46	14178.0	11.0	10.3	0.9	49.0
CK02-47	158.0	145.0	2.8	0.5	454.0
CK02-48	462.0	15.0	0.8	0.6	584.0
CK02-49	4420.0	4060.0	82.0	0.3	5663.0
CK02-50	123.0	65.0	0.6	0.3	131.0
CK02-51	980.0	182.0	0.7	0.3	473.0
CK02-52	55.0	35.0	4.9	0.2	166.0
CK02-53	46.0	25.0	0.6	0.7	253.0
CK02-54	96.0	N	0.2	0.1	29.0
CK02-55	84.0	10.0	20.2	1.6	1651.0
CK02-56	216.0	14.0	0.5	1.1	105.0
GM-1	20.0	14.0	0.2	1.0	55.0
GM-2	15.0	N	N	2.0	56.0
GM-3	12.0	N	N	1.4	11.0

Sample	B ppm	Ba ppm	Bi ppm	Ca %	Cd ppm	Co ppm	Cr ppm
CK02-22	23.0	62.0	42.0	0.2	4.5	1.0	24.0
CK02-23	53.0	138.0	63.0	0.0	10.5	1.0	21.0
CK02-24	9.0	92.0	14.0	0.0	3.7	N	25.0
CK02-25	7.0	66.0	4.0	0.1	1.0	N	34.0
CK02-26	12.0	47.0	6.0	0.0	10.0	16.0	68.0
CK02-27	6.0	105.0	1.0	0.5	0.5	3.0	50.0
CK02-28	22.0	14.0	35.0	0.0	1.6	N	33.0
CK02-29	67.0	3.0	84.0	0.0	5.2	N	9.0
CK02-30	40.0	153.0	98.0	0.2	6.5	1.0	129.0
CK02-31	40.0	60.0	39.0	0.3	62.5	N	18.0
CK02-32	18.0	239.0	13.0	0.2	22.3	1.0	66.0
CK02-33	7.0	425.0	3.0	2.8	0.8	13.0	29.0
CK02-34	39.0	317.0	31.0	0.4	43.4	N	32.0
CK02-35	15.0	60.0	7.0	0.1	2.7	1.0	34.0
CK02-36	58.0	47.0	31.0	0.1	11.2	1.0	22.0
CK02-37	25.0	30.0	16.0	0.3	448.7	3.0	26.0
CK02-38	4.0	27.0	N	0.9	1.5	N	26.0
CK02-39	3.0	123.0	N	1.6	1.3	1.0	23.0
CK02-40	5.0	41.0	N	0.7	N	2.0	24.0
CK02-41	9.0	41.0	2.0	0.5	N	7.0	55.0
CK02-42	7.0	75.0	2.0	0.7	0.8	3.0	28.0
CK02-43	15.0	32.0	7.0	2.0	1.8	7.0	52.0
CK02-44	12.0	23.0	6.0	0.1	0.8	N	53.0
CK02-45	11.0	74.0	5.0	2.3	2.7	7.0	49.0
CK02-46	11.0	14.0	5.0	0.1	0.8	2.0	50.0
CK02-47	13.0	72.0	12.0	1.2	1.7	5.0	22.0
CK02-48	11.0	186.0	9.0	0.1	0.6	N	40.0
CK02-49	41.0	118.0	90.0	0.1	4.7	N	30.0
CK02-50	5.0	125.0	2.0	0.1	N	N	36.0
CK02-51	9.0	105.0	7.0	0.1	N	N	29.0
CK02-52	9.0	106.0	41.0	0.1	N	N	42.0
CK02-53	10.0	262.0	4.0	2.0	3.9	5.0	25.0
CK02-54	5.0	29.0	2.0	0.0	N	N	67.0
CK02-55	43.0	275.0	29.0	0.2	4.4	N	27.0
CK02-56	9.0	43.0	5.0	0.1	2.4	2.0	36.0
GM-1	11.0	120.0	4.0	0.8	0.7	7.0	91.0
GM-2	15.0	244.0	5.0	0.7	0.8	15.0	41.0
GM-3	12.0	265.0	3.0	0.4	0.6	10.0	50.0

Sample	Cu ppm	Fe %	K %	La ppm	Mg %	Mn ppm	Mo ppm	Na %
CK02-22	611.0	5.4	0.2	N	0.0	25.0	13.0	0.0
CK02-23	266.0	13.7	0.0	N	0.0	169.0	4.0	0.0
CK02-24	426.0	1.3	0.0	N	0.0	42.0	1.0	0.0
CK02-25	8.0	0.5	0.0	N	0.2	187.0	1.0	0.0
CK02-26	221.0	2.1	0.0	N	0.0	5663.0	4.0	0.0
CK02-27	14.0	0.9	0.0	2.0	0.9	201.0	N	0.0
CK02-28	90.0	4.5	0.0	N	0.0	12.0	2.0	0.0
CK02-29	292.0	17.4	0.0	N	0.0	N	N	0.0
CK02-30	540.0	10.1	0.0	3.0	0.0	50.0	28.0	0.0
CK02-31	470.0	10.2	0.0	2.0	0.0	142.0	15.0	0.1
CK02-32	190.0	4.1	0.0	N	0.0	290.0	21.0	0.0
CK02-33	46.0	1.3	0.1	13.0	0.1	955.0	N	0.0
CK02-34	433.0	9.5	0.0	N	0.0	547.0	184.0	0.0
CK02-35	123.0	2.8	0.0	4.0	0.0	773.0	106.0	0.0
CK02-36	633.0	14.7	0.0	N	0.1	731.0	195.0	0.0
CK02-37	1295.0	5.8	0.0	3.0	0.1	7159.0	8.0	0.0
CK02-38	16.0	0.4	0.0	N	0.4	237.0	5.0	0.0
CK02-39	6.0	0.1	0.1	2.0	0.1	71.0	1.0	0.0
CK02-40	2.0	0.2	0.0	5.0	0.2	33.0	1.0	0.0
CK02-41	4.0	1.1	0.1	7.0	0.5	69.0	1.0	0.2
CK02-42	31.0	0.6	0.1	7.0	0.2	229.0	2.0	0.0
CK02-43	110.0	3.1	0.0	5.0	1.2	777.0	2.0	0.0
CK02-44	475.0	2.0	0.0	N	0.1	100.0	378.0	0.0
CK02-45	394.0	2.0	0.0	2.0	1.1	742.0	18.0	0.0
CK02-46	1520.0	1.7	0.0	N	0.5	346.0	141.0	0.0
CK02-47	456.0	2.5	0.2	11.0	0.1	492.0	4.0	0.1
CK02-48	182.0	1.8	0.2	11.0	0.1	33.0	4.0	0.1
CK02-49	240.0	9.9	0.0	3.0	0.0	21.0	121.0	0.0
CK02-50	15.0	0.3	0.2	4.0	0.0	14.0	21.0	0.0
CK02-51	77.0	1.2	0.1	5.0	0.0	14.0	46.0	0.0
CK02-52	64.0	1.0	0.1	5.0	0.0	24.0	28.0	0.0
CK02-53	309.0	1.5	0.1	12.0	0.1	2125.0	26.0	0.0
CK02-54	30.0	0.3	0.0	N	0.0	92.0	4.0	0.0
CK02-55	667.0	10.2	0.0	11.0	0.1	182.0	255.0	0.0
CK02-56	557.0	1.2	0.2	7.0	0.6	474.0	6.0	0.0
GM-1	6.0	2.2	0.1	3.0	0.6	550.0	N	0.0
GM-2	7.0	3.1	1.0	4.0	1.0	644.0	N	0.0
GM-3	2.0	2.3	1.0	4.0	0.7	439.0	1.0	0.0

Sample	Ni ppm	P ppm	Pb ppm	Sb ppm	Se ppm
CK02-22	N	N	10000.0	500.0	69.0
CK02-23	23.0	N	7952.0	42.0	N
CK02-24	2.0	N	10000.0	36.0	30.0
CK02-25	4.0	N	215.0	4.0	N
CK02-26	14.0	N	2324.0	4.0	N
CK02-27	8.0	N	26.0	3.0	N
CK02-28	2.0	N	863.0	53.0	14.0
CK02-29	N	N	10000.0	434.0	94.0
CK02-30	N	N	5003.0	409.0	N
CK02-31	4.0	N	10000.0	111.0	23.0
CK02-32	5.0	N	10000.0	47.0	17.0
CK02-33	19.0	N	241.0	5.0	N
CK02-34	26.0	N	10000.0	157.0	16.0
CK02-35	7.0	N	8471.0	21.0	109.0
CK02-36	12.0	N	10000.0	43.0	195.0
CK02-37	11.0	N	10000.0	117.0	30.0
CK02-38	4.0	N	414.0	2.0	4.0
CK02-39	2.0	N	105.0	N	N
CK02-40	3.0	N	38.0	N	N
CK02-41	14.0	N	20.0	N	N
CK02-42	4.0	N	41.0	N	N
CK02-43	8.0	N	38.0	N	N
CK02-44	3.0	N	33.0	N	N
CK02-45	8.0	N	184.0	N	N
CK02-46	6.0	N	49.0	N	N
CK02-47	10.0	N	69.0	125.0	N
CK02-48	3.0	N	139.0	7.0	21.0
CK02-49	1.0	N	4071.0	179.0	114.0
CK02-50	2.0	N	59.0	10.0	N
CK02-51	4.0	N	53.0	43.0	N
CK02-52	4.0	N	179.0	25.0	N
CK02-53	14.0	N	157.0	26.0	N
CK02-54	3.0	N	42.0	2.0	N
CK02-55	6.0	N	2866.0	18.0	13.0
CK02-56	6.0	N	332.0	2.0	N
GM-1	7.0	590.0	14.0	N	N
GM-2	10.0	611.0	13.0	N	N
GM-3	5.0	437.0	6.0	N	N

Sample	Sr ppm	Ti %	Th ppm	V ppm	W ppm	Zn ppm
CK02-22	45.0	0.0	N	13.0	N	58.0
CK02-23	N	0.0	N	85.0	N	1721.0
CK02-24	N	0.0	N	5.0	N	261.0
CK02-25	N	0.0	N	6.0	N	78.0
CK02-26	N	0.0	3.2	5.0	N	2225.0
CK02-27	52.0	0.0	N	16.0	N	37.0
CK02-28	N	0.0	N	3.0	N	49.0
CK02-29	N	0.0	0.8	6.0	N	64.0
CK02-30	28.0	0.0	1.0	48.0	N	176.0
CK02-31	35.0	0.0	N	73.0	N	2323.0
CK02-32	58.0	0.0	0.5	41.0	N	908.0
CK02-33	13.0	0.0	0.6	33.0	N	79.0
CK02-34	20.0	0.0	N	90.0	N	2755.0
CK02-35	N	0.0	N	35.0	N	518.0
CK02-36	N	0.0	N	68.0	N	2548.0
CK02-37	N	0.0	3.9	25.0	N	10000.0
CK02-38	56.0	0.0	N	10.0	N	245.0
CK02-39	274.0	0.1	N	3.0	N	163.0
CK02-40	57.0	0.0	N	6.0	N	14.0
CK02-41	30.0	0.1	N	19.0	N	12.0
CK02-42	88.0	0.1	N	17.0	N	57.0
CK02-43	104.0	0.1	N	52.0	N	89.0
CK02-44	N	0.0	N	11.0	N	37.0
CK02-45	322.0	0.1	N	27.0	N	154.0
CK02-46	N	0.0	N	13.0	N	49.0
CK02-47	52.0	0.0	0.8	15.0	N	94.0
CK02-48	24.0	0.0	N	27.0	N	9.0
CK02-49	39.0	0.0	5.3	15.0	N	33.0
CK02-50	N	0.0	N	7.0	N	5.0
CK02-51	6.0	0.0	1.1	10.0	N	27.0
CK02-52	N	0.0	N	11.0	N	21.0
CK02-53	21.0	0.0	0.6	25.0	N	243.0
CK02-54	N	0.0	N	4.0	N	22.0
CK02-55	7.0	0.0	N	66.0	N	232.0
CK02-56	N	0.0	N	25.0	N	94.0
GM-1	18.0	0.1	N	44.0	N	46.0
GM-2	27.0	0.2	N	67.0	N	66.0
GM-3	19.0	0.2	N	42.0	N	43.0

Sample	Mine / Area	UTMX	UTMY
GM-4	Granite Mountain	521449.14	4472187.93
GM-5	Granite Mountain	521469.83	4472039.27
GM-6	Granite Mountain	522909.23	4469785.5
GM-7	Granite Mountain	521740.26	4471599.07
GM-8	Granite Mountain	521344.81	4471461.82
GM-9	Granite Mountain	521829.38	4470763.37
GM-10	Granite Mountain	521829.38	4470763.37
GM-11	Granite Mountain	520791	4471059
GM-12	Granite Mountain	520791	4471059
GM-13	Granite Mountain	520833	4471046
GM-14	Granite Mountain	520965	4471129
GM-15	Granite Mountain	520672	4470270
GM-16	Granite Mountain	520965	4471129
GM-17	Granite Mountain	520965	4471129
GM-18	Granite Mountain	520965	4471129
KATT-1	Kattenhorn	514657.12	4473852.35
KATT-2	Kattenhorn	514657.12	4473852.35
KATT-3	Kattenhorn	514529.86	4473791.26
KATT-4	Kattenhorn	514529.86	4473791.26
KATT-5	Kattenhorn	514529.86	4473791.26
KATT-6	Kattenhorn	514486.87	4473734.67
KATT-7	Kattenhorn	514183.13	4474071.21
KATT-8	Kattenhorn	514183.13	4474071.21
KATT-9	Kattenhorn	514183.13	4474071.21
KATT-10	Kattenhorn	514183.13	4474071.21
KATT-11	Kattenhorn	514211.66	4474172.42
KATT-12	Kattenhorn	514211.66	4474172.42
KATT-13	Kattenhorn	514211.66	4474172.42
KATT-14	Kattenhorn	514211.66	4474172.42
KATT-15	Kattenhorn	514211.66	4474172.42
KATT-16	Kattenhorn	514350.54	4473963.62
KATT-17	Kattenhorn	514335.45	4474002.15
KATT-18	Kattenhorn	514335.45	4474002.15
KATT-19	Kattenhorn	514335.45	4474002.15
KATT-20	Kattenhorn	514440.39	4473852.71
KATT-21	Kattenhorn	514313.9	4474098.09
KATT-22	Kattenhorn	514472.41	4474049.15
KATT-23	Kattenhorn	514472.41	4474049.15

Sample	Au ppb	Hg ppb	Ag ppm	Al %	As ppm
GM-4	10.0	N	N	1.0	9.0
GM-5	5.0	N	N	1.4	8.0
GM-6	11.0	N	N	1.0	5.0
GM-7	8.0	N	N	0.7	8.0
GM-8	6.0	N	N	1.3	7.0
GM-9	6.0	30.0	N	2.0	18.0
GM-10	2.0	27.0	N	2.5	12.0
GM-11	12.0	1320.0	0.1	0.3	80.0
GM-12	14.0	1050.0	N	0.2	6.0
GM-13	4.0	65.0	0.1	0.0	N
GM-14	55.0	1010.0	2.4	0.2	259.0
GM-15	16.0	39.0	0.1	1.0	N
GM-16	10.0	236.0	0.3	0.1	13.0
GM-17	5.0	23.0	0.1	0.0	N
GM-18	8.0	305.0	0.1	0.2	25.0
KATT-1	252.0	249.0	307.9	0.1	34.0
KATT-2	251.0	620.0	93.0	0.2	72.0
KATT-3	1918.0	4170.0	807.8	0.1	861.0
KATT-4	178.0	1050.0	297.3	0.0	96.0
KATT-5	1548.0	1220.0	343.3	0.1	2275.0
KATT-6	18.0	82.0	1.1	0.5	87.0
KATT-7	233.0	500.0	56.0	0.1	100.0
KATT-8	182.0	610.0	75.0	0.2	96.0
KATT-9	355.0	226.0	118.0	0.0	86.0
KATT-10	160.0	710.0	115.0	0.1	101.0
KATT-11	209.0	80.0	67.0	0.1	83.0
KATT-12	208.0	149.0	47.0	0.0	101.0
KATT-13	57.0	2750.0	12.3	0.1	47.0
KATT-14	145.0	296.0	23.3	0.1	58.0
KATT-15	108.0	205.0	16.2	0.2	78.0
KATT-16	628.0	1320.0	713.7	0.3	362.0
KATT-17	147.0	1390.0	22.7	0.1	61.0
KATT-18	44.0	850.0	49.0	0.1	37.0
KATT-19	263.0	1080.0	27.3	0.1	156.0
KATT-20	99.0	261.0	26.1	0.2	61.0
KATT-21	193.0	8360.0	39.3	0.2	40.0
KATT-22	31.0	502.0	7.5	0.2	277.0
KATT-23	137.0	610.0	74.0	0.2	65.0

Sample	B ppm	Ba ppm	Bi ppm	Ca %	Cd ppm	Co ppm	Cr ppm
GM-4	11.0	136.0	2.0	0.5	N	7.0	76.0
GM-5	12.0	246.0	3.0	0.4	0.6	9.0	34.0
GM-6	11.0	129.0	4.0	0.3	0.5	8.0	44.0
GM-7	9.0	129.0	2.0	0.2	N	5.0	59.0
GM-8	12.0	47.0	4.0	0.6	0.6	9.0	99.0
GM-9	17.0	363.0	6.0	1.0	1.1	16.0	92.0
GM-10	17.0	414.0	10.0	2.3	1.0	17.0	97.0
GM-11	37.0	104.0	9.0	0.1	1.3	6.0	17.0
GM-12	6.0	28.0	N	0.1	N	N	29.0
GM-13	4.0	2418.0	N	0.0	N	N	4.0
GM-14	18.0	1810.0	7.0	0.1	0.8	2.0	15.0
GM-15	14.0	1154.0	2.0	0.4	N	8.0	32.0
GM-16	4.0	2619.0	N	0.0	N	N	7.0
GM-17	4.0	2702.0	N	0.0	N	N	3.0
GM-18	5.0	2657.0	N	0.1	N	N	20.0
KATT-1	5.0	372.0	1.0	0.0	8.0	N	65.0
KATT-2	6.0	697.0	2.0	0.0	N	N	56.0
KATT-3	6.0	2591.0	3.0	0.0	N	N	51.0
KATT-4	5.0	1581.0	1.0	0.0	N	N	17.0
KATT-5	6.0	483.0	3.0	0.0	N	N	41.0
KATT-6	5.0	437.0	2.0	0.0	N	N	16.0
KATT-7	7.0	117.0	4.0	0.0	N	2.0	51.0
KATT-8	7.0	90.0	4.0	0.0	0.7	2.0	79.0
KATT-9	5.0	725.0	3.0	0.0	1.4	N	34.0
KATT-10	6.0	1301.0	2.0	0.0	N	N	69.0
KATT-11	6.0	2179.0	1.0	0.0	N	N	63.0
KATT-12	6.0	1915.0	2.0	0.0	N	N	12.0
KATT-13	6.0	500.0	2.0	0.0	N	1.0	48.0
KATT-14	6.0	430.0	3.0	0.0	N	1.0	31.0
KATT-15	7.0	66.0	6.0	0.0	N	3.0	35.0
KATT-16	6.0	87.0	5.0	0.6	1.3	3.0	26.0
KATT-17	6.0	221.0	N	0.0	N	N	71.0
KATT-18	5.0	137.0	N	0.1	N	N	69.0
KATT-19	6.0	108.0	2.0	0.0	N	N	65.0
KATT-20	7.0	76.0	2.0	0.0	N	1.0	54.0
KATT-21	5.0	105.0	3.0	0.0	N	N	48.0
KATT-22	12.0	87.0	5.0	0.0	0.6	N	48.0
KATT-23	50.0	7.0	27.0	0.0	3.0	45.0	44.0

Sample	Cu ppm	Fe %	K %	La ppm	Mg %	Mn ppm	Mo ppm	Na %
GM-4	3.0	1.8	0.6	3.0	0.6	399.0	N	0.2
GM-5	2.0	2.2	0.9	4.0	0.7	434.0	1.0	0.0
GM-6	3.0	1.9	0.7	4.0	0.6	377.0	N	0.2
GM-7	10.0	1.2	0.4	5.0	0.3	203.0	3.0	0.2
GM-8	6.0	2.1	0.1	4.0	0.8	561.0	N	0.2
GM-9	10.0	3.8	0.7	31.0	1.0	623.0	N	0.1
GM-10	17.0	4.1	0.5	31.0	1.8	515.0	N	0.2
GM-11	N	5.4	0.0	13.0	0.0	432.0	8.0	0.0
GM-12	1.0	0.4	0.1	19.0	0.0	23.0	1.0	0.1
GM-13	N	0.1	0.0	N	0.0	24.0	N	0.0
GM-14	6.0	2.4	0.1	5.0	0.0	427.0	N	0.0
GM-15	1.0	1.8	0.6	6.0	0.5	335.0	N	0.2
GM-16	N	0.1	0.0	N	0.0	16.0	N	0.0
GM-17	N	0.0	0.0	N	0.0	5.0	N	0.0
GM-18	2.0	0.2	0.1	7.0	0.0	50.0	3.0	0.0
KATT-1	56.0	0.2	0.0	N	0.0	157.0	4.0	0.0
KATT-2	33.0	0.4	0.0	N	0.0	30.0	4.0	0.0
KATT-3	34.0	0.4	0.0	N	0.0	12.0	5.0	0.0
KATT-4	168.0	0.1	0.0	N	0.0	3.0	7.0	0.0
KATT-5	127.0	0.6	0.0	2.0	0.0	11.0	3.0	0.0
KATT-6	6.0	0.4	0.3	21.0	0.0	6.0	2.0	0.0
KATT-7	44.0	0.6	0.0	N	0.0	10.0	5.0	0.0
KATT-8	40.0	0.7	0.1	N	0.0	19.0	7.0	0.0
KATT-9	78.0	0.3	0.0	N	0.0	76.0	2.0	0.0
KATT-10	131.0	0.3	0.0	N	0.0	23.0	4.0	0.0
KATT-11	11.0	0.4	0.1	4.0	0.0	18.0	7.0	0.0
KATT-12	5.0	0.3	0.0	N	0.0	3.0	2.0	0.0
KATT-13	10.0	0.4	0.1	N	0.0	14.0	5.0	0.0
KATT-14	16.0	0.4	0.1	N	0.0	6.0	9.0	0.0
KATT-15	16.0	0.8	0.1	N	0.0	6.0	10.0	0.0
KATT-16	75.0	0.6	0.1	2.0	0.3	201.0	21.0	0.0
KATT-17	4.0	0.3	0.1	5.0	0.0	19.0	4.0	0.0
KATT-18	5.0	0.2	0.0	N	0.0	41.0	3.0	0.0
KATT-19	15.0	0.3	0.0	N	0.0	16.0	4.0	0.0
KATT-20	23.0	0.6	0.0	N	0.0	8.0	5.0	0.0
KATT-21	19.0	0.2	0.1	N	0.0	14.0	4.0	0.0
KATT-22	92.0	2.0	0.0	N	0.0	5.0	55.0	0.0
KATT-23	49.0	11.8	0.0	N	0.0	N	80.0	0.0

Sample	Ni ppm	P ppm	Pb ppm	Sb ppm	Se ppm
GM-4	17.0	466.0	5.0	N	N
GM-5	4.0	386.0	5.0	N	N
GM-6	5.0	368.0	5.0	N	N
GM-7	4.0	184.0	10.0	N	N
GM-8	26.0	528.0	6.0	N	N
GM-9	45.0	865.0	8.0	N	N
GM-10	47.0	850.0	6.0	N	N
GM-11	7.0	335.0	16.0	N	N
GM-12	3.0	332.0	12.0	N	N
GM-13	N	10.0	2.0	N	N
GM-14	3.0	158.0	36.0	N	N
GM-15	6.0	377.0	4.0	N	N
GM-16	1.0	24.0	9.0	N	N
GM-17	N	5.0	3.0	N	N
GM-18	3.0	103.0	21.0	4.0	N
KATT-1	3.0	N	1797.0	98.0	26.0
KATT-2	5.0	N	207.0	65.0	3.0
KATT-3	2.0	N	61.0	311.0	2.0
KATT-4	1.0	N	22.0	241.0	4.0
KATT-5	3.0	N	16.0	266.0	8.0
KATT-6	1.0	N	19.0	5.0	N
KATT-7	6.0	N	92.0	76.0	N
KATT-8	11.0	N	85.0	101.0	N
KATT-9	2.0	N	242.0	232.0	8.0
KATT-10	4.0	N	657.0	291.0	N
KATT-11	3.0	N	36.0	27.0	N
KATT-12	1.0	N	54.0	43.0	2.0
KATT-13	6.0	N	21.0	9.0	N
KATT-14	5.0	N	227.0	64.0	N
KATT-15	9.0	N	278.0	52.0	N
KATT-16	29.0	N	22.0	1485.0	81.0
KATT-17	3.0	N	22.0	38.0	N
KATT-18	3.0	N	8.0	26.0	N
KATT-19	3.0	N	8.0	22.0	N
KATT-20	9.0	N	22.0	27.0	N
KATT-21	2.0	N	20.0	23.0	N
KATT-22	3.0	N	13.0	43.0	N
KATT-23	301.0	N	57.0	41.0	N

Sample	Sr ppm	Ti %	Th ppm	V ppm	W ppm	Zn ppm
GM-4	15.0	0.1	N	33.0	N	35.0
GM-5	27.0	0.2	N	38.0	N	42.0
GM-6	15.0	0.1	N	38.0	N	35.0
GM-7	13.0	0.1	N	17.0	N	21.0
GM-8	12.0	0.1	N	32.0	N	45.0
GM-9	36.0	0.1	N	60.0	N	60.0
GM-10	157.0	0.1	N	62.0	N	63.0
GM-11	8.0	0.0	N	35.0	N	109.0
GM-12	3.0	0.0	N	20.0	N	7.0
GM-13	65.0	0.0	N	N	N	2.0
GM-14	22.0	0.0	N	8.0	N	46.0
GM-15	18.0	0.2	N	37.0	N	34.0
GM-16	48.0	0.0	N	N	N	4.0
GM-17	60.0	0.0	N	N	N	N
GM-18	53.0	0.0	N	4.0	N	11.0
KATT-1	N	0.0	N	2.0	12.0	1867.0
KATT-2	11.0	0.0	0.7	6.0	N	54.0
KATT-3	23.0	0.0	N	N	24.0	6.0
KATT-4	60.0	0.0	N	N	17.0	23.0
KATT-5	20.0	0.0	0.6	N	10.0	19.0
KATT-6	3.0	0.0	N	4.0	N	3.0
KATT-7	N	0.0	0.5	5.0	N	10.0
KATT-8	N	0.0	N	12.0	N	78.0
KATT-9	68.0	0.0	N	N	3.0	251.0
KATT-10	N	0.0	N	5.0	4.0	46.0
KATT-11	61.0	0.0	N	5.0	N	3.0
KATT-12	46.0	0.0	N	6.0	N	N
KATT-13	N	0.0	N	4.0	N	4.0
KATT-14	N	0.0	N	4.0	N	9.0
KATT-15	N	0.0	0.5	5.0	N	20.0
KATT-16	12.0	0.0	0.9	14.0	23.0	193.0
KATT-17	115.0	0.0	N	5.0	N	7.0
KATT-18	103.0	0.0	N	5.0	N	5.0
KATT-19	65.0	0.0	N	4.0	N	3.0
KATT-20	2.0	0.0	N	5.0	N	25.0
KATT-21	4.0	0.0	N	3.0	N	4.0
KATT-22	N	0.0	N	71.0	N	6.0
KATT-23	N	0.0	0.9	21.0	N	38.0

Sample	Mine / Area	UTMX	UTMY
KATT-24	Kattenhorn	514183.13	4474071.21
KATT-25	Kattenhorn	513920.75	4474103.52
KATT-26	Kattenhorn	513920.75	4474103.52
KATT-27	Kattenhorn	513920.75	4474103.52
KATT-28	Kattenhorn	513920.75	4474103.52
KATT-29	Kattenhorn	513920.75	4474103.52
KATT-30	Kattenhorn	513926.05	4474059.54
KATT-31	Kattenhorn	513804.69	4474224.31
KATT-32	Kattenhorn	513804.69	4474224.31
KATT-33	Kattenhorn	513715.08	4474391.99
KATT-34	Kattenhorn	513715.08	4474391.99
KATT-35	Kattenhorn	513715.08	4474391.99
KATT-36	Kattenhorn	513737.51	4474355.87
KATT-37	Kattenhorn	513632.16	4474278.81
KATT-38	Kattenhorn	513632.16	4474278.81
KATT-39	Kattenhorn	513653.43	4474257.96
KATT-40	Kattenhorn	513685.76	4474251.71
KATT-41	Kattenhorn	513685.76	4474251.71
KATT-42	Kattenhorn	513632.16	4474278.81
KATT-43	Kattenhorn	513632.16	4474278.81
BD-1	Blue Dick	514072.5	4473771.94
BD-2	Blue Dick	514072.5	4473771.94
BD-3	Blue Dick	514072.5	4473771.94
BD-4	Blue Dick	514013.4	4473797.85
BD-5	Blue Dick	514013.4	4473797.85
BD-6	Blue Dick	513929.24	4473817.15
BD-7	Blue Dick	513864.2	4473881.55
BD-8	Blue Dick	513864.2	4473881.55
BD-9	Blue Dick	513864.2	4473881.55
BD-10	Blue Dick	513729.38	4473964
BD-11	Blue Dick	513729.38	4473964
BD-12	Blue Dick	513729.38	4473964
BD-13	Blue Dick	513729.38	4473964
BD-14	Blue Dick	513729.38	4473964
BD-15	Blue Dick	513963.81	4473902.47
BD-16	Blue Dick	513963.81	4473902.47
BD-17	Blue Dick	513985.13	4473891.38
BD-18	Blue Dick	513985.13	4473891.38

Sample	Au ppb	Hg ppb	Ag ppm	Al %	As ppm
KATT-24	148.0	1320.0	246.0	0.1	72.0
KATT-25	108.0	77.0	9.7	0.2	37.0
KATT-26	147.0	1440.0	6.0	0.1	27.0
KATT-27	380.0	15100.0	127.0	0.0	33.0
KATT-28	15137.0	5640.0	16.0	0.1	1234.0
KATT-29	107.0	610.0	14.3	0.1	45.0
KATT-30	696.0	104.0	1.1	0.1	105.0
KATT-31	93.0	2480.0	3.5	0.0	89.0
KATT-32	63.0	1420.0	11.3	0.1	287.0
KATT-33	167.0	6440.0	64.0	0.1	37.0
KATT-34	42.0	200.0	28.0	0.1	42.0
KATT-35	605.0	5680.0	97.0	0.5	1111.0
KATT-36	40.0	116.0	10.9	0.1	60.0
KATT-37	271.0	11200.0	15.4	0.2	119.0
KATT-38	2849.0	215.0	27.2	0.1	1493.0
KATT-39	81.0	940.0	43.0	0.1	80.0
KATT-40	207.0	352.0	102.0	0.1	37.0
KATT-41	102.0	294.0	3.6	0.1	15.0
KATT-42	288.0	3160.0	121.0	0.1	55.0
KATT-43	203.0	11800.0	600.0	0.1	71.0
BD-1	144.0	52.0	16.5	0.0	46.0
BD-2	2466.0	3120.0	20.1	0.5	912.0
BD-3	403.0	102.0	5.7	0.1	221.0
BD-4	603.0	197.0	8.4	0.3	109.0
BD-5	327.0	102.0	5.5	0.1	166.0
BD-6	537.0	339.0	312.6	0.1	67.0
BD-7	208.0	14.0	0.8	2.0	12.0
BD-8	444.0	670.0	70.0	0.1	76.0
BD-9	142.0	1000.0	8.5	0.1	35.0
BD-10	115.0	1780.0	296.5	0.1	24.0
BD-11	733.0	1560.0	179.0	0.1	21.0
BD-12	7386.0	2770.0	418.8	0.1	74.0
BD-13	236.0	206.0	64.0	0.1	45.0
BD-14	76.0	680.0	48.0	0.1	63.0
BD-15	3108.0	33.0	8.4	0.2	1037.0
BD-16	1987.0	100.0	4.6	0.3	66.0
BD-17	6438.0	270.0	8.9	0.2	3921.0
BD-18	2221.0	335.0	3.7	0.2	946.0

Sample	B ppm	Ba ppm	Bi ppm	Ca %	Cd ppm	Co ppm	Cr ppm
KATT-24	6.0	1077.0	2.0	0.0	0.8	N	56.0
KATT-25	16.0	86.0	7.0	0.1	0.6	4.0	22.0
KATT-26	6.0	322.0	4.0	0.0	N	N	34.0
KATT-27	4.0	1454.0	3.0	0.0	N	N	17.0
KATT-28	30.0	11.0	16.0	0.0	1.3	8.0	23.0
KATT-29	9.0	414.0	5.0	0.1	N	N	61.0
KATT-30	12.0	103.0	5.0	0.0	N	4.0	44.0
KATT-31	7.0	556.0	2.0	0.0	N	N	32.0
KATT-32	33.0	260.0	15.0	0.0	1.4	N	40.0
KATT-33	5.0	1451.0	3.0	0.1	N	N	69.0
KATT-34	4.0	955.0	2.0	0.1	N	N	46.0
KATT-35	40.0	632.0	15.0	0.2	1.9	3.0	165.0
KATT-36	5.0	173.0	N	0.1	N	N	78.0
KATT-37	16.0	50.0	30.0	0.0	0.6	8.0	21.0
KATT-38	6.0	540.0	3.0	0.0	N	2.0	72.0
KATT-39	7.0	85.0	72.0	0.0	N	2.0	26.0
KATT-40	5.0	204.0	3.0	0.0	N	N	76.0
KATT-41	5.0	65.0	2.0	0.0	N	N	36.0
KATT-42	7.0	99.0	9.0	0.0	N	2.0	50.0
KATT-43	5.0	1382.0	2.0	0.1	N	N	38.0
BD-1	5.0	126.0	2.0	0.0	N	N	74.0
BD-2	14.0	99.0	7.0	0.0	0.8	N	19.0
BD-3	7.0	32.0	2.0	0.0	N	N	59.0
BD-4	5.0	114.0	2.0	0.1	N	N	36.0
BD-5	6.0	102.0	3.0	0.0	N	N	69.0
BD-6	6.0	492.0	4.0	0.0	N	N	47.0
BD-7	9.0	154.0	2.0	8.3	N	5.0	30.0
BD-8	8.0	72.0	5.0	0.0	N	1.0	49.0
BD-9	6.0	60.0	1.0	0.1	N	N	39.0
BD-10	7.0	51.0	4.0	0.0	1.0	2.0	36.0
BD-11	7.0	62.0	3.0	0.0	N	2.0	35.0
BD-12	11.0	69.0	5.0	0.0	0.5	N	78.0
BD-13	8.0	93.0	4.0	0.0	N	1.0	71.0
BD-14	11.0	67.0	4.0	0.0	N	4.0	42.0
BD-15	42.0	113.0	21.0	0.1	1.8	N	9.0
BD-16	5.0	109.0	4.0	0.1	N	N	23.0
BD-17	10.0	106.0	6.0	0.1	N	N	39.0
BD-18	10.0	426.0	9.0	0.1	N	N	30.0

Sample	Cu ppm	Fe %	K %	La ppm	Mg %	Mn ppm	Mo ppm	Na %
KATT-24	187.0	0.3	0.0	N	0.0	21.0	4.0	0.0
KATT-25	8.0	2.9	0.2	N	0.0	29.0	4.0	0.0
KATT-26	7.0	0.6	0.0	N	0.0	15.0	32.0	0.0
KATT-27	125.0	0.3	0.0	N	0.0	7.0	38.0	0.0
KATT-28	32.0	5.7	0.0	N	0.0	42.0	28.0	0.0
KATT-29	10.0	1.3	0.1	N	0.0	22.0	68.0	0.0
KATT-30	9.0	1.7	0.0	4.0	0.0	25.0	11.0	0.0
KATT-31	6.0	0.9	0.1	N	0.0	21.0	4.0	0.0
KATT-32	69.0	6.3	0.2	N	0.0	56.0	9.0	0.0
KATT-33	9.0	0.3	0.0	N	0.1	135.0	11.0	0.0
KATT-34	7.0	0.3	0.0	N	0.0	36.0	5.0	0.0
KATT-35	542.0	7.9	0.0	N	0.1	199.0	24.0	0.1
KATT-36	6.0	0.4	0.0	N	0.0	77.0	4.0	0.0
KATT-37	6.0	2.7	0.1	N	0.0	26.0	2.0	0.0
KATT-38	58.0	0.6	0.0	N	0.0	26.0	3.0	0.0
KATT-39	13.0	1.0	0.1	2.0	0.0	20.0	3.0	0.0
KATT-40	8.0	0.4	0.0	N	0.0	15.0	3.0	0.0
KATT-41	6.0	0.3	0.0	N	0.0	12.0	2.0	0.0
KATT-42	109.0	0.9	0.1	3.0	0.0	18.0	3.0	0.0
KATT-43	69.0	0.4	0.0	N	0.0	17.0	1.0	0.0
BD-1	17.0	0.2	0.0	N	0.0	9.0	4.0	0.0
BD-2	142.0	2.5	0.0	7.0	0.0	N	55.0	0.0
BD-3	21.0	0.6	0.0	N	0.0	6.0	17.0	0.0
BD-4	5.0	0.2	0.1	3.0	0.0	10.0	5.0	0.0
BD-5	7.0	0.6	0.1	2.0	0.0	13.0	10.0	0.0
BD-6	22.0	0.5	0.0	N	0.0	7.0	7.0	0.0
BD-7	8.0	1.5	0.3	12.0	0.4	665.0	N	0.1
BD-8	56.0	1.0	0.1	2.0	0.0	15.0	9.0	0.0
BD-9	13.0	0.4	0.0	N	0.0	9.0	3.0	0.0
BD-10	267.0	0.7	0.1	8.0	0.0	5.0	8.0	0.0
BD-11	65.0	0.7	0.0	N	0.0	6.0	16.0	0.0
BD-12	70.0	1.6	0.1	N	0.0	6.0	178.0	0.0
BD-13	40.0	0.9	0.0	N	0.0	9.0	7.0	0.0
BD-14	29.0	1.7	0.0	N	0.0	17.0	44.0	0.0
BD-15	58.0	7.8	0.5	N	0.0	55.0	20.0	0.1
BD-16	5.0	0.6	0.2	N	0.0	12.0	2.0	0.0
BD-17	36.0	1.4	0.2	N	0.0	21.0	9.0	0.0
BD-18	17.0	1.4	0.1	N	0.0	15.0	10.0	0.0

Sample	Ni ppm	P ppm	Pb ppm	Sb ppm	Se ppm
KATT-24	5.0	N	451.0	311.0	3.0
KATT-25	3.0	45.0	12.0	16.0	N
KATT-26	3.0	23.0	6.0	60.0	5.0
KATT-27	N	12.0	23.0	7920.0	152.0
KATT-28	59.0	46.0	21.0	119.0	23.0
KATT-29	10.0	26.0	18.0	63.0	25.0
KATT-30	18.0	18.0	7.0	9.0	N
KATT-31	4.0	404.0	53.0	21.0	N
KATT-32	3.0	678.0	174.0	54.0	N
KATT-33	4.0	66.0	149.0	50.0	N
KATT-34	4.0	128.0	302.0	43.0	2.0
KATT-35	15.0	1350.0	220.0	165.0	N
KATT-36	6.0	215.0	42.0	5.0	N
KATT-37	20.0	57.0	81.0	12.0	3.0
KATT-38	16.0	56.0	15.0	60.0	N
KATT-39	8.0	86.0	105.0	56.0	3.0
KATT-40	6.0	118.0	25.0	35.0	N
KATT-41	4.0	14.0	9.0	5.0	N
KATT-42	9.0	23.0	22.0	101.0	N
KATT-43	5.0	59.0	20.0	422.0	N
BD-1	4.0	N	10.0	7.0	N
BD-2	2.0	N	29.0	68.0	16.0
BD-3	3.0	N	6.0	12.0	2.0
BD-4	4.0	N	7.0	12.0	N
BD-5	4.0	N	7.0	13.0	N
BD-6	5.0	N	31.0	168.0	20.0
BD-7	12.0	N	8.0	N	N
BD-8	8.0	N	16.0	49.0	4.0
BD-9	4.0	N	7.0	21.0	7.0
BD-10	10.0	N	29.0	205.0	6.0
BD-11	8.0	N	11.0	65.0	7.0
BD-12	3.0	N	64.0	255.0	2.0
BD-13	8.0	N	31.0	32.0	4.0
BD-14	15.0	N	24.0	31.0	3.0
BD-15	N	303.0	46.0	1388.0	2.0
BD-16	2.0	36.0	20.0	18.0	N
BD-17	3.0	42.0	33.0	53.0	N
BD-18	3.0	42.0	22.0	34.0	N

Sample	Sr ppm	Ti %	Th ppm	V ppm	W ppm	Zn ppm
KATT-24	N	0.0	N	2.0	9.0	80.0
KATT-25	7.0	0.0	N	7.0	N	3.0
KATT-26	N	0.0	N	3.0	N	3.0
KATT-27	40.0	0.0	1.9	N	3.0	4.0
KATT-28	N	0.0	1.8	6.0	N	5.0
KATT-29	3.0	0.0	0.9	6.0	N	1.0
KATT-30	N	0.0	0.6	4.0	N	8.0
KATT-31	29.0	0.0	0.6	10.0	N	2.0
KATT-32	93.0	0.0	0.8	153.0	N	4.0
KATT-33	22.0	0.0	N	8.0	N	11.0
KATT-34	25.0	0.0	N	8.0	N	5.0
KATT-35	26.0	0.0	3.8	241.0	N	152.0
KATT-36	10.0	0.0	N	7.0	N	4.0
KATT-37	4.0	0.0	N	3.0	N	8.0
KATT-38	8.0	0.0	0.7	N	N	15.0
KATT-39	N	0.0	N	3.0	N	6.0
KATT-40	6.0	0.0	N	N	N	3.0
KATT-41	N	0.0	N	N	N	3.0
KATT-42	16.0	0.0	N	2.0	N	25.0
KATT-43	13.0	0.0	N	3.0	23.0	13.0
BD-1	N	0.0	N	N	N	3.0
BD-2	75.0	0.0	N	49.0	N	10.0
BD-3	16.0	0.0	0.6	14.0	N	4.0
BD-4	14.0	0.0	N	8.0	N	3.0
BD-5	4.0	0.0	N	21.0	N	3.0
BD-6	6.0	0.0	N	6.0	9.0	4.0
BD-7	277.0	0.0	N	27.0	N	25.0
BD-8	N	0.0	0.7	8.0	N	10.0
BD-9	N	0.0	N	N	N	5.0
BD-10	N	0.0	N	6.0	7.0	40.0
BD-11	N	0.0	N	3.0	N	15.0
BD-12	10.0	0.0	N	35.0	N	13.0
BD-13	N	0.0	N	4.0	N	3.0
BD-14	N	0.0	0.7	7.0	N	11.0
BD-15	27.0	0.0	0.5	84.0	N	4.0
BD-16	7.0	0.0	N	5.0	N	3.0
BD-17	6.0	0.0	N	7.0	N	6.0
BD-18	16.0	0.0	N	8.0	N	3.0

Sample	Mine / Area	UTMX	UTMY
BD-19	Blue Dick	513985.13	4473891.38
BD-20	Blue Dick	513985.13	4473891.38
BD-21	Blue Dick	513685.75	4473977.59
BD-22	Blue Dick	513927.99	4473540.6
BD-23	Blue Dick	513985.13	4473891.38
BD-24	Blue Dick	513985.13	4473891.38
BD-25	Blue Dick	513985.13	4473891.38
TEN-1	Tenabo	526858	4461408
TEN-2	Tenabo	527168	4461285
TEN-3	Tenabo	527184	4461111
TEN-4	Tenabo	527174	4461070
TEN-5	Tenabo	527174	4461070
TEN-6	Tenabo	527051	4461242
TEN-7	Tenabo	526722	4461319
TEN-8	Tenabo	526543	4461280
TEN-9	Tenabo	526543	4461280
TEN-10	Tenabo	524854	4463093
TEN-11	Tenabo	527051	4461242
GRIT-01	Betty O'Neal	509478.0	4478062.5
GRIT-02	Betty O'Neal	509482.5	4478053.1
GRIT-03	Betty O'Neal	509482.7	4478053.1
GRIT-04	Betty O'Neal	509477.8	4478049.1
GRIT-05	Betty O'Neal	509476.8	4478049.3
GRIT-06	Betty O'Neal	509480.0	4478042.1
GRIT-07	Betty O'Neal	509480.4	4478042.4
GRIT-08	Betty O'Neal	509476.2	4478041.7
GRIT-09	Betty O'Neal	509487.3	4478035.2
GRIT-10	Betty O'Neal	509483.4	4478027.7
GRIT-11	Betty O'Neal	509476.6	4478037.6
GRIT-12	Betty O'Neal	509507.0	4478039.2
GRIT-13	Betty O'Neal	509541.4	4477959.3
GRIT-14	Betty O'Neal	509541.8	4477956.7
GRIT-15	Betty O'Neal	509542.7	4477955.3
GRIT-16	Betty O'Neal	509542.7	4477952.7
GRIT-17	Betty O'Neal	509543.2	4477953.2
GRIT-18	Betty O'Neal	509548.6	4477953.3
GRIT-19	Betty O'Neal	509535.5	4477964.7
GRIT-20	Betty O'Neal	509535.4	4477964.8

Sample	Au ppb	Hg ppb	Ag ppm	Al %	As ppm
BD-19	288.0	46.0	5.1	0.1	237.0
BD-20	864.0	55.0	6.5	0.2	521.0
BD-21	809.0	4000.0	1036.7	0.1	193.0
BD-22	44.0	120.0	16.9	0.6	36.0
BD-23	8767.0	323.0	13.1	0.2	1451.0
BD-24	1152.0	110.0	2.0	0.2	450.9
BD-25	1068.0	140.0	4.8	0.1	2309.9
TEN-1	14.0	34.0	0.2	2.9	N
TEN-2	407.0	26.0	3.6	0.1	61.0
TEN-3	16.0	N	0.8	2.1	N
TEN-4	39.0	18.0	0.3	0.2	N
TEN-5	120.0	18.0	1.4	0.3	17.0
TEN-6	1722.0	20.0	0.4	0.7	N
TEN-7	29.0	11.0	3.4	4.1	N
TEN-8	90.0	25.0	2.5	1.7	N
TEN-9	41.0	13.0	0.2	0.7	N
TEN-10	319.0	151.0	10.9	0.6	1479.0
TEN-11	176.0	N	1.2	0.4	4.0
GRIT-01	57.0	12.0	1.5	0.0	N
GRIT-02	113.0	16.0	0.5	0.0	4.0
GRIT-03	7.0	N	N	0.0	N
GRIT-04	115.0	24.0	9.1	0.1	203.0
GRIT-05	44.0	153.0	273.1	0.0	21.0
GRIT-06	548.0	1100.0	2389.6	0.0	78.0
GRIT-07	25.0	31.0	13.9	0.3	59.0
GRIT-08	778.0	15.0	17.4	0.0	698.0
GRIT-09	32.0	14.0	N	0.7	17.0
GRIT-10	44.0	312.0	2.2	0.0	33.0
GRIT-11	34.0	304.0	112.5	0.1	16.0
GRIT-12	29.0	39.0	0.5	0.2	34.0
GRIT-13	59.0	30.0	25.0	0.2	79.0
GRIT-14	42.0	21.0	12.4	0.2	75.0
GRIT-15	77.0	23.0	7.1	0.3	122.0
GRIT-16	42.0	20.0	N	0.8	48.0
GRIT-17	33.0	58.0	N	0.4	109.0
GRIT-18	25.0	44.0	0.4	0.2	29.0
GRIT-19	62.0	30.0	9.4	0.2	65.0
GRIT-20	68.0	22.0	N	0.3	157.0

Sample	B ppm	Ba ppm	Bi ppm	Ca %	Cd ppm	Co ppm	Cr ppm
BD-19	7.0	74.0	4.0	0.0	N	3.0	37.0
BD-20	4.0	50.0	3.0	0.1	N	N	25.0
BD-21	13.0	44.0	14.0	0.1	1.9	4.0	54.0
BD-22	60.0	177.0	23.0	0.1	2.9	3.0	30.0
BD-23	7.0	95.0	6.0	0.1	N	N	51.0
BD-24	33.3	126.2	1.2	0.0	0.4	4.7	7.5
BD-25	35.7	416.2	1.1	0.0	0.1	1.3	15.0
TEN-1	9.0	1351.0	N	1.2	N	3.0	30.0
TEN-2	6.0	472.0	24.0	0.0	1.2	N	42.0
TEN-3	14.0	254.0	4.0	0.6	0.9	6.0	24.0
TEN-4	5.0	94.0	N	0.0	N	2.0	40.0
TEN-5	5.0	112.0	4.0	0.1	N	N	37.0
TEN-6	5.0	123.0	1.0	1.3	N	N	37.0
TEN-7	11.0	243.0	2.0	1.4	1.0	4.0	35.0
TEN-8	10.0	1022.0	2.0	0.7	0.7	7.0	30.0
TEN-9	6.0	85.0	N	0.2	N	N	11.0
TEN-10	80.0	119.0	35.0	0.1	57.6	7.0	51.0
TEN-11	4.0	81.0	N	1.1	N	N	33.0
GRIT-01	N	3.0	3.0	0.0	N	N	4.0
GRIT-02	N	9.0	N	2.8	N	N	78.0
GRIT-03	N	1343.0	3.0	10.0	N	N	3.0
GRIT-04	16.0	12.0	2.0	0.7	3.0	8.0	77.0
GRIT-05	2.0	39.0	N	10.0	1.9	N	71.0
GRIT-06	2.0	42.0	4.0	10.0	62.6	N	63.0
GRIT-07	5.0	55.0	N	2.1	1.0	3.0	54.0
GRIT-08	39.0	N	17.0	0.5	3.0	14.0	22.0
GRIT-09	4.0	48.0	N	2.3	N	3.0	21.0
GRIT-10	3.0	19.0	N	10.0	22.3	N	53.0
GRIT-11	2.0	44.0	N	2.8	22.1	N	115.0
GRIT-12	5.0	113.0	N	3.8	1.0	2.0	46.0
GRIT-13	4.0	85.0	N	0.1	0.8	1.0	77.0
GRIT-14	4.0	115.0	N	0.1	N	1.0	50.0
GRIT-15	3.0	98.0	N	0.2	N	1.0	51.0
GRIT-16	5.0	73.0	1.0	0.3	0.9	2.0	21.0
GRIT-17	6.0	247.0	N	0.1	1.1	4.0	47.0
GRIT-18	2.0	78.0	N	0.1	1.2	1.0	57.0
GRIT-19	2.0	90.0	N	0.1	N	N	72.0
GRIT-20	4.0	37.0	N	0.4	0.5	2.0	18.0

Sample	Cu ppm	Fe %	K %	La ppm	Mg %	Mn ppm	Mo ppm	Na %
BD-19	16.0	0.9	0.1	N	0.0	13.0	6.0	0.0
BD-20	8.0	0.4	0.1	N	0.0	8.0	4.0	0.0
BD-21	320.0	2.0	0.0	N	0.0	75.0	4.0	0.0
BD-22	49.0	10.0	0.0	N	0.0	128.0	N	0.0
BD-23	48.0	1.0	0.1	N	0.0	15.0	11.0	0.0
BD-24	13.6	2.8	0.2	1.3	0.0	57.3	10.9	0.0
BD-25	35.2	2.7	0.2	1.6	0.0	108.2	27.2	0.0
TEN-1	8.0	1.0	0.4	3.0	0.6	130.0	2.0	0.0
TEN-2	94.0	0.5	0.0	N	0.0	41.0	2.0	0.0
TEN-3	7.0	2.0	0.5	5.0	0.6	201.0	N	0.0
TEN-4	8.0	0.2	0.0	N	0.1	34.0	1.0	0.0
TEN-5	23.0	0.3	0.1	N	0.1	43.0	2.0	0.0
TEN-6	61.0	0.4	0.3	17.0	0.3	66.0	2.0	0.1
TEN-7	114.0	1.5	0.4	5.0	0.6	161.0	2.0	0.0
TEN-8	348.0	1.3	0.5	4.0	0.5	141.0	26.0	0.0
TEN-9	4.0	0.5	0.2	8.0	0.1	196.0	1.0	0.1
TEN-10	307.0	13.3	0.0	6.0	0.1	132.0	40.0	0.1
TEN-11	31.0	0.2	0.2	5.0	0.1	33.0	5.0	0.1
GRIT-01	N	0.0	0.0	N	0.3	5437.0	N	0.0
GRIT-02	3.0	0.2	0.0	N	0.0	1114.0	8.0	0.0
GRIT-03	N	0.1	0.0	3.0	0.2	5987.0	N	0.0
GRIT-04	89.0	4.8	0.0	N	0.2	187.0	9.0	0.0
GRIT-05	389.0	0.4	0.0	3.0	1.1	10316.0	7.0	0.0
GRIT-06	2170.0	0.4	0.0	N	0.5	7903.0	15.0	0.0
GRIT-07	42.0	1.4	0.1	6.0	0.9	1005.0	4.0	0.0
GRIT-08	200.0	10.0	0.0	N	0.1	610.0	N	0.0
GRIT-09	22.0	1.2	0.2	5.0	1.3	627.0	2.0	0.0
GRIT-10	8.0	0.6	0.0	N	1.4	8654.0	N	0.0
GRIT-11	163.0	0.4	0.0	N	0.4	7243.0	8.0	0.0
GRIT-12	50.0	1.4	0.1	4.0	1.8	1679.0	8.0	0.0
GRIT-13	22.0	0.8	0.1	4.0	0.1	233.0	6.0	0.0
GRIT-14	15.0	0.7	0.1	5.0	0.0	86.0	6.0	0.0
GRIT-15	6.0	0.9	0.2	7.0	0.0	665.0	4.0	0.0
GRIT-16	3.0	1.3	0.3	11.0	0.3	786.0	3.0	0.0
GRIT-17	28.0	1.6	0.2	7.0	0.1	199.0	4.0	0.0
GRIT-18	11.0	0.4	0.1	7.0	0.0	898.0	7.0	0.0
GRIT-19	7.0	0.5	0.1	3.0	0.0	129.0	5.0	0.0
GRIT-20	1.0	1.2	0.3	6.0	0.1	860.0	3.0	0.0

Sample	Ni ppm	P ppm	Pb ppm	Sb ppm	Se ppm
BD-19	7.0	13.0	14.0	11.0	N
BD-20	4.0	29.0	14.0	17.0	N
BD-21	26.0	12.0	122.0	588.0	10.0
BD-22	14.0	855.0	19.0	59.0	N
BD-23	6.0	19.0	22.0	59.0	5.0
BD-24	52.8	20.3	41.3	21.5	4.3
BD-25	107.5	30.4	24.6	64.8	4.2
TEN-1	7.0	330.0	11.0	N	N
TEN-2	5.0	69.0	58.0	N	N
TEN-3	4.0	364.0	7.0	N	N
TEN-4	4.0	17.0	4.0	N	N
TEN-5	4.0	295.0	16.0	N	N
TEN-6	24.0	5250.0	2.0	N	N
TEN-7	6.0	264.0	5.0	N	N
TEN-8	14.0	375.0	10.0	N	N
TEN-9	N	30.0	3.0	N	N
TEN-10	51.0	1575.0	511.0	25.0	N
TEN-11	4.0	4373.0	5.0	N	N
GRIT-01	N	7.0	73.0	N	N
GRIT-02	4.0	8.0	54.0	N	N
GRIT-03	N	4.0	22.0	N	N
GRIT-04	60.0	51.0	200.0	38.0	15.0
GRIT-05	6.0	299.0	544.0	259.0	N
GRIT-06	15.0	250.0	8915.0	1412.0	21.0
GRIT-07	10.0	196.0	123.0	12.0	N
GRIT-08	61.0	44.0	192.0	93.0	47.0
GRIT-09	10.0	207.0	35.0	N	N
GRIT-10	7.0	51.0	42.0	3.0	3.0
GRIT-11	12.0	68.0	311.0	87.0	N
GRIT-12	23.0	409.0	23.0	14.0	N
GRIT-13	9.0	149.0	61.0	14.0	N
GRIT-14	4.0	191.0	20.0	8.0	N
GRIT-15	3.0	254.0	32.0	2.0	N
GRIT-16	13.0	438.0	21.0	N	N
GRIT-17	12.0	240.0	87.0	12.0	N
GRIT-18	13.0	135.0	69.0	4.0	N
GRIT-19	3.0	67.0	31.0	2.0	N
GRIT-20	2.0	358.0	16.0	N	N

Sample	Sr ppm	Ti %	Th ppm	V ppm	W ppm	Zn ppm
BD-19	N	0.0	N	2.0	N	5.0
BD-20	4.0	0.0	N	3.0	N	3.0
BD-21	N	0.0	N	3.0	24.0	257.0
BD-22	N	0.0	N	114.0	N	154.0
BD-23	N	0.0	N	9.0	N	10.0
BD-24	7.1	0.0	N	4.8	0.1	14.0
BD-25	8.6	0.0	N	9.7	0.1	7.4
TEN-1	204.0	0.1	N	30.0	N	30.0
TEN-2	N	0.0	N	13.0	N	35.0
TEN-3	75.0	0.1	N	31.0	N	43.0
TEN-4	N	0.0	N	2.0	N	9.0
TEN-5	N	0.0	N	7.0	N	62.0
TEN-6	9.0	0.0	N	97.0	N	14.0
TEN-7	240.0	0.1	N	34.0	N	33.0
TEN-8	55.0	0.1	N	35.0	N	36.0
TEN-9	40.0	0.0	N	N	N	21.0
TEN-10	7.0	0.0	N	169.0	N	678.0
TEN-11	9.0	0.0	N	43.0	N	22.0
GRIT-01	296.0	0.0	9.1	N	N	9.0
GRIT-02	43.0	0.0	1.9	N	N	7.0
GRIT-03	501.0	0.0	9.5	N	N	8.0
GRIT-04	8.0	0.0	1.7	10.0	N	167.0
GRIT-05	58.0	0.0	12.9	17.0	7.0	114.0
GRIT-06	131.0	0.0	11.7	18.0	77.0	5894.0
GRIT-07	51.0	0.0	1.8	3.0	N	110.0
GRIT-08	N	0.0	2.2	3.0	N	20.0
GRIT-09	31.0	0.0	N	5.0	N	22.0
GRIT-10	29.0	0.0	76.7	4.0	N	3396.0
GRIT-11	36.0	0.0	10.4	13.0	N	2436.0
GRIT-12	55.0	0.0	3.0	21.0	N	141.0
GRIT-13	6.0	0.0	N	6.0	N	99.0
GRIT-14	7.0	0.0	N	3.0	N	30.0
GRIT-15	7.0	0.0	1.0	N	N	47.0
GRIT-16	12.0	0.0	1.0	2.0	N	180.0
GRIT-17	14.0	0.0	N	5.0	N	148.0
GRIT-18	17.0	0.0	0.5	3.0	N	93.0
GRIT-19	4.0	0.0	N	N	N	34.0
GRIT-20	9.0	0.0	1.5	N	N	47.0

Sample	Mine / Area	UTMX	UTMY
GRIT-21	Betty O'Neal	509539.6	4477959.8
GRIT-22	Betty O'Neal	509539.5	4477959.9
GRIT-23	Betty O'Neal	509539.2	4477959.9
GRIT-24	Betty O'Neal	509542.5	4477962.2
GRIT-25	Betty O'Neal	509725.5	4477762.1
GRIT-26	Betty O'Neal	509725.5	4477762.7
GRIT-27	Betty O'Neal	509725.5	4477762.9
GRIT-28	Betty O'Neal	509790.2	4477934.4
GRIT-29	Betty O'Neal	509789.2	4477935.6
GRIT-30	Betty O'Neal	509536.4	4478004.3
GRIT-31	Betty O'Neal	509530.0	4477641.2
GRIT-32	Betty O'Neal	509557.9	4477625.4
GRIT-33	Betty O'Neal	509557.7	4477625.5
GRIT-34	Betty O'Neal	509557.8	4477625.4
GRIT-35	Betty O'Neal	509715.7	4477784.5
GRIT-36	Betty O'Neal	509718.6	4477787.4
GRIT-37	Betty O'Neal	509718.2	4477788.3
GRIT-38	Betty O'Neal	509806.2	4477788.4
GRIT-39	Betty O'Neal	509806.1	4477788.4
GRIT-40	Betty O'Neal	509815.6	4477814.2
GRIT-41	Betty O'Neal	509588.6	4477961.4
GRIT-42	Betty O'Neal	509585.7	4477956.4
GRIT-43	Betty O'Neal	509718.5	4477997.4
GRIT-44	Betty O'Neal	509765.5	4478102.4
GRIT-45	Betty O'Neal	509931.1	4477990.7
GRIT-46	Betty O'Neal	510054.2	4478083.5
GRIT-47	Betty O'Neal	510013.2	4478011.7
GRIT-48	Betty O'Neal	509961.4	4477687.2
GRIT-49	Betty O'Neal	509920.3	4477672.0
GRIT-50	Betty O'Neal	509918.4	4477672.2
GRIT-51	Betty O'Neal	509922.8	4477668.7
GRIT-52	Betty O'Neal	509729.2	4477780.7
GRIT-53	Betty O'Neal	509425.8	4477751.1
GRIT-54	Betty O'Neal	509427.0	4477751.0
GRIT-55	Betty O'Neal	509251.1	4478277.1
GRIT-56	Betty O'Neal	507924.2	4476626.8
GRIT-57	Betty O'Neal	507924.5	4476625.9
GRIT-58	Betty O'Neal	507926.2	4476626.1

Sample	Au ppb	Hg ppb	Ag ppm	Al %	As ppm
GRIT-21	28.0	N	N	0.7	9.0
GRIT-22	19.0	N	N	1.3	6.0
GRIT-23	23.0	41.0	N	0.3	68.0
GRIT-24	21.0	39.0	N	0.1	17.0
GRIT-25	12.0	44.0	112.8	0.0	N
GRIT-26	20.0	133.0	535.0	0.0	16.0
GRIT-27	23.0	116.0	479.7	0.0	12.0
GRIT-28	29.0	42.0	20.3	0.1	51.0
GRIT-29	40.0	51.0	6.6	0.0	23.0
GRIT-30	874.0	880.0	41.6	0.1	1578.0
GRIT-31	24.0	181.0	2.1	0.3	94.0
GRIT-32	16.0	32.0	N	0.0	22.0
GRIT-33	23.0	54.0	4.5	0.1	58.0
GRIT-34	19.0	33.0	3.2	0.1	11.0
GRIT-35	21.0	135.0	601.9	0.0	13.0
GRIT-36	30.0	25.0	0.3	0.3	133.0
GRIT-37	80.0	351.0	1388.9	0.1	92.0
GRIT-38	172.0	1960.0	2891.7	0.0	169.0
GRIT-39	53.0	370.0	450.0	0.0	56.0
GRIT-40	8.0	40.0	13.1	0.3	4.0
GRIT-41	7.0	32.0	2.2	0.1	13.0
GRIT-42	120.0	221.0	7.7	0.2	371.0
GRIT-43	892.0	37.0	20.0	0.1	648.0
GRIT-44	20.0	15.0	0.7	0.2	37.0
GRIT-45	116.0	18.0	N	0.4	121.0
GRIT-46	22.0	26.0	2.8	0.2	48.0
GRIT-47	61.0	30.0	N	1.7	241.0
GRIT-48	256.0	90.0	334.1	0.4	1069.0
GRIT-49	44.0	26.0	30.6	0.1	95.0
GRIT-50	10.0	27.0	N	2.2	N
GRIT-51	52.0	502.0	1145.0	0.0	337.0
GRIT-52	16.0	28.0	11.5	0.0	9.0
GRIT-53	20.0	48.0	12.1	3.1	2.0
GRIT-54	8.0	20.0	N	2.6	N
GRIT-55	155.0	126.0	0.8	0.0	131.0
GRIT-56	15.0	18.0	0.5	1.2	N
GRIT-57	13.0	29.0	N	1.0	3.0
GRIT-58	50.0	12.0	N	0.9	7.0

Sample	B ppm	Ba ppm	Bi ppm	Ca %	Cd ppm	Co ppm	Cr ppm
GRIT-21	3.0	45.0	N	0.3	0.5	3.0	24.0
GRIT-22	5.0	78.0	2.0	0.2	N	2.0	11.0
GRIT-23	4.0	146.0	N	0.1	2.1	5.0	18.0
GRIT-24	N	45.0	N	0.0	N	N	45.0
GRIT-25	N	1049.0	N	0.0	N	N	87.0
GRIT-26	N	76.0	N	0.0	5.1	N	92.0
GRIT-27	N	203.0	N	10.0	3.8	N	104.0
GRIT-28	3.0	1408.0	N	0.0	N	N	135.0
GRIT-29	2.0	67.0	N	10.0	0.8	N	69.0
GRIT-30	36.0	284.0	9.0	3.5	19.6	14.0	28.0
GRIT-31	4.0	287.0	N	0.2	N	N	25.0
GRIT-32	N	20.0	N	10.0	2.0	N	14.0
GRIT-33	3.0	25.0	N	0.7	0.6	2.0	79.0
GRIT-34	N	20.0	N	3.0	N	N	75.0
GRIT-35	N	780.0	N	0.0	2.1	N	103.0
GRIT-36	4.0	52.0	N	0.8	N	2.0	31.0
GRIT-37	4.0	64.0	N	0.1	23.6	1.0	106.0
GRIT-38	3.0	714.0	N	0.2	71.7	N	93.0
GRIT-39	2.0	184.0	N	0.1	12.6	N	130.0
GRIT-40	3.0	130.0	N	0.1	0.8	1.0	108.0
GRIT-41	N	28.0	N	0.1	N	N	96.0
GRIT-42	6.0	91.0	2.0	0.2	0.9	3.0	39.0
GRIT-43	9.0	96.0	6.0	0.1	1.4	N	54.0
GRIT-44	N	60.0	N	0.4	N	N	9.0
GRIT-45	11.0	64.0	N	0.1	0.8	5.0	34.0
GRIT-46	3.0	1241.0	N	0.0	N	N	28.0
GRIT-47	12.0	136.0	2.0	0.3	1.0	10.0	10.0
GRIT-48	11.0	1500.0	N	0.6	6.6	15.0	50.0
GRIT-49	3.0	1205.0	N	0.0	N	N	15.0
GRIT-50	8.0	156.0	4.0	0.7	0.6	16.0	62.0
GRIT-51	3.0	4855.0	N	0.8	19.8	N	75.0
GRIT-52	N	1217.0	N	0.0	N	N	25.0
GRIT-53	8.0	595.0	3.0	2.3	1.1	14.0	32.0
GRIT-54	8.0	1073.0	4.0	1.4	0.9	14.0	110.0
GRIT-55	9.0	11.0	N	0.0	10.8	2.0	10.0
GRIT-56	6.0	46.0	1.0	1.5	N	5.0	23.0
GRIT-57	4.0	88.0	N	2.4	N	4.0	40.0
GRIT-58	8.0	65.0	1.0	1.1	N	9.0	40.0

Sample	Cu ppm	Fe %	K %	La ppm	Mg %	Mn ppm	Mo ppm	Na %
GRIT-21	N	1.0	0.2	14.0	0.2	351.0	2.0	0.0
GRIT-22	N	1.6	0.2	10.0	0.4	119.0	1.0	0.0
GRIT-23	24.0	1.4	0.1	8.0	0.1	1123.0	3.0	0.0
GRIT-24	3.0	0.3	0.1	3.0	0.0	66.0	5.0	0.0
GRIT-25	120.0	0.2	0.0	N	0.0	27.0	5.0	0.0
GRIT-26	496.0	0.2	0.0	N	0.0	78.0	9.0	0.0
GRIT-27	234.0	0.2	0.0	N	0.0	21.0	7.0	0.0
GRIT-28	34.0	0.6	0.0	N	0.0	85.0	14.0	0.0
GRIT-29	10.0	0.5	0.0	N	0.2	2032.0	5.0	0.0
GRIT-30	186.0	10.0	0.0	2.0	0.2	8490.0	18.0	0.0
GRIT-31	17.0	1.2	0.2	N	0.1	91.0	2.0	0.1
GRIT-32	4.0	0.3	0.0	N	0.1	1805.0	N	0.0
GRIT-33	19.0	0.6	0.0	N	0.0	627.0	9.0	0.0
GRIT-34	13.0	0.2	0.0	N	0.0	473.0	5.0	0.0
GRIT-35	465.0	0.2	0.0	N	0.0	52.0	11.0	0.0
GRIT-36	5.0	1.2	0.2	4.0	0.2	2864.0	2.0	0.0
GRIT-37	893.0	1.0	0.0	N	0.0	382.0	11.0	0.0
GRIT-38	2542.0	0.7	0.0	2.0	0.0	10000.0	22.0	0.0
GRIT-39	183.0	0.4	0.0	2.0	0.0	10000.0	13.0	0.0
GRIT-40	38.0	0.5	0.0	N	0.1	855.0	10.0	0.0
GRIT-41	8.0	0.3	0.0	N	0.0	469.0	10.0	0.0
GRIT-42	242.0	1.8	0.1	2.0	0.0	89.0	5.0	0.0
GRIT-43	17.0	2.9	0.0	N	0.0	104.0	38.0	0.0
GRIT-44	22.0	0.3	0.1	3.0	0.0	115.0	2.0	0.0
GRIT-45	93.0	3.6	0.0	3.0	0.1	826.0	7.0	0.0
GRIT-46	40.0	0.7	0.0	3.0	0.0	24.0	1.0	0.0
GRIT-47	24.0	4.9	0.0	8.0	0.7	3035.0	N	0.0
GRIT-48	222.0	3.9	0.0	7.0	0.2	10000.0	N	0.0
GRIT-49	47.0	0.4	0.0	N	0.1	605.0	N	0.0
GRIT-50	38.0	2.6	0.0	4.0	2.4	478.0	N	0.0
GRIT-51	1039.0	0.6	0.0	6.0	0.3	10000.0	11.0	0.1
GRIT-52	105.0	0.1	0.0	N	0.0	1411.0	N	0.0
GRIT-53	41.0	3.0	0.1	6.0	2.1	2949.0	N	0.3
GRIT-54	22.0	3.2	0.1	6.0	2.7	567.0	N	0.0
GRIT-55	55.0	3.2	0.0	4.0	3.7	10000.0	N	0.0
GRIT-56	123.0	1.9	0.0	4.0	0.6	990.0	7.0	0.1
GRIT-57	45.0	1.2	0.0	5.0	0.7	2007.0	3.0	0.0
GRIT-58	71.0	2.6	0.1	4.0	0.7	1967.0	19.0	0.0

Sample	Ni ppm	P ppm	Pb ppm	Sb ppm	Se ppm
GRIT-21	10.0	405.0	9.0	N	N
GRIT-22	7.0	361.0	10.0	N	N
GRIT-23	26.0	220.0	25.0	12.0	N
GRIT-24	3.0	74.0	15.0	N	N
GRIT-25	4.0	5.0	52.0	44.0	N
GRIT-26	3.0	8.0	589.0	264.0	N
GRIT-27	4.0	5.0	395.0	447.0	N
GRIT-28	7.0	12.0	25.0	21.0	N
GRIT-29	4.0	26.0	116.0	8.0	N
GRIT-30	70.0	1075.0	2902.0	190.0	N
GRIT-31	7.0	52.0	28.0	6.0	N
GRIT-32	3.0	11.0	10.0	3.0	N
GRIT-33	7.0	33.0	68.0	12.0	N
GRIT-34	3.0	7.0	47.0	8.0	N
GRIT-35	3.0	3.0	248.0	264.0	N
GRIT-36	2.0	296.0	12.0	N	N
GRIT-37	9.0	43.0	7330.0	1118.0	7.0
GRIT-38	22.0	116.0	10000.0	1782.0	10.0
GRIT-39	5.0	20.0	1688.0	419.0	N
GRIT-40	7.0	27.0	157.0	12.0	N
GRIT-41	7.0	39.0	19.0	3.0	N
GRIT-42	25.0	412.0	835.0	24.0	N
GRIT-43	11.0	600.0	6401.0	14.0	5.0
GRIT-44	2.0	15.0	115.0	2.0	N
GRIT-45	28.0	292.0	27.0	22.0	14.0
GRIT-46	2.0	98.0	48.0	11.0	N
GRIT-47	12.0	823.0	11.0	N	N
GRIT-48	15.0	480.0	658.0	102.0	N
GRIT-49	2.0	24.0	27.0	19.0	N
GRIT-50	85.0	267.0	21.0	N	N
GRIT-51	3.0	113.0	1610.0	414.0	11.0
GRIT-52	2.0	24.0	263.0	49.0	N
GRIT-53	74.0	228.0	37.0	N	N
GRIT-54	72.0	239.0	8.0	N	N
GRIT-55	N	12.0	107.0	4.0	N
GRIT-56	40.0	740.0	13.0	N	N
GRIT-57	26.0	992.0	11.0	N	N
GRIT-58	43.0	760.0	11.0	2.0	N

Sample	Sr ppm	Ti %	Th ppm	V ppm	W ppm	Zn ppm
GRIT-21	11.0	0.0	N	N	N	141.0
GRIT-22	7.0	0.0	0.6	2.0	N	102.0
GRIT-23	6.0	0.0	1.0	4.0	N	192.0
GRIT-24	9.0	0.0	N	2.0	N	22.0
GRIT-25	11.0	0.0	N	N	1.0	50.0
GRIT-26	N	0.0	N	N	49.0	341.0
GRIT-27	N	0.0	N	N	14.0	53.0
GRIT-28	4.0	0.0	N	3.0	N	95.0
GRIT-29	101.0	0.0	3.2	2.0	N	70.0
GRIT-30	209.0	0.0	12.2	67.0	N	2561.0
GRIT-31	15.0	0.0	1.1	6.0	N	33.0
GRIT-32	380.0	0.0	3.0	N	N	52.0
GRIT-33	13.0	0.0	1.0	3.0	N	99.0
GRIT-34	49.0	0.0	1.1	N	N	20.0
GRIT-35	7.0	0.0	N	N	18.0	88.0
GRIT-36	11.0	0.0	4.5	N	N	28.0
GRIT-37	3.0	0.0	0.5	4.0	42.0	2450.0
GRIT-38	93.0	0.0	83.7	6.0	71.0	4585.0
GRIT-39	69.0	0.0	34.7	2.0	11.0	1491.0
GRIT-40	5.0	0.0	0.7	4.0	N	71.0
GRIT-41	2.0	0.0	N	6.0	N	53.0
GRIT-42	67.0	0.0	N	23.0	N	108.0
GRIT-43	12.0	0.0	0.5	5.0	N	200.0
GRIT-44	8.0	0.0	N	N	N	28.0
GRIT-45	4.0	0.0	1.1	14.0	N	141.0
GRIT-46	18.0	0.0	N	4.0	N	28.0
GRIT-47	16.0	0.0	2.7	52.0	N	143.0
GRIT-48	38.0	0.0	14.9	9.0	N	956.0
GRIT-49	15.0	0.0	0.8	N	N	83.0
GRIT-50	16.0	0.1	N	31.0	N	61.0
GRIT-51	284.0	0.0	188.2	N	33.0	3004.0
GRIT-52	24.0	0.0	1.5	N	N	89.0
GRIT-53	112.0	0.1	N	47.0	N	92.0
GRIT-54	38.0	0.0	N	48.0	N	39.0
GRIT-55	96.0	0.0	26.7	N	N	386.0
GRIT-56	39.0	0.0	N	40.0	N	25.0
GRIT-57	68.0	0.0	N	31.0	N	27.0
GRIT-58	32.0	0.0	N	82.0	N	30.0

Sample	Mine / Area	UTMX	UTMY
GRIT-59	Betty O'Neal	507903.6	4476624.3
GRIT-60	Betty O'Neal	507877.4	4476640.5
GRIT-61	Betty O'Neal	507894.9	4476601.4
GRIT-62	Betty O'Neal	508035.0	4476587.1
GRIT-63	Betty O'Neal	508034.6	4476586.6
GRIT-64	Betty O'Neal	508133.0	4476638.3
GRIT-65	Betty O'Neal	508133.6	4476639.8
GRIT-66	Betty O'Neal	508191.4	4476637.1
GRIT-67	Betty O'Neal	508195.1	4476679.2
GRIT-68	Betty O'Neal	508081.1	4476702.5
GRIT-69	Betty O'Neal	508080.6	4476702.9
GRIT-70	Betty O'Neal	508078.2	4476703.8
GRIT-71	Betty O'Neal	508074.9	4476695.5
GRIT-72	Betty O'Neal	507749.6	4476731.0
LOVIE-01	Lovie	523146.7	4467226.7
LOVIE-02	Lovie	523146.7	4467226.7
LOVIE-03	Lovie	523146.5	4467226.6
LOVIE-04	Lovie	523146.5	4467226.6
LOVIE-05	Lovie	523146.5	4467226.5
LOVIE-06	Lovie	523146.5	4467226.4
LOVIE-07	Lovie	523146.4	4467226.3
LOVIE-08	Lovie	523146.3	4467226.4
LOVIE-09	Lovie	523144.3	4467216.6
LOVIE-10	Lovie	523060.2	4467103.0
LOVIE-11	Lovie	523061.2	4467102.6
LOVIE-12	Lovie	523048	4467098
LOVIE-13	Lovie	523048	4467098
LOVIE-14	Lovie	523048	4467098
LOVIE-15	Lovie	523112.6	4467100.8
LOVIE-16	Lovie	523142.9	4467075.2
LOVIE-17	Lovie	523141.4	4467072.0
LOVIE-18	Lovie	523242.7	4467023.4
LOVIE-19	Lovie	523243.0	4467023.1
LOVIE-20	Lovie	523243.7	4467015.8
LOVIE-21	Lovie	523299.1	4467000.6
LOVIE-22	Lovie	523298.1	4467114.5
LOVIE-23	Lovie	523298.1	4467114.3
LOVIE-24	Lovie	523424.5	4467260.5

Sample	Au ppb	Hg ppb	Ag ppm	Al %	As ppm
GRIT-59	19.0	21.0	0.5	0.8	N
GRIT-60	11.0	30.0	0.3	0.1	3.0
GRIT-61	93.0	21.0	N	0.1	N
GRIT-62	1854.0	26.0	67.6	0.8	712.0
GRIT-63	6093.0	25.0	96.8	1.4	448.0
GRIT-64	9.0	31.0	N	0.1	3.0
GRIT-65	472.0	22.0	N	0.9	132.0
GRIT-66	91.0	29.0	0.2	0.7	4.0
GRIT-67	899.0	21.0	6.5	0.7	782.0
GRIT-68	374.0	23.0	0.2	0.9	46.0
GRIT-69	12.0	15.0	N	1.2	5.0
GRIT-70	15.0	N	N	0.9	13.0
GRIT-71	1048.0	N	2.0	0.4	45.0
GRIT-72	41.0	N	N	0.9	36.0
LOVIE-01	2583.0	4560.0	462.9	0.1	4255.0
LOVIE-02	940.0	4860.0	538.7	0.2	5332.0
LOVIE-03	747.0	11200.0	30.0	0.0	1661.0
LOVIE-04	250.0	150.0	13.5	0.5	778.0
LOVIE-05	198.0	7200.0	30.2	0.0	628.0
LOVIE-06	214.0	303.0	17.6	0.7	1463.0
LOVIE-07	593.0	113.0	13.3	0.1	854.0
LOVIE-08	99.0	7300.0	24.3	0.0	203.0
LOVIE-09	8151.0	2090.0	172.7	0.2	7797.0
LOVIE-10	2014.0	5000.0	143.1	1.4	5351.0
LOVIE-11	974.0	540.0	16.9	0.5	1044.0
LOVIE-12	29.0	910.0	1.2	1.2	1040.0
LOVIE-13	907.0	1430.0	11.4	0.7	2169.0
LOVIE-14	341.0	622.0	23.8	0.2	1041.0
LOVIE-15	2145.0	6060.0	31.9	0.3	2203.0
LOVIE-16	2238.0	5540.0	847.8	0.3	3450.0
LOVIE-17	550.0	254.0	8.9	0.3	840.0
LOVIE-18	24.0	124.0	2.0	1.1	104.0
LOVIE-19	250.0	212.0	7.4	0.6	269.0
LOVIE-20	1433.0	4600.0	344.2	0.6	2327.0
LOVIE-21	1922.0	267.0	14.1	0.4	1424.0
LOVIE-22	1052.0	590.0	131.8	0.1	1863.0
LOVIE-23	42.0	142.0	6.6	0.8	106.0
LOVIE-24	363.0	760.0	89.9	0.5	1058.0

Sample	B ppm	Ba ppm	Bi ppm	Ca %	Cd ppm	Co ppm	Cr ppm
GRIT-59	7.0	29.0	N	1.6	0.6	3.0	28.0
GRIT-60	N	21.0	N	0.0	N	N	18.0
GRIT-61	N	18.0	N	0.3	N	N	14.0
GRIT-62	26.0	88.0	16.0	0.2	2.3	6.0	13.0
GRIT-63	12.0	26.0	48.0	0.4	2.1	13.0	42.0
GRIT-64	N	22.0	N	0.0	N	N	1.0
GRIT-65	11.0	85.0	15.0	1.8	0.7	3.0	12.0
GRIT-66	2.0	79.0	N	0.6	N	2.0	28.0
GRIT-67	12.0	179.0	16.0	0.7	1.3	7.0	24.0
GRIT-68	15.0	100.0	8.0	0.3	1.3	12.0	16.0
GRIT-69	4.0	404.0	N	0.3	N	3.0	40.0
GRIT-70	5.0	35.0	N	1.1	N	2.0	7.0
GRIT-71	13.0	87.0	15.0	0.4	0.9	4.0	15.0
GRIT-72	5.0	67.0	N	0.4	N	4.0	32.0
LOVIE-01	69.0	14.0	19.0	0.0	270.6	5.0	63.0
LOVIE-02	36.0	34.0	12.0	0.0	474.8	9.0	36.0
LOVIE-03	62.0	3.0	19.0	0.0	1686.9	27.0	18.0
LOVIE-04	28.0	57.0	7.0	0.0	20.9	7.0	31.0
LOVIE-05	69.0	2.0	20.0	0.0	1984.1	30.0	11.0
LOVIE-06	21.0	76.0	6.0	0.0	8.7	3.0	18.0
LOVIE-07	36.0	28.0	10.0	0.0	17.7	8.0	103.0
LOVIE-08	55.0	4.0	17.0	0.0	2038.4	44.0	13.0
LOVIE-09	30.0	21.0	10.0	0.0	48.7	4.0	80.0
LOVIE-10	93.0	493.0	27.0	0.1	62.2	27.0	14.0
LOVIE-11	39.0	519.0	10.0	0.1	4.6	5.0	21.0
LOVIE-12	50.0	474.0	13.0	0.1	9.9	12.0	86.0
LOVIE-13	37.0	241.0	10.0	0.3	7.5	2.0	25.0
LOVIE-14	33.0	185.0	9.0	0.1	1.8	2.0	122.0
LOVIE-15	21.0	145.0	6.0	0.0	4.7	2.0	30.0
LOVIE-16	40.0	522.0	13.0	0.2	245.9	26.0	52.0
LOVIE-17	43.0	221.0	12.0	0.1	5.2	5.0	22.0
LOVIE-18	22.0	370.0	4.0	0.2	9.7	17.0	18.0
LOVIE-19	31.0	418.0	6.0	0.0	5.4	8.0	9.0
LOVIE-20	69.0	225.0	20.0	0.3	17.8	13.0	56.0
LOVIE-21	53.0	260.0	14.0	0.1	2.7	6.0	17.0
LOVIE-22	44.0	31.0	12.0	0.2	102.0	26.0	63.0
LOVIE-23	49.0	97.0	12.0	0.6	4.4	21.0	45.0
LOVIE-24	163.0	41.0	80.0	0.1	16.1	12.0	15.0

Sample	Cu ppm	Fe %	K %	La ppm	Mg %	Mn ppm	Mo ppm	Na %
GRIT-59	334.0	2.2	0.0	N	0.8	922.0	2.0	0.0
GRIT-60	8.0	0.1	0.0	N	0.0	97.0	1.0	0.0
GRIT-61	3.0	0.2	0.1	2.0	0.0	200.0	1.0	0.0
GRIT-62	6793.0	9.5	0.0	3.0	0.3	236.0	6.0	0.0
GRIT-63	10000.0	4.0	0.0	4.0	0.9	810.0	2.0	0.0
GRIT-64	39.0	0.3	0.0	5.0	0.1	2314.0	N	0.0
GRIT-65	628.0	3.8	0.0	4.0	0.5	398.0	N	0.0
GRIT-66	89.0	0.4	0.1	2.0	0.4	100.0	7.0	0.0
GRIT-67	1957.0	4.3	0.2	5.0	0.4	409.0	N	0.0
GRIT-68	1107.0	5.1	0.0	4.0	0.6	656.0	N	0.0
GRIT-69	43.0	0.8	0.2	3.0	0.7	88.0	1.0	0.1
GRIT-70	14.0	1.3	0.1	6.0	0.4	191.0	N	0.0
GRIT-71	1175.0	4.1	0.0	N	0.2	212.0	N	0.1
GRIT-72	50.0	1.2	0.0	N	0.5	229.0	1.0	0.1
LOVIE-01	440.0	5.4	0.0	8.0	0.0	574.0	6.0	0.0
LOVIE-02	437.0	3.3	0.3	31.0	0.0	1106.0	5.0	0.0
LOVIE-03	1131.0	4.8	0.0	3.0	0.0	5283.0	N	0.0
LOVIE-04	18.0	2.6	0.3	8.0	0.0	81.0	N	0.1
LOVIE-05	706.0	5.2	0.0	2.0	0.0	10000.0	N	0.0
LOVIE-06	37.0	1.9	0.5	14.0	0.1	87.0	4.0	0.1
LOVIE-07	22.0	3.2	0.0	N	0.0	155.0	N	0.0
LOVIE-08	268.0	4.5	0.0	6.0	0.0	10000.0	N	0.0
LOVIE-09	144.0	2.8	0.2	9.0	0.0	181.0	50.0	0.0
LOVIE-10	275.0	6.0	0.0	14.0	0.1	880.0	28.0	0.2
LOVIE-11	31.0	3.6	0.0	17.0	0.1	234.0	9.0	0.2
LOVIE-12	55.0	4.2	0.0	23.0	0.0	249.0	N	0.0
LOVIE-13	50.0	3.3	0.0	20.0	0.1	160.0	N	0.0
LOVIE-14	32.0	3.0	0.4	9.0	0.1	101.0	3.0	0.0
LOVIE-15	19.0	1.9	0.3	10.0	0.0	110.0	1.0	0.1
LOVIE-16	871.0	3.6	0.0	10.0	0.0	10000.0	15.0	0.0
LOVIE-17	16.0	3.8	0.0	6.0	0.0	262.0	N	0.0
LOVIE-18	33.0	2.1	0.5	39.0	0.2	681.0	N	0.0
LOVIE-19	15.0	2.8	0.6	29.0	0.0	147.0	N	0.0
LOVIE-20	309.0	5.2	0.0	17.0	0.1	10000.0	43.0	0.1
LOVIE-21	18.0	4.3	0.0	7.0	0.1	318.0	2.0	0.0
LOVIE-22	518.0	3.7	0.0	N	0.2	1054.0	N	0.0
LOVIE-23	159.0	4.1	0.0	8.0	0.8	2131.0	3.0	0.0
LOVIE-24	274.0	7.2	0.0	5.0	0.1	578.0	16.0	0.1

Sample	Ni ppm	P ppm	Pb ppm	Sb ppm	Se ppm
GRIT-59	12.0	496.0	6.0	N	N
GRIT-60	2.0	11.0	7.0	N	N
GRIT-61	N	17.0	20.0	N	N
GRIT-62	22.0	347.0	46.0	47.0	N
GRIT-63	33.0	339.0	75.0	29.0	N
GRIT-64	N	3.0	2.0	N	N
GRIT-65	6.0	335.0	11.0	N	N
GRIT-66	14.0	252.0	8.0	N	N
GRIT-67	7.0	192.0	30.0	7.0	N
GRIT-68	13.0	220.0	24.0	3.0	N
GRIT-69	13.0	121.0	5.0	N	N
GRIT-70	N	357.0	7.0	N	N
GRIT-71	4.0	105.0	14.0	5.0	5.0
GRIT-72	6.0	180.0	10.0	N	N
LOVIE-01	15.0	163.0	39842.0	502.0	76.0
LOVIE-02	10.0	252.0	10000.0	299.0	24.0
LOVIE-03	29.0	117.0	2678.0	37.0	N
LOVIE-04	12.0	567.0	2027.0	17.0	N
LOVIE-05	89.0	32.0	850.0	30.0	N
LOVIE-06	7.0	462.0	3681.0	66.0	N
LOVIE-07	23.0	86.0	1637.0	170.0	N
LOVIE-08	68.0	34.0	2371.0	16.0	N
LOVIE-09	17.0	365.0	10000.0	237.0	24.0
LOVIE-10	40.0	3031.0	10000.0	173.0	N
LOVIE-11	14.0	896.0	777.0	29.0	N
LOVIE-12	40.0	1655.0	125.0	25.0	N
LOVIE-13	11.0	2417.0	604.0	20.0	7.0
LOVIE-14	8.0	845.0	1643.0	58.0	N
LOVIE-15	6.0	391.0	5769.0	43.0	5.0
LOVIE-16	54.0	1224.0	10000.0	342.0	N
LOVIE-17	18.0	702.0	317.0	27.0	N
LOVIE-18	27.0	2210.0	116.0	4.0	N
LOVIE-19	12.0	1014.0	175.0	13.0	N
LOVIE-20	24.0	4193.0	10000.0	195.0	N
LOVIE-21	19.0	827.0	1130.0	14.0	N
LOVIE-22	51.0	168.0	10000.0	86.0	N
LOVIE-23	64.0	876.0	132.0	6.0	N
LOVIE-24	34.0	1514.0	7578.0	61.0	N

Sample	Sr ppm	Ti %	Th ppm	V ppm	W ppm	Zn ppm
GRIT-59	26.0	0.0	N	27.0	N	43.0
GRIT-60	N	0.0	N	N	N	11.0
GRIT-61	10.0	0.0	N	N	N	25.0
GRIT-62	9.0	0.0	N	47.0	N	92.0
GRIT-63	8.0	0.0	0.7	38.0	9.0	125.0
GRIT-64	836.0	0.0	2.1	N	N	5.0
GRIT-65	64.0	0.0	N	15.0	N	36.0
GRIT-66	19.0	0.0	N	32.0	8.0	21.0
GRIT-67	21.0	0.0	N	13.0	N	78.0
GRIT-68	16.0	0.0	N	24.0	24.0	109.0
GRIT-69	16.0	0.0	N	24.0	N	13.0
GRIT-70	17.0	0.0	N	11.0	N	29.0
GRIT-71	23.0	0.0	N	11.0	N	64.0
GRIT-72	13.0	0.0	N	17.0	N	23.0
LOVIE-01	10.0	0.0	0.7	4.0	N	12681.0
LOVIE-02	3.0	0.0	N	4.0	N	10000.0
LOVIE-03	N	0.0	4.7	N	N	10000.0
LOVIE-04	8.0	0.0	N	11.0	N	1928.0
LOVIE-05	N	0.0	10.2	N	N	10000.0
LOVIE-06	6.0	0.0	N	10.0	N	1397.0
LOVIE-07	4.0	0.0	0.7	2.0	N	2315.0
LOVIE-08	N	0.0	22.3	N	N	10000.0
LOVIE-09	13.0	0.0	N	6.0	N	4097.0
LOVIE-10	123.0	0.0	1.7	20.0	N	6143.0
LOVIE-11	121.0	0.0	N	18.0	N	196.0
LOVIE-12	75.0	0.0	N	151.0	N	586.0
LOVIE-13	152.0	0.0	N	33.0	N	551.0
LOVIE-14	120.0	0.0	N	21.0	N	199.0
LOVIE-15	15.0	0.0	1.9	5.0	N	532.0
LOVIE-16	36.0	0.0	11.6	9.0	N	10000.0
LOVIE-17	42.0	0.0	N	37.0	N	959.0
LOVIE-18	34.0	0.0	N	13.0	N	500.0
LOVIE-19	147.0	0.0	N	8.0	N	516.0
LOVIE-20	51.0	0.0	8.0	26.0	N	6074.0
LOVIE-21	35.0	0.0	N	38.0	N	572.0
LOVIE-22	13.0	0.0	1.0	4.0	N	10000.0
LOVIE-23	19.0	0.0	1.4	53.0	N	482.0
LOVIE-24	32.0	0.0	2.2	63.0	N	5048.0

Sample	Mine / Area	UTMX	UTMY
LOVIE-25	Lovie	523317.1	4466795.4
LOVIE-26	Lovie	523317.1	4466795.4
LOVIE-27	Lovie	523321.7	4466792.7
LOVIE-28	Lovie	523321.5	4466792.4
LOVIE-29	Lovie	523328.7	4466794.3
LOVIE-30	Lovie	523342.3	4466805.2
LOVIE-31	Lovie	523293.4	4466787.0
LOVIE-32	Lovie	523293.9	4466787.4
LOVIE-33	Lovie	523174.2	4466794.7
LOVIE-34	Lovie	523174.2	4466794.5
LOVIE-35	Lovie	523173.4	4466785.0
LOVIE-36	Lovie	523229.6	4466708.1
LOVIE-37	Lovie	523398.5	4466692.4
LOVIE-38	Lovie	523397.3	4466693.7
LOVIE-39	Lovie	523374.2	4466732.0
LOVIE-40	Lovie	523374.3	4466731.9
LOVIE-41	Lovie	523374.3	4466731.8
LOVIE-42	Lovie	523374.2	4466731.4
LOVIE-43	Lovie	523258.2	4466941.6
LOVIE-44	Lovie	523325.1	4466897.7
LOVIE-45	Lovie	523325.7	4466897.5
GE-01	Grey Eagle	520590.3	4469560
GE-02	Grey Eagle	520589.7	4469559.5
GE-03	Grey Eagle	520589.6	4469559.3
GE-04	Grey Eagle	520589.5	4469559.1
GE-05	Grey Eagle	520589.6	4469559
GE-06	Grey Eagle	520589.5	4469559
GE-07	Grey Eagle	520589.5	4469558.9
GE-08	Grey Eagle	520589.4	4469558.7
GE-09	Grey Eagle	520589.4	4469558.7
GE-10	Grey Eagle	520589.4	4469558.7

Sample	Au ppb	Hg ppb	Ag ppm	Al %	As ppm
LOVIE-25	82.0	770.0	125.7	0.3	302.0
LOVIE-26	17.0	530.0	97.7	0.1	49.0
LOVIE-27	20.0	1760.0	70.1	0.1	272.0
LOVIE-28	27.0	1720.0	389.0	0.1	361.0
LOVIE-29	29.0	460.0	15.2	0.0	133.0
LOVIE-30	148.0	2160.0	150.9	0.7	368.0
LOVIE-31	98.0	1090.0	1003.1	1.1	524.0
LOVIE-32	68.0	442.0	30.0	0.8	302.0
LOVIE-33	21.0	580.0	120.8	0.0	125.0
LOVIE-34	114.0	1000.0	98.7	0.0	2097.0
LOVIE-35	218.0	9300.0	6494.4	0.0	2136.0
LOVIE-36	27.0	74.0	15.1	0.7	22.0
LOVIE-37	37.0	11.0	2.6	0.5	3.0
LOVIE-38	23.0	177.0	11.4	0.5	61.0
LOVIE-39	12.0	15.0	1.0	3.5	N
LOVIE-40	3.0	10.0	N	3.4	N
LOVIE-41	64.0	14.0	1.7	2.6	86.0
LOVIE-42	11.0	17.0	0.7	4.1	N
LOVIE-43	63.0	441.0	758.9	0.4	259.0
LOVIE-44	21.0	176.0	51.3	0.2	15.0
LOVIE-45	22.0	110.0	4.1	0.8	30.0
GE-01	1064.0	455.0	176.0	0.0	1509.9
GE-02	456.0	1205.0	29.5	0.1	5279.7
GE-03	394.0	400.0	199.0	0.0	2580.0
GE-04	200.0	165.0	24.0	0.1	819.6
GE-05	2560.0	500.0	145.0	0.0	3119.9
GE-06	1706.0	1000.0	393.0	0.0	2200.0
GE-07	13750.0	410.0	204.9	0.0	17000.0
GE-08	12250.0	1200.0	529.9	0.0	2810.0
GE-09	3528.0	360.0	357.9	0.0	3060.0
GE-10	1342.0	240.0	159.0	0.0	4999.9

Sample	B ppm	Ba ppm	Bi ppm	Ca %	Cd ppm	Co ppm	Cr ppm
LOVIE-25	17.0	43.0	4.0	0.0	3.1	2.0	36.0
LOVIE-26	10.0	10.0	2.0	0.0	2.5	N	91.0
LOVIE-27	10.0	39.0	2.0	0.0	2.9	N	79.0
LOVIE-28	10.0	17.0	2.0	0.0	1.7	N	99.0
LOVIE-29	11.0	301.0	3.0	0.0	0.8	2.0	57.0
LOVIE-30	35.0	384.0	9.0	0.1	8.0	25.0	30.0
LOVIE-31	15.0	61.0	2.0	0.1	9.9	3.0	64.0
LOVIE-32	63.0	285.0	15.0	0.6	16.2	39.0	30.0
LOVIE-33	14.0	377.0	3.0	0.0	6.4	8.0	52.0
LOVIE-34	141.0	725.0	41.0	0.1	98.2	156.0	28.0
LOVIE-35	19.0	26.0	4.0	0.1	62.0	4.0	3.0
LOVIE-36	13.0	71.0	2.0	0.5	1.0	1.0	55.0
LOVIE-37	9.0	28.0	1.0	10.0	N	7.0	17.0
LOVIE-38	30.0	62.0	7.0	0.6	4.7	9.0	40.0
LOVIE-39	35.0	22.0	10.0	10.0	1.5	18.0	42.0
LOVIE-40	33.0	82.0	8.0	10.0	1.4	25.0	76.0
LOVIE-41	34.0	111.0	9.0	10.0	1.5	20.0	64.0
LOVIE-42	40.0	9.0	11.0	10.0	1.9	19.0	17.0
LOVIE-43	13.0	66.0	2.0	0.1	2.9	3.0	96.0
LOVIE-44	9.0	43.0	1.0	0.0	1.3	1.0	122.0
LOVIE-45	27.0	186.0	6.0	0.1	8.2	7.0	39.0
GE-01	1.5	8.5	163.0	0.0	33.5	16.0	5.3
GE-02	1.5	13.0	8.5	1.8	823.2	7.7	4.9
GE-03	1.5	2.2	184.9	0.0	25.3	23.6	4.6
GE-04	1.5	56.3	16.1	1.9	14.9	4.5	6.8
GE-05	1.5	18.0	23.7	0.7	305.3	6.7	8.4
GE-06	1.5	1.0	225.9	0.0	124.4	39.2	7.0
GE-07	1.5	0.0	31.4	0.0	8.0	12.6	6.1
GE-08	1.5	0.0	253.9	0.0	18.9	33.9	8.0
GE-09	1.5	0.0	232.9	0.0	18.7	36.1	3.7
GE-10	1.5	0.4	248.9	1.2	8.6	28.3	6.1

Sample	Cu ppm	Fe %	K %	La ppm	Mg %	Mn ppm	Mo ppm	Na %
LOVIE-25	450.0	1.4	0.1	6.0	0.0	249.0	3.0	0.0
LOVIE-26	181.0	0.7	0.0	N	0.0	51.0	N	0.0
LOVIE-27	230.0	0.6	0.0	N	0.0	36.0	1.0	0.0
LOVIE-28	215.0	0.7	0.0	N	0.0	58.0	N	0.0
LOVIE-29	171.0	0.8	0.0	N	0.0	77.0	2.0	0.0
LOVIE-30	1538.0	3.2	0.3	11.0	0.1	2173.0	20.0	0.0
LOVIE-31	10000.0	1.2	0.1	10.0	0.0	64.0	121.0	0.0
LOVIE-32	578.0	4.8	0.0	13.0	0.1	2888.0	2.0	0.1
LOVIE-33	334.0	1.1	0.0	N	0.0	1753.0	11.0	0.0
LOVIE-34	2158.0	6.8	0.0	11.0	0.1	10000.0	62.0	0.1
LOVIE-35	9690.0	1.7	0.0	2.0	0.0	1306.0	225.0	0.0
LOVIE-36	60.0	0.9	0.3	7.0	0.1	53.0	11.0	0.0
LOVIE-37	5.0	0.6	0.2	4.0	0.2	1733.0	N	0.1
LOVIE-38	187.0	2.5	0.2	6.0	0.6	912.0	7.0	0.1
LOVIE-39	N	3.1	0.0	13.0	1.8	1171.0	N	0.1
LOVIE-40	6.0	3.1	0.0	9.0	1.7	716.0	N	0.1
LOVIE-41	18.0	3.1	0.0	8.0	1.5	2511.0	N	0.1
LOVIE-42	N	3.5	0.0	3.0	2.2	1365.0	N	0.0
LOVIE-43	1540.0	1.0	0.0	3.0	0.0	62.0	173.0	0.0
LOVIE-44	217.0	0.4	0.0	N	0.0	88.0	36.0	0.0
LOVIE-45	179.0	2.4	0.1	6.0	0.1	316.0	19.0	0.0
GE-01	316.3	8.9	0.0	1.3	0.0	48.4	7.7	0.0
GE-02	670.6	6.3	0.1	3.1	0.5	799.7	5.8	0.0
GE-03	466.2	14.2	0.0	0.8	0.0	39.3	6.2	0.0
GE-04	123.1	2.7	0.1	4.8	0.5	431.4	7.3	0.0
GE-05	662.1	6.2	0.0	1.6	0.2	232.9	11.1	0.0
GE-06	588.1	13.7	0.0	0.6	0.0	65.8	9.2	0.0
GE-07	842.1	19.7	0.0	0.6	0.0	37.6	8.0	0.0
GE-08	844.3	20.4	0.0	0.6	0.0	59.3	10.1	0.0
GE-09	479.0	23.5	0.0	0.7	0.0	25.9	4.9	0.0
GE-10	181.5	13.6	0.0	1.8	0.4	153.8	12.8	0.0

Sample	Ni ppm	P ppm	Pb ppm	Sb ppm	Se ppm
LOVIE-25	7.0	2147.0	10000.0	294.0	5.0
LOVIE-26	5.0	124.0	1184.0	103.0	N
LOVIE-27	5.0	130.0	1233.0	195.0	N
LOVIE-28	4.0	174.0	2513.0	586.0	4.0
LOVIE-29	12.0	69.0	423.0	41.0	N
LOVIE-30	68.0	1539.0	3882.0	302.0	N
LOVIE-31	13.0	3199.0	10000.0	274.0	N
LOVIE-32	170.0	2324.0	1493.0	47.0	N
LOVIE-33	33.0	511.0	10000.0	133.0	N
LOVIE-34	377.0	1196.0	7447.0	224.0	N
LOVIE-35	7.0	4449.0	10000.0	7418.0	8.0
LOVIE-36	9.0	3987.0	1146.0	34.0	N
LOVIE-37	18.0	455.0	42.0	3.0	N
LOVIE-38	33.0	1955.0	488.0	5.0	N
LOVIE-39	36.0	3967.0	22.0	N	N
LOVIE-40	58.0	755.0	20.0	N	N
LOVIE-41	58.0	975.0	90.0	N	N
LOVIE-42	26.0	50.0	10.0	N	N
LOVIE-43	8.0	2818.0	10000.0	308.0	11.0
LOVIE-44	13.0	179.0	978.0	14.0	N
LOVIE-45	95.0	906.0	131.0	5.0	N
GE-01	36.9	24.1	4414.6	252.9	0.3
GE-02	30.9	213.9	238.0	128.8	0.2
GE-03	30.9	25.3	4561.4	304.1	0.5
GE-04	38.3	254.2	2148.3	29.4	0.2
GE-05	58.2	0.3	3296.2	623.8	0.2
GE-06	50.0	0.3	6831.7	954.3	0.2
GE-07	38.0	3.2	1358.1	868.2	0.2
GE-08	52.4	0.3	5797.7	2013.0	0.6
GE-09	21.6	0.3	2895.8	402.0	0.2
GE-10	40.8	39.4	1471.8	234.3	0.9

Sample	Sr ppm	Ti %	Th ppm	V ppm	W ppm	Zn ppm
LOVIE-25	15.0	0.0	N	16.0	N	411.0
LOVIE-26	N	0.0	N	3.0	N	376.0
LOVIE-27	3.0	0.0	N	3.0	N	502.0
LOVIE-28	2.0	0.0	N	4.0	13.0	154.0
LOVIE-29	N	0.0	N	7.0	N	184.0
LOVIE-30	23.0	0.0	1.2	24.0	N	1383.0
LOVIE-31	30.0	0.0	N	76.0	37.0	899.0
LOVIE-32	117.0	0.0	1.3	74.0	N	1613.0
LOVIE-33	8.0	0.0	1.0	4.0	N	421.0
LOVIE-34	170.0	0.0	23.6	15.0	N	5669.0
LOVIE-35	58.0	0.0	0.9	N	134.0	564.0
LOVIE-36	64.0	0.0	N	70.0	N	61.0
LOVIE-37	156.0	0.0	N	21.0	N	26.0
LOVIE-38	23.0	0.0	N	35.0	N	326.0
LOVIE-39	169.0	0.0	N	66.0	N	58.0
LOVIE-40	68.0	0.1	N	89.0	N	59.0
LOVIE-41	128.0	0.0	N	65.0	N	81.0
LOVIE-42	142.0	0.0	N	50.0	N	87.0
LOVIE-43	28.0	0.0	N	8.0	27.0	260.0
LOVIE-44	4.0	0.0	N	6.0	N	169.0
LOVIE-45	38.0	0.0	N	43.0	N	545.0
GE-01	2.8	0.0	N	0.7	0.0	1066.3
GE-02	27.3	0.0	N	2.2	297.0	3249.6
GE-03	1.7	0.0	N	0.1	0.0	947.4
GE-04	66.8	0.0	N	3.6	0.0	611.6
GE-05	14.5	0.0	N	2.1	68.4	2419.6
GE-06	7.4	0.0	N	0.5	19.3	2108.8
GE-07	0.5	0.0	N	0.1	7.6	389.8
GE-08	11.0	0.0	N	0.2	0.0	774.6
GE-09	0.6	0.0	N	0.1	0.0	739.8
GE-10	22.9	0.0	N	0.7	0.0	437.6

APPENDIX B

$^{40}\text{Ar} / ^{39}\text{Ar}$ data

ID	Temp (°C)	$^{40}\text{Ar}/^{39}\text{Ar}$	$^{37}\text{Ar}/^{39}\text{Ar}$	$^{36}\text{Ar}/^{39}\text{Ar}$ ($\times 10^{-3}$)	$^{39}\text{Ar}_K$ ($\times 10^{-15}$ mol)	K/Ca	$^{40}\text{Ar}^*$ (%)	^{39}Ar (%)	Age (Ma)	$\pm 1\sigma$ (Ma)
GRIT-53, biotite, 2.60 mg, J=0.0016165, D=1.0037±0.0005, NM-181C, Lab#=55055-01										
# A	650	139.4	2.707	462.0	0.273	0.19	2.3	0.3	9.5	5.9
# B	700	60.50	4.890	184.6	0.269	0.10	10.5	0.6	18.4	5.9
# C	750	37.70	2.211	90.40	0.434	0.23	29.6	1.1	32.3	3.5
D	800	19.56	0.5480	22.13	2.18	0.93	66.8	3.5	37.72	0.73
E	850	14.84	0.0689	4.870	5.38	7.4	90.3	9.4	38.69	0.29
F	900	14.21	0.0400	2.540	6.31	12.7	94.7	16.3	38.84	0.24
G	950	14.15	0.0379	1.990	8.32	13.5	95.9	25.5	39.13	0.18
# H	1000	23.02	0.0409	33.81	9.8	12.5	56.6	36.3	37.61	0.22
I	1100	15.18	0.0382	5.643	24.8	13.4	89.0	63.6	38.981	0.080
J	1250	14.23	0.0993	2.443	32.7	5.1	95.0	99.6	38.991	0.062
# K	1300	19.14	0.0878	18.30	0.366	5.8	71.8	100.0	39.6	3.9
Total gas age ± 1σ		n=11			90.9		K2O=8.31 %		38.616	0.079
Plateau ± 1σ steps D-J		n=6		MSWD=1.01	79.8	9.2		87.7	38.979	0.060
PH-156 260, biotite, 6.96 mg, J=0.0016139, D=1.0037±0.0005, NM-181C, Lab#=55052-01										
A	650	144.0	0.9132	465.2	1.28	0.56	4.6	0.5	19.1	2.0
B	700	56.77	2.242	157.3	1.08	0.23	18.5	1.0	30.3	1.5
C	750	53.68	1.366	136.6	1.02	0.37	25.0	1.4	38.7	1.7
D	800	27.68	0.3357	51.35	5.34	1.5	45.3	3.6	36.13	0.38
E	850	15.80	0.0332	8.190	12.4	15.4	84.7	8.6	38.55	0.15
F	900	14.64	0.0264	2.993	15.8	19.3	94.0	15.1	39.60	0.11
G	950	14.43	0.0359	2.370	12.4	14.2	95.2	20.2	39.54	0.13
H	1000	14.90	0.0445	3.890	9.68	11.5	92.3	24.1	39.60	0.17
I	1100	14.74	0.0441	3.307	34.9	11.6	93.4	38.4	39.640	0.062
J	1250	14.22	0.0793	2.326	89.4	6.4	95.2	75.0	38.985	0.042
K	1300	14.30	0.0739	4.150	61.2	6.9	91.5	100.0	38.62	0.06
Total gas age ± 1σ		n=11			244.5		K2O=8.36 %		38.619	0.064
HT02-5, biotite, 1.86 mg, J=0.001612, D=1.0037±0.0005, NM-181C, Lab#=55050-02										
# A	650	428.8	1.227	1441.0	0.575	0.42	0.7	2.3	9.0	5.7
# B	700	49.61	2.182	143.7	0.440	0.23	14.8	4.1	21.3	3.1
# C	750	25.95	1.063	62.70	0.474	0.48	29.0	6.0	21.8	2.7
# D	800	18.99	0.7621	25.90	0.697	0.67	60.0	8.7	32.9	1.8
# E	850	15.74	0.0774	10.58	1.70	6.6	80.2	15.6	36.34	0.73
F	900	16.73	0.0600	8.620	2.38	8.5	84.8	25.1	40.79	0.53
G	950	15.35	0.0736	6.460	2.41	6.9	87.6	34.7	38.70	0.51
H	1000	16.46	0.1203	7.200	1.91	4.2	87.1	42.4	41.23	0.66
I	1100	15.77	0.1650	5.730	5.25	3.1	89.3	63.3	40.52	0.25
J	1250	14.71	0.1279	4.149	9.10	4.0	91.7	99.7	38.81	0.14
K	1300	17.50	0.1780	-20.3000	0.064	2.9	134.0	100.0	67.0	18.0
Total gas age ± 1σ		n=11			25.0		K2O=3.20 %		37.97	0.22
Plateau ± 1σ steps F-K		n=6		MSWD=11.24	21.1	4.6		84.4	39.33	0.38

GM-3, biotite, 6.75 mg, J=0.0016112, D=1.0037±0.0005, NM-181C, Lab#=55049-01

# A	650	175.5	0.3495	573.0	0.702	1.5	3.5	0.3	17.8	6.4
# B	700	55.79	0.0813	154.3	1.61	6.3	18.3	1.1	29.4	2.7
# C	750	19.38	0.0283	23.60	3.95	18.0	64.0	2.9	35.7	1.1
D	800	14.34	0.0151	3.720	16.3	33.8	92.4	10.3	38.10	0.26
E	850	13.86	0.0160	1.640	20.2	31.9	96.5	19.6	38.45	0.21
F	900	13.78	0.0151	1.210	20.8	33.9	97.4	29.1	38.61	0.21
G	950	13.93	0.0209	1.870	17.1	24.4	96.0	36.9	38.48	0.25
H	1000	14.32	0.0390	3.120	19.8	13.1	93.6	45.9	38.53	0.23
I	1100	14.08	0.0341	2.220	61.1	15.0	95.4	73.9	38.614	0.082
J	1250	13.87	0.0882	1.459	57.2	5.8	96.9	100.0	38.670	0.088
Integrated age ± 1σ			n=10		218.9		K2O=7.73 %		38.370	0.080
Plateau ± 1σ steps D-J			n=7	MSWD=0.86	212.6	18.0		97.1	38.593	0.064

CK02-14, amphibole, 24.95 mg, J=0.0016165, D=1.0064±0.0005, NM-181C, Lab#=55056-02

# B	800	-3.1100	0.0540	-36.8000	0.130	9.4	-250.0	0.5	22.5	4.5
# C	1000	60.28	1.472	171.3	0.97	0.35	16.2	4.6	28.3	1.6
D	1030	30.05	3.303	59.60	0.590	0.15	42.3	7.1	36.7	1.5
E	1060	19.39	4.728	21.84	2.85	0.11	68.7	19.0	38.57	0.35
F	1090	17.15	5.017	12.88	7.15	0.10	80.2	49.0	39.82	0.21
G	1120	16.51	4.935	11.85	6.41	0.10	81.3	75.9	38.86	0.25
H	1170	22.43	4.773	32.71	1.80	0.11	58.7	83.4	38.10	0.69
I	1200	21.99	4.911	31.77	2.11	0.10	59.1	92.3	37.66	0.48
J	1250	23.24	5.190	35.27	1.79	0.098	57.0	99.8	38.37	0.56
K	1300	107.1	6.050	350.0	0.058	0.084	3.9	100.0	12.0	15.0
Total gas age ± 1σ			n=10		23.8		K2O=0.23 %		38.34	0.17
Plateau ± 1σ steps D-K			n=8	MSWD=4.76	22.7	0.105		95.4	39.03	0.29

GE-02, muscovite, 1.98 mg, J=0.0016233, D=1.0037±0.0005, NM-181F, Lab#=55084-01

A	600	113.3	-0.0038	343.4	0.494	-	10.5	1.4	34.4	3.5
B	680	17.04	0.0015	11.90	1.63	340.1	79.4	5.8	39.17	0.93
C	700	14.47	-0.0006	1.600	0.594	-	96.7	7.5	40.5	2.4
D	750	14.78	0.0015	4.510	1.79	340.1	91.0	12.4	38.94	0.82
H	920	13.37	0.0005	1.270	5.99	981.2	97.2	28.8	37.65	0.37
I	960	13.56	0.0008	1.230	9.62	622.2	97.3	55.2	38.23	0.16
J	1000	13.65	0.0015	1.620	5.17	342.4	96.5	69.4	38.18	0.29
K	1040	13.68	0.0028	1.370	3.76	185.5	97.0	79.7	38.47	0.40
L	1080	13.77	0.0026	1.750	4.18	194.7	96.2	91.1	38.39	0.36
M	1120	14.64	0.0087	3.640	1.20	58.6	92.7	94.4	39.3	1.2
N	1160	12.90	0.0291	-4.5000	0.401	17.5	110.0	95.5	41.2	3.5
O	1200	12.40	0.0457	-2.3000	0.306	11.2	106.0	96.4	38.0	4.6
P	1250	17.40	0.0550	10.30	0.246	9.3	82.0	97.1	41.5	5.8
Q	1350	15.32	0.0551	5.600	0.677	9.3	89.2	98.9	39.6	2.1
R	1700	24.22	0.1814	34.70	0.394	2.8	57.7	100.0	40.5	3.7
Total gas age ± 1σ			n=15		36.5		K2O=4.36 %		38.37	0.17
Plateau ± 1σ steps A-R			n=15	MSWD=0.68	36.5	463.4		100.0	38.25	0.12

GM-6 Hornblende, A10:170, 20.08 mg, J=0.0008103, NM-170, Lab#=54259-02

# A	800	238.9	0.7910	750.9	3.04	0.64	7.1	5.6	24.8	1.8
# B	900	45.13	0.1515	61.83	5.78	3.4	59.5	16.3	38.88	0.29
# C	1000	42.63	0.3824	53.87	6.00	1.3	62.7	27.3	38.69	0.31
# D	1030	43.39	1.209	55.14	3.31	0.42	62.7	33.4	39.36	0.35
# E	1060	44.13	3.393	61.55	2.83	0.15	59.4	38.7	38.02	0.41
F	1090	42.05	4.765	51.70	4.66	0.11	64.6	47.3	39.42	0.28
G	1120	34.39	4.791	25.97	10.3	0.11	78.8	66.2	39.35	0.18
H	1170	32.38	4.020	19.58	8.2	0.13	83.2	81.3	39.04	0.19
I	1200	35.72	2.359	28.93	3.13	0.22	76.6	87.1	39.64	0.25
J	1250	40.77	4.353	49.40	5.50	0.12	65.1	97.3	38.49	0.25
K	1300	38.88	6.244	40.59	1.48	0.082	70.5	100.0	39.79	0.36
Integrated age ± 1σ			n=11		54.2		K2O=1.29 %		38.24	0.20
Plateau ± 1σ steps F-K			n=6	MSWD=3.13	33.3	0.12		61.3	39.23	0.17

GM-6 Biotite, A9:170, 5.17 mg, J=0.00080803, NM-170, Lab#=54258-01

# A	650	703.6	0.0956	2359.3	0.93	5.3	0.9	1.1	9.3	6.2
# B	750	71.88	0.0426	165.9	2.58	12.0	31.8	4.1	33.01	0.72
# C	850	30.69	0.0145	14.13	10.5	35.2	86.4	16.2	38.25	0.13
# D	920	28.77	0.0095	6.381	13.3	53.7	93.4	31.7	38.78	0.11
E	1000	28.95	0.0132	5.962	11.9	38.5	93.9	45.6	39.21	0.10
F	1075	28.86	0.0185	6.352	11.7	27.5	93.5	59.2	38.92	0.12
G	1110	28.41	0.0182	3.875	6.34	28.1	96.0	66.5	39.32	0.15
H	1180	28.11	0.0210	3.943	14.5	24.3	95.9	83.3	38.86	0.12
I	1210	27.78	0.0536	2.844	9.8	9.5	97.0	94.7	38.86	0.11
# J	1250	27.79	0.1693	1.496	4.58	3.0	98.5	100.0	39.45	0.18
Integrated age ± 1σ			n=10		86.1		K2O=7.97 %		38.40	0.12
Plateau ± 1σ steps E-I			n=5	MSWD=3.03	54.2	25.9		63.0	39.02	0.10

GM-15 Hornblende, A12:170, 22.62 mg, J=0.00081397, NM-170, Lab#=54261-01

# A	800	203.6	5.484	608.7	2.12	0.093	11.9	4.1	35.4	1.7
# B	900	37.37	0.4616	35.81	4.40	1.1	71.8	12.6	38.98	0.27
# C	1000	33.53	0.7134	22.23	5.09	0.72	80.6	22.4	39.26	0.24
# D	1030	33.42	2.235	23.95	2.95	0.23	79.4	28.1	38.60	0.34
E	1060	33.18	4.340	23.56	2.83	0.12	80.1	33.6	38.72	0.36
F	1090	31.48	5.135	17.62	6.08	0.099	84.8	45.3	38.92	0.22
G	1120	29.65	4.757	10.93	9.9	0.11	90.4	64.4	39.09	0.14
H	1170	29.85	3.587	11.92	4.51	0.14	89.2	73.1	38.78	0.24
I	1200	31.13	4.328	15.81	3.16	0.12	86.1	79.2	39.08	0.36
J	1250	31.56	5.070	17.19	9.5	0.10	85.2	97.6	39.22	0.16
K	1300	34.29	7.255	28.64	1.27	0.070	77.1	100.0	38.59	0.64
Integrated age ± 1σ			n=11		51.8		K2O=1.09 %		38.86	0.14
Plateau ± 1σ steps E-K			n=7	MSWD=0.70	37.3	0.11		71.9	39.03	0.09

GM-15 Biotite, A11:170, 7.26 mg, J=0.00081246, NM-170, Lab#=54260-01

# A	650	217.0	0.2931	699.9	0.485	1.7	4.7	0.4	14.9	2.7
# B	750	75.11	0.0621	163.0	2.13	8.2	35.9	2.1	39.09	0.89
# C	850	29.47	0.0093	10.36	14.4	54.6	89.6	13.5	38.30	0.11
D	920	27.98	0.0055	2.481	16.2	93.4	97.4	26.3	39.50	0.10
E	1000	27.87	0.0088	2.430	16.0	58.1	97.4	38.9	39.36	0.08
F	1075	27.89	0.0164	2.201	15.7	31.2	97.7	51.3	39.49	0.09
G	1110	27.67	0.0220	2.337	9.4	23.2	97.5	58.7	39.12	0.11
H	1180	27.66	0.0188	2.135	25.7	27.1	97.7	79.0	39.19	0.09
I	1210	27.49	0.0522	1.596	17.4	9.8	98.3	92.7	39.18	0.08
J	1250	27.33	0.1207	1.209	9.3	4.2	98.7	100.0	39.12	0.13
Integrated age ± 1σ			n=10		126.8		K2O=8.31 %		39.08	0.07
Plateau ± 1σ steps D-J			n=7	MSWD=2.96	109.7	37.0		86.5	39.29	0.07

T99413-570 Biotite, A15:170, 7.96 mg, J=0.00081488, NM-170, Lab#=54262-01

# A	650	246.4	0.6033	817.4	0.391	0.85	2.0	0.3	7.2	3.4
# B	750	87.89	0.4013	208.7	2.02	1.3	29.9	1.8	38.18	0.92
# C	850	29.52	0.0127	9.914	14.9	40.3	90.1	12.9	38.67	0.11
D	920	27.47	0.0083	1.670	17.6	61.1	98.2	25.9	39.23	0.08
E	1000	27.46	0.0098	1.486	15.3	52.1	98.4	37.3	39.30	0.09
F	1075	27.71	0.0143	1.510	15.0	35.8	98.4	48.4	39.65	0.08
G	1110	27.34	0.0153	1.077	10.7	33.4	98.8	56.3	39.30	0.11
H	1180	27.47	0.0260	1.447	13.5	19.6	98.5	66.3	39.32	0.08
I	1210	27.30	0.0323	1.179	13.2	15.8	98.7	76.1	39.20	0.11
J	1250	27.12	0.0551	0.8330	20.3	9.3	99.1	91.1	39.09	0.08
K	1300	27.40	0.0522	0.9500	9.9	9.8	99.0	98.5	39.44	0.11
# L	1700	32.12	0.1089	20.71	2.06	4.7	81.0	100.0	37.84	0.38
Integrated age ± 1σ			n=12		134.9		K2O=8.04 %		39.10	0.07
Plateau ± 1σ steps D-K			n=8	MSWD=4.12	115.4	30.5		85.6	39.32	0.07

Notes:

Isotopic ratios corrected for blank, radioactive decay, and mass discrimination, not corrected for interfering reactions.
 Errors quoted for individual analyses include analytical error only, without interfering reaction or J uncertainties.
 Total gas age calculated by combining isotopic measurements of all steps.
 Total gas age error calculated by combining errors of isotopic measurements of all steps.
 Plateau age is inverse-variance-weighted mean of selected steps.
 Plateau age error is inverse-variance-weighted mean error (Taylor, 1982) times square root MSWD where MSWD>1.
 Decay constants and isotopic abundance after Steiger and Jager (1977).
 # symbol preceding sample ID denotes analyses excluded from plateau age calculations.
 Ages calculated relative to FC-2 Fish Canyon Tuff sanidine interlaboratory standard at 28.02 Ma (cf. Renne et al., 1998)
 Decay Constant (LambdaK (total)) = 5.543e-10/a
 D= 1 AMU mass discrimination in favor of light isotopes
 K20 estimated from ³⁹Ar, sample weight, J-factor and mass spectrometer sensitivity.

Correction factors:	NM-181	NM-170
	$(^{39}\text{Ar}/^{37}\text{Ar})_{\text{Ca}} = 0.00070 \pm 0.00005$	$(^{39}\text{Ar}/^{37}\text{Ar})_{\text{Ca}} = 0.00070 \pm 0.00002$
	$(^{36}\text{Ar}/^{37}\text{Ar})_{\text{Ca}} = 0.00028 \pm 0.00001$	$(^{36}\text{Ar}/^{37}\text{Ar})_{\text{Ca}} = 0.000280 \pm 0.000005$
	$(^{38}\text{Ar}/^{39}\text{Ar})_{\text{K}} = 0.01077$	$(^{38}\text{Ar}/^{39}\text{Ar})_{\text{K}} = 0.01077$
	$(^{40}\text{Ar}/^{39}\text{Ar})_{\text{K}} = 0 \pm 0.0004$	$(^{40}\text{Ar}/^{39}\text{Ar})_{\text{K}} = 0.0002 \pm 0.0003$

Sample	Step	Laser Power (%)	$^{40}\text{Ar}/^{39}\text{Ar}$	$^{38}\text{Ar}/^{39}\text{Ar}$	$^{37}\text{Ar}/^{39}\text{Ar}$	$^{36}\text{Ar}/^{39}\text{Ar}$	Ca/K	Cl/K
GM-3 (U)	1	2	30.56	0.14	0.35	0.10	1.50	0.02
Biotite	2	2.3	10.30	0.08	0.30	0.03	1.35	0.01
	3	2.6	10.81	0.08	0.07	0.02	0.29	0.01
	4	2.9	8.94	0.08	0.02	0.01	0.06	0.02
	5	# 3.2	7.28	0.08	0.01	0.00	0.04	0.02
	6	# 3.5	7.26	0.08	0.01	0.00	0.03	0.02
	7	# 3.8	7.53	0.08	0.02	0.00	0.08	0.02
	8	# 4	7.32	0.08	0.02	0.00	0.10	0.02
	9	# 4.3	7.28	0.08	0.03	0.00	0.12	0.02

Total gas age **n = 9** **J = 0.00313**
Plateau steps 5-9 **n = 5** **MSWD = 0.46**

CK02-08	1	# 2	24.03	0.03	0.01	0.06	0.04	0.00
Potassium	2	# 2.4	8.77	0.01	0.01	0.01	0.04	0.00
Feldspar	3	# 2.7	9.05	0.02	0.01	0.01	0.02	0.00
	4	# 2.9	11.40	0.02	0.01	0.02	0.04	0.00
	5	3.2	18.97	0.02	0.03	0.04	0.11	0.00
	6	3.6	36.58	0.04	0.04	0.10	0.16	0.00

Total gas age **n = 6** **J = 0.00315**
Plateau steps 5-9 **n = 4** **MSWD = 2.2**

Sample	^{40}Ar atm (%)	^{39}Ar (%)	$^{40}\text{Ar}^*/^{39}\text{Ar}_K$	Age (Ma)	$\pm 2\sigma$ (Ma)
GM-3	92.33	0.27	1.90	10.67	11.02
Biotite	73.01	0.77	2.23	12.54	2.01
	52.35	1.88	4.75	26.65	2.69
	23.20	6.24	6.67	37.28	0.82
	1.82	14.67	7.04	39.30	0.32
	1.50	19.72	7.07	39.46	0.24
	5.25	23.07	7.07	39.49	0.26
	1.94	16.32	7.08	39.56	0.31
	1.40	17.05	7.08	39.56	0.31
Total gas age		99.99		31.61	2.00
Plateau steps 5-9		90.83		39.47	0.29
CK02-08	71.28	5.13	6.49	36.53	3.60
Potassium	18.83	24.15	6.87	38.61	0.87
Feldspar	22.21	39.23	6.89	38.76	0.50
	35.17	15.58	7.08	39.81	1.22
	57.37	9.08	7.75	43.50	2.07
	77.02	6.83	8.16	45.81	2.99
Total gas age		100		40.50	1.88
Plateau steps 5-9		84.09		38.43	1.55

Sample	Step		Laser Power (%)	$^{40}\text{Ar}/^{39}\text{Ar}$	$^{38}\text{Ar}/^{39}\text{Ar}$	$^{37}\text{Ar}/^{39}\text{Ar}$	$^{36}\text{Ar}/^{39}\text{Ar}$	Ca/K	Cl/K
CK02-08									
Muscovite	1	#	2	8.46	0.01	0.01	0.01	0.01	0.00
	2	#	2.2	7.29	0.01	0.00	0.00	0.01	0.00
	3	#	2.4	7.40	0.01	0.00	0.00	0.00	0.00
	4	#	2.6	7.30	0.01	0.00	0.00	0.01	0.00
	5	#	2.8	7.51	0.01	0.00	0.00	0.01	0.00
	6		3	10.04	0.01	0.01	0.02	0.00	0.00
Total gas age				n = 6	J = 0.003151				
Plateau steps 5-9				n = 5	MSWD = 1.4				
GM-10	1		2	27.17	0.03	0.01	0.06	0.00	0.00
Potassium	2		2.2	17.43	0.02	0.01	0.03	0.01	0.00
Feldspar	3		2.4	11.40	0.01	0.01	0.01	0.01	0.00
	4	#	2.6	10.35	0.02	0.00	0.01	0.01	0.00
	5	#	2.8	12.84	0.02	0.00	0.02	0.01	0.00
	6	#	3	9.52	0.01	0.01	0.01	0.02	0.00
	7		3.2	15.75	0.02	0.00	0.03	0.01	0.00
	8		3.5	63.21	0.05	0.02	0.19	0.03	0.00
Total gas age				n = 8	J = 0.003146				
Plateau steps 5-9				n = 3	MSWD = 1.7				

Volumes are $1\text{E-}13\text{ cm}^3$ NPT

Neutron flux monitors: 28.02 Ma FCs (Renne et al., 1998)

Isotope production ratios: $(^{40}\text{Ar}/^{39}\text{Ar})_{\text{K}}=0.0302$, $(^{37}\text{Ar}/^{39}\text{Ar})_{\text{Ca}}=1416.4306$,

$(^{36}\text{Ar}/^{39}\text{Ar})_{\text{Ca}}=0.3952$, $\text{Ca/K}=1.83(37\text{ArCa}/39\text{ArK})$.

= steps used in plateau calculations.

Sample	⁴⁰ Ar atm (%)	³⁹ Ar (%)	⁴⁰ Ar*/ ³⁹ Ar _K	Age (Ma)	± 2σ (Ma)
CK02-08					
Muscovite	11.56	10.36	6.72	37.81	2.29
	0.74	23.07	6.85	38.52	0.94
	0.84	22.96	6.95	39.10	0.98
	1.02	24.55	6.86	38.61	0.91
	3.32	16.50	6.74	37.92	0.65
	4.16	2.55	6.30	35.46	6.79
Total gas age		99.99		37.90	2.09
Plateau steps 5-9		97.44		38.39	1.15
GM-10					
Potassium	56.54	1.93	10.93	60.99	1.39
Feldspar	52.35	5.98	7.99	44.77	0.59
	30.91	8.58	7.55	42.33	0.41
	29.90	15.87	7.07	39.69	0.20
	44.56	30.63	7.04	39.53	0.50
	24.97	28.46	7.03	39.47	0.33
	47.87	6.28	7.88	44.15	0.35
	83.47	2.26	10.19	56.94	4.12
Total gas age		99.99		45.98	0.99
Plateau steps 5-9		74.96		39.56	0.34

T ^a	⁴⁰ Ar ^b / ³⁹ Ar	³⁸ Ar ^b / ³⁹ Ar	³⁷ Ar ^b / ³⁹ Ar	³⁶ Ar ^b / ³⁹ Ar (x100)
Sample GM-3 (biotite)				
Run #72B8 (J = 0.007030 wt. = 5.4070mg, 2 Grains 7.9 wt% K)				
600	135.7	0.1844	0.188	44.8
650	24.2	0.1058	0.0735	7.405
675	10.63	0.0977	0.0265	2.559
700	10.37	0.0991	0.0185	2.47
725	5.197	0.0946	0.0076	0.7245
750	3.787	0.0955	0.0068	0.2566
770	3.438	0.0945	0.0059	0.1277
790	3.282	0.0953	0.0064	0.079
810	3.246	0.0956	0.0081	0.0645
830	3.196	0.096	0.0087	0.04
850	3.196	0.0957	0.0108	0.0409
880	3.195	0.0949	0.0112	0.0469
910	3.223	0.0951	0.01	0.0536
930	3.251	0.0943	0.0174	0.0634
950	3.238	0.0932	0.0189	0.0604
970	3.17	0.0938	0.0187	0.0375
990	3.168	0.0929	0.0159	0.0358
1000	3.142	0.094	0.0163	0.0232
1010	3.147	0.0953	0.0171	0.0303
1020	3.132	0.0958	0.0218	0.0265
1030	3.188	0.0956	0.0442	0.042
1040	3.636	0.0966	0.1947	0.1687
1050	5.504	0.098	0.0889	0.7467
1065	16.6	0.1196	1.259	4.518
1080	20.98	0.1507	1.522	6.12
Integrated	4.322	0.0956	0.0209	0.4277

Spectrum analysis:

fractions 700 – 1030°C (96% of ³⁹Ar)

Isotope Correlation analysis: intercept ⁴⁰Ar/³⁶Ar = 293 ± 3

fractions 600 – 1080°C N = 25 MSWD = 1.7

F ^c	³⁹ Ar ^d (%)	⁴⁰ Ar ^{*e} (%)	Ca/K ^f	Cl/K ^g	Apparent Age (Ma)
Sample GM-3 (biotite)					
Run #72B8 (J = 0.007030 wt. = 5.4070mg, 2 Grains 7.9 wt% K)					
3.318	0.49	2.44	0.359	0.0169	41.60 ± 13.3
2.3	0.7	9.51	0.14	0.0153	28.90 ± 2.8
3.039	1.01	28.68	0.051	0.0155	38.10 ± 1.2
3.044	1.84	29.44	0.035	0.0158	38.20 ± 0.7
3.03	2.88	58.66	0.014	0.0156	38.00 ± 0.4
3.003	4.7	79.95	0.013	0.0159	37.70 ± 0.2
3.036	5.4	89.07	0.011	0.0158	38.10 ± 0.2
3.023	5.63	92.97	0.012	0.016	37.90 ± 0.1
3.03	5.5	94.23	0.015	0.016	38.00 ± 0.2
3.053	4.89	96.43	0.017	0.0161	38.30 ± 0.2
3.05	4.49	96.36	0.021	0.0161	38.30 ± 0.2
3.032	4.57	95.79	0.021	0.0159	38.00 ± 0.2
3.039	4.49	95.21	0.019	0.0159	38.10 ± 0.2
3.04	3.41	94.37	0.033	0.0158	38.10 ± 0.2
3.035	3.61	94.62	0.036	0.0156	38.10 ± 0.2
3.035	4.95	96.66	0.036	0.0157	38.10 ± 0.2
3.037	6.33	96.81	0.03	0.0155	38.10 ± 0.1
3.049	7.5	97.99	0.031	0.0157	38.30 ± 0.1
3.033	8.96	97.32	0.033	0.016	38.10 ± 0.1
3.03	10.36	97.68	0.042	0.0161	38.00 ± 0.1
3.041	6.39	96.33	0.085	0.016	38.20 ± 0.1
3.127	1.42	86.73	0.372	0.0162	39.20 ± 0.4
3.264	0.35	59.64	0.17	0.0162	40.90 ± 1.4
3.329	0.09	20.07	2.41	0.019	41.70 ± 5.2
2.994	0.04	14.28	2.91	0.0244	37.60 ± 14.3
3.034	100	70.7	0.04	0.0159	38.10 ± 0.1
					*** ± 0.4
Spectrum analysis:					
fractions	700 – 1030°C (96% of ³⁹ Ar)				38.1 ± 0.1
					*** ± 0.4
Isotope Correlation analysis:					
fractions	600 – 1080°C N = 25 MSWD = 1.7				38.1 ± 0.1
					*** ± 0.4

T (C)	$^{40}\text{Ar}/^{39}\text{Ar}$	$^{38}\text{Ar}/^{39}\text{Ar}$	$^{37}\text{Ar}/^{39}\text{Ar}$	$^{36}\text{Ar}/^{39}\text{Ar}$ (x100)
Sample DSC BXA (clay)				
Run #727C (J = 0.007006 wt. = 0.6442mg)				
uncorrected for Ar recoil loss (2.2 wt% K)				
550	15.58	0.0345	0.048	3.549
725	5.947	0.0174	0.2513	0.5475
1050	83.45	0.0677	0.5435	24.61
Integrated	13.56	0.0259	0.202	2.916

Isotope Correlation analysis:

fractions 550 – 1050°C N = 3 MSWD = 0.16 $^{40}\text{Ar}/^{36}\text{Ar} = 321 \pm 1$

corrected for Ar recoil loss of 31.6% ^{39}Ar and 13.4% ^{37}Ar (3.3 wt% K)

550	10.65	0.0236	0.0379	2.427
725	4.068	0.0119	0.1981	0.3747
1050	57.08	0.0463	0.429	16.83
Integrated	9.278	0.0177	0.1593	1.995

Isotope Correlation analysis:

fractions 550 – 1050°C N = 3 MSWD = 0.17 $^{40}\text{Ar}/^{36}\text{Ar} = 321 \pm 1$

F	³⁹ Ar (%)	⁴⁰ Ar* (%)	Ca/K	Cl/K	Apparent Age (Ma)
Sample DSC BXA (clay)					
Run #727C (J = 0.007006 wt. = 0.6442mg)					
uncorrected for Ar recoil loss (2.2 wt% K)					
5.065	32.57	32.58	0.092	0.0031	62.9 ± 1.2
4.32	61.65	73	0.481	0.0009	53.8 ± 0.4
10.75	5.78	12.88	1.04	0.0018	130.9 ± 9.2
4.934	100	36.45	0.386	0.0016	61.3 ± 0.7
					*** ± 0.9
Isotope Correlation analysis:					
fractions 550 – 1050°C					52.1 ± 0.4
3.455	32.57	32.52	0.072	0.0014	43.1 ± 1.2
2.946	61.65	72.97	0.379	0.0003	36.9 ± 0.4
7.344	5.78	12.87	0.821	0.0005	90.5 ± 9.2
3.366	100	36.4	0.305	0.0004	42.1 ± 0.7
					*** ± 0.9
Isotope Correlation analysis:					
fractions 550 – 1050°C					35.7 ± 0.4

Notes on data from RIL:

These data are shown as initially reported relative to 27.84 Ma Fish Canyon sanidine.

Sample ages relative to 28.02 Ma Fish Canyon sanidine are reported in Table 3.5 and shown in Figure 3.8 and in the accompanying age spectra.

For DSC BXA, the sample amount was severely limited so that only a single aliquot was feasible for the step-heating analysis using sample removed from the #72C7 ampoule after measuring the recoiled Ar. The “uncorrected” data are the step-heating results. For the “corrected” entries, the measured values are corrected for ^{39}Ar and ^{37}Ar recoil losses as measured for the ampoules.

All fractions were corrected uniformly using the recoil % for ^{39}Ar and for ^{37}Ar measured independently for each sample.

a Temperature °C measured via thermocouple outside of the Ta crucible.

b The isotope ratios given are not corrected for Ca, K and Cl derived Ar isotopic interference but, ^{37}Ar is corrected for decay using a half-life of 35.1 days. The ratios are corrected for line blanks.

c F is the ratio of radiogenic ^{40}Ar to K-derived ^{39}Ar . It is corrected for atmospheric argon and other nuclear reactions using the following factors:

$(^{40}\text{Ar}/^{36}\text{Ar})_{\text{air}}$	=	295.5
$(^{38}\text{Ar}/^{39}\text{Ar})_{\text{K}}$	=	0.01185
$(^{38}\text{Ar}/^{37}\text{Ar})_{\text{Ca}}$	=	3.5×10^{-5}
$(^{36}\text{Ar}/^{38}\text{Ar})_{\text{Cl}}$	=	-6 per day after irradiation.
$(^{39}\text{Ar}/^{37}\text{Ar})_{\text{Ca}}$	=	7.524×10^{-4}
$(^{36}\text{Ar}/^{37}\text{Ar})_{\text{Ca}}$	=	2.678×10^{-4}
$(^{40}\text{Ar}/^{39}\text{Ar})_{\text{K}}$	=	0.0305298

d Relative percent of the total ^{39}Ar released in the fraction.

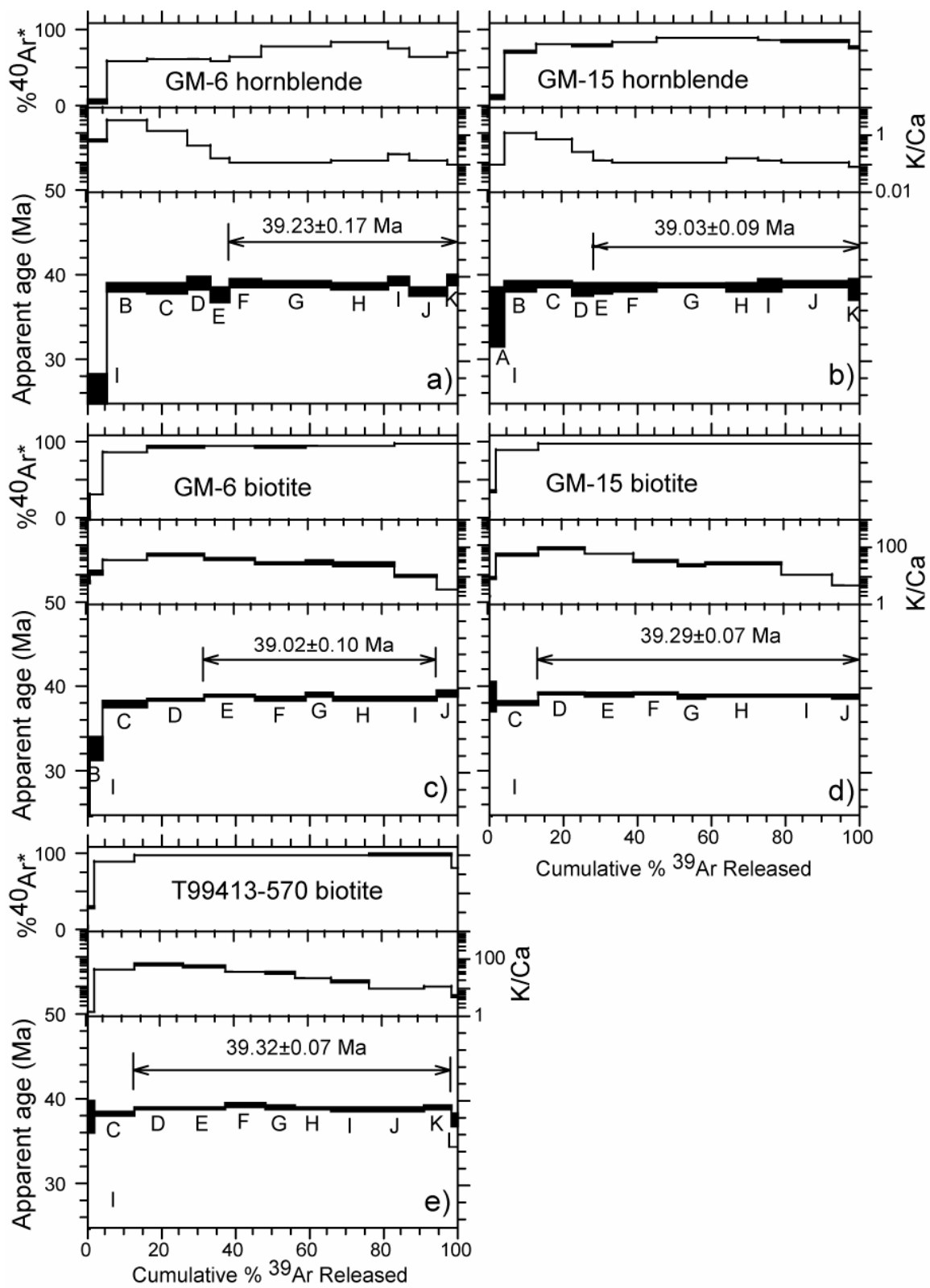
e Percent of the total ^{40}Ar in the fraction that is radiogenic.

f Weight ratio calculated using the relationship: $\text{K}/\text{Ca} = 0.523 \times (^{39}\text{Ar}/^{37}\text{Ar})_{\text{Ca}}$

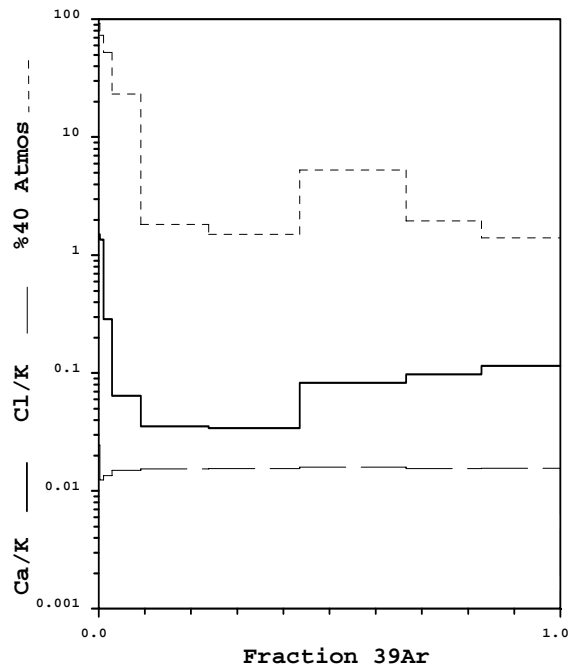
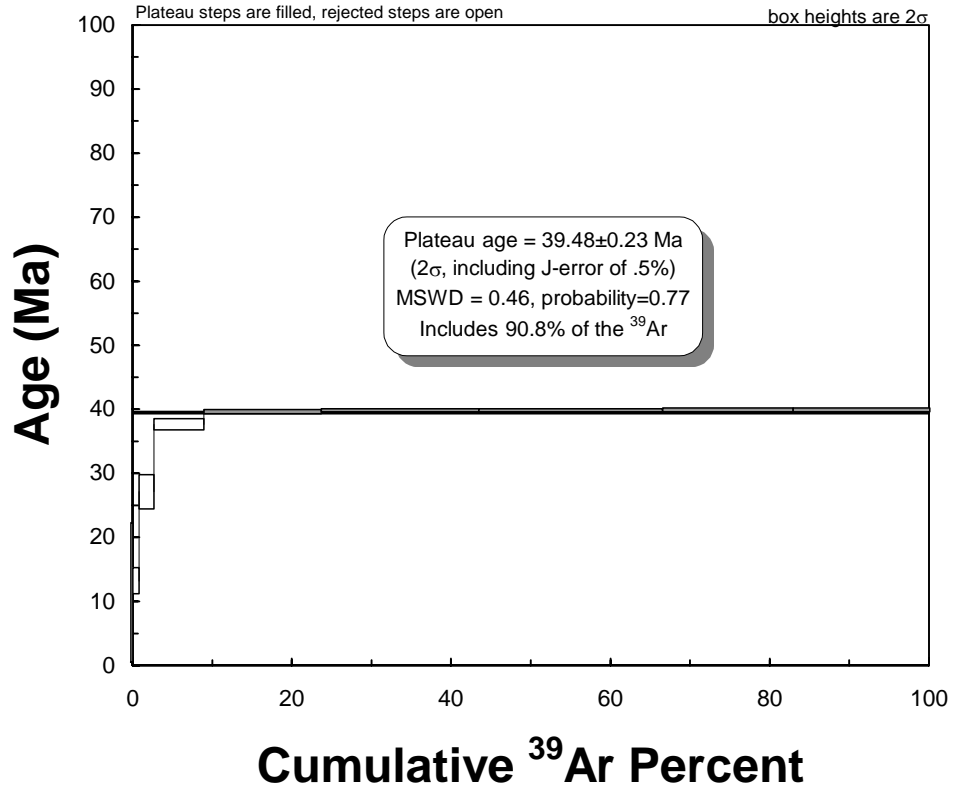
g Weight ratio calculated using the relationship: $\text{K}/\text{Cl} = 5.220 \times (^{39}\text{Ar}/^{38}\text{Ar})_{\text{Cl}}$.

h Ages calculated with a total decay constant of $5.543 \times 10^{-10} \text{ y}^{-1}$. Uncertainties are given at the one-sigma level. For individual fractions they do not include an uncertainty in J value; these uncertainties are appropriate for comparing fractions of a run. For integrated, plateau, and correlation ages, an uncertainty in J of 0.20% is used; this is appropriate for comparison with analogous ages for other samples and aliquots analyzed. An overall systematic uncertainty of $\pm 1\%$ is assigned to all ages. The monitor used was an intralaboratory muscovite with a $^{40}\text{Ar}/^{39}\text{Ar}$ age of 165.3 Ma that is assigned an uncertainty of $\pm 1\%$.

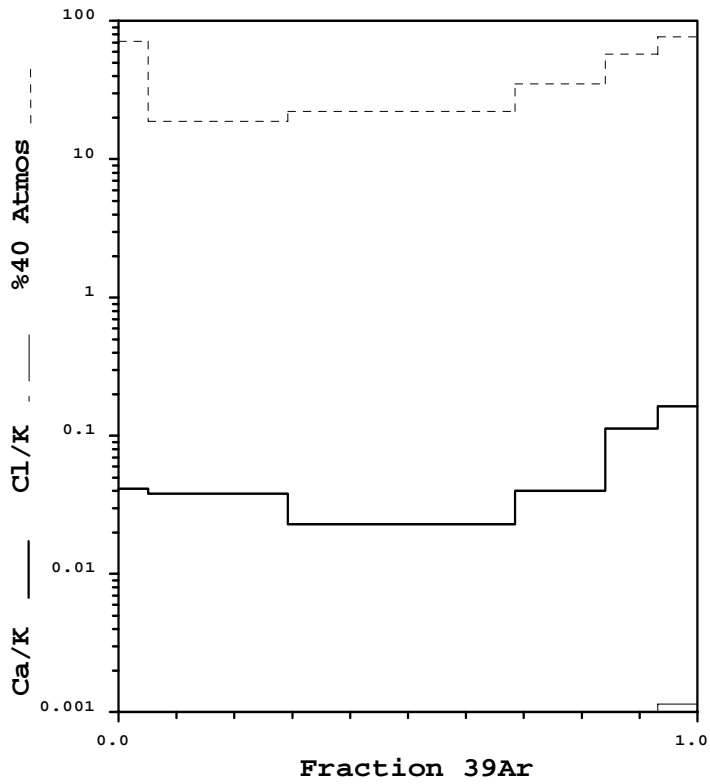
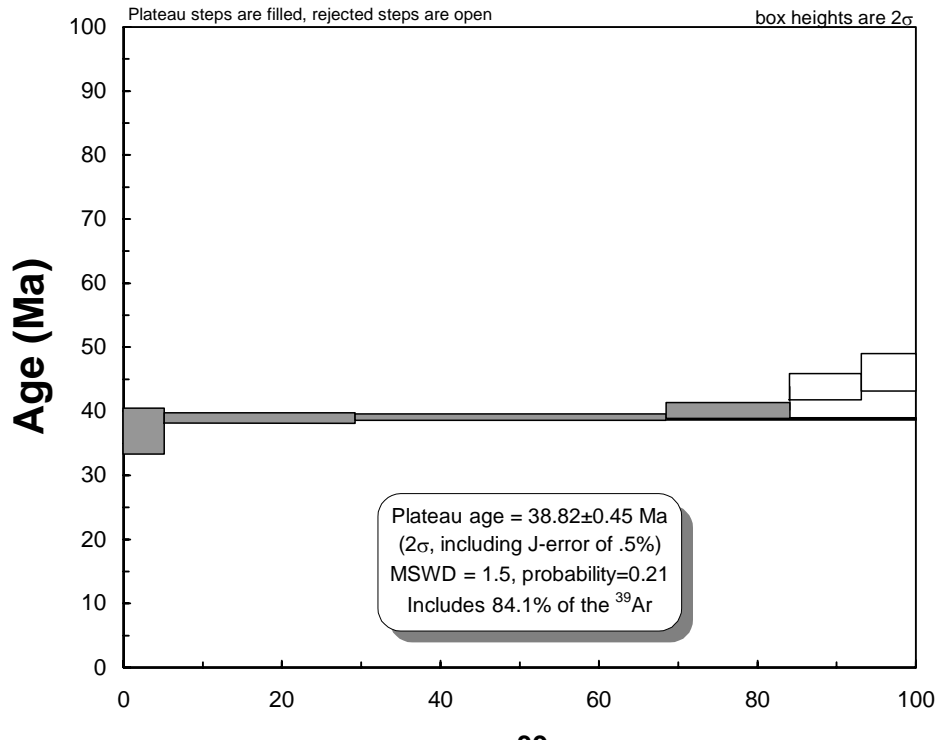
Uncertainties for integrated, plateau, and correlation ages noted by *** apply this $\pm 1\%$ uncertainty quadratically; these uncertainties are appropriate for comparison to other data sets. Uncertainties for recoil-corrected ages do not taken into account any recoil uncertainties.

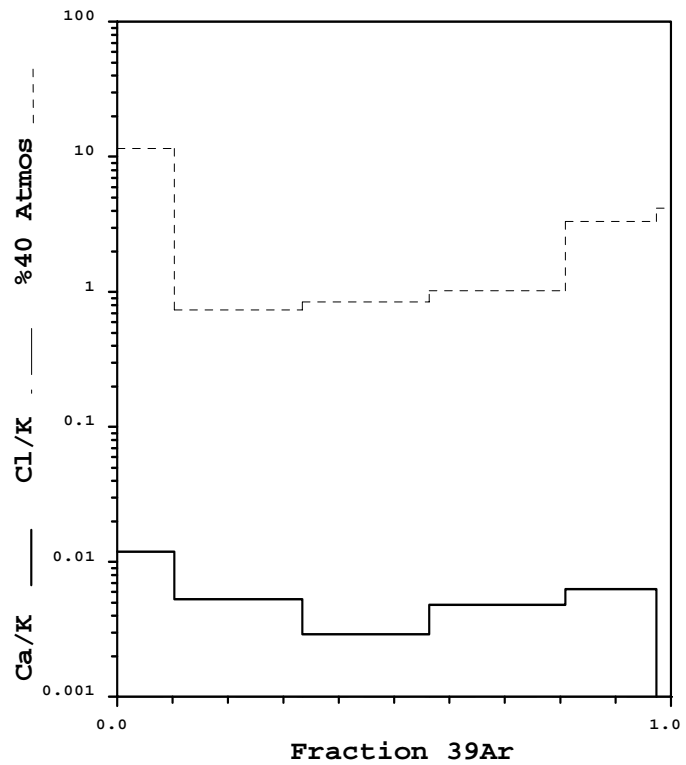
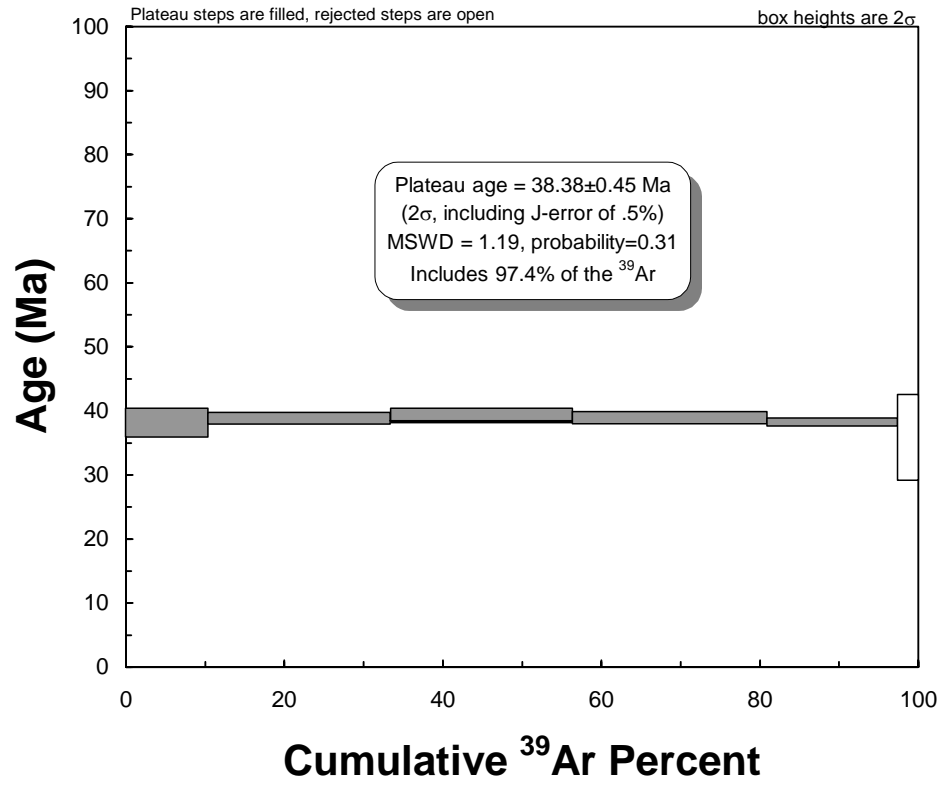


GM-3 Biotite

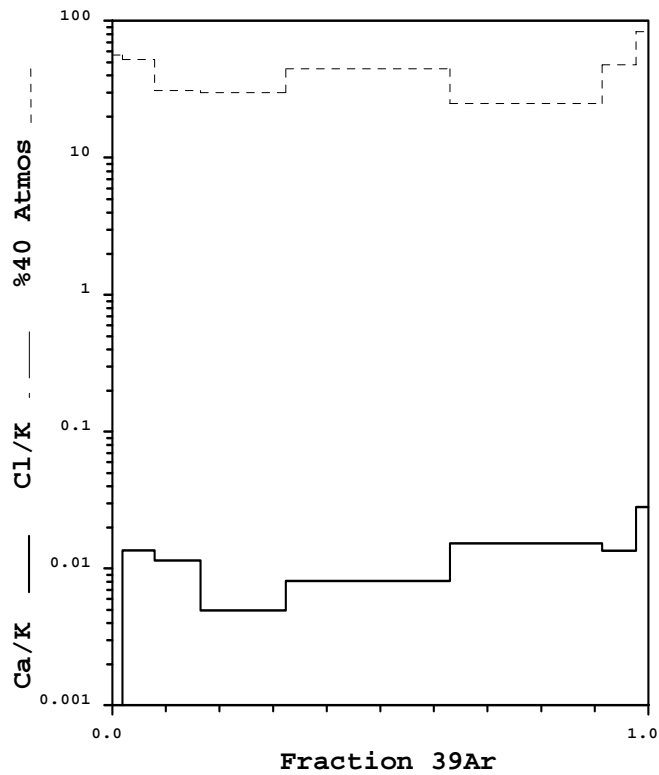
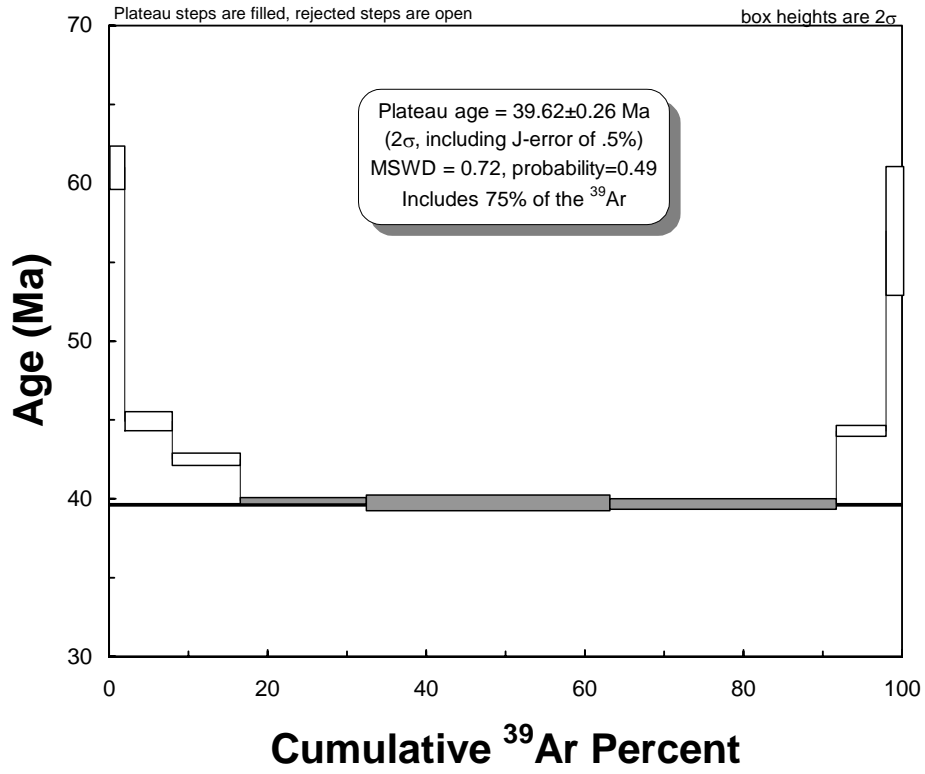


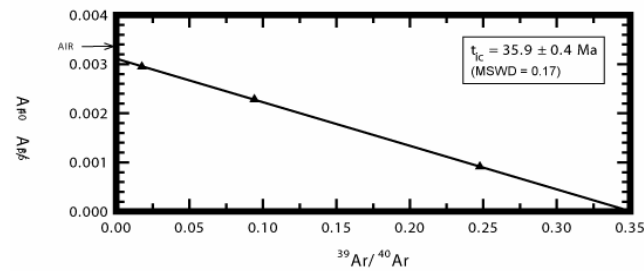
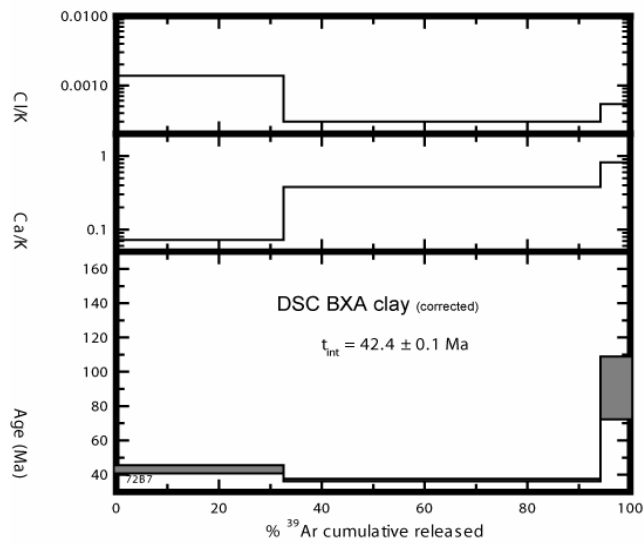
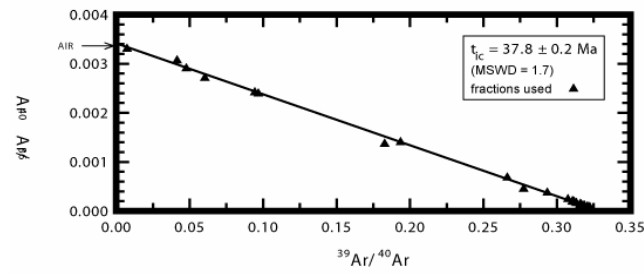
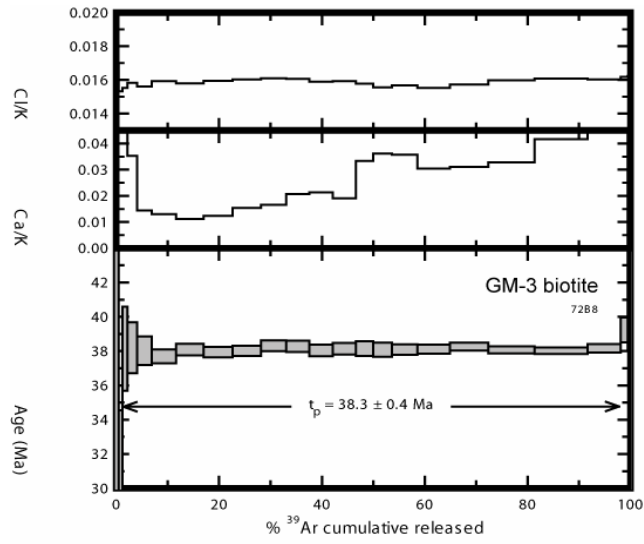
CK-02-8 Potassium Feldspar





GM-10 Potassium Feldspar





APPENDIX C

Quartz vein-hosted mineral species delineated by sample and deposit.

Sample	Py	Sph	Gal	Stib	Elec	Fah	Bour	Cpy	Mo	Asp
GRIT 01										
02										
03										
04	X	X	X							
05	X		X							
06	X	X	X			X				
07	X									
08	X		X					X		
09										
10	X					X				
12										
24										
26	X					X				
27				X		X				
28	X									
29										
32										
33	X									
34	X									
35			X			X	X	X		
38	X					X				
49										
51S	X					X				
52										
55										
56	X									
57										
63										
64										

Sample	OC	Clay	Chi ± Ep	Ser	Carb	Arg	Bar	Cu-ox	Cor	Cir ± Bro ± Em	Ac
GRIT 01			X		X						
02					X						
03					X						
04											
05					X						
06					X	X					
07				X	X						
08											
09			X								
10					X						
12	X				X						
24		X		X							
26									X		
27										X	
28											
29		X			X						
32					X						
33											
34					X						
35							X	X			
38									X	X	X
49							X				
51S							X				
52							X				
55					X						
56		X		X							
57					X		X				
63			X		X						
64					X						

Sample	Py	Sph	Gal	Stib	Elec	Fah	Bour	Cpy	Mio	Asp
BD										
01										
06										
09	X									
11										
12										
13	X									
14	X									
17	X	X						X		X
19	X									
21	X		X			X				
23	X									
25	X									
LOVIE										
01										
02	X	X	X			X		X		X
03	X	X	X	X						
05	X	X						X		X
06	X					X				
08	X	X	X							
09	X	X	X					X		X
12										
15	X									
17										
21S										
22	X	X	X			X		X		
25										
26										
27										
28	X									
29										
31		X								
35	X	X	X			X		X		
36	X									
37										
39										
40										
41	X									
42										

Sample	OC	Clay	Chl ± Ep	Ser	Carb	Arg	Bar	Cu-ox	Cor	Clr ± Bro ± Em	Ac
BD	01	X					X				
	06	X					X				
	09										
	11		X								
	12		X								
	13										
	14		X	X							
	17		X							X	
	19		X		X						
	21									X	
	23		X								
	25	X									
LOVIE	01			X							
	02					X					
	03				X						
	05										
	06										
	08										
	09		X				X				
	12		X	X							
	15		X								
	17		X								
	21S		X								
	22		X		X	X					
	25				X						
	26		X								
	27				X						
	28										
	29		X								
	31										
	35									X	
	36										
37					X						
39		X	X		X						
40		X			X						
41			X		X						
42			X		X						

Sample		Py	Sph	Gal	Stib	Elec	Fah	Bour	Cpy	Mo	Asp
UN	CK02-11	X	X	X			X				X
	CK02-13	X	X				X				X
GE	X1-B	X		X			X				
	02	X	X	X			X		X		X
	04	X		X			X		X		X
	05	X	X	X		X			X		X
KATT	01	X	X	X			X				
	03										
	06		X	X			X				
	07	X									
	08	X									
	09	X									
	10	X	X	X			X				
	12										
	13	X									
	14	X									
	15	X									
	17										
	24										
	27										
	30	X									
31	X										
37	X										
41											

Sample		Py	Sph	Gal	Stib	Elec	Fah	Bour	Cpy	Mo	Asp
HT	BURNS 05	X		X			X		X		
	CK02-4	X	X	X			X				
	CK02-5	X									X
	DSC BXA					X					
	HT02-12	X			X						
	HT02-14	X	X	X		X					
	IND N ADIT		X	X			X		X		X
	97-2 172		X	X					X		
	97-8 107	X	X	X					X		
	97-10 106.1	X								X	
	97-10 1084.5	X	X	X			X				
	97-10 1161.7	X	X	X			X	X			X
	97-10 1168	X	X	X			X	X			X
	97-10 1181.5	X	X	X			X				
	97-11 665.3	X	X				X		X		X
	97-12-330.3	X							X		
	97-13 221	X	X	X		X	X		X		

Sample	Ac	Clr ± Bro ± Em	Cor	Cu-ox	Bar	Arg	Carb	Ser	Chl ± Ep	Clay	OC
HT BURNS 05											
CK02-4											
CK02-5										X	
DSC BXA										X	
HT02-12					X						
HT02-14											
IND N ADIT											
97-2 172							X				
97-8 107											
97-10 106.1											
97-10 1084.5											
97-10 1161.7											
97-10 1168											
97-10 1181.5											
97-11 665.3							X			X	
97-12-330.3											
97-13 221											

Notes: Py, pyrite; sph, sphalerite; gal, galena; stib, stibnite; elec, electrum; fah, fahlore; bour, bourmonite; cpy, chalcopyrite; mo, molybdenite; asp, arsenopyrite; ac, acanthite; clr, chlorargyrite; bro, bromargyrite; em, embolite; cor, coronadite; Cu-ox, copper oxide; bar, barite; arg, argentite; carb, carbonate; ser, sericite; chl, chlorite; ep, epidote; clay, clay (unidentified); OC, organic carbon.
GRIT = Betty O'Neal mine; BD = Blue Dick mine; Lovie = Love mine;
UN = Unnamed prospect; GE = Gray Eagle mine; KATT = Kattenhorn mine;
HT = Hilltop deposit